Intergovernmental Oceanographic Commission
technical series

60

Interdisciplinary Approaches to Geoscience on the North East Atlantic Margin and Mid-Atlantic Ridge

Preliminary results of investigations during the TTR-10 cruise of
RV *Professor Logachev*
July-August, 2000

Editors: N.H. Kenyon
M.K. Ivanov
A.M. Akhmetzhanov
G.G. Akhmanov

UNESCO 2001

The designations employed and the presentation of the material in this publication do not imply the expression of any opinion whatever on the part of the Secretariats of UNESCO and IOC concerning the legal status of any country or territory, or its authorities, or concerning the delimitation of the frontiers of any country or territory.

For bibliographic purposes, this document should be cited as follows:
Interdisciplinary Approaches to Geoscience on the North East Atlantic Margin and Mid-Atlantic Ridge
IOC Technical Series No. 60, UNESCO, 2001
(English)

Printed in 2001
by the United Nations Educational,
Scientific and Cultural Organisation
7, place de Fontenoy, 75352 Paris 07 SP

Printed in UNESCO's Workshops

© UNESCO 2001
Printed in France

SC-2002/WS/02

TABLE OF CONTENTS

ABSTRACT ..... (iii)

ACKNOWLEDGEMENTS ..... (iv)

INTRODUCTION 1

METHODS 5

I. PORTUGUESE MARGIN AND GULF OF CADIZ (LEG 1) 8

I.1 Introduction and objectives of the TTR-10 Leg 1 and first part of Leg 2 8

I.2. The Marques de Pombal Area 9

I.2.1 Introduction and geological setting 9
I.2.2 Summary of work 11
I.2.3 Seismic and acoustic data 11

I.2.3.1 Seismic data acquisition and processing 11
I.2.3.2 Seismic data interpretation 12
I.2.3.3 Sidescan sonar data (OKEAN and OREtech) 17

I.2.4 Bottom sampling results 21
I.2.5 Discussion and main conclusions 21

I.3. Algarve margin and Gulf of Cadiz 26

I.3.1 Introduction and geological setting 26
I.3.2 Seismic and acoustic data 26

I.3.2.1 Seismic data acquisition and processing 26
I.3.2.2 Seismic data interpretation 27
I.3.2.3 Sidescan sonar data (OKEAN and OREtech) 30

I.3.3 Bottom sampling results 32
I.3.4 Micropalaeontological investigation of matrix from mud volcanic deposits 40
I.3.5 Geochemical sampling 42
I.3.6 Main conclusions 45

II. MID-ATLANTIC RIDGE: LUCKY STRIKE FIELD (LEG 2) 46

II.1 Introduction and geological setting 46
II.2 Aims and Objectives 49
II.3 Main results 49

II.3.1 30 kHz sidescan sonar OREtech imagery and 7 kHz sub-bottom profiling 49
II.3.2 Bottom sampling 51

II.4 Conclusions 51

III. NORTH-EAST ATLANTIC EUROPEAN MARGIN (LEG 3) 57

III.1. Porcupine Seabight Mouth: short study 57

III.2. Northeastern Rockall Trough Margin 59

III.2.1. Introduction 59
III.2.2 Single channel seismic profiling 60
III.2.3 3.5 kHz hull-mounted sediment profiler data 70
III.2.4 Side-scan sonographs 76
III.2.5 Ground-truthing of 3.5 kHz profiler, OKEAN and OREtech sidescan sonographs 79
III.2.6 Main conclusions 88

III.3. Northern Rockall Trough and Southern Faeroe continental margin 89

III.3.1 Objectives 89
III.3.2 Methodology 89
III.3.3 Summary of work 91

III.4. Southern Vøring Plateau 94

III.4.1 Introduction 94
III.4.2 Seismic and OKEAN profiling 95
III.4.3 Bottom sampling 99
III.4.4 Main results 101

REFERENCES 102

ANNEX I. CORE LOGS

ANNEX II. LIST OF TTR-RELATED REPORTS

ABSTRACT

The areas visited during the 10th Training-through-Research Programme were the Portuguese Margin, the Gulf of Cadiz, the Lucky Strike area of the Mid-Atlantic Ridge, the Rockall Trough, the Southern Faeroe margin, and the Vøring Plateau (Norwegian margin). The investigations were aimed at studying such geological processes as neotectonics, fluid migration and escape, sediment processes in canyons and sediment reworking and benthic biology in areas swept by deep-sea bottom currents as well as hydrothermal manifestations on mid-ocean ridges.

A seismic and sidescan survey of the Marques de Pombal structure (Portuguese margin) allowed a better understanding of a fault system known here from previous studies such as the ARRI-FANO and BIGSET projects. The fault pattern has been mapped and acoustic images have helped to evaluate the status of their activity. The Marques de Pombal structure showed little evidence of recent activity and is being covered by sediments. Shallow slides found in the vicinity of the structure may, however, indicate some occasional activity disturbing the overlying sedimentary cover. The Pereira de Sousa fault was found to be much more active.

Six new mud volcanoes were discovered and studied in the Gulf of Cadiz. Most of them were proved to be recently active. The mud volcanism of the Gulf of Cadiz can be considered as two characteristic regions with different mud breccia lithological composition.

Several types of lava sulphite ores sampled during the Azores campaign of Leg 2 allowed a better understanding of volcanic evolution and associated processes of this area.

A short 3.5 kHz survey across the Porcupine Seabight mouth, combined with existing swath bathymetry data and a few cores from the area, confirmed the findings of the TTR-7 cruise that the Gollum channel system is currently inactive.

The study of a canyon on the northeastern Rockall Trough margin showed that the system is inactive at the present time and the last pulse of active downslope sediment transport took place in immediate pre-Holocene time. Debris flows were found mostly on the flanks of the canyon while the axial zone showed numerous signs of erosion. Sand was not particularly common in the studied area. It is suggested that significant amounts of sand are trapped in the canyon head, possibly due to slumps blocking the narrower waist area. Abundant traces of seabed erosion found immediately beyond the canyon mouth indicate that this area is a bypass zone and sand deposition may occur further into the basin plain.

An extensive collection of TV-guided grab samples and seafloor video records, obtained from sites in the Northern Rockall Trough, Wyville-Thomson Ridge and Southern Faeroe Plateau, provided good insight on the distribution of bottom fauna, including deep-water corals, and of coarse glaciagenic debris.

New data on a BSR distribution pattern were obtained on the southeastern part of the Vøring Plateau and they suggest that the formation of the Storegga Slide was not directly related to the dissolution of gas hydrates. The investigation also provided a new insight into gas hydrate formation and distribution in the area.

ACKNOWLEDGEMENTS

The 10th Training-Through-Research Cruise became a reality due to financial support from various sources, among which were: the Intergovernmental Oceanographic Commission (IOC) of UNESCO, GEOTEK (UK) Ltd., Instituto Geologico e Mineiro (Portugal), Challenger Division of the Southampton Oceanography Centre (UK), the Russian Ministry of Science and Technological Policy, the Polar Marine Geological Exploration Expedition of the Russian Ministry of Natural Resources and the Moscow State University (Russia). Logistic support was provided by the Netherlands Sea Research Institute (The Netherlands).

A number of people from different organizations supported the Training-through-Research Programme and were involved into the cruise preparation. The editors would like to express their gratitude for the contributions made by Prof. I. F. Glumov (Ministry of Natural Resources of the Russian Federation), Dr. P. Bernal (Executive Secretary, IOC), Dr. A. Suzyumov (UNESCO) and Mr. V. Zhivago (Ministry of Science and Technological Policy of the Russian Federation).

Credit also should be given to Dr. Maarten van Arkel of the Netherlands Institute for Sea Research and Prof. Dr. B. A. Sokolov (Moscow State University) for administrative support.

Thanks are due to the administration and staff of the Polar Marine Geological Exploration Expedition (St. Petersburg) for their co-operation and assistance with the cruise organization. Captain A. Arutyunov and the skilful crew of the RV *Professor Logachev* are thanked for the successful carrying out of the operations at sea.

Staff and students of the UNESCO-MSU Marine Geosciences Centre were very instrumental in processing the acoustic data and the preparation of figures.

INTRODUCTION

In summer of the year 2000 the 10th anniversary cruise (TTR-10) was successfully conducted within the framework of the UNESCO-IOC 'Training-through-Research' programme on board RV *Professor Logachev* (Russia) from 13 July to 28 August. The cruise started from Santa Cruz de Tenerife (Canaries, Spain) and terminated in Bergen (Norway). The cruise was subdivided into three legs with two intermediate port calls, where partial exchange of the Scientific Party was made: in Cadiz (Spain) on 24-25 July and in Ponta Delgada (Azores Islands, Portugal) on 7-8 August. An international team of 58 scientists, post- and undergraduate students (in addition to a group of Russian technicians who had been working with the *Logachev* equipment) from 10 countries (Belgium, Brazil, Georgia, Italy, Morocco, Portugal, Russia, Spain, Switzerland, U.K.) participated in the cruise.

The main idea behind this cruise as well as of all the previous TTR cruises combines the training of students and young scientists with advanced research in the field of marine geosciences.

During the cruise, the participating students were actively involved in all stages of acquisition and preliminary processing of a multidisciplinary set of geophysical, geological and biological data. Daily seminars, lectures and discussions of the data, that have been collected facilitated a high-level of on-the-job training of the students and young scientists from different countries.

The major scientific objectives of the cruise were to study geological processes on the European continental margin as well as hydrothermal activity on a portion of the Mid-Atlantic Ridge. The scientific programme of the expedition included work in seven areas located on the Portuguese Margin, in the Gulf of Cadiz, in the Lucky Strike area of the Mid-Atlantic Ridge, near the Porcupine Basin, on the Rockall Trough and the Faeroe margins, and on the Vøring Plateau on the Norwegian Margin.

The work on the Portuguese margin continued investigations conducted during TTR-8 and TTR-9 cruises and was aimed to study main structural elements of the margin and recent fault activity.

Investigations of fluid escape features and gas hydrate accumulations were undertaken in the Gulf of Cadiz, continuing the study commenced by TTR in 1999.

The main goal of the study on the Mid-Atlantic Ridge, in the Lucky Strike area, was to investigate relations between volcanic and tectonic structures and distribution of hydrothermal activities leading to sulphide ore formation. An extensive sampling programme with a TV-controlled grab was planned in order to groundtruth the existing detailed sidescan sonar and video observation data.

On the Irish margin, a hitherto poorly known canyon system was the focus of investigation with a wide range of geophysical and geological equipment including single channel seismic profiling, 3.5 kHz profiler, and two types of sidescan sonars. The bottom sampling was aimed to sedimentologically characterise different parts of the system and to ground-truth acoustic facies observed at different frequencies.

The work in the northern Rockall Trough and on the Faeroe margin was primarily an environmental survey with the main aim to obtain a representative collection of TV-guided grab samples of bottom sediments and epifauna with visual control of sampling sites. The work took place on 3 sites. In the northern Rockall Trough a field of small cold-water carbonate mounds was a target for sampling. On the Wyville-Thomson Ridge and on the southern Faeroe margin areas covered by coarse glacial lag deposits and the sites of Tertiary rock outcrops were sampled.

A study area on the Norwegian margin was located at the northern edge of the giant Storegga Slide extending to the southwestern edge of the Vøring Plateau. Previous expeditions (including RV *Professor Logachev* cruises in 1994 and 1998) discovered here numerous fluid escape features. This year study was conducted in the area in order to better understand how fluid escape features and gas hydrate accumulations can affect slope instability processes.

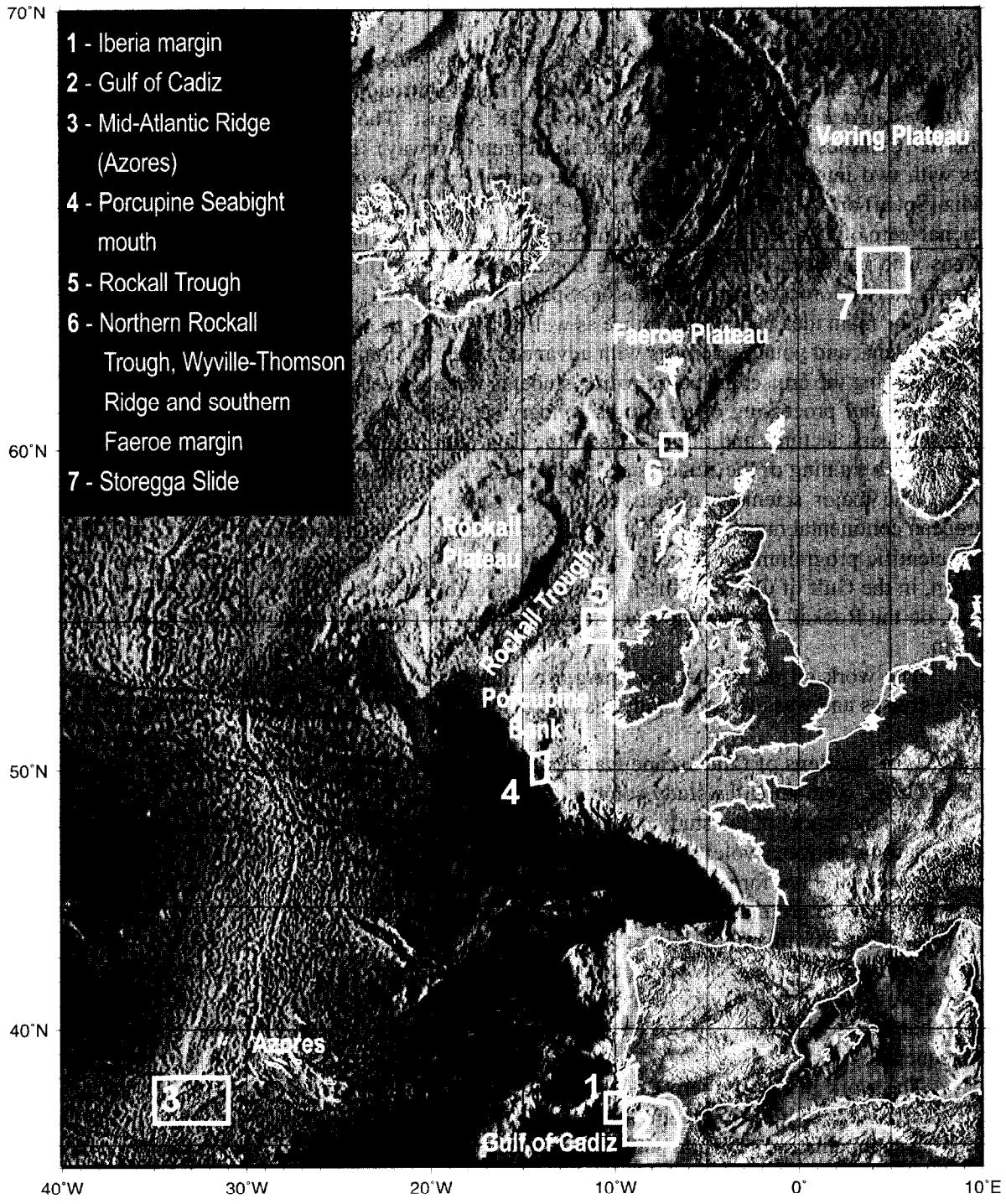

TTR-10 cruise location map

LIST OF PARTICIPANTS

TTR-10 "Floating University" Cruise, 13 July - 28 August 2000,
RV *Professor Logachev*

BELGIUM	**Jean-Pierre Henriet**	***Gent University***
	Peggy Vermeersch	***Gent University)***
	Samuel Deleu	***Gent University***
BRAZIL	**Waldemar de Almeida**	***Petrobras***
	Dennis Miller	***Petrobras***
GEORGIA	**Zurab Savaneli**	***Tbilisi State University***
ITALY	**Marzia Rovere**	***Institute for Marine Geology, Bologna***
	Adriano Mazzini	***University of Genoa***
MOROCCO	**Naima Hamoumi**	***Mohammed V University, Rabat***
PORTUGAL	**Luis Pinheiro***	***Aveiro University***
	Marina da Cunha	***Aveiro University***
	Anna Hilario	***Instituto de Ciences Biomedicas Abel Salazar***
	Isabel Gomes Teixeira	***Instituto de Ciences Biomedicas Abel Salazar***
	Francisco Teixeira	***Instituto Geologico e Mineiro***
	Jose Monteiro*	***Instituto Geologico e Mineiro***
	Manuel Quartau	***Instituto Geologico e Mineiro***
	Pedro Terrinha	***Instituto Geologico e Mineiro***
	Vitor Hugo	***Instituto Geologico e Mineiro***
	Tiago Cunha	***Instituto Geologico e Mineiro***
	Cristina Dias Lopes	***Instituto Geologico e Mineiro***
	Pedro Ferreira	***Instituto Geologico e Mineiro***
	Alvaro Pinto	***Instituto Geologico e Mineiro***
	Emilia Salgueiro	***Instituto Geologico e Mineiro***
	Luis Matias	***University of Lisbon***
RUSSIA	**Michael Ivanov***	***Moscow State University (MSU)***
	Sergey Buryak	***MSU***
	Ivan Denisenko	***MSU***
	Igor Kuvaev	***MSU***
	Vasily Galaktionov	***MSU***
	Pavel Shashkin	***MSU***
	Anna Volkonskaya	***MSU***
	Sergey Shkarinov	***MSU***
	Ksenia Ivanova	***MSU***
	Grigorii Akhmanov	***MSU***
	Elena Kozlova	***MSU***
	Dmitry Ovsyannikov	***MSU***
	Valentina Blinova	***MSU***
	Alexey Stepanov	***MSU***
	Alexander Sautkin	***MSU***
	Ivan Pasechnik	***MSU***
	Alina Stadnitskaya	***MSU***
	Irina Belenkaya	***MSU***
	Nikolay Galin	***MSU***
	Alexandr Arutyunov	***Polar Marine Geological Exploration Expedition (PMGRE)***
	Mikhail Maslov	***PMGRE***
	Alexandr Ashadze	***PMGRE***

	Alexandr Machulin	***PMGRE***
	Evgeny Samsonov	***PMGRE***
	Igor Tyunyakin	***PMGRE***
	Gennady Antipov	***PMGRE***
	Irina Antipova	***PMGRE***
	Victor Sheremet	***PMGRE***
	Victor Tsybulsky	***PMGRE***
	Valentin Konfetkin	***PMGRE***
	Anatoly Shagin	***PMGRE***
	Alexandr Shagin	***PMGRE***
	Alexandr Plakhotnik	***PMGRE***
	Sergey Luybimov	***PMGRE***
	Konstantin Plakhotnik	***PMGRE***
	Vyacheslav Gladush	***PMGRE***
	Vladimir Kyasper	***PMGRE***
	Alexandr Nescheretov	***PMGRE***
	Vladislav Malin	***PMGRE***
	Vladimir Zakharychev	***PMGRE***
	Leonid Mazurenko	***VNII Okeangeologia***
SPAIN	**Luis Somoza**	***Geological Survey of Spain***
SWITZERLAND	**Pierre-Michel Brudder**	***Institute of Geology, University of Neuchatel***
	Gaelle Dupont	
U.K.	**Paul Barnett**	***GEOTEK CO.***
	Bramley Murton	***Southampton Oceanography Centre (SOC)***
	Najeeb Rasul	***SOC***
	Juliette Biggs	***University of Cambridge***
	Ana Paula Teles	***SOC***
	Arnaud Mille	***SOC***
	Robert Swift	***SOC***
	Andrey Akhmetzhanov*	***SOC***
	Bryan Cronin	***University of Aberdeen***

* co-chief scientists

METHODS

VESSEL

The RV *Professor Logachev* is a Russian 104.5 m marine geology research and survey vessel equipped with seismic and seabed sampling equipment. She is operated by the State Enterprise "Polar Marine Geosurvey Expedition" St. Petersburg. The vessel has: a draught of 6.66 m, width of 16 m, net tonnage of 1351 ton, displacement of 5700 ton and is powered by two 3500 hp diesel engines.

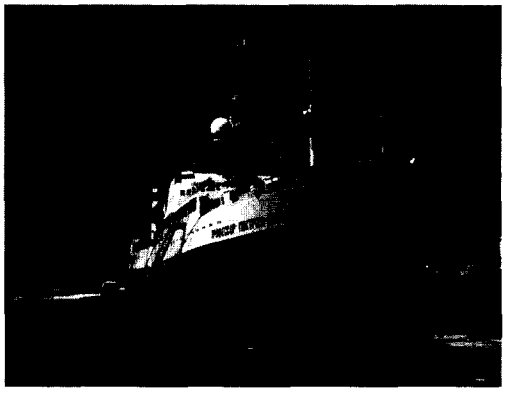

RV *Professor Logachev*

EQUIPMENT

Most of the equipment available onboard RV *Professor Logachev* has been already described in detail in the previous reports (Kenyon et al., 1998; Kenyon et al., 2000). This chapter will give a brief overview of the methods used. Where some of the equipment was used for the first time a more detailed description is provided.

Navigation

Positioning of the ship is acquired using an Ashtech GG24 GPS + GLONASS receiver. The use of both the GPS and GLONASS satellite configurations allows a far greater accuracy than is available from conventional GPS alone, with up to 60% greater satellite availability. Positions are calculated in real-time code differential mode with 5 measurements per second and an accuracy of +/- 35cm (75cm at 95% confidence limits) with optimal satellite configuration. Realistic positioning accuracy under normal satellite configuration for European waters is assumed as c. 5 m. OREtech sidescan, OKEAN sidescan, TV controlled grab and deep-tow video system are all fitted with pingers allowing precise navigation between the vessel and sub-sea surface position. This is necessary as deep-towed equipment is subject to greater spacial differences with respect to the vessel. This underwater navigation is based on the Sigma-1001 hydroacoustic system. Four stationary aerials, spaced 14 m apart, are hull mounted and receive acoustic signals from pingers attached to deployed equipment in short-base mode operating between 7-15 kHz. Four additional thrusters connected with the navigation system allow dynamic positioning of the ship. This is particularly useful during high resolution surveys or precise bottom sampling operations.

Seismic profiling

See section 1.2.3.1

3.5 kHz subbottom penetrating echosounder

A hull-mounted 3.5 kHz profiler was routinely used during most of the operations with a continuous paper output and selective recording of the digital data.

Sidescan sonars

Sidescan sonar survey was carried out simultaneously with seismic profiling using the

OKEAN 10 kHz long-range system. At selected areas where higher resolution of the seabed features was considered necessary, an OREtech deep-towed sidescan sonar operating at 30 and 100 kHz frequencies and equipped with a 7.5 kHz subbottom penetrating echosounder was employed. All data were digitally recorded and geographically registered onboard.

Sampling Tools

Gravity cores

Coring was performed using a 6 m long c. 1500 kg gravity corer with an internal diameter of 14.7 cm.

One half of the opened core was described on deck, paying particular attention to changes in lithology, colour and sedimentary structures. All colours relate to Munsell Colour Charts. The other half was measured for changes in magnetic susceptibility using a Bartington Instruments Magnetic Susceptibility meter with a MS2E1 probe. Magnetic susceptibility reflects the ease at which a material can be magnetised. This property is most strongly influenced by grain-size, heavy mineral content and inversely related to carbonate content and diagenetic ferric mineral reduction. Samples were also taken for coccolith and micropalaeontological assays from smear slides. This was done to generate a preliminary chronostratigraphy for the cores.

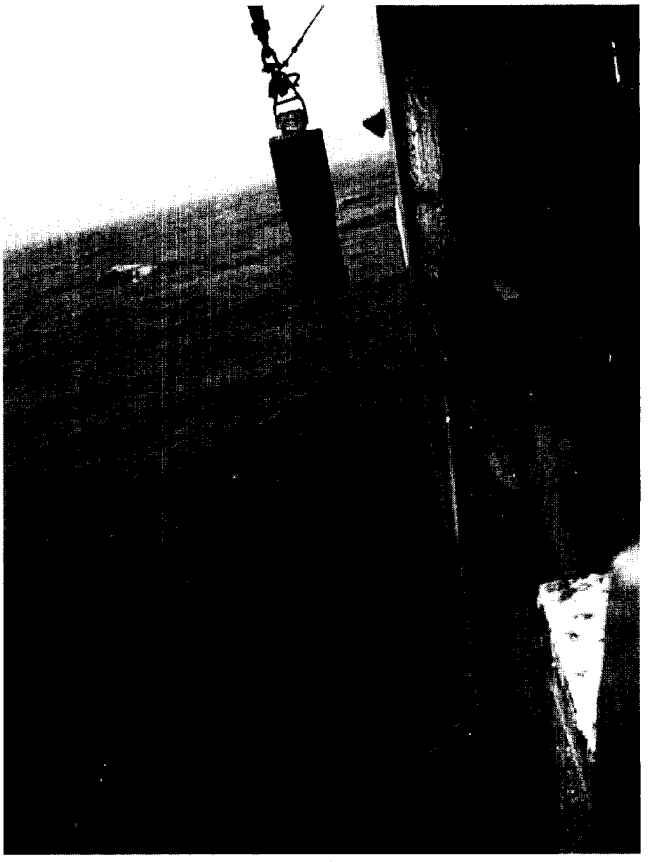

Deployment of gravity corer

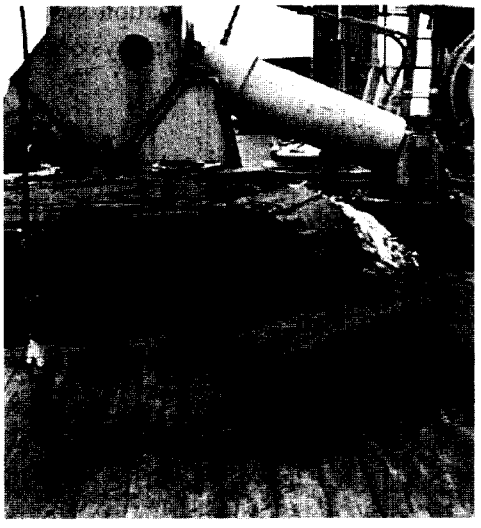

Dredge

Dredge

The dredge comprises a 1m^2, circular steel gate with chain mesh bag trailing behind and a 0.5 tonne weight leading by 3 m in front of the gate. The mesh bag also has a rope bag inside and the mesh size is ~5 cm. The dredge was deployed ~250 m in front of the identified target site and the ship moved at 0.5 kts for between 500 and 1500 m, ensuring the dredge was pulled up-slope. On some sites, the bottom was monitored with a 3.5 kHz hull-mounted single-beam echosounder. At all times, the ship's velocity and position were monitored using GPS. Tension on the trawl-wire was monitored in the winch cab by both ink-line paper roll and with a tension meter. "Bites" of up to 10 tonnes on the trawl wire were recorded in this way.

TV-guided grab

A new DG-1 grab system was used during the TTR-10 cruise. The 1500 kg system is able to sample dense clayey and sandy sediments as well as deep water basalts and sulphide ores. DG-1 can be used at depths down to 6000 m and closes by the difference in hydrostatic pressure. The maximum sample volume for soft sediment is 0.4 m^3. The triggering mechanism is set off by onboard control after the grab is lowered to the seabed. The grab is positioned with the short base SIGMA 1000 underwater navigation system. The grab is equipped with a build-in camcorder which uses 90 min cassettes and records in Hi-Fi Video8 format. Video signal is also transmitted on board to enable control for the grab operation and back-up recording is made as well. The lights are powered by a rechargeable battery, enabling 1 hour of continuous operation. A second battery kept on board is used to perform consequent deployments.

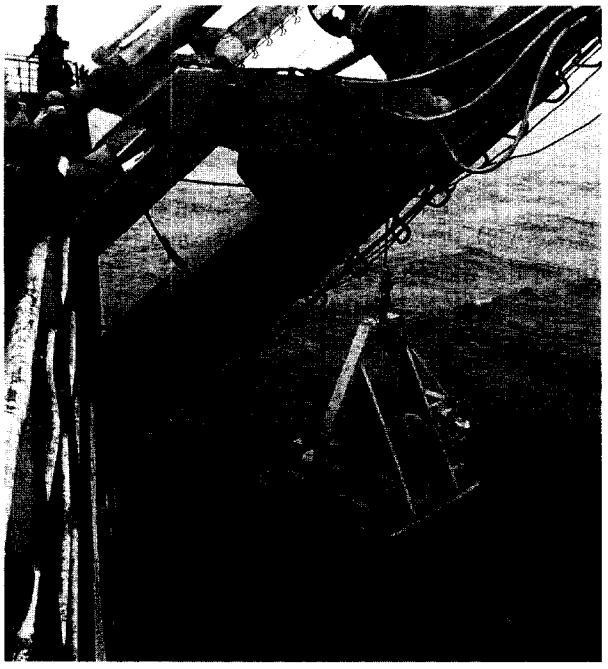

TV guided grab

I. PORTUGUESE MARGIN AND GULF OF CADIZ (LEG I)

I.1. INTRODUCTION AND OBJECTIVES OF THE TTR-10 LEG 1 AND FIRST PART OF LEG 2

L. PINHEIRO, J. MONTEIRO, L. MATIAS, P. TERRINHA

The aim of the first Leg of the TTR-10 Cruise was to use seismics, long range sidescan sonar (OKEAN), deep-towed sidescan sonar (OREtech), hull mounted 3.5 kHz profiler and coring, to investigate the morphology, sedimentation, tectonics and fluid escape structures in two distinct areas: (1) the Marques de Pombal area, on the continental slope of Baixo Alentejo, off W. Portugal, and (2) the

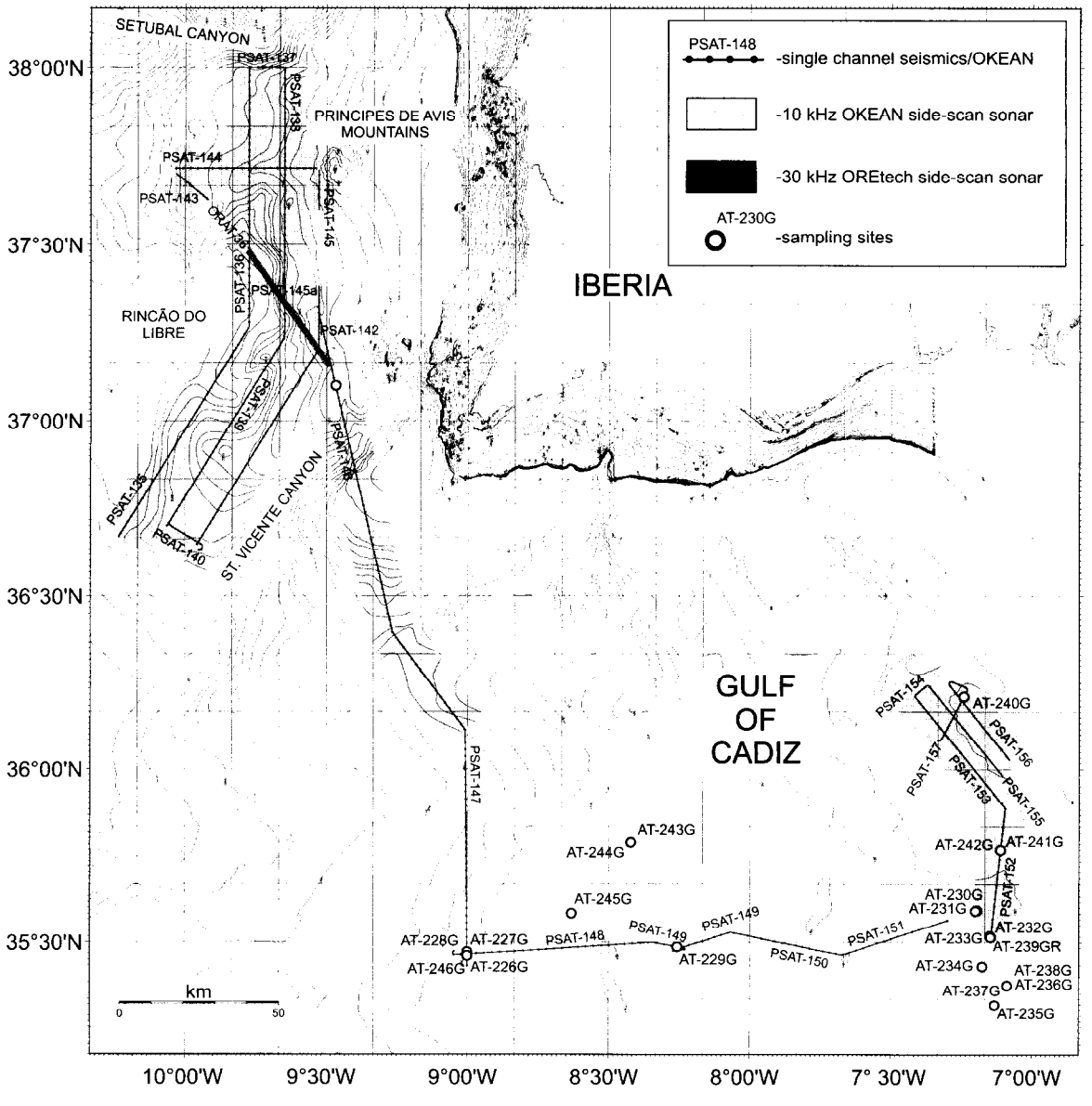

Figure 1. Location of the two study areas off south and southwest Iberia and the Gulf of Cadiz. Profile lines, sidescan coverage and sampling sites are shown.

South Iberia margin and Gulf of Cadiz (Fig.1).

The Marques de Pombal Structure

The Marques de Pombal fault (MPF) is thought to be part of the seismogenic structure of the 1755 earthquake (estimated Mw=8.7) and is named after the the Prime Minister in charge of the reconstruction of Lisbon. The earthquake provoked a large tsunami that destroyed a significant part of Lisbon, caused damage in a large part of the SW coast of Portugal and Morocco, and was felt as far as Switzerland and Finland. It consists of an active thrust fault that is clearly imaged on several multichannel seismic profiles acquired in the scope of the recent ARRIFANO and BIGSETS projects (Zitellini et al., 1999). The length of the fault trace (~50 km), however, is not long enough to explain the large magnitude of both the earthquake and the tsunami which require at least triple this fault length, even considering a large slip on the fault plane (2 m) (Baptista et al., 1998). A fault scarp, northwest of the MPF is a good candidate for a northward en-echelon continuation of this fault. In that area, tectonic deformation is observed on the shaded relief image of the multibeam data (BIGSETS).

The main objectives of the first part of Leg 1 of the TTR-10 cruise were: (1) to investigate the MPF and it's possible prolongation to the north; (2) to study the deformation west of the active fault zone; (3) to determine if there are any related fluid escape features and sediment slides/slumps. For this purpose, an OKEAN mosaic and single channel seismic profiles were collected in the study area.

S. Iberia and Gulf of Cadiz

During the TTR-9 cruise a large mud volcano field was investigated in the Gulf of Cadiz and the Moroccan margin, based on a sidescan mosaic and multibeam bathymetry collected in the area by the Naval Research Laboratory (NRL), Washington DC (courtesy of Joan Gardner). Several interesting features that could also be mud volcanoes or fluid escape structures were visible on another sidescan mosaic of the western portion of the Gulf of Cadiz and S. Iberia, made available for this cruise by Joan Gardner (NRL).

The main objective of the second part of Leg was to investigate mud volcanoes, gas hydrates and gas seeps off S. Iberia and in the Gulf of Cadiz, using seismic reflection, 3.5 kHz profiling, sidescan imagery and ground truthing (cores and grabs).

I.2. THE MARQUES DE POMBAL AREA

I.2.1. Introduction and Geological Setting

The Portuguese Continental Margin between Setubal and S. Vicente

The Baixo Alentejo continental margin is characterized by the absence of general breaks in the relief. It consists of a plane of moderate dip that extends from the coast line to the Iberian abyssal plain.

The shoreline is mainly made of active and uplifted cliffs with pocket beaches related to small river valleys. The inner shelf is a narrow shoulder with an inner surface cut into the basement (up to 120 m deep) and an outer surface that is completely overlain by the Neogene progradation shaping a convex slope. The outer shelf between 200 and 700 m in depth is a large accumulation of sediments of moderate dip, with no outer edge except at the northern and southern limits where the Principes de Avis and the Descobridores Mountains are bounded by steep "cuestas" corresponding to a sharp and seaward elevation of deep-bedded structures (Fig. 1). The outer shelf is the remnant part of an ancient continental shelf formed from the upper Eocene to the late Miocene.

The outer shelf passes into a continental slope that is an important sedimentary filling where a succession of alternating well stratified and transparent units have been recognized by seismic reflection overlaying a diffracting horizon (acoustic basement) cut by faults. The sediment cover of the slope

is also prone to gravity sliding. The outer part of the slope is being covered by the discordant turbiditic filling of the Tagus Abyssal Plain. The S. Vicente submarine canyon differs from the other canyons by the width of its valley which follows a graben (Fig.1).

To the south the continental shelf is very narrow and disappears below the sediment progradation of Neogene beds. It gives to the slope a a smooth profile (1.5°). At 2000 m a steep slope with a drop of 1400 m can be followed for 45 km. At the base of this slope the semicircular Rincao do Lebre (Fig. 1) is covered by sediments. Its limit in the N is a tectonic feature oriented at 60°.

At 10° W the sediment cover of the lower slope is intersected by a 50 km long scarp with a drop of 800 m. In the south, the scarp is limited by the S. Vicente Canyon which follows the offshore prolongation of the onshore Odemira-Avila fault.

The Marques de Pombal Structure and the 1755 Earthquake

Much research has been devoted to the study of tsunamigenic structures like the one that caused the 1st of November 1755 Lisbon earthquake (Mw=8.7) (Baptista et al., 1998). Hydrodynamic modelling of the 1755 event and comparison with the tsunami of the 28th of February 1969 earthquake, generated at Gorringe Bank and felt in Lisbon with tide gauges of 20 cm amplitude, has shown that the structure responsible for the 1969 event, amplified to the estimated magnitude Mw=8.7 of the 1755 event, cannot account for the historical observations of the 1755 earthquake (Baptista et al., 1998). Alternative sources, selected as the most probable ruptures for the 1755 earthquake, all involve high displacements on the seafloor (>20 m) along a fault with over 200 km length, trending approximately N-S, which must be closer to the coast than Gorringe Bank.

In 1992, the ARRIFANO seismic survey (Torelli et al, 1997; Sartori et al., 1994) crossed the epicentre of the 1755 earthquake as indicated in some historical catalogues. The MCS line AR92-10 revealed a huge thrust fault, offsetting the seafloor with over 1000 m relief, which appears to sole out in the deeper levels of the crust or even below (Zitellini et al., 1999). As part of the EC funded BIGSETS Project (Big Sources of Earthquake and Tsunami), the thrust was well imaged by seismic refraction profiles, together with multibeam survey. Dating of the turbidites from one of the cores in front of the fault trace yielded an age of 300±100 y BP which is compatible with gravitational sliding on the Marques de Pombal 60 km long fault scarp during the 1755 event. The thrust fault attenuates to the N and S, becomes a fold and then disappears.

The relocation of seismic events recorded in the area by the National Seismic Networks of Portugal and Spain, show that the earthquake depth can be larger than 30 km. Recently, the 26th March 2000 event M=4.2 was located at 30 km depth and, further west, near Gorringe, large earthquakes at a depth of 70 km were recorded (Grimison and Chen, 1998). Based on this data, an estimated thickness of 60 km was proposed for the schizosphere where single event failure might occur (BIGSETS team). Considering that the 1755 event was an intra-plate earthquake with high stress-drop, an average 20 m slip could be attained for a Mw=8.7 event; based on this, the minimum length for the tsunamigenic fault that originated the 1755 earthquake should be 150 km. This value disqualifies the MPF as the single tsunamigenic source responsible for this destructive earthquake as well as the other fault structures identified so far in the target area. However, it has been observed in many large earthquakes that the surface rupture can be split into several segments, connected at depth to a main fault. It is therefore necessary to identify the major fault at depth and its surface expression next to the Marques de Pombal structure, either to the north or to the south of it.

The pattern of seismic activity off Iberia is diffuse with a few patches of concentrated seismicity in the Gorringe Bank (particularly the southern flank), the Guadalquivir Bank and the S. Vicente Canyon. Focal mechanisms obtained offshore SW Iberia from P-wave polarity studies for small and large events show a consistent NW-SE direction for the maximum inferred compressive stress. Most of the mechanisms are strike-slip (left lateral for the near E-W plane) but a few of the events are dip-slip. Near the MPF structure, all events are strike-slip, including the preliminary solution for the recent

26th March 2000 earthquake. If this latter event is related to the activity in the MPF, then it can only be interpreted in terms of regional tectonics, considering a transfer fault at depth offsetting the MPF to the south. On the other hand, the earthquake activity concentrated in the S. Vicente Canyon is elongated along this morphological feature where active faults are identified and its tectonic control is well established.

Recent analysis of onshore cores recovered from alluvial deposits near the coast has revealed the existence of tsunami deposits between fine-grained sediments. These deposits were dated and the determined age plus error bars coincides with the 1755 event and thus corresponds to the tsunami invasion of shallow plains (Hindson and Andrade, 1999). Systematic drilling and coring revealed that this deposit is unique in the sedimentary sequence sampled. Two explanations are possible for this, either the paleogeographic conditions that allowed the formation of such a deposit were unique, or the previous "1755-like" earthquake occurred more than several thousand years ago. If the latter explanation is true then the seismic cycle is very long and the return period for such an extreme event is very large. It may therefore be that after 245 years of the main shock we are still in a post-seismic gap of activity. The seismicity pattern should then be read in reverse, that is, the active tectonic structures that currently show none or little activity may be the ones that ruptured during the 1755 event. This could be the case for the MPF and also for other structures identified north and northwest of it.

I.2.2. Summary of Work

Leg 1 started in Santa Cruz de Tenerife, in the Canary Islands, 13/7/2000, at 22:30 and ended in Cadiz, 24/7/2000, at 08:00. The first leg started one day later than initially planned because of a problem with one engine of the ship. We arrived at the MPF area on the 17th of July at 04:00 when both OKEAN and the seismics started to be collected for testing. Simultaneous seismic and OKEAN lines were collected in this area between 05:30 of the 17/7 (start of line PSAT-135) and 02:17 20/7 end of line PSAT-145A. Line 135 was recorded in two parts, with an overlap, because of a problem with the OKEAN.

One core - AT-225G - was collected (Table 2) and one 30kHz OREtech line (ORAT-136) (Figure 2).

On the 20/7, Line PSAT-146, with both OKEAN and single channel seismics, was recorded on the way from this area to the first target in the S. Iberia margin: a structure, visible on a SEABEAM mosaic, interpreted as a possible mud volcano.

Figure 2 shows the coverage of seismic lines, OKEAN sidescan data and high resolution deep-tow OREtech sidescan images.

I.2.3. Seismic and Acoustic Data

I.2.3.1. Seismic Data Acquisition and Processing

Single channel seismic reflection profiles were acquired throughout Leg 1. After a period of testing, the most suitable configuration for the working conditions was adopted. The source consisted of one 3.5 litre airgun on Lines PSAT 135-138 and lines PSAT 147-157 and two 3.5 litres airguns on Lines PSAT 139-146. The airguns were towed at a depth of approximately 2-2.5 m and were fired every 10 seconds (i.e. approximately every 30 m). The streamer consisted of one active section, 7.5 m long, with 16 hydrophones, towed at a depth of approximately 2.5-3 m. The offset between the seismic source and the centre of the live hidrophone array was 230 m on lines PSAT 135-142 and 180 meters from line PSAT 143 onwards. The signals were filtered analogically to 50-250 Hz in the acquisition stage. The sample interval was 1 ms and the record length 3 seconds.

The data was acquired digitally using the MSU developed software and preliminary processed with the RadExPro software, which was provided to the UNESCO-MSU Centre for Marine Geosciences by GSD Productions, Moscow. A strong bubble pulse was observed in places (e.g. Line

PSAT-138), which was sometimes confused with a possible BSR.

All the single seismic data collected during the cruise was preliminarily processed on board, using the SPW software (Seismic Processing Workshop, from Parallel Geoscience Coorporation) running on a Power-PC. The basic processing sequence consisted of definition of the acquisition geometry, static shifts correction, amplitude recovery by spherical divergence correction and Butterworth bandpass filtering (20-230 Hz). For some of the seismic lines a preliminary f-k migration was attempted.

The location of the seismic and sidescan sonar lines were based on the interpretation of the available MCS seismic lines and multibeam data, as well as on the structural maps, earthquake data and tsunamigenic models. Considering the available shiptime, it was decided to investigate the Marques de Pombal Fault and the N-S trending morphological scarp which is located to the northeast: the Pereira de Sousa fault (see location on Figure 5), which could represent its northward prolongation.

I.2.3.2. Seismic Data Interpretation

L. PINHEIRO, J. MONTEIRO, L. MATIAS, P. TERRINHA, F. TEIXEIRA, M. QUARTAU, V. HUGO, T. CUNHA, A. VOLKONSKAYA AND S. BOURIAK

The study of active tectonics in offshore SW Portugal relied on the integration of the data acquired during the cruise and data brought onboard by participating scientists. These included: (1) 2000 km of MCS seismic data (raw-stack) acquired by the BIGSETS project in 1998; (2) 600 km of deep-penetration MCS data (final stack and final migration) acquired by the IAM project in 1993; (3) 200 km of deep-penetration MCS data (migrated time section) acquired by the ARRIFANO survey in 1992; (3) Multibeam data acquired by the BIGSETS project in May 2000: shaded relief image and colour contours for a 400 m grid spacing and a digital grid at 500 m spacing; (4) A GLORIA mosaic acquired in this area by SOC. The TTR-10 seismic dataset consisted of 470 km of single channel seismic data and 3.5 kHz high-resolution profiles. The coverage of seismic profiles collected during the TTR-10 cruise in the study area is illustrated on Fig. 2. The penetration in general was good, reaching over 1.5 secs, in places. The seismic lines were first interpreted on a line-by-line basis and then the main structures were plotted on a structural map based on a previous interpretation of the BIGSETS and ARRIFANO data.

PSAT 135: This profile was aquired along a NE direction (Fig. 2) cutting across the NNE-SSW trending MPF (Figs. 3 and 5). Due to a failure in the acquisition system there is a data gap in the zone of the fault trace. Nevertheless, the hanging-wall anticline and the foot-wall syncline are well imaged as well as the morphological scarp that marks the transition from this structure to the Rincão do Lebre plain, in the north.

PSAT 136: This N-S trending profile (Fig. 2) imaged the vertical structure across the ENE-WSW scarp that lies at approximately 37° 38' and the fold-like structures to the south (Figs. 4 and 5). These structures were well imaged on the sea bottom during the BIGSETS/PARSIFAL multibeam cruise. The ENE-WSW trending scarp appears to be due to a northward dipping thrust fault while the fold-like structures were interpreted as channels and levees caused by sediment drainage across the Pereira de Sousa fault (Fig. 5). The interpretation of these fold-like features as sedimentary was decided on the basis of their positioning with respect to the N-S trending scarp and also on the systematic existence of high amplitude reflectors (HAR) in the troughs and low amplitude reflectors on the highs.

PSAT 137: This is a short transit line between the PSAT 136 and PSAT 138. A normal fault dipping to the west and a Neogene basin could be correlated by comparison with IAM-5I profile.

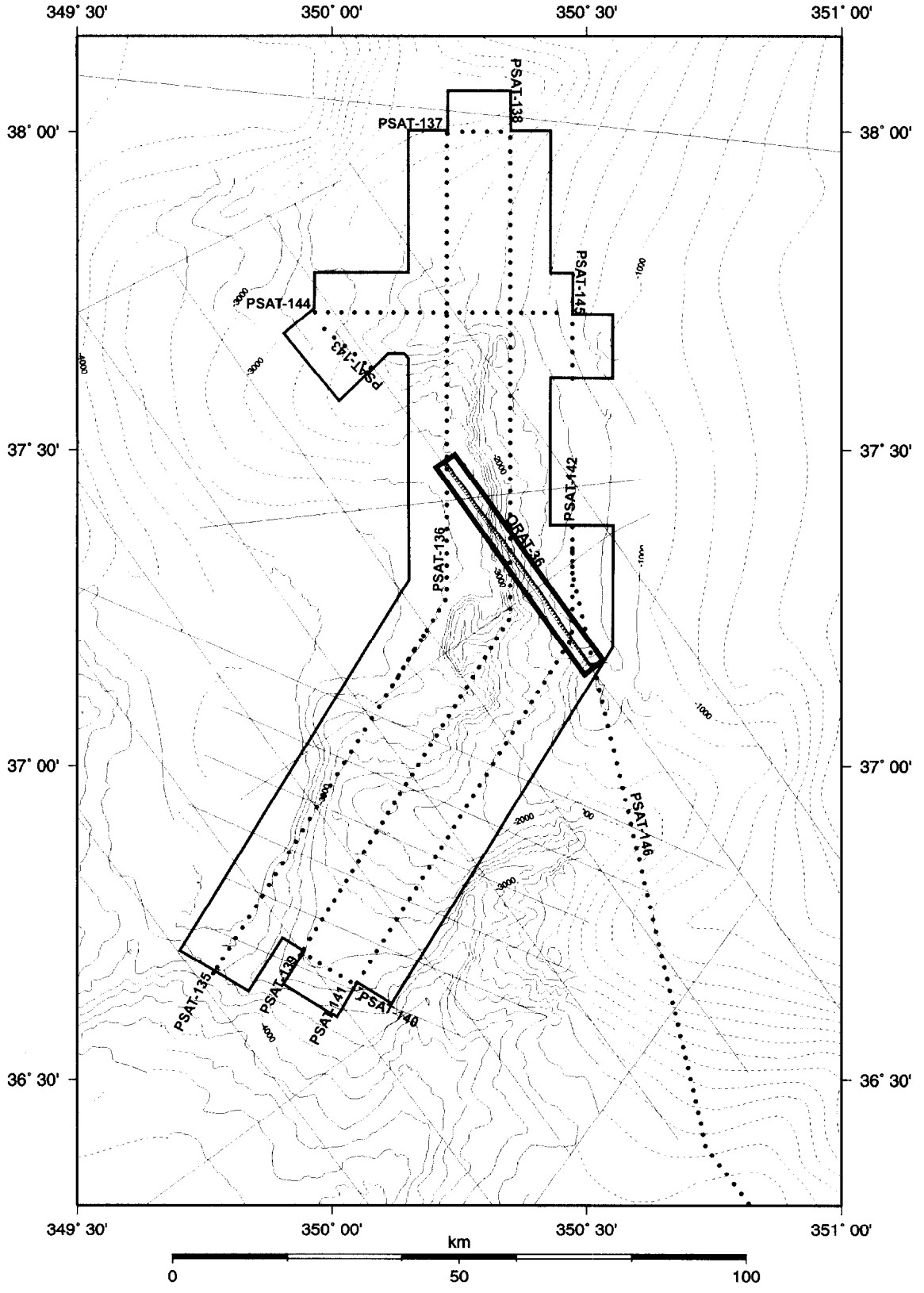

Figure 2. Seismic, OKEAN and OREtech coverage in the Marques de Pombal area. Also shown as thin lines is the multichannel seismic coverage in this area (BIGSETS, ARRIFANO and IAM), used for interpretation.

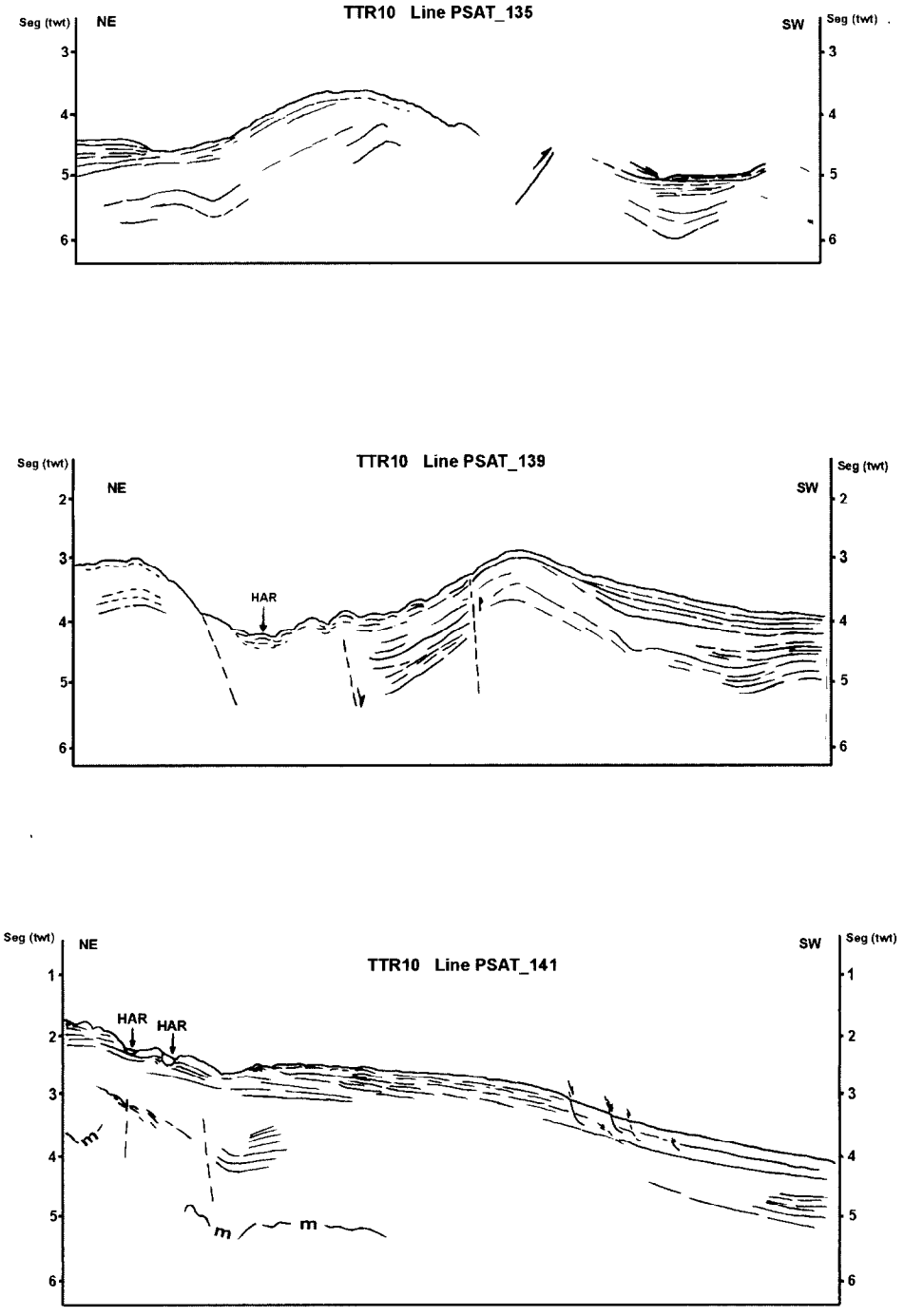

Figure 3. Interpreted seismic lines PSAT 135, 139 and 141 (for location see Figure 2). ***HAR*** *indicates high amplitude reflector,* ***m*** *indicates water bottom multiple.*

PSAT 138: Various sedimentary and tectonic structures are well imaged on this profile (Fig. 4), such as the valleys that cut the N-S trending Pereira de Sousa fault, the E-W striking F1 fault and compressional structures of probable Miocene age.

PSAT 139: This NE-SW trending line (Fig. 2) shows two segments of continuous and little disturbed horizons at the northern and southern ends of the line (Fig. 3). The morphological depression in the centre of the line shows many diffraction hyperbolae overlain by fold-like structures that were

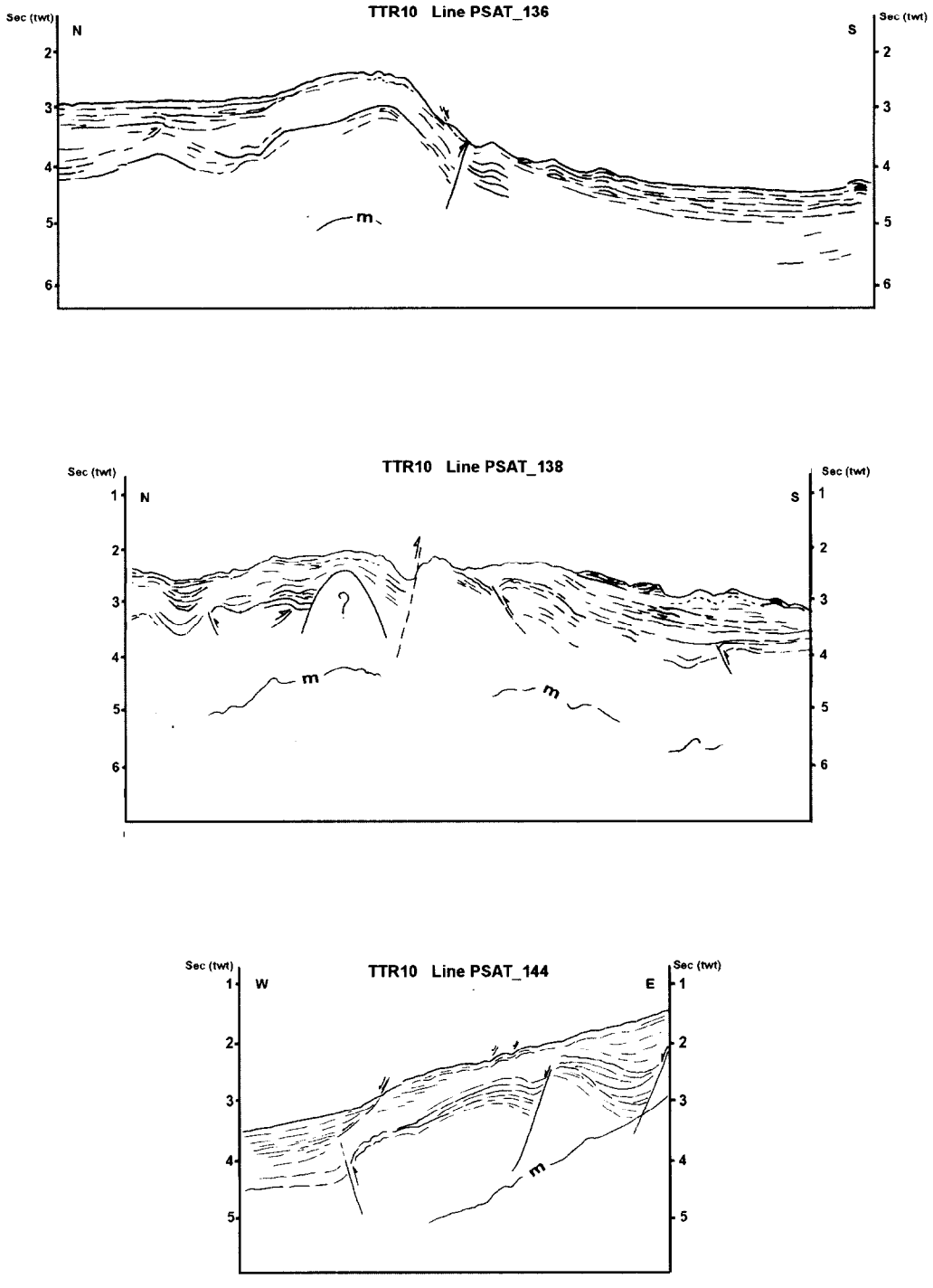

Figure 4. Interpreted seismic lines PSAT 136, 138 and 144. For location see Figure 2. ***m*** *indicates water bottom multiple.*

interpreted as channels and levees, as in line PSAT 136. It also appears that the two elevated blocks are separated by transverse faults.

PSAT 140: This is a short transit line between the PSAT 139 and PSAT 141 that displays a segment of gentle anticline, the crest of the Marques de Pombal hanging-wall anticline.

PSAT 141: This NE-SW trending seismic line shows some slope instability features on the slope of the Marques de Pombal plateau (Figs. 3 and 5). Further north, the transition from this plateau

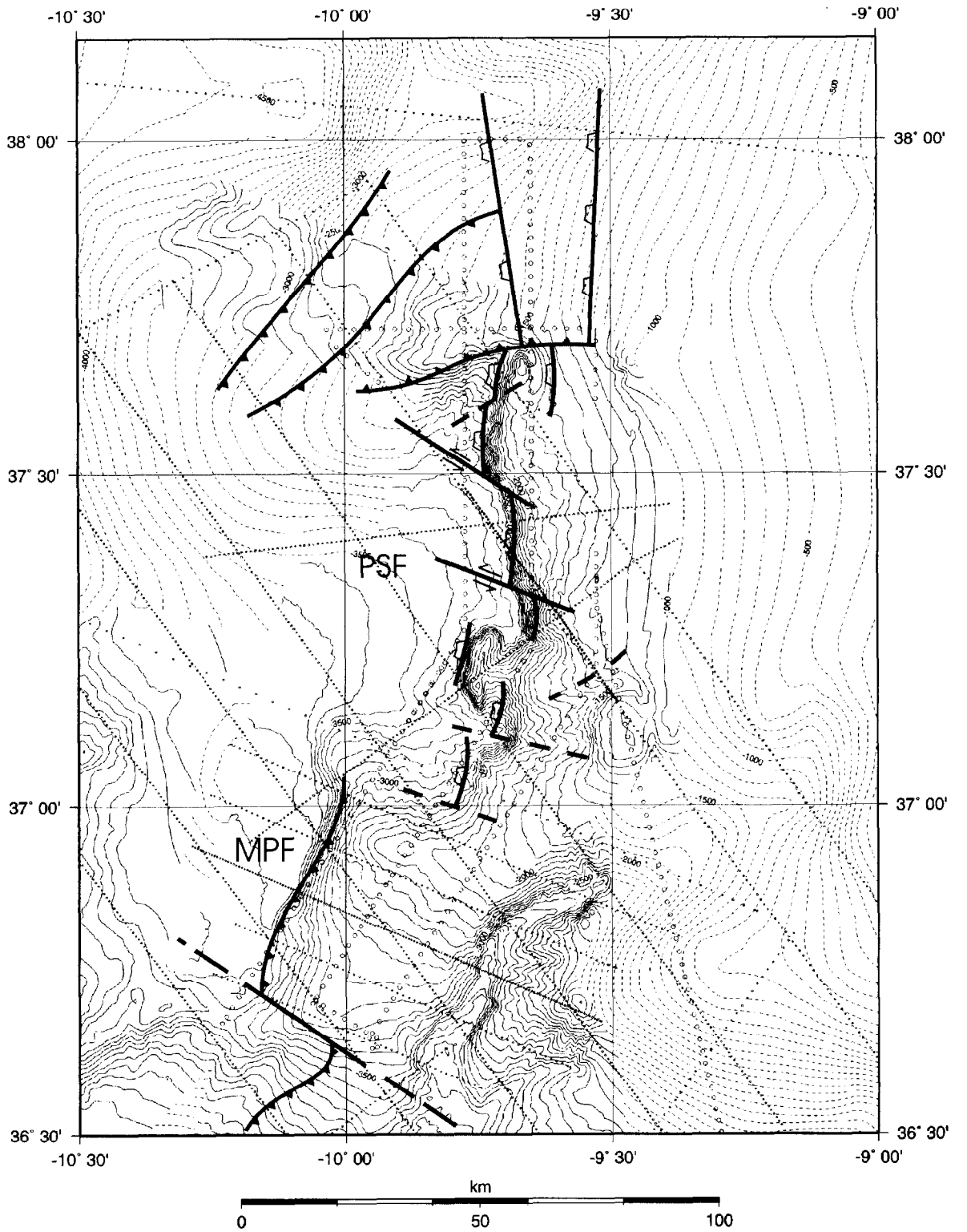

Figure 5. Interpreted fault structures in the Marques de Pombal area. Dotted lines show location of the MCS ARRIFANO, BIGSETS and IAM lines and the single channel TTR-10 profiles. Detailed bathymetry from a multibeam survey carried out by the BIGSETS team (courtesy L. Matias, J. Danobeitia). MPF denotes the Marques de Pombal fault and PSF - the Pereira de Sousa fault, offset by transfer zones/faults.

to the Pereira de Sousa plateau is marked by a series of channels and levees. Two possible faults were marked underneath the transparent sedimentary unit at the transition of the Marques de Pombal and the the Pereira de Sousa structure.

PSAT 142: This is a short N-S profile, shot along strike of the the Principes de Avis plateau, showing well layered sediments resting on top of a transparent sedimentary package. A possible fault has been marked.

PSAT 143: This is a short transit line shot between the OREtech line and seismic lines.

PSAT 144 shows rotated blocks along west-dipping normal faults, reactivated by compression (Fig. 4).

The interpreted structural map for the Marques de Pombal area is represented in Figure 5. It shows the main fault structures that were identified based on the integration of the available datasets.

I.2.3.3. Sidescan Sonar Data (OKEAN and OREtech)

A. AKMETZHANOV, J.-P. HENRIET, J. MONTEIRO, M. ROVERE AND P. SHASHKIN

An extensive acoustic data set has been acquired on the Iberian margin. The set comprises about 450 km of seismic survey together with simultaneous acquisition of 10 kHz long-range OKEAN sidescan and hull-mounted 3.5 kHz profiler data.

Although OKEAN imagery shows mostly low backscattering uniform seafloor, several interesting features can be identified (Fig.6). In the south, the Marques de Pombal (MPF) structure is expressed as a step on the seafloor and is seen on the OKEAN record as a NNE-SSW trending linear feature about 60 km long. East of the structure there is an area of higher backscatter whose morphology resembles three tongue-like patches. They are located on the slope of a pronounced ledge and are thought to be recent thin debris flows. This is confirmed by 3.5 kHz records showing acoustically transparent lens-like bodies on the slope of the ledge. OKEAN data suggest that sediment failure occurred at a water depth of about 2200 m and then sediments were transported to the base of the ledge bounded by the MPF at 3800 m water depth. The length of the debris flows reaches up to 20 km.

From 37°10'N and up to 37°15'N there is an elongate hill, about 25 km long on its longer axis, recognised in the seafloor topography and expressed on the OKEAN record as an ellipse like object with highly backscattering edges. Such a backscatter pattern suggests that the edges of the hill are outcrops of older rocks or consolidated sediments and the hill is an uplifted basement block. To the north of the basement block (37°16'N-37°40'N) the OKEAN record shows a narrow N-S trending linear zone of high backscatter with a length of about 45 km and a width of about 2 km. The zone corresponds to the area of significant increase of slope gradient in the seabed topography, probably a fault scarp. High backscatter is caused by outcropping of hard rocks or lithified sediments. The height of the escarpment is about 600 m. To the west of the escarpment the OKEAN image shows a finger-like pattern of downslope running debris flows, seen as high backscatter streaks. The presence of debris flows suggests that the escarpment is a local source for redeposition of sediments by gravitational processes. To the east of the escarpment, at about 9°35'W, the record shows several subparallel, sinuous high backscattering features which are interpreted as slump folds. At 37°40'N/9°30'W there is an area of high backscatter representing outcrops of bedrocks on the slopes of Principes de Avis Mountains.

A 30 kHz OREtech line was run oblique to the seismic and OKEAN profiles in order to better understand the acoustic facies seen on the OKEAN imagery and to observe seabed morphology with higher resolution.

The most common acoustic facies observed along the line is a uniform low backscatter representing undisturbed hemipelagic sediments. The subbottom profiler also shows a well stratified

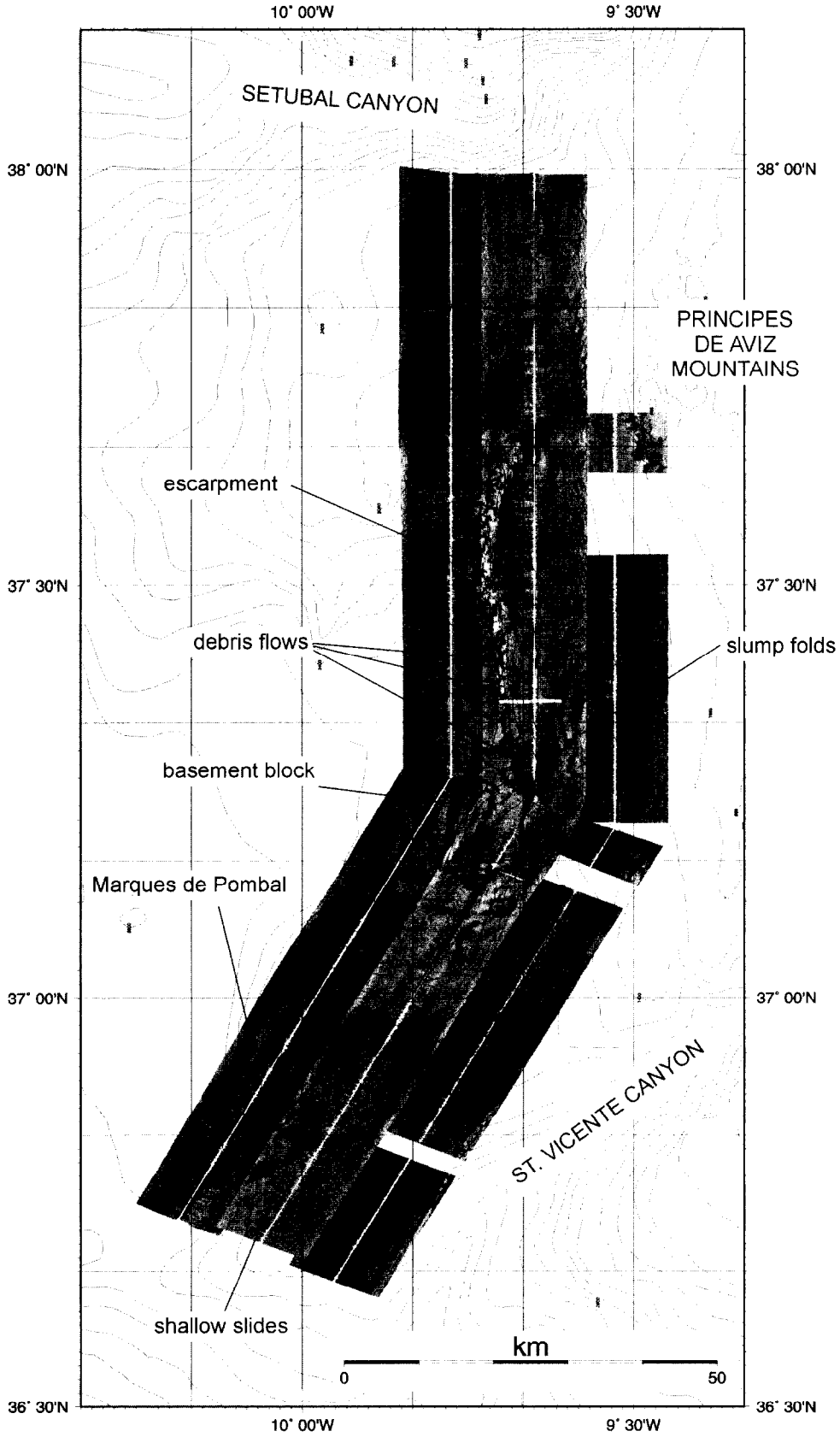

Figure 6. OKEAN mosaic from the Marques de Pombal area with main features shown.

sequence, although penetration is limited to the upper 10 m. At one point the line crosses a NE-SW trending small canyon, with high backscattering on the SW flank due to outcropping of older rocks/lithified sediments (Fig. 7).

The flat bottom of the canyon has low backscatter, suggesting that the canyon is not an active turbidity current pathway. However, there seems to be a redistribution of sediments by gravity processes mainly due to failures from canyon walls. Interestingly, the major failures had happened on the gentler northwestern flank. This may indicate tectonic control on the present stage of the canyon's development or show that occasionally bypassing turbiditic currents are deflected to the right by Coriolis effect.

A shallow depression, about 40 m deep, is seen on the subbottom profiler record but has almost no expression on the sonograph. On the flanks of the depression there are truncated reflectors indicating the erosion. To the SW of this depression there is a vague wrinkle-like pattern probably caused by sediments disturbed by sliding. These features seem to be evidence of sediment instability on the local slopes in the area causing shallow sliding within the hemipelagic cover. Another interesting feature is observed between time marks 4:00 and 5:20 where there is a 200 m wide sinuous band of parallel streaks, characterised by relatively higher backscatter, which could be confused with a channel. A more careful analysis revealed that the feature follows along the slope of a local elevation and most likely is a zone of outcropping of older sediments resulted from sediment failure. The streaked acoustic pattern observed on the sonograph within this zone reflects the layered character of the outcropping sedimentary sequence. The thickness of the uppermost unconsolidated hemipelagic cover is about 50 m according to the subbottom profiler data. From 6:00 to 10:00 the sonograph reveals a more complex acoustic pattern in an area with increased slope gradient close to the escarpment. Evidence of sediment failure is common. At 0:00 the line crosses an escarpment, seen as a band of high backscatter. A strong return on the profile also suggests that the escarpment is an outcrop of hard rocks. At the base of the escarpment the seabed has moderate backscatter and some roughness on the sonograph (Fig. 8). This corresponds to one of the debris flow deposits. The subbottom profiler record does not offer much penetration. However, the uppermost part of the succession is built by several acoustically transparent lens-like bodies, up to 5 m thick, which are believed to be debris flows.

Further to the NW the seabed becomes flat and smooth and has a uniform low backscatter.

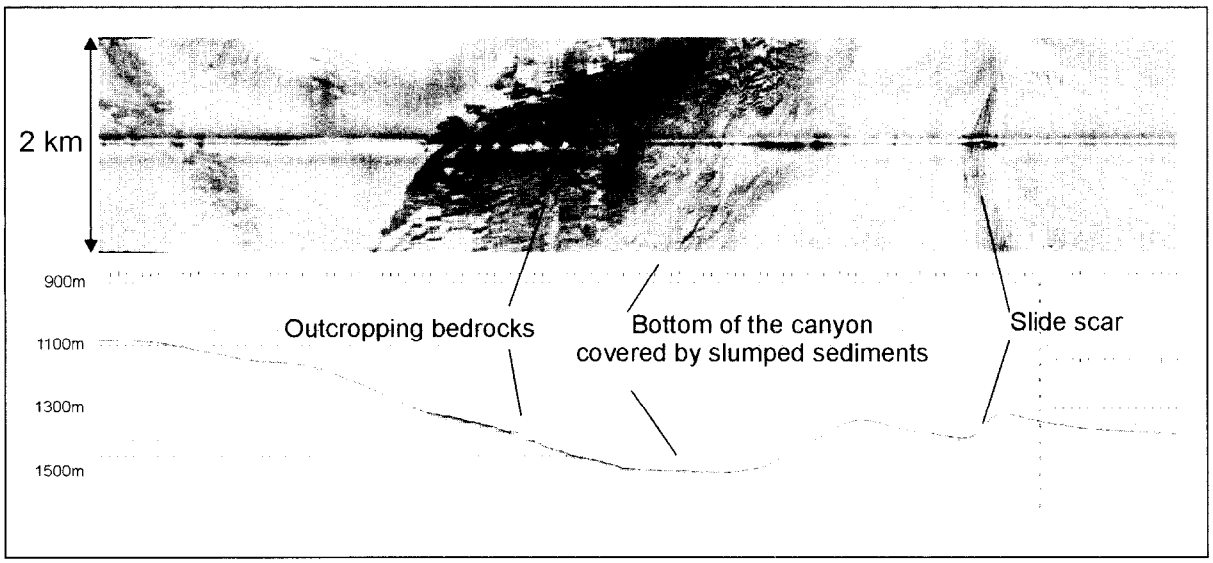

Figure 7. Fragment of ORAT-36 line showing a small canyon with sediment failures on the SW flank and slumped sediments covering the bottom of the canyon, suggesting the absence of recent turbidity currents.

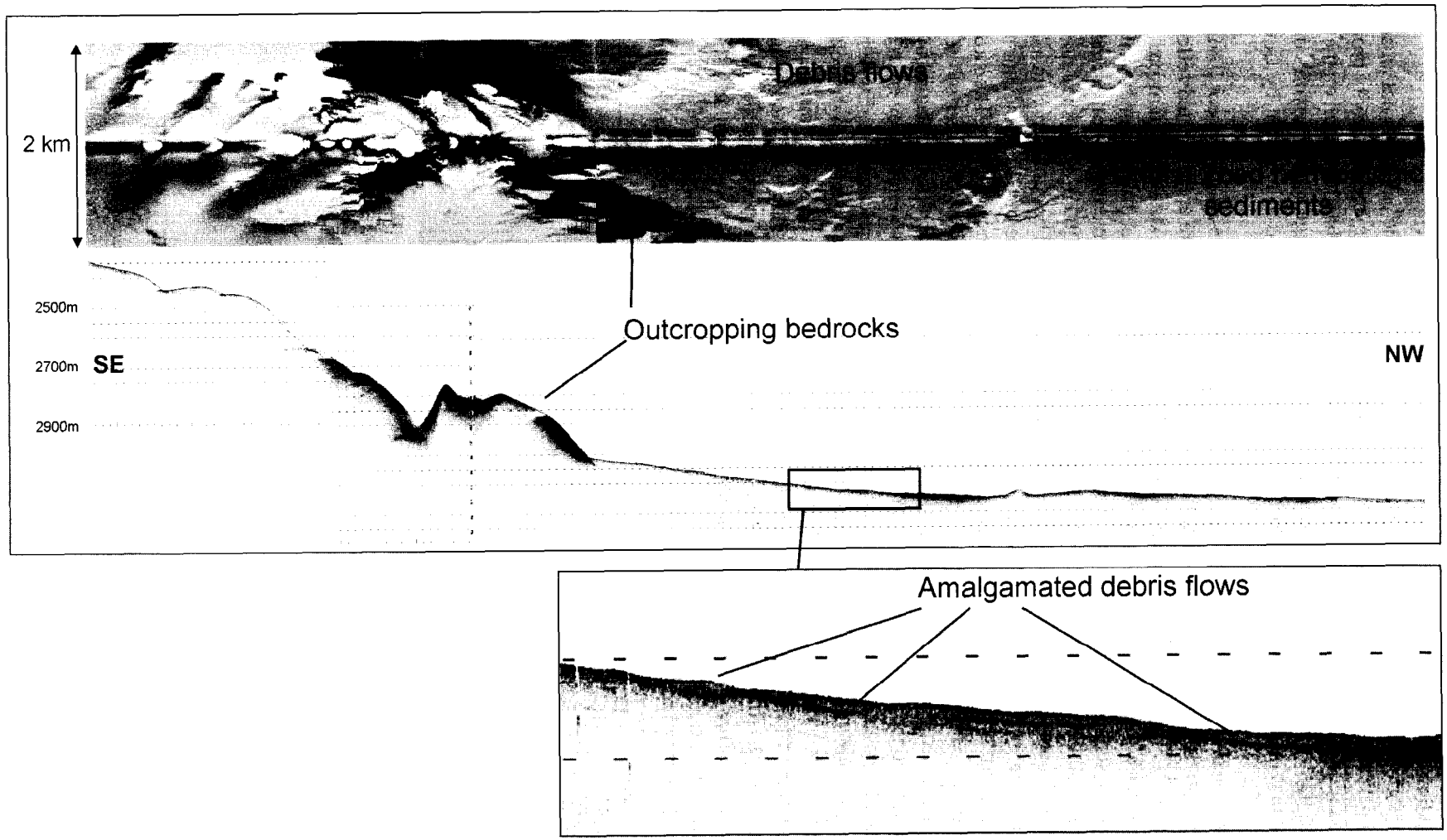

Figure 8. Fragment of ORAT-36 line showing high backscattering escarpment with debris flow deposits at the base. Blow up of the subbottom profiler shows details of the sedimentary section build up by amalgamated debris flows.

Summary

There are a number of features observed on the sidescan sonar records which are thought to be related to recent tectonic activity in the area. Major faults are expressed in the seabed topography as prominent escarpments. Lack of sedimentary cover on some of the escarpments and the existence of outcrops of older rocks suggest that there is some recent activity along these faults. Another indication of active tectonics in this area is the widespread occurrence of slope instability features on the local slopes. Earthquakes are considered good candidates for the triggering mechanism for shallow slides and local sediment failures within a relatively thin cover of unconsolidated sediments.

The different expression of major faults on the OKEAN record provides a clue to understanding the character of the tectonic activity along these structures. Thus, the MPF shows little evidence of recent activity and is being covered by sediments. Shallow slides found in the vicinity of the structure may, however, indicate occasional activity disturbing the overlying sedimentary cover. The 37°16'N-37°40'N fault appears to be much more active and as a result a prominent escarpment has been formed. The presence of numerous debris flows at the base of the escarpment and widespread traces of slope instability in the surroundings suggest that movements along the structure may occur frequently.

I.2.4. Bottom Sampling Results

Only one core was taken on the western Portuguese margin. The target was to sample a kind of plateau on the continental rise in order to characterise hemipelagic sedimentation in the area. Technical information about the core is summarized in Tables 1 and 2 (see also Annexe I for core log).

The coring site TTR10-AT225G was selected in order to determine the character of the sediments present where the hull-mounted pinger showed layered sequence. The core consisted of 248 cm of olive grey clayey sediments, mainly homogeneous and structureless, occasionally bioturbated, with silty admixture and some foraminifera. The recovery suggests high terrigenous clay supply to the area and a prevalence of hemipelagic clay settling over carbonate sedimentation.

Table 1. General information on the core from the Marques de Pombal Area.

Core No	Date	Time, GMT	Latitude	Longitude	Cable length, m	Depth, m	Recovery, cm
TTR-10-AT-225G	18.07.00	22:00	37°06.002' N	09° 28.051' W	990	1000	248

Table 2. Sedimentological, acoustic and geological characteristics of sampling stations. The Marques de Pombal Area

Core No	Geographical Setting	Sedimentary Summary	Instrumentation	Acoustic Characteristics
TTR-10-AT-225G	Portuguese margin, upper part of the plateau	Hemipelagic sediments	3,5 kHz profiler	Layered sequence on the subbottom profiler

I.2.5. Discussion and Main Conclusions

L. PINHEIRO, J-P. HENRIET, L. MATIAS, P. TERRINHA, J. MONTEIRO, M. IVANOV

Tsunamigenic Structures, Active Tectonics and Structural Interpretation

The integrated analysis of side-scan sonar images, 3.5 kHz profiler, and the TTR-10 single channel seismic lines have shown no scars of a huge land slide that might have been triggered by the

1755 earthquake. Thus, the tsunami observed after the earthquake must have a tectonic origin and computations made so far based on that assumption remain valid. A few landslides were neverthless identified on the southern border of the MPF, extending to the floor of the footwall plain. It remains to be confirmed if the core taken during the BIGSETS Urania cruise in 1998, when turbidites dated 300±100 y BP were sampled, lies within one of these land slides. This could date the event(s) and allow hydrodynamic modelling of its tsunamigenic contribution.

Several presently active tectonic structures were identified on the seismic profiles, displacing the seafloor and/or affecting the most recent post-Miocene sedimentary sequence. These active tectonic features have the same trend as the predominant NW-SE tardi-hercynian faults or the ESE-WNW Mesozoic structures and therefore correspond to a reactivation of these older structures. In several places normal faults appear to have been reactivated as thrust faults. Sometimes the structure is less developed and the reverse movement along the normal fault is the cause of folding of the shallower sediments. In other cases, when the fault plane is steep and under compression, this dip is increased and block rotation and folding of the shallower sediments is observed due to near vertical movement. With increased compressional deformation a new thrust fault, antithetic to the first, may be created; one such example can be seen on line PSAT-144 (see Fig. 4).

To the north of the MPF and offset 50 km to the west, a large N-S fault system (Fig. 5) with a total length of almost 90 km is observed offsetting a reference seismic reflector by 2.8 s TWT. This fault was imaged as a normal fault on the deep penetrating MCS profiles and no signs of recent activity could be seen. Prior to TTR-10 cruise this tectonic feature was a serious candidate for the northward continuation of the MPF. Both faults together have a total length of 150 km, compatible with the minimum fault length estimated for the source of the 1755 earthquake (Baptista et al., 1998). The new data acquired during TTR-10 cruise, namely the OKEAN and OREtech sidescan images, together with the BIGSETS multibeam coverage have shown that this steeply dipping fault is the most active feature in the studied area with strong carving of the fault scarp by erosional canyons. Since there is no evidence for a thrust fault plane dipping to the east, however, these results are interpreted as a reactivation of a Mesozoic growth fault by a vertical movement, indicating reactivation under compression. These results disqualify this fault system as the northward continuation of the MPF. The source for the 1755 earthquake must therefore be sought for elsewhere.

Based on the interpretation of all seismic lines available in the area, a structural map for offshore SW Portugal was prepared (Fig. 5), illustrating the main active/recent structures. Thanks to new data acquired during the TTR-10 cruise, the geodynamic framework of the area north of the MPF is now much better constrained. Several thrust faults, folds, flexures and vertically reactivated normal faults can be followed on several seismic lines but no continuous band of deformation can be followed in the whole area (Fig. 5); this implies that transfer faults must be active. Transfer faults are however much more difficult to detect on the seismic lines. Generally these are only inferred from discontinuities of reference seismic horizons. This is the case for some minor strike-slip faults but also the case for the large transfer fault south of MPF. These strike-slip faults trend ESE-WNW and their orientation is compatible with the inferred orientation of maximum compressive stress (Ribeiro et al., 1996) and also are compatible with the source mechanisms computed for earthquakes in the area. The MPF must also be limited to the north by a transfer fault that cannot be imaged properly in the whole northern flank. New data shows some indication of strike-slip movement to the east but this trend cannot be followed to the northern tip of MPF. This may be related to the fact the in the north the MPF terminates as a gentle half circle fold, and doesn't seem to abut against a tectonic feature.

Slope Failures and Slope-to-basin Sediment Pathways

Structural and morphological setting

The structural and morphological assessment of the first study area of Leg 1 of TTR-10 benefitted immensely from the outstanding quality of the multibeam coverage and seismic data sets

acquired in the area. The higher resolution of the seismic and acoustic imaging tools deployed in the framework of TTR-10 however has yielded the interpretation keys for identifying and understanding some intriguing morphological patterns and for translating them into a model of slope sediment pathways in this seismically very active margin zone.

The MPF zone and the northward relaying N-S basement fault, which were prime components of the Mesozoic North Atlantic extension, still form impressive escarpments on the Iberian continental slope. Structurally, they are truly major accidents, with vertical throws of about 1800 m (1.3 s TWT, MPF) and close to 4000 m (2.8 s TWT, the northern N-S basement fault). Within the recent compressional context, these faults have locally been driven into thrust or strike-slip movements.

The MPF has shaped a NNE trending, 50 km long escarpment of about 1600 m height, which is the western boundary of a large rectangular terrace, advancing some 30 km in the direction of Gorringe Bank. The top of this terrace dips oceanward from about 2000 to 2500 m depth, while the facing abyssal plain has a depth close to 4000 m. The back of this large terrace is deeply incised by the WSW trending S. Vicente canyon, which is the seat of significant present-day seismic activity. A relatively smaller but still intriguing terrace extends some 60 km further north, within approximately the same depth range as the southern platform. Its alongslope extent in a N-S direction amounts to some 20 km. The E-W axis of this high links in the upslope direction with the Infante Dom Henrique peak of the Montanhas dos Principes de Avis.

The TTR-10 seismic survey confirms the horst-type structure of this northern terrace. Its E-W trending boundary faults can be traced further into the margin, thus intersecting the major N-S basement fault. The PSAT 144 profile however verified that the north trending basement fault does not abut against the horst, but is crosscutting it. The exact spatial and temporal relationship between these complex intersecting fault sets and the resulting mosaic of faulted blocks can, with difficultly, be resolved in an unambiguous way with the present dataset, and should be the object of further research. The outline of the faults on the interpretation map (Fig. 5) should be regarded as preliminary.

Both terraces and the steep scarp of the N-S trending basement fault frame the Rincao do Lebre, a half-open, box-shaped basin which logically has trapped a thick sequence of (probably largely turbiditic) sediments deposited on the downthrown limb of the fault.

A most remarkable morphological feature protruding from the 1900 m high hanging wall is a hammer-shaped promontory, with an elevation of 800 m above the facing abyssal plain. This promontory and its upslope extension, located straight west of the Estevao Gomes high from the Montanhas dos Descobridores, segments the slope into two large, individual drainage basins. For further convenience in this text, we shall refer to these basins informally with the names of the peaks adjacent to the highest reaches of the drainage valleys, the Infante Dom Henrique basin in the north and the Estevao Gomes basin south of the "hammer" promontory.

Seismotectonic setting

Remarkably, the MPF area and the Rincao do Lebre show up as "gaps" on maps of recent earthquake epicentres, but the close proximity of a major elongated, NNW trending cluster of epicentres following the axis of the S. Vicente canyon , probably accounts for the promotion of the slope sediments into failure and gravitational mass movements. Three fault plane solutions of earthquake foci located under the Infante D. Henrique peak and the Montanhas dos Descobridores (see Fig. 1 for location) argue for WNW trending dextral strike-slip movements (or for NNE trending sinistral displacements), while the southern edge of the Rincao do Lebre has been the seat of two recent thrust fault movements, respectively in E-W and SSW-NNE directions.

Sediment pathways in the Infante Don Henrique slope basin

The most intriguing morphological feature which showed up on the BIGSETS multibeam backscatter image was a set of parallel, narrow and long sigmoidal ridges, an unconventional fishbone

with a southward vergence of the western, downslope limbs and a northward vergence of the upslope limbs. Initially, some considerations could support a structural origin, linked e.g. to the deformation of a ductile sedimentary cover over a strike-slip basement fault. Although a certain degree of structural control of the upslope valley orientations cannot be ruled out, it has been demonstrated by the interpretation of the TTR high-resolution seismic data, supported by the analysis of the sidescan sonar images, that those ridges are pure depositional features: they are levee-type deposits flanking the main transit channels which funnel and convey the slope sediments from the upper slope realms to the abyssal plain.

Up to 21 ridges have been identified on the slopes of the Rincao do Lebre on base of the seismic data supported by the multibeam bathymetry, and only very minor one on the MPF. The striking morphodynamic contrast between the slopes of the Rincao do Lebre and MPF, the latter barely affected by two singular slope failures, will be discussed later.

Within the confines of the Dom Henrique slope basin, three major ridges flank and delineate the steep valleys which drain the higher reaches of the Infante Dom Henrique peak. The arcuate shape of their lower extension at the foot of the slope and upon the abyssal plain is strikingly imaged by the shaded multibeam bathymetric model, while the associated distal, still coarse-grained channel deposits show up as long, high-backscatter streaks on the OKEAN 136. The longest ridge is more than 20 km long.

The seismic sections bear witness to a gradual buildup of these levees in a regime of episodic and probably frequent discharges. One of the ridges for instance, which has a length of some 12 km, displays on profile PSAT 136 (Fig. 4) a gradual buildup of 300 m (350 ms TWT) above a smoothly dipping basal plane. It has an elevation of some 40 - 50 m (50 - 60 ms TWT) above the present adjacent valley floor. The buried valley deposits are characterized by irregular and sometimes chaotic high amplitude reflectors (HAR).

The exceptional length and thickness of the three major ridges described above no doubt reflect the size of the drainage basins and the exceptional height of the slope which feeds the gravity flows. In contrast to "normal" situations where gravity flows in canyons or slope channels result in diverging distal depositional patterns, building wide spreads of fan lobes in an "open" abyssal plain, the main Infante Dom Henrique channels are forced to converge when reaching the abyssal plain. Their sediment load is funneled into a confined basin corner, which leads to build-up of the levees separating the three main channels.

South of the main levees, only short ridges are observed, remarkably on the steepest, lower part of the slope. The associated channels discharge coarse-grained sediment into elongated lobes, 1-3 km long, which are easily traced along the foot of the scarp by their high backscatter, both on the multibeam images and on the OKEAN record PSAT 136. One small ridge (PSAT 136) is observed on the northern edge of the "hammer" shaped promontory.

Sediment pathways in the Estevao Gomes slope basin

The Estevao Gomes slope basin takes a hinge position between the Infante Dom Henrique basin and the MPF escarpment. Just like in the Infante Dom Henrique basin, it is the fault-controlled northeastern corner that hosts the major valley. The upper reaches of this valley on the steep northern flank of the Estevao Gomes high are affected by an important slide, beautifully imaged by the ORAT 36 line (Fig. 8).

Four elongated ridges have been observed on the upper valley slopes, one of them displaying a length of 20 km, between 1400 m and 3200 m depth. Two shorter ridges frame the bowl-shaped lower valley, where again the coarse-grained channel fills show up as elongated high-backscatter streaks on the OKEAN records. Four more ridges can be identified on the southern flank of the basin.

Sediment pathways on the Marques de Pombal slope.

In contrast to the eastern slope of the Rincao do Lebre, the Marques de Pombal slope is virtually unaffected by channels and - with one minor exception - displays neither levee-like ridges nor narrow downslope high-backscatter streaks, so frequently observed in the northern basins. Downslope sediment transport has here a totally different aspect, in the form of only a few slides and wide tongues of debris flows. Three slides seem to originate at about 2500 m depth on the SW flank of the Marques de Pombal promontory. Two of them give rise to large avalanche flows, 15 and 25 km long and up to 2 km wide, and well visible on PSAT 135 (Fig. 3).

The depocentres in the abyssal plain.

The joint interpretation of the BIGSETS and TTR-10 seismic lines allows assessment of the size and extent of the depocentres of probably mainly turbiditic sediments, accumulated through slope processes in the Rincao do Lebre and in front of the Marques de Pombal slope. The continuity between the slope sequences of the Infante Dom Henrique basin observed on PSAT 136 (Fig. 3) and a spatially confined upper sequence of basin deposits, clearly onlapping on a regional unconformity, provides the key to a full analysis of downslope sediment transport on this margin, from source to sink.

The isochrons of the considered basin sequence (in ms, which with a velocity hypothesis of 2000 m/s can be read in terms of m) show a major depocentre of 1000 ms in front of the Rincao do Lebre slopes. A much more modest depocentre of some 700 ms is locked between the Marques de Pombal slope and the western slope of Gorringe Bank. It may have been fed partly from the latter high.

Conclusions

The downslope sediment transport on the eastern slopes of the Rincao do Lebre and off the Marques de Pombal escarpment shows a striking contrast.

The northern basement fault bordering the Rincao do Lebre seems to be the source of a quasi continuous or short-period episodic process of slope erosion and downslope transport through long valleys flanked by narrow, levee-like depositional ridges. The lower reaches feature elongated streaks of coarse-grained deposits. Slope failures and avalanching appear to be confined to the very upper reaches of the main valleys, where the morphology is strongly structurally controlled. The probably mainly turbiditic deposits in the proximal zone of the abyssal plain reach a thickness of about 1000 m at the foot of the fault.

Such a channelled transport mode, with associated levee-type deposits seems to be virtually absent on the Marques de Pombal slope. Only three (apparently recent) slides, with relatively wide debris flows, provide some clue towards downslope processes in this margin sector. This is a surprising observation, considering the very close proximity of an important seismogenic zone in the S. Vicente canyon. The seismic profiles provide little evidence of slope disturbance in a more distant past (but still recent in geological terms).

The identification of the full downslope sediment pathway - from source to sink - paves the way for mass balance analysis and - through targeted (long) coring - for translating the sedimentary record locked in both the levees and the deeper turbitic depocentre into a high-resolution record of the tectonic activity of this major seismogenic zone.

Open questions and future lines of investigation

A detailed description of the tectonic structure that may be the origin of the 1755 Lisbon earthquake remains to be done. The largest fault north of the MPF cannot be associated with it at depth because data shows that it has been reactivated essentially with vertical movements along a Mesozoic normal fault dipping to the west and not to the east like the Marques de Pombal thrust.

If the MPF is bounded to the north by a major left-lateral transform fault trending ESE-WNW, then at depth the MPF may be linked to a set of WSW-ENE thrust faults with large dip and a length smaller than 50 km. Taken together the shortening along a NW-SE direction is accommodated by the MPF and these smaller faults. Each segment is most active where the others are attenuating or absent. To generate the 1755 earthquake all these segments should merge at depth along a major detachment that would allow them to move co-seismically during an extreme earthquake like the 1755 event. If this is true then future work should by applied to the detection of this transfer zone and to the imaging of the deep crustal detachment. It is therefore necessary to complement the multibeam coverage of BIGSETS, acquire additional deep penetrating seismic profiles and also use OBS's to obtain a detailed velocity image of the crust through refraction and wide-angle reflection modelling. An open question still remains: why is the MPF near N-S when the associated fault ruptures trend WSW-ENE

To the south of MPF a transfer fault is clearly seen on MCS profiles but no high resolution seismics exist. In this area, west of the MPF we reach the greatly deformed Gorringe Bank area where a number of huge faults are identified, but the dating of the compressional event that originated them is still controversial. East and south of the MPF a large thrust fault is observed that is offset by the transfer fault. North of this transfer fault recent movements are very small or absent, but to the south its expression is similar to the MPF. On the sparse network of available MCS lines this feature can be followed in the NE-SW direction for more than 150 km, into the Horseshoe Abyssal Plain. This fault offsets the seafloor and coincides with a major geomorphological feature appearing on public domain bathymetry maps. This is the most serious candidate for the continuation of the MPF to the south. However their differing orientations must be explained taking into consideration the Gorringe Bank influence. Future work needs to be done to detect this transfer zone, obtain a detailed image of the fault and to define the deep crustal detachment linking both tectonic features.

I.3. ALGARVE MARGIN AND GULF OF CADIZ

L. PINHEIRO, M. IVANOV AND L. SOMOZA

I.3.1. Introduction and Geological Setting

The Gulf of Cadiz is an area of active tectonics related to the NW directed convergence between the Africa and the Eurasia plates. During the TTR-9 cruise (Kenyon et al., 2000) several mud volcanoes were discovered and investigated in this area, based on high quality sidescan sonar images and multibeam bathymetry brought to the cruise by Joan Gardner from the Naval Research Laboratory (NRL), Washington, USA. These were collected during a survey conducted in the Gulf of Cadiz and the Moroccan Margin in 1992 by the Marine Physics Branch of the NRL, in cooperation with the Hawaii Mapping Group (HMRG) and the Naval Oceanographic Office (NAVOCEANO).

For the planning of the TTR-10 cruise, a further sidescan mosaic and multibeam bathymetry from the S. Portuguese margin was provided by Joan Gardner.

Three regions of mud volcanism have been investigated and they will be referred to as the South Portuguese Field (SPF), the Moroccan Field (WMF) and the Spanish TASYO field (SF).

The work in this area was split into two parts: the second part of Leg1 (Tenerife - Cadiz) and the first part of Leg 2 (Cadiz - Ponta Delgada, Azores).

I.3.2. Seismic and Acoustic Data

I.3.2.1. Seismic Data Acquisition and Processing

Single channel seismic reflection profiles were acquired throughout the first Leg of the TTR-10 cruise. The same configuration as in the Marques de Pombal area was used.

The location of the seismic and sidescan sonar lines were based on the SeaMap sidescan mosaic where several structures (S1-S9) were identified as possible mud volcanoes.

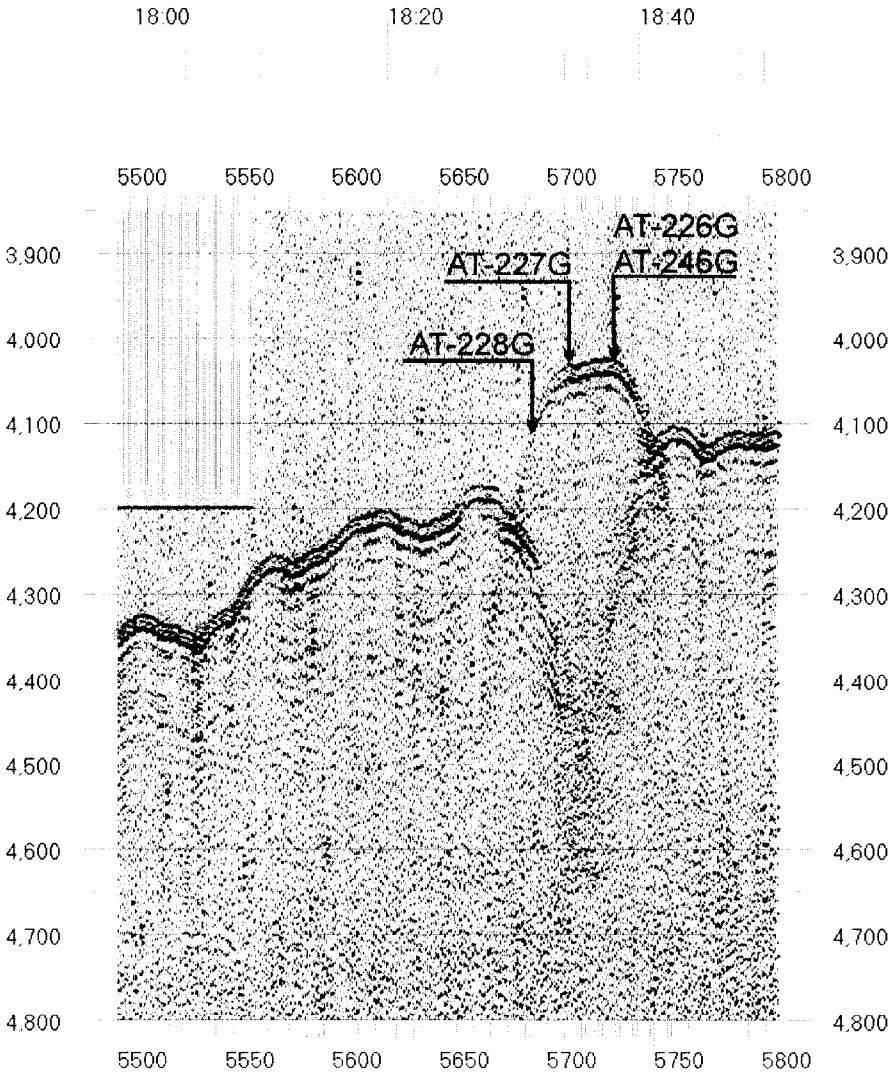

Figure 9. Southern end of the seismic profile PSAT-146, showing the Bonjardim mud volcano.

I.3.2.2. Seismic Data Interpretation

L. M. PINHEIRO, M. IVANOV, A. VOLKONSKAYA, J. H. MONTEIRO, P. TERRINHA, L. MATIAS

On the transit from the Marques de Pombal area to the S. Iberia margin a high quality seismic profile (PSAT-146) showed a target structure that looked like a mud volcano (Fig. 9). One reflector, visible at approximately 100 ms below the seafloor, was interpreted as a bubble effect of the airguns rather than a BSR (Bottom Simulating Reflector).

Along Lines PSAT-147/148 two other interesting structures were surveyed (Fig. 10) and a core was taken at the S3 structure. The marls and pelagic sediments recovered did not confirm it as a mud volcano. Future work in this area is required.

Line PSAT-149 crossed two (S4 and S5, in Fig. 11) of a group of three interesting features identified on the sidescan mosaic. The seismic profile did not confirm them as likely mud volcanoes and they were therefore not investigated further.

Line 150 crossed the structure S6, which did not look like a mud volcano.

Line PSAT-151 crossed two other promising structures: S7 and S8 (Fig. 12). S8 was cored and proved to be a mud volcano named the Jesus Baraza mud volcano.

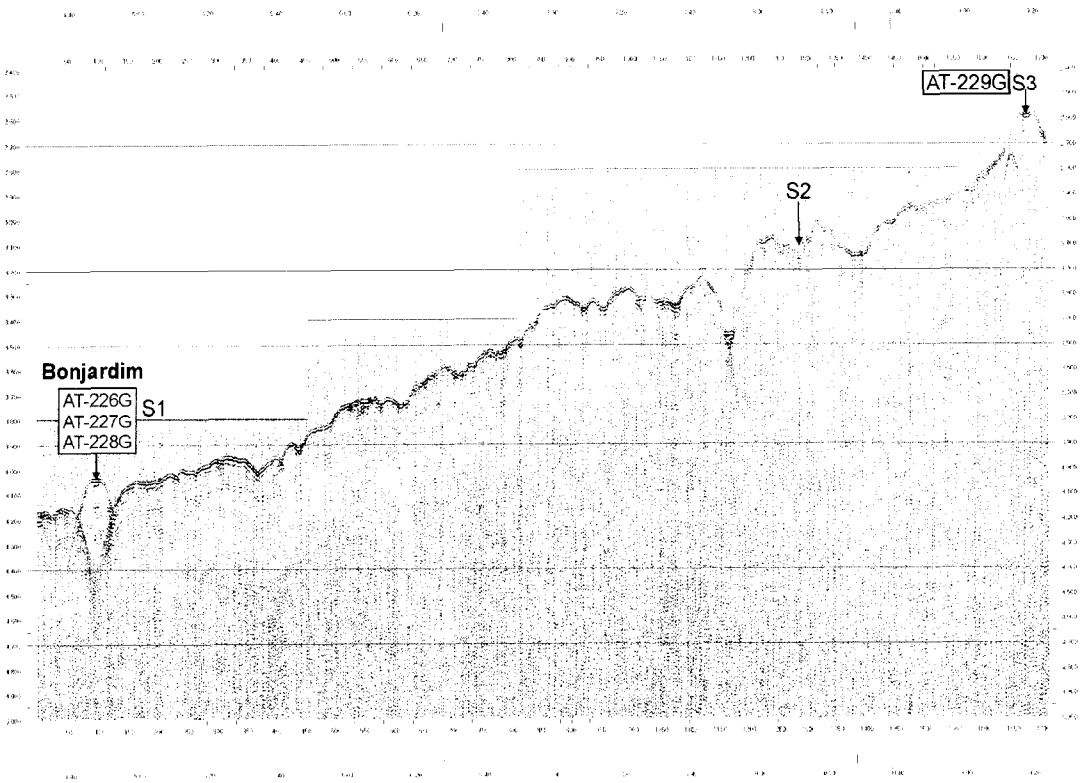

Figure 10. Seismic profiles PSAT-147/148, showing the image of structure S2 and S3. A core was taken at the structure S3 (AT-229G).

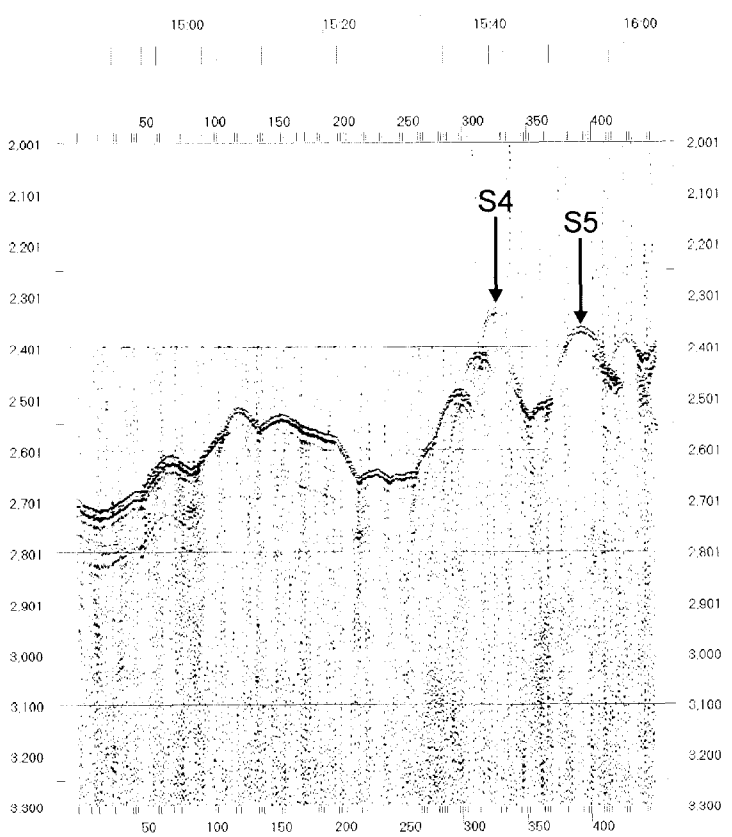

Figure 11. Seismic profile Line PSAT-149 crossing two (S4 and S5) of a group of three potential mud volcanoes, seen on the sidescan mosaic.

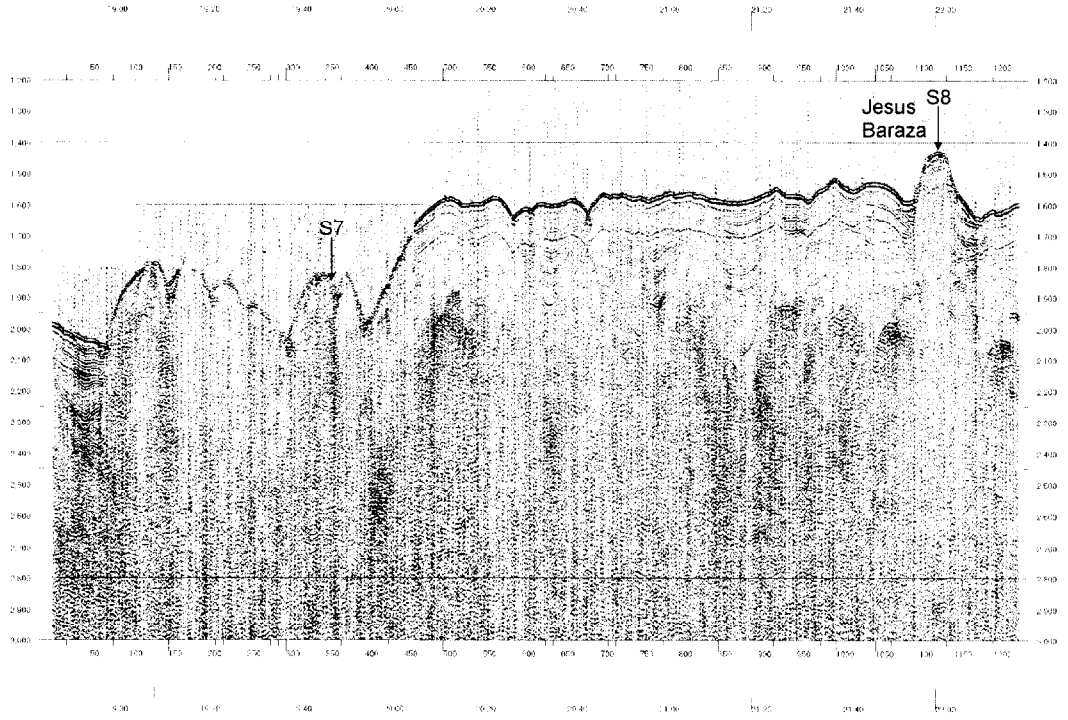

Figure 12. Seismic profile PSAT-151, showing the structures S7 and S8 (Jesus Baraza mud volcano) identified on the NRL sidescan mosaic.Two cores were taken at the Jesus Baraza mud volcano (AT-230G and AT-231G).

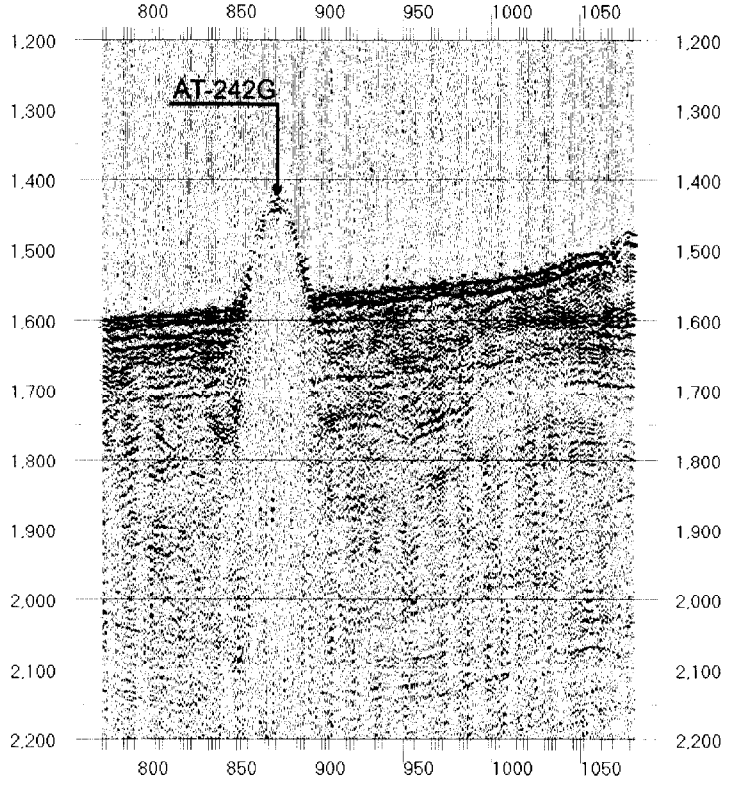

Figure 13. Seismic profile PSAT-152, showing the TASYO mud volcano.

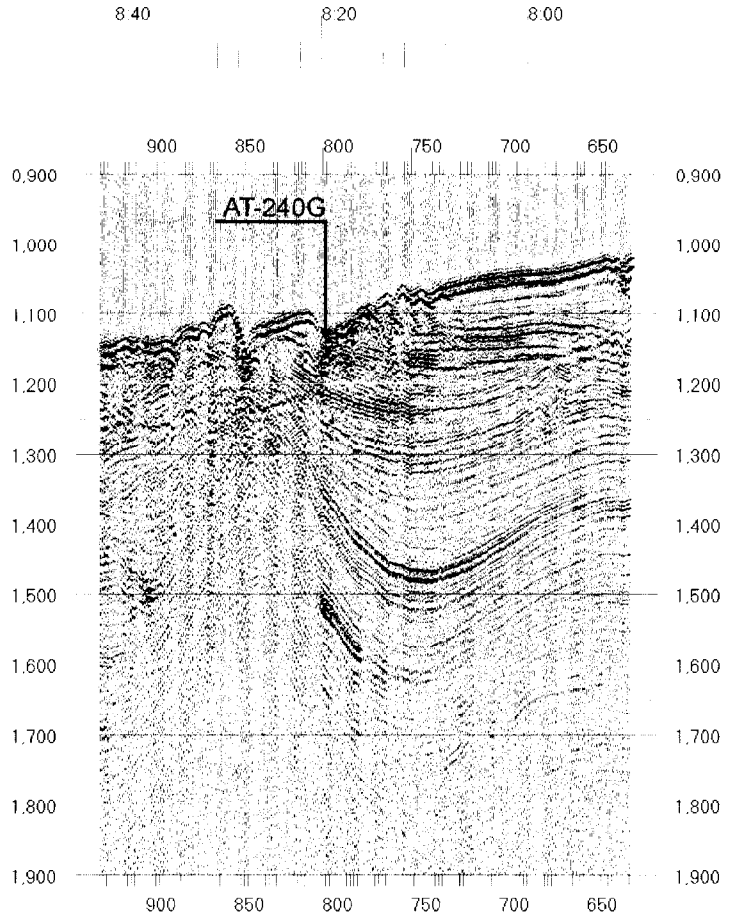

Figure 14. Seismic profile PSAT-156, showing a contourite channel with levees.

Only 3.5 kHz profiles were taken between the Jesus Baraza mud volcano and line PSAT 152. PSAT 152 crossed the Student mud volcano and the TASYO mud volcano (Fig. 13).

Seismic profile PSAT-156 (Fig. 14) shows a zone of seabed erosion with a channel-like feature.

I.3.2.3. Sidescan Sonar Data (OKEAN and OREtech)

A. AKHMETZHANOV, J.-P. HENRIET, J. MONTEIRO, M. ROVERE

An extensive acoustic data set has been acquired on the Iberian margin and Gulf of Cadiz. This set comprises about 950 km of seismic profiles accompanied by simultaneous acquisition of 10 kHz long-range OKEAN and hull-mounted 3.5 kHz profiler data.

The survey was run in the eastern Gulf of the Cadiz aimed to detect potential mud volcanic structures, which were expected here by Spanish researchers on the basis of high resolution seismic data (L. Somoza, pers. comm.). The area is located north of the mud volcanic provinces discovered during TTR-9 cruise on the Moroccan margin (Kenyon et al., 2000). A grid of survey lines (PSAT-152 to PSAT-157) enabled about 700 km^2 of OKEAN images to be aquired (Fig. 15).

North of 35°50' the imagery shows a very complicated acoustic pattern resulting mainly from complex bottom topography due to the presence of sand dunes, mud waves, diapiric ridges and incised channels cut by Mediterranean Outflow Water (Kenyon and Belderson, 1973; Nelson et al., 1993). Channels are characterised by slightly higher uniform backscatter. A 3.5 kHz profiler shows most of the area has a wavy character with deeply incised narrow channels. In places where channels become broader the seabed is normally flatter and has a strong acoustic return or shows the presence of strati-

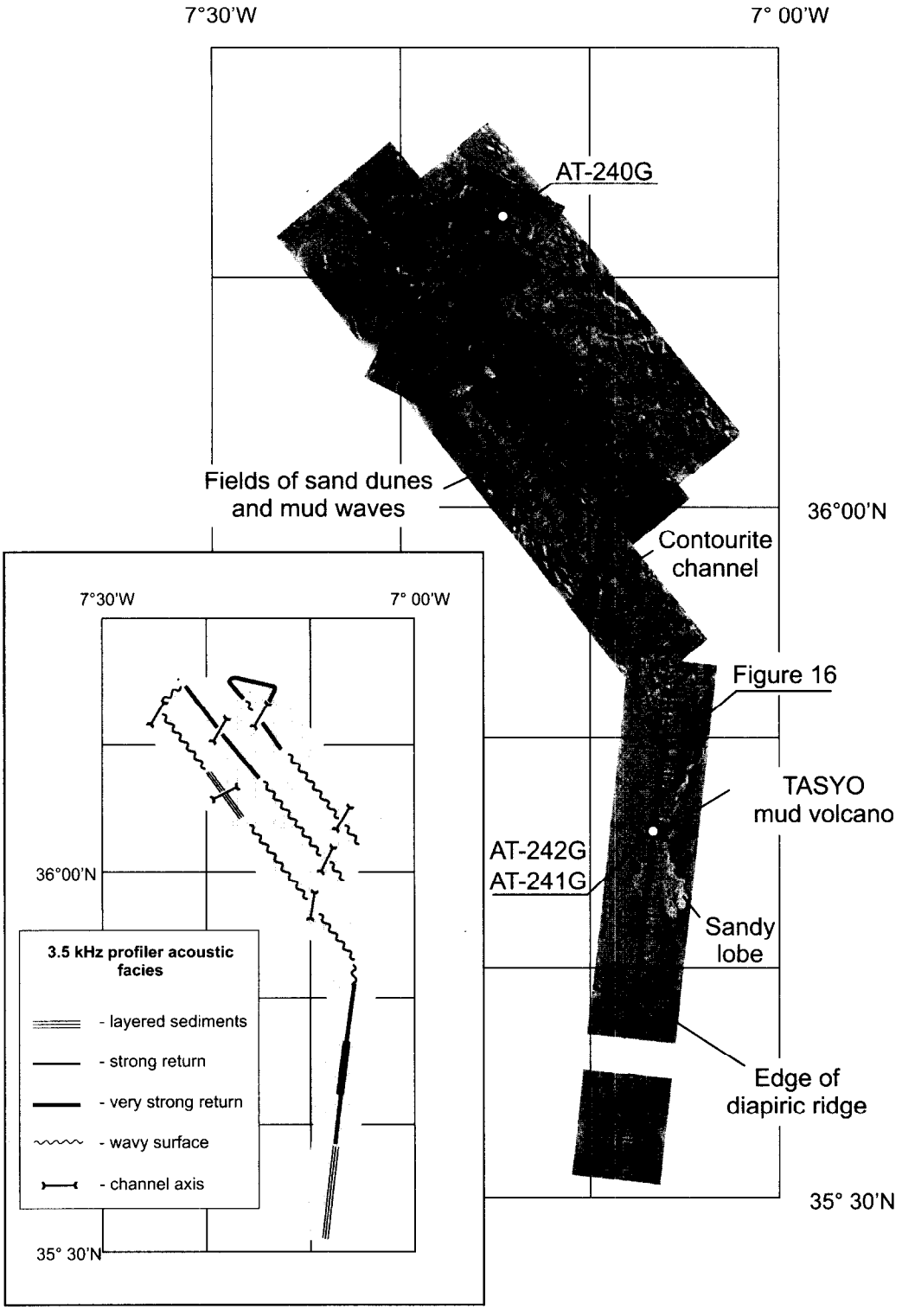

Figure 15. OKEAN mosaic from the Gulf of Cadiz area and types of echoes observed on the 3.5 kHz records.

fied sediments. South of 36°50' the seabed is more uniform and characterised by moderate backscatter. A prominent lobe of low backscatter is observed on the line PSAT- 152 representing an area of deposition of fine-medium grained, well-sorted sand at the mouth of a down-slope running contourite channel (N. Kenyon, pers. comm.). The 3.5 kHz data shows relatively smooth seafloor with a thin sed-

imentary lens underneath. It has a strong acoustic return and a slight elevation is seen over the lobe and the return becomes stronger (Fig. 16). This pattern is believed to be caused by the presence of sandy deposits filling up a local depression fed by a contourite channel. This is supported by seismic data (PSAT-152) showing a local sedimentary basin with a sequence about 700 ms thick. The basin is bounded by a diapiric ridge to the south and by a sediment drift to the north. The ridge is about 175 m high and is well expressed in the seabed topography and is also recognised on the OKEAN image as a linear high backscattering feature. The sandy lobe appears to be a recent feature formed by spasmodic discharges of well-sorted material from the channel.

No obvious mud volcanic structures were observed on the OKEAN data. The only mud volcano found in the area was located within the sandy lobe and is not well seen on the sonograph as the ship's track runs directly over the structure. It is best recognised on the 3.5 kHz record (Fig. 16) where there is a prominent conical hill up to 120 m high.

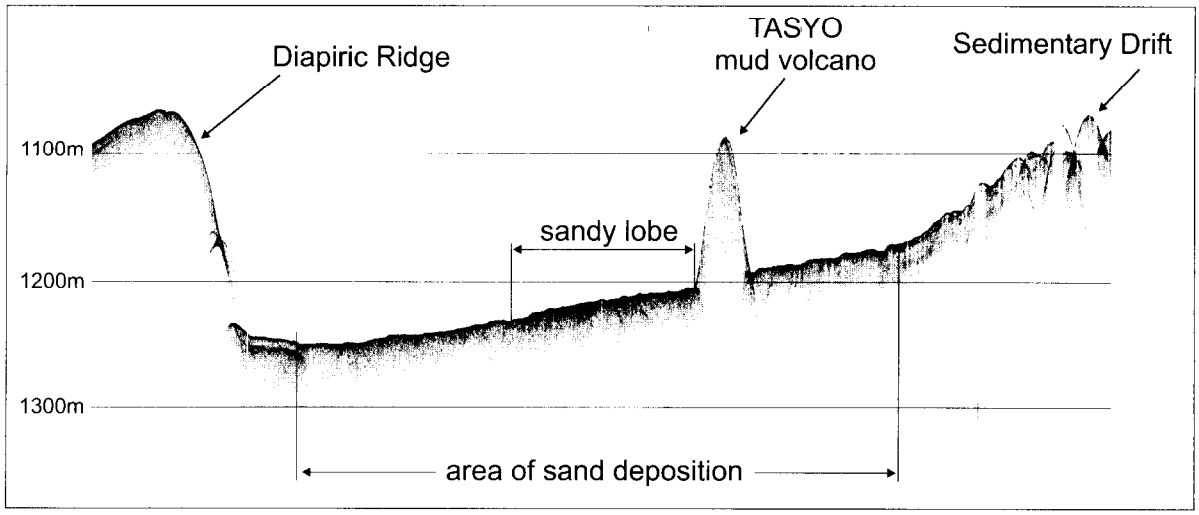

Figure 16. Fragment of PSAT-152 3.5 kHz record showing TASYO mud volcano and an area of sand deposition fed by a contourite channel.

I.3.3. Bottom Sampling Results

G. Akhmanov, M. Ivanov, A. Stadnitskaya, I. Belenkaya, D. Ovsyannikov, M. da Cunha, E. Kozlova, V. Blinova, A. Stepanov, I. Pasechnik, C. Lopes and N. Hamoumi

The TTR programme began working in the Gulf of Cadiz in 1999 when a number of inferred mud volcanoes were confirmed by bottom sampling for the first time on the Moroccan and Spanish margin of the Gulf of Cadiz and mud volcanic deposits were recovered (Kenyon et al., 2000). Bottom sampling on the South Portuguese margin and further investigation of the mud volcanic provinces discovered in 1999 were the main aims of the second part of first leg and the first part of the second leg of the TTR-10 cruise.

Several assumed mud volcanic edifices were to be checked out by bottom sampling, based on Seamap mosaic provided by US Naval Research Laboratory (courtesy Joan Gardner). They were well expressed in the seafloor topography and characterised by particular reflectivity patterns. In addition, a number of seismic and 3.5 kHz profiler lines and a mosaic of the OKEAN long range sidescan sonar images, obtained during the TTR-9 cruise on the Moroccan margin, provided a precise position for most sites (Kenyon et al., 2000). A new area of assumed mud volcanic activity (the TASYO mud volcanic field) on the Spanish margin of the Gulf of Cadiz was proposed for bottom sampling by Luis Somoza, based on results of a previous survey made in 1999 by the Spanish Geological Survey. During the cruise new surveys with air gun seismic and OKEAN sidescan sonar systems, as well as 3.5 kHz profiler were carried out in all areas chosen for bottom sampling.

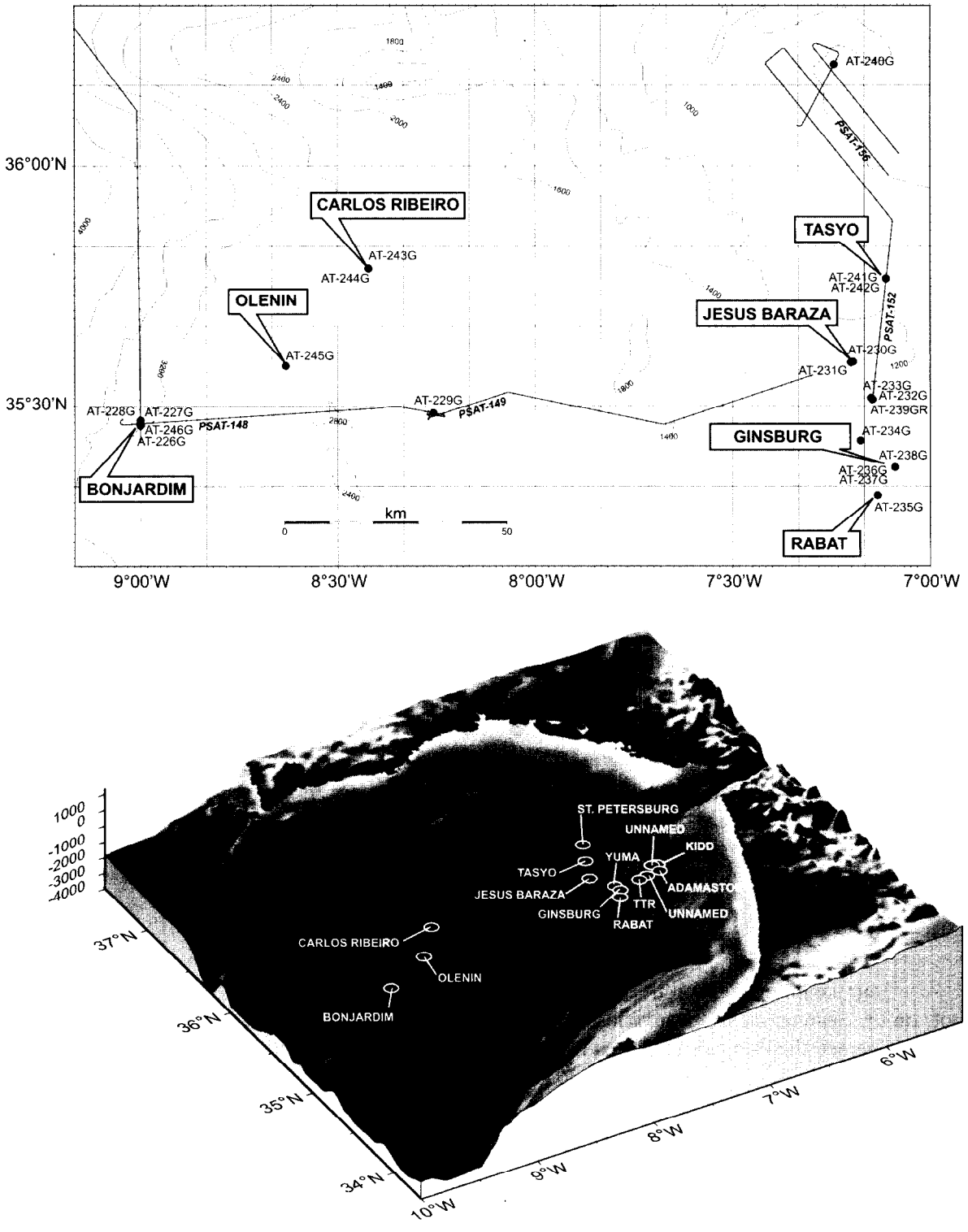

Figure 17. General map of the study area with the locations of the cores and the mud volcanoes sampled.

Table 3. General information on the cores from the Gulf of Cadiz.

Core No	Date	Time, GMT	Latitude	Longitude	Cable length, m	Depth, m	Recovery, cm
AT-226G	20.07.00	21:59	35°27.603' N	09° 00.023' W	3059	3059	151
AT-227G	21.07.00	00:01	35°27.851' N	09° 00.028' W	3066	3060	234
AT-228G	21.07.00	02:55	35°28.234' N	09° 00.030' W	3170	3150	283
AT-229G	21.07.00	11:19	35°29.129' N	08° 15.442' W	1960	1962	276
AT-230G	21.07.00	23:56	35°35.539' N	07° 11.693' W	1175	1159	211
AT-231G	22.07.00	00:58	35°35.452' N	07° 12.048' W	1090	1091	125
AT-232G	22.07.00	03:32	35°30.849' N	07° 08.744' W	940	940	CC
AT-233G	22.07.00	04:38	35°31.068' N	07° 08.964' W	948	955	36
AT-234G	22.07.00	06:57	35°25.724' N	07° 10.556' W	1140	1140	241
AT-235G	22.07.00	10:19	35°18.858' N	07° 07.997' W	1050	1060	288.5
AT-236G	22.07.00	12:03	35°22.409' N	07°05.328' W	910	910	159
AT-237G	22.07.00	12:46	35°22.410' N	07° 05.343' W	910	910	145
AT-238G	22.07.00	13:25	35°22.409' N	07° 05.330' W	910	910	182
AT-239GR	22.07.00	15:46 16:32	35°30.854' N 35°30.853' N	07° 08.749' W 07° 08.816' W	956 961	955	
AT-240G	23.07.00	12:58	36°12.624' N	07° 14.540' W	845	845	337
AT-241G	26.07.00	03:08	35°45.967' N	07° 06.720' W	1105	1100	150
AT-242G	26.07.00	04:15	35°45.962' N	07° 06.684' W	1105	1098	134
AT-243G	26.07.00	13:59	35°47.217' N	08° 25.313' W	2200	2200	136
AT-244G	26.07.00	15:28	35°47.221' N	08° 25.333' W	2200	2200	163
AT-245G	26.07.00	19:55	35°35.007' N	08° 37.901' W	2604	2614	287
AT-246G	27.07.00	00:11	35°27.610' N	09° 00.030' W	3064	3060	184

A total of 21 sites (Fig. 17), 20 by gravity corer (total recovery 36.87 m) and one by TV-controlled grab system were sampled. The main sampling site parameters and sedimentological, acoustic and relevant information are summarized in Table 3.

Core logs are given in the Annex I. The discussion of the bottom sampling results is divided into the Portuguese margin, the Moroccan margin and the Spanish margin of the Gulf of Cadiz.

Portuguese margin

Four sampling sites on the Portuguese margin and expressed as high reflectivity subcircular spots on the Seamap mosaic were chosen. Three of them were confirmed as new mud volcanic structures and named the Bonjardim, Carlos Ribeiro and Olenin mud volcanoes.

Bonjardim mud volcano

Core TTR-10-AT226G

The top of Bonjardim mud volcano was sampled (Fig. 18). The recovery consists of 151 cm of mud breccia, matrix supported with angular and subangular clasts of different size (from millimetric to 3 cm) and lithology, mainly represented by brownish grey mudstone. Lack of a pelagic veneer and only a few uppermost cm of oxidized mud volcanic deposits suggest that the mud volcano is active.

Different layers of mud breccia were observed with a paler and water saturated type alternating with darker and more consolidated mud breccia. This could indicate different flows and stages of activity of the volcano. A strong smell of H_2S was detected.

Core TTR-10-AT227G

A terrace just below the top of the Bonjardim mud volcano was sampled. The mud breccia recovered was very similar to the one previously sampled (although it was quite homogeous through the whole core) but the top 42 cm comprise brown marl, soupy for the first 6 cm and then bioturbated and rich in foraminifera. A strong smell of H_2S and a *Pogonophora* layer observed at the very top of the core, indicate active fluid venting.

Core TTR-10-AT228G

The flank of the mud volcano was sampled in order to define the extension of the mud flows. The recovery consisted of 283 cm thick intercalation of olive brown pelagic marl and brown marly turbitites enriched in foraminifera, the latter easily distinguishable due to the sharp boundaries and the coarser texture. The turbitides redeposit pelagic material within the basin (in this case from the upper slope of mud volcanic edifice to the lower part and foot of the slope) and might be related to uplift or collapse of the mud volcanic structure. Bioturbation activity is very strong throughout the whole core. No mud breccia was recovered, suggesting a long period of non-deposition of mud breccia on this part of the mud volcano.

Core TTR-10-AT246G

An attempt was made to sample the top of the Bonjardim mud volcano and to recover gas hydrates for further analysis. The recovery was comparable with the station TTR-10-AT226G, with a 12 cm layer of more soupy and oxidized mud breccia on the top. There is the usual structureless mud

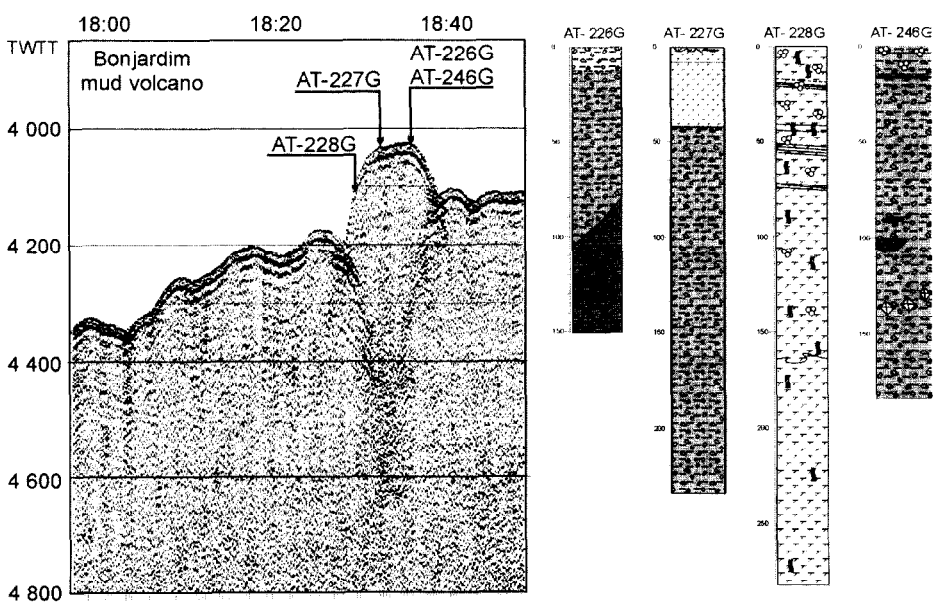

Figure 18. Location of the sampling stations AT-226G, AT-227G, AT-228G and AT-246G along seismic line PSAT-146. Core logs are shown.

breccia with angular and subangular clasts of different size and lithology. Between 135-156 cm darker mud breccia was observed, indicating a different stage of activity of the mud volcano. Gas hydrates were sampled below 156 cm. A strong smell of H_2S was detected.

Carlos Ribeiro mud volcano

Cores TTR-10-AT243G and TTR-10-AT244G

The Carlos Ribeiro mud volcanic structure, expressed as a high reflectivity subcircular spot on the Seamap mosaic was sampled with two cores. Both had a very similar succession of grey structureless very poorly sorted mud breccia, slightly oxidized and bioturbated at the very top. The clasts were subangular and angular rock fragments of different lithologies and shapes. Clast sizes sometimes reached 15 cm. A fragment of semi-consolidated claystone with thin bituminous film at the surface was the most impressive in core TTR10-AT243G. A strong smell of H_2S throughout the cores and lack of pelagic veneer at the top of both successions confirmed the recent activity of the mud volcano.

Olenin mud volcano

Core TTR-10-AT245G

The core was taken from a dome-like structure with high reflectivity on the Seamap mosaic. 287 cm of recovery was represented mainly by pelagic yellowish brown and olive grey marl with olive brown and grey clay. The sediments were bioturbated and contained a silty and foraminiferal admixture. Several oxidized layers were observed throughout the core and traces of reduction front were described for the lowermost part of the succession, suggesting possible fluid venting at the site. Between 60-65 cm and 210-215 cm the core consisted of two thin layers of mud volcanic deposits. Both were characterised by sharp irregular contacts and contained millimetric to centimetric subangular clasts of different lithologies in a silty clayey matrix.

Although the presence of mud volcanic deposits confirmed the discovery of a new mud volcano, the site is worth further sampling and investigation.

Dome-like structure

Core TTR-10-AT-229G (Fig. 10)

This core was taken in order to determine the characteristics of the sediments of a dome-shaped structure on the Portuguese margin observed on the OKEAN sidescan sonar records and on the seismic profile (Fig. 11). The recovery was a hemipelagic succession of alternating light olive brown, marl, rich in foraminifera and more greyish marl. Both were intesively bioturbated. The succession contained a number of thin, reddish brown oxidized layers with high foraminiferal content and sharp planar boundaries, indicating interbasinal turbidite activity. This activity might reflect recent dome growth.

Although no mud breccia was recovered from this site, a mud volcanic origin of the dome-like structure cannot be excluded.

Moroccan margin

Five sites were chosen for bottom sampling on the Moroccan margin of the Gulf of Cadiz (Fig. 1). Two of them were confirmed to be new mud volcanic structures and named as the Jesus Baraza and Rabat mud volcanoes. One site was sampled with three coring stations from the previously known Ginsburg mud volcano. The other stations were taken from high reflectivity spots on the Seamap and OKEAN sonar mosaic.

Jesus Baraza mud volcano

Core TTR-10-AT231G

This core sampled the top of the mud volcano. The first 4 cm consisted of light brown soupy and water saturated marl very rich in foraminifera and with a few *Pogonophora* within the interval. The rest of the core was divided in two main units. The first one (4-27 cm) showed structureless, water saturated brownish mud breccia with clayey matrix and numerous clasts of different colour, roundness and lithology. The oxidation of this interval and the bioturbation with burrows, filled with sediment from the upper marl layer, might indicate that the mud volcano had not been active in recent times. The second unit (27-1254 cm) presented the same mud breccia found above but more consolidated and without oxidation and bioturbation. Strong smell of H_2S was detected. Mud breccia unit was relatively well stratified with several intervals representing different mud flows.

Core TTR-10-AT-230G

The flank of the Jesus Baraza mud volcano was sampled. An hemipelagic marly succession was recovered with bioturbation and foraminifera distributed throughout the whole core. The usual few centimeters of soupy brownish marl were found at the top. Downcore the sediment became more consolidated. Slump structures are visible below 120 cm where darker layers and burrows are tilted and bent in oblique orientation. No mud breccia was recovered. This indicates that hemipelagic and slump deposition was prevalent on this slope for a relatively long period, while mud breccia flows were reaching other sides of the mud volcanic edifice.

Rabat mud volcano

Core TTR-10-AT235G

A single attempt to sample the top of the Rabat mud volcano was made. 288.5 cm of sediment were recovered. The first 19 cm consisted of yellowish brown marl, intensively bioturbated and water saturated for the first 6 cm. Foraminifera and shell-coral debris was also found throughout the interval. From 19 to 129 cm the core showed the same marl but with a greyish colour becoming darker towards the bottom. Coral debris were present throughout whole interval. Bioturbation was extremely intense, with large burrows filled with soupy sandy silty clay, presumably derived from the underlying interval. The rest of the core was mud breccia varying from grey to dark grey. The intervals separated by sharp boundaries are interpreted as different mud flows. Surprisingly the mud breccia showed intense bioturbation. This, and the cover of marly sediments, may indicate that the mud volcano had a relatively long period of inactivity.

Ginsburg mud volcano

Cores TTR-10-AT236G, TTR-10-AT237G, and TTR-10-AT238G

Three cores were taken from the top of the previously discovered Ginsburg mud volcano, varying in recovery from 145 to 182 cm. They all showed the same lithology - structureless, grey mud breccia with a thin oxidized interval at the very top, and very gasified. The target, to recover gas hydrate crystals, was successfully reached in core TTR-10-AT238G. Ice-like gas hydrates, up to 5 cm in size, were collected from the interval below 150 cm and stored in the cold laboratory for further geochemical analyses. According to data obtained during two expeditions (TTR-9 and TTR-10), the Ginsburg structure is the most recently active mud volcano in the Gulf of Cadiz.

Seepage area; carbonate mound and slabs

Core TTR-10-AT232G

A high reflectivity, subcircular spot on the OKEAN sonar mosaic detected during the TTR-9 cruise was a target for bottom sampling. The recovery was only some material in the core catcher. It was represented by a grey mud, enriched in foraminifera with numerous coral branches of *Lophelia pertusa* and *Madrepora oculata* and with abundant fragments of mollusc. *Pogonophora* worms were observed in a clayey matrix as well as echinodea spikes and one live crab. Three pieces of carbonate crusts were collected.

Core TTR-10-AT233G

An attempt to core the same structure was made. The recovery consisted of 36 cm of yellowish brown and greyish brown marl, very enriched in foraminifera, with *Pogonophora* tubes at the top, and fragments of bivalve shells and coral branches. A large (5 cm in diameter) carbonate crust was found in the middle of the recovered sequence.

TV Grab TTR-10-AT239Gr

The same structure was revisited again with the TV-controlled grab system. The video profile confirmed the assumption of active seepage through the area and showed the presence of gas-related carbonate build-ups, live corals and coral debris.

The TV grab was lowered to the seabed from 35°30.854'W, 07° 08.749'N to 35°30.853'W, 07° 08.816'N with a water depth varying from 956 to 961 m. The bottom surface is mainly characterised by a relatively flat relief with discontinuously distributed fragments of cemented sediment and bulky build-ups. Generally, a number of distinct seabed types appeared as the camera progressed along the transect.

On spatially restricted areas covered by fine sediments, numerous burrows and hummocks were observed, indicating intense bioturbation typical of deep-sea soft bottom communities. Build-ups were represented by meter-scale irregular slabs composed of consolidated carbonate crust. Crust samples from the area, showed a large diversity in texture and shape. Their size varied from 2 cm up to 50 cm and the cement was mainly composed of calcite and "complex" carbonates. A large amount of dead bivalves and corals fragments, trapped during the crust's cementation process, was found in the sample (Fig. 20). The bright yellow to reddish colour, observed in the fresh cuts, indicated enrichment with metal oxides, which means that carbonate was formed in an oxygen-rich environment. Such massive carbonate-cemented edifices serve as prominent indicators of microbial activity maintained by processes of intensive methane oxidation near the water-sediment interface.

Apparent fluid venting was recognised in certain areas during the TV survey. It was recorded as pale-grey, vaguely visible seeps released from isolated soft sediment areas in the cemented carbonate crust. It is presumable that due to the high water pressure those gas escapes do not create apparent bubbling.

An abundance of juvenile corals were observed to have settled on exposed hard boulders. The corals were differentiated by colour. An orange red-colour were recognised as *Madrepora sp.* while pale colour is characteristic for *Lophelia sp.* In the same area a large variety of faunas, including shrimps, lobsters, small fish and anemones, was also observed.

High biomass concentrations appeared in small areas generally not exceeding a few meters. They occurred as continuos fields of dead shell debris or beds composed largely of coral remains of different species. The local and ephemeral occurrence of chemosynthetic fauna can be attributed to spatial and temporal variations in the fluid supply. Among the fauna sampled with the grab, needles of echinoids, large solitary corals, and valves of *Bathymodiolus* spp., reaching of up to 10 cm in length, were recognised.

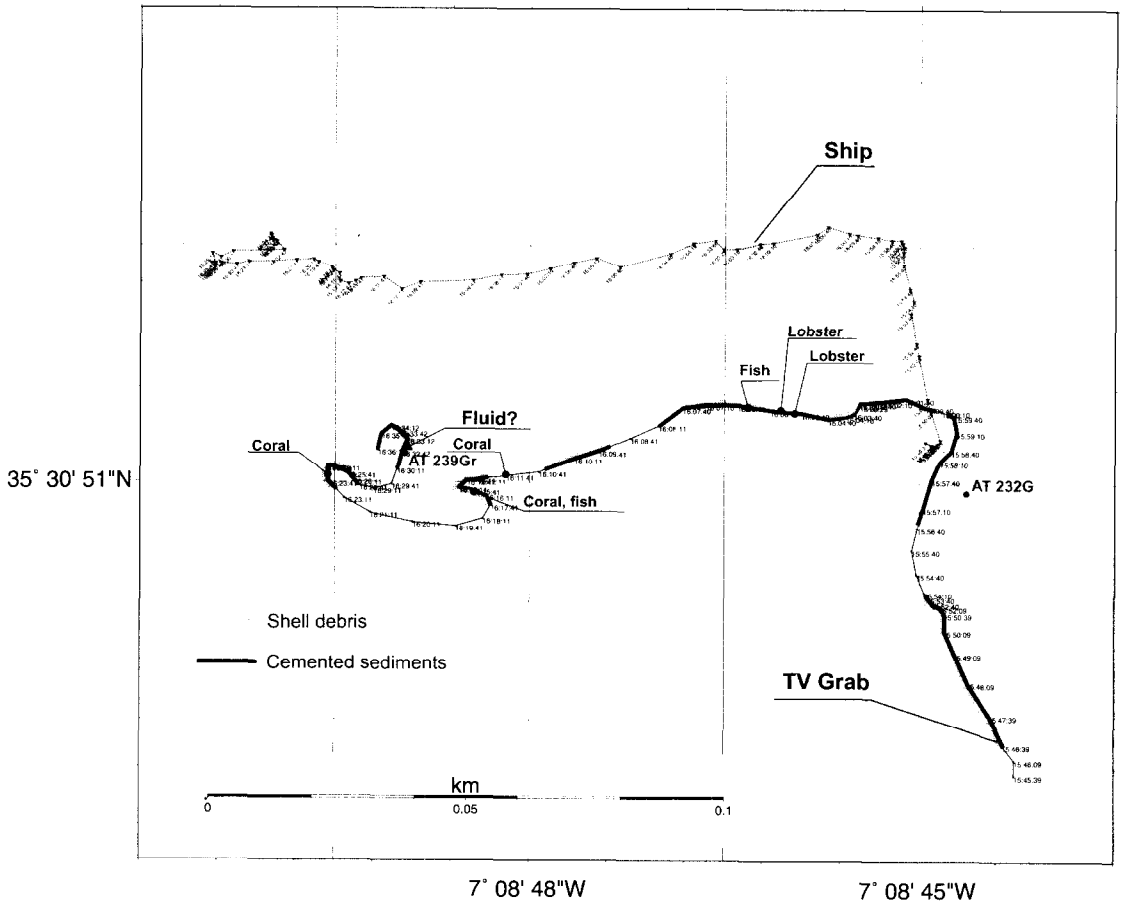

Figure 19. Track chart of the AT-239GR video survey showing the bottom features observed.

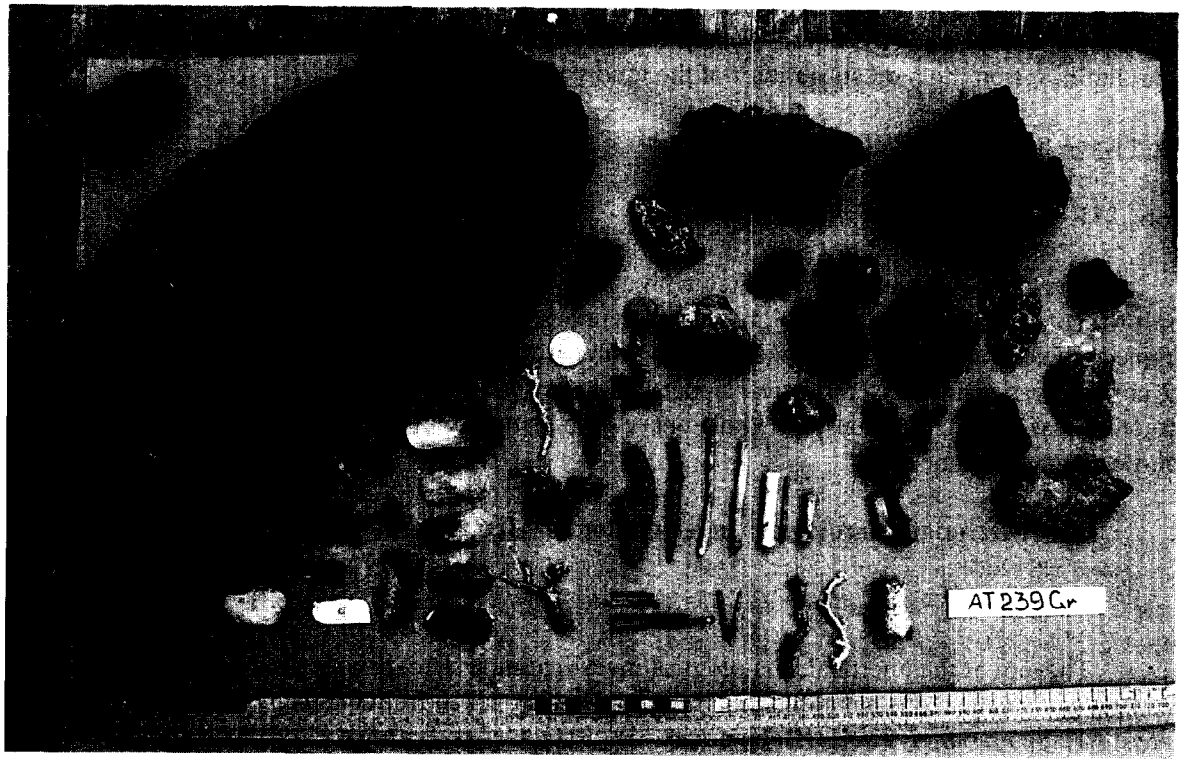

Figure 20. Carbonate crusts and coral fragments recovered from site AT-239GR.

Diapir-like structure

Core TTR-10-AT234G

A dome-shaped structure, expressed as an isometric high reflectivity spot on the OKEAN sidescan mosaic of the TTR-9 cruise, was cored. A 241 cm of marly succession was recovered, showing an intensive bioturbation throughout the core and presence of shell and coral fragments at some intervals. The lower half of the succession was represented by an unusual intercalation of oxidized and reduced lamina and was characterised by smell of H_2S. All this suggested intensive fluid venting through the sea-floor. Although no more cores were taken from this structure, its gas escape origin was confirmed. The site would be interesting for further investigation.

Spanish margin

Two sites were sampled on the Spanish margin of the Gulf of Cadiz. One is a dome-like structure discovered and mapped during the Spanish Geological Institute expedition in 1999. This structure was cored twice, confirmed to be a new mud volcano and named as TASYO mud volcano. The other site was situated within a sand wave field in a contourite channel.

Tasyo mud volcano

Core TTR-10-AT241G and Core TTR-10-AT242G

These stations can be easily compared since they both sampled the top of the mud volcano seen on the 3.5 kHz profile. The two cores showed a marly unit on the top. In both cases the yellowish brown marl was found to be rich in foraminifera containing a coral supported layer at about 15cm. For core AT241G the coral fragments showed up again in the lower part of the marly unit, between 50 and 69 cm where the sediment appeared to be more greyish and enriched in foraminifera. The lower half of these cores was mud breccia, homogeneous and structureless with a large amount of clasts of different roundness and size (up to 9 cm in diameter). Both cores showed a possible development of coral build-ups on the hard substratum of the mud volcanic edifice.

Sand wave field within a contourite channel

Core TTR-10-AT240G

The core was taken from an area with a very complex, bumpy seafloor morphology. The 337 cm of recovery consisted of olive grey, homogeneous, water-saturated, well-sorted, fine to medium grained siliciclastic sand with some silty admixture. A more clayey sand interval was observed at 12-22 cm and was characterised by clear upper and lower boundaries. Although no visible depositional structure was seen throughout the whole succession sampled, the core is believed to represent contourite channel sediments.

I.3.4. Micropalaeontological Investigation of Matrix from Mud Volcanic Deposits

A. SAUTKIN

The aim of the micropalaeontological investigation was to date the matrix of the mud volcanic deposits using calcareous nannofossils. The samples were taken from the matrix of the mud breccia in cores AT226G and AT227G (Bonjardim), AT231G (Jesus Baraza), AT235G (Rabat), AT236G, AT237G (Ginsburg), AT241G, AT242G (mud volcano TASYO, AT243G, AT244G (mud volcano Carlos Ribeiro) for preliminary determination of the time range.

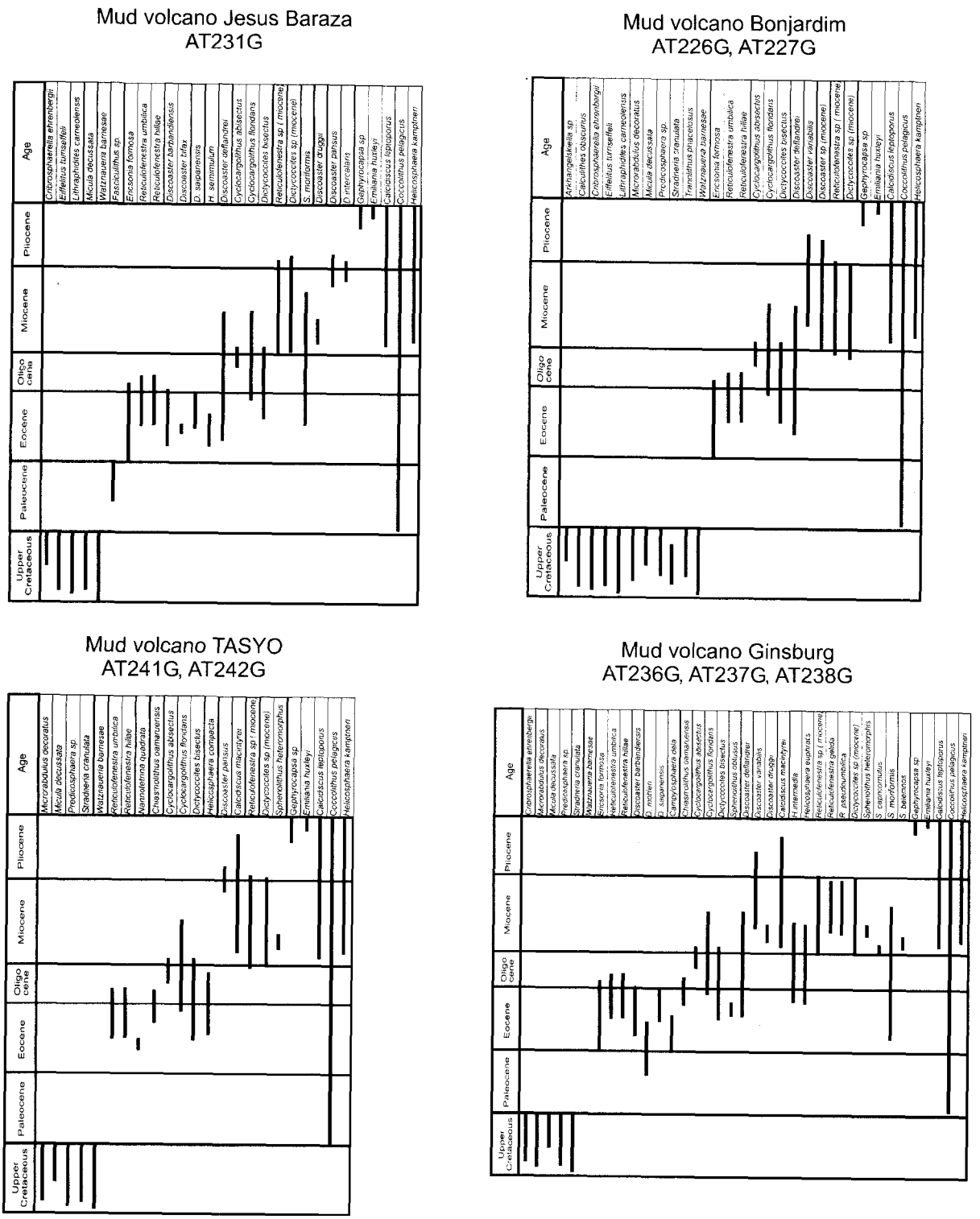

Figure 21. Distribution of calcareous nannofossils species in the mud volcano cores.

Smear slides were prepared from raw samples and examined using an "Olympus" light microscope with magnifications x1000. The method of calcareous nannofossils identification by Perch-Nielsen (Bolli et al.,1985) was applied on coccoliths.

Calcareous nannofossils from different ages have been found in the matrix of mud breccia (Fig. 21). Preservation of the calcareous nannofossils is moderate to poor. They seem to be partially dissolved which makes it difficult to identify small forms. Relatively big coccoliths show good preservation. In general, discoasters are found to be damaged and at times their arms broken, making their identification difficult. Some representatives of the discoasters show overcalcification patterns that obscure important features and cause complications during the process of identification and classification of species.

Some Upper Cretaceous species are common in the samples from the mud volcanoes. In each sample 4 to 6 species of Upper Cretaceous coccoliths were identified in the mud volcanoes. The most abundant species are *Micula decussata* and *Watznaueria barnesae* and others. These species could have been derived from a hemipelagic source or from slope sediment by the process of resedimentation. They are also present in the pelagic sediments observed on the superficial sediments of some mud volcanoes. Thus, the presence of these species cannot be firm evidence of Upper Cretaceous age. Only the mud volcanoes discovered in the S. Portuguese margin show an assemblage of Upper Cretaceous coccoliths. It is probable that Upper Cretaceous deposits are located near the roots of the mud volcanoes on the Portuguese margin.

The Paleocene species occur very sporadically in only two sediment samples. The most probable explanation for this is the absence of any Paleocene deposits near the roots of the studied mud volcanoes. Calcareous nannofossils, typical of Eocene deposits are found in abundance. Among them *R. umbilica, R. hillae, Discoaster barbendiensis, D. saipanensis, Ericsonia formosa* are frequently observed in smear slides. Based on these nannofossils it is confirmed that the roots of the mud volcanoes have Eocene deposits. There are also some transitional species through the Oligocene (*D. deflandrei, Cyclicargolithus floridanus, C. abisectus, Dictycoccites bisectus*). However, the presence of the Oligocene sediments cannot be confirmed because of lack of evidence of marker species. The most abundant species in the matrix are Miocene-Pliocene coccoliths and discoasters. There are numerous species in all the studied samples of the matrix. The following species are observed most frequently in the smear-slides: *Discoaster variabilis, D. druggii, D. pansus, R. pseudoumbilica, R. gelida, Reticulofenestra* spp., *Dictycoccites* spp., *Sphenolithus heteromorphus, Calcidiscus macintyrei* and many more. The presence of the Miocene-Pliocene species suggests that sediments of these ages have been actively involved in the process of mud volcanism in the region.

Quantitative analysis of the coccoliths was carried out in the samples of matrix from mud breccia in core AT227G. Amongst the 145 specimens of calcareous nannofossils, 45 are from Upper Cretaceous (mainly *Micula decussata* 26, *Watznaueria barnesae* 15, *Cribrospherella ehrinbergii* 5, etc.), 25 specimens are from Eocene (*Ericsonia formosa* 7, *Reticulofenestra umbilica* 5, *R. hillae* 3), 15 specimens are transitional from Upper Eocene through Oligocene to lower Miocene, 37 specimens are from Miocene-Pliocene (mainly different types of *Discoasters*, small *Reticulofenestra, R. pseudoumbilica, R. gelida* and *Dictycoccithes* spp.). The other species are recent coccoliths namely *Emiliania huxley, Gephyrocapsa* spp., *Coccolithus pelagicus, Calcidiscus leptoporus, Rhabdosphaera claviger* and *Syracosphaera pulchra.*

I.3.5. Geochemical Sampling

A.STADNITSKAIA, I.BELENKAYA, P.FERREIRA, L.MAZURENKO, V. BLINOVA AND N. GALIN

The main aim of the geochemical programme on board was to collect samples for geochemical investigation, including both organic and inorganic domains.

Hydrocarbon gas and pore water analysis

Due to diagenesis only an insignificant part of extinct organic material is preserved in marine sediments. Other organic substance either decays because of physico-chemical rearrangement, or is dissolved in pore waters and then microbiologically utilized. Crude organic matter consists of a diverse variety of compounds, each differing in its inherent biochemical characteristics and susceptibility to microbial attack (Tyson, 1995). Microorganisms require energy for growth and cell maintenance, which is obtained in metabolising organic material by a series of coupled oxidation-reduction reactions. The conversion of organic matter to biogenic gas takes place by bacterial decomposition under anaerobic conditions. These metabolic processes result in the production of gases including methane (Rice and Claypool, 1981).

The investigations of hydrocarbon gas composition in the areas of active fluid flux and gas venting is one of the main subjects leading to a better understanding of its formation processes, accumulation and migration mechanisms. An intensive hydrocarbon gas flux through the sediment sequence supports high bacterial activity that leaves indelible marks on the chemistry of pore fluids, serving as transport media for the microbial metabolic products. Authigenic carbonates associated with gas saturated sediments also serve as prominent indicators of microbial activity. This is because hydrocarbon-consuming bacteria produce extremely high levels of alkalinity and dissolved inorganic carbon which lead to supersaturating of pore fluid with the carbonate and subsequent precipitation of diagenetic cement.

Samples for hydrocarbon gas, pore water and organic matter investigations were collected from the gravity-corer stations taken from upper part of mud volcanoes (AT-226G, AT-227G, AT-231G, AT-235G, AT-236G, AT-237G, AT-238G, AT-241G, AT-242G, AT-243G, AT-244G, and AT-246G). Core AT-225G was subsampled in order to use it as a reference.

According to lithological description, these cores can be divided into two groups. The first group represents cores which recovered fluidised homogenous silty/sandy mud breccia containing up to several centimetres rock clasts which are uniformly dispersed in matrix (AT-226G, AT-236G, AT-237G, AT-243G, AT-244G and AT-246G). Another group includes cores with mud breccia overlain by pelagic sediments (AT-227G, AT-231G, AT-235G, AT-241G, and AT-242G). All these cores contained gas saturated sediments that crumbled away on the deck under the influence of gas discharge after being extracted from the core barrel. All of them were noted for gas saturation, especially cores AT-238G and AT-246G, which contained gas hydrate accumulations.

Hydrocarbon gas

The composition and distribution of C1 to C5 hydrocarbon gases in pelagic sediments and mud volcanic deposits will be determined for the presence of hydrocarbons that have migrated through the sediments from subsurface accumulations. Particular interest will be directed to content and correlation between individual hydrocarbons along the cores in order to surmise the relation to a deep source.

For identification of hydrocarbon gas composition, its distribution and stable isotope signatures, the standard sub-sampling and degassing procedures of the sampled sediments were applied. It was done using a syringe with a cut tip. Sediments of 30 cm^3 were taken every 10 cm and from all different lithological intervals. The degassing was accomplished according to the Head-Space analysis adapted for shipboard conditions (Bolshakov and Egorov, 1987).

One of the main factors controlling the quantity of produced hydrocarbon gas is the amount of organic mater preserved in sediments. The hydrocarbon gas production in deep-sea sediments is strongly related to total organic carbon (TOC) content. This means that without influence of migrated fluids, the hydrocarbon gas formed in situ is characterized by a strike lithological control. Therefore, for determination of TOC content and for bituminological investigations, mud breccia matrix were sub-sampled from the same core intervals as for gas analysis and dried at a temperature of 60°C.

Gas hydrates

Two cores, AT-238G (Ginsburg mud volcano) and AT-246G (Bonjardim mud volcano) contained gas hydrates. Gas hydrate samples (Fig. 22) were stored in plastic bags in a cool room at -10°C. The morphology of gas hydrates accumulations was documented in the cool room.

Pore water

The pore-water subsampling has been undertaken for the following objectives: (1) transient changes in Alkalinity (Alk-), sulfate (SO_4^{2-}), Ca^{2+}, and Mg^{2+} content in order to infer the geochemical and microbiological history of gas-influenced sediment; (2) to evaluate the precipitation rate of authigenic minerals such as carbonates; (3) to assess gas hydrate amounts in hydrate-bearing sediments on the basis of chloride anomalies measured along the cores with the oxygen isotopes in pore waters.

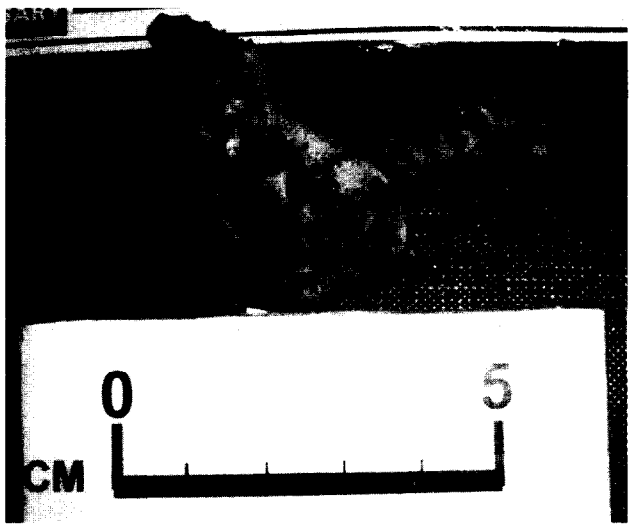

Figure 22. Gas hydrate aggregates sampled from the Ginsburg mud volcano.

Water saturated tops of the cores were selected to collect samples of sediment moisture using "Rhizon soil moisture samplers (SMS)" linked by two females luer connectors to plastic luer lock syringes of 10 ml (Kenyon et al., 1998). Pore waters were extracted with the standard titanium/stainless-steel squeezer and/or centrifuged using a Heraeus Megafuge 1.0. An amount of $HgCl_2$ was added into the each pore water sample in order to suppress microbiological activity which could considerably change the carbon isotopic values. Then the pore water samples were stored at a temperature of +5°C.

For the detailed isotope study (δ13C and δ18O) each core was subsampled in accordance with the pore water and gas sampling intervals.

In addition, gas saturated sediments were collected for the microbiological study in the uppermost 0-10 cm. Samples were packed in the sterile plastic boxes with size 2x2 cm and stored in a cold room at a temperature of -10°C.

Major and trace elements

The subsampling for inorganic geochemistry studies was carried out in order to analyze major and trace elements with special emphasis on immobile elements, such as Zn, Hf, Ta,Th, Nb, Rare Earth Elements, etc. Further investigations will be directed to:

1. Identification of key-elements leading to geochemical deriviation of different lithologies present in the mud breccia;
2. Find elemental differences between pelagic sediments and mud volcanic deposits;
3. Cooperative study of interrelations between pore water/mineral compositions for understanding geochemical balances in mud breccia matrix;
4. Study of sampling precision (within Sampling and Uncertainly Group of IAG - International Association of Geoanalysts).

The subsampling was made on the two most characteristic lithological units: pelagic sediments and mud breccia matrix. Subsampling was carried out using plastic syringes with a cut tip. The vol-

ume of the samples varied between 20 and 40 ml. The syringes were washed in distilled water before being used. Subsequently, the samples inside the syringes were put in the plastic bags that were closed and stored at 0°C for later analyses after the cruise.

For each gravity core all the different lithological (and/or textural) sections were sampled. In cases of homogeneity, a systematic sampling was made from the top to the bottom of the core. On average, two samples per section were taken (one at the top and the other at the middle of the section)

For the study of sampling precision, laterally contiguous sabsamples from the same levels were taken (15-20% of the all samples).

In order to analyse short spaced variations in terms of elemental concentrations, two vertical contiguous levels were subsampled (both levels having similar lithological and textural characteristics).

I.3.6. Main Conclusions

G. AKHMANOV, M. IVANOV AND L. PINHEIRO

The following conclusions can be made:

- A large variety of sediment types present in the Gulf of Cadiz study area were recovered and described during bottom sampling, implying a superposition of different depositional environments in this region of very complex geology and hydrology.
- Mud volcanism is a widespread phenomenon in the Gulf of Cadiz and six new mud volcanoes were discovered in the area during the TTR-10 cruise. Most of them were proved to be recently active.
- Mud volcanism is characterized by a zonal pattern in terms of mud breccia lithology typical of different mud volcanoes. In general, relatively thin mud breccia flows, intensively bioturbated at the top, having semi-consolidated clasts, within a matrix with high carbonate content, are characteristic for mud volcanoes sampled on the Spanish and Moroccan margins of the Gulf of Cadiz. Non-stratified, thick, stiff mud breccia, only occasionally bioturbated, and numerous well-lithified clasts within a matrix lacking significant carbonate admixture, were found to be typical for mud volcanoes from the Portuguese margin of the Gulf of Cadiz.
- Beside mud volcanism, active fluid venting in the Gulf of Cadiz is expressed by formation of coral-rich carbonate mounds and carbonate slabs on the sea-floor. Also a geochemical front, as a result of sediment reduction due to upward fluid migration, was noticed in the study area.
- The co-existence of coral-rich carbonate build-ups and mud volcanic activity was confirmed to be widely present in the Gulf of Cadiz. Mud volcanic deposits serve as a hard substratum to facilitate the growth of coral colonies.

II. MID-ATLANTIC RIDGE: LUCKY STRIKE FIELD (LEG 2)

II.1. INTRODUCTION AND GEOLOGICAL SETTING

J. MONTEIRO, B. MURTON, L. PINHEIRO AND A. PINTO

Bathymetry

The Lucky Strike segment of the slow-spreading Mid-Atlantic Ridge is characterised by an unusually large central volcanic complex. Fouquet et al. (1996) presented a map of the field derived from diving operations conducted with the Nautile in 1994. Langmuir et al. 1997, presented results of the French American Ridge Atlantic (FARA) program showing that the depth and chemistry of the ridge segment are influenced by the Azores hot spot. Fouquet (1999), listed the Lucky Strike field as one of the 14 major sulfide deposits in the oceans. This ~65 km long, second order ridge segment is centred on 37°17.5'N and 32°16.5'W. At its deepest ends, the segment is ~3200 m deep. At its centre the depth rises to 1650 m. Here the width of the axial valley is about 8 km. The central volcanic complex comprises a plateau that rises from a mean basal depth of 2200 m. This plateau is 5 km wide (east to west) and 6 km long (north to south). To the south and north, the plateau is constructed from six to seven lobate terraces that cause a series of steps in the bathymetric gradient. To the east and west, the plateau has a more complex structure. The eastern side comprises two sub-terraces. The main terrace is divided in two by a 015°-trending valley that is 60-80 m deeper than the terrace, and 0.6 km wide. This small valley divides the main terrace from an elongate ridge, also with a 015° strike. At the centre of the volcanic complex there are three elliptical cones, two to the north aligned east-west and elongated with an 015° trend, and one to the south with an east-west elongation. These cones rise 100 m above the main plateau. Their peaks are 1 km apart and at their centre, 140 m below the summits of the three cones, is a circular depression with a 150 m radius (Fig. 23).

Steep, linear scarps, of probable tectonic origin, cut the main plateau to the north of the three cones. These are aligned with a trend of 015°. The eastern-most scarp has the greatest height, of 100 m, but decreases northward (Fig. 23). The width of the scarp is about 100 m. It intersects the eastern slope of the eastern cone, causing an elongated shoulder on the eastern flank. The western scarp also has about a 100 m height, but is 500 m wide. The trend of this scarp is continuous with the western wall of the approximately north-south striking, narrow valley that dissects the western side of the main volcanic plateau. Between these two major linear scarps are several parallel scarps with heights of about 30-40 m. Along with the main scarps, the strike of these lesser ones curve inwards towards the centre of the volcanic complex. To the south, and along strike from the main scarps in the north, there are a series of buttress-like structures that parallel the trend of the main scarps in the north. In the west, the steepest of these buttresses forms a gully, 10-20 m deep, that is parallel to the major, western scarp to the north of the western cone. In the east, there is a similar gully, but that is only 10-15 m deep. The northern flank of the three cones is cut by a steep, 100° trending, roughly linear scarp, that faces to the north and has a height of ~40-50 m. When traced westwards, this scarp crosses the narrow valley dissecting the western part of the plateau and off-sets the crest of the N-S elongated ridge on the western side of the central plateau. To the south, there are three to four curved terraces in the volcanic plateau that are elongated either southwards or towards 190°.

Geochemical and volcanic setting

The Lucky Strike segment lies about 700 km to the southwest of the Azores archipelago that is the result of volcanism above a mantle hot-spot. Geochemical gradients between N-MORB and enriched plume mantle, characteristic of the Azores archipelago, extend as far south as the Lucky Strike segment. The central volcanic complex in the segment has a K_2O/TiO_2 ratio of up to 0.5, similar to the ratio for the Azores archipelago. In contrast, N-MORB compositions 100 km to the south of

Lucky Strike have K_2O/TiO_2 ratios of ~0.2. Clearly the Lucky Strike central volcano is influenced by mantle compositions typical for the Azores mantle plume.

The central volcanic complex has geochemical variations that reflect magmatic fractionation processes. The three cones at the top of the volcanic complex, in the centre of the plateau, are enriched in incompatible elements, with up to 300 ppm Ba and 300 ppm Sr, compared to the plateau that has only 60 ppm Ba and 110 ppm Sr (Langmuir et al., 1997). The three central cones are also highly vesicular compared with the subjacent plateau. The central depression located between the three cones comprises fresh and vitreous collapsed lobate flows and lava pillars, and has been described as a recently active lava lake (Fouquet, 1999).

Fouquet (1999) also reports that there are hyaloclastic and volcanic breccias deposited on the flanks of the three cones and around the periphery of the lava lake. Built upon these deposits, and a basement of pillow lavas, are numerous high-temperature sulphide structures (Langmuir et al., 1997; Fouquet, 1999). Many of these are active with temperatures of up to 220°C. Broad areas of diffuse activity also surround the sulphide structures and three regions comprise altered and sulphide mineralised hyaloclastite deposits.

The bathymetry and sidescan sonar imagery together reveal a slow-spreading ridge segment that has a large composite volcanic plateau at its centre. The volcanic plateau comprises up to seven constructional terraces with three conical edifices at its highest point in the centre. The three volcanic cones are relatively old and comprise late-stage fractionated and highly vesicular basalt. The presence of hyaloclastites associated with these cones indicates explosive submarine activity. In between the three central cones is a circular depression of recent volcanic activity and subsidence. To the north and south, the central volcanic complex is characterised by recent and extensive sheet-like flows. To the north and south of these sheet-like flows, the ridge segment contains regions of hummocky flows, as well as more sediment. An exception to these trends are two sheet-like flows that occur in the extreme north and south of the segment.

Brittle tectonic deformation in the form of fault scarps has recently bifurcated the central volcanic plateau and post-dates the three central cones. This activity forms a north-south trending graben that forms the small valley immediately to the west of the three cones. Subsidence is centred on the volcanic plateau where it has a maximum, observed, throw of 100 m. However, the extensive sheet flows, to the north and south of the central cones, are retained by the graben walls and probably mask several metres of additional tectonic subsidence. Brittle deformation is still continuing, with abundant small throw faults and fissures breaking-up the recent sheet flows. The steep, east-west striking northern flank of the three centrally located cones is probably fault controlled.

Previous Sidescan Sonar Imagery

Deep-towed 30 kHz sidescan sonar data acquired by Southampton Oceanography Centre (Parson et al., 2000), are useful in that they reveal high-frequency bathymetric changes and variations in acoustic texture of the axial floor. The central volcanic complex is characterised by high backscattered energy. The three central cones have high-frequency variations in backscatter and are cut by 6-8 linear reflectors, 10-20 m wide, that bifurcate and join together in a general trend of 015°. Centred on the 300 m wide depression between the three cones is an area of mottled backscatter and arcuate shadows and strong reflectors consistent with a circular depression. To the north and south of the three central cones are areas of high but relatively homogeneous backscatter. These areas lie between the major north-south trending scarps identified from the bathymetry. The smooth acoustic texture is interrupted by a series of parallel linear reflectors and shadows that parallel the main bathymetric scarps. These parallel features are 4-6 km-long, 40-100 m wide and face towards a central zone that lies along the centre of the small western valley. The smooth and high amplitude backscatter acoustic facies extend to this north-south trending ridge to the west of the three cones. The eastern flank and plateau has a lower backscatter amplitude, that is also mottled in texture. The deepest part of the eastern axial valley has low backscatter intensity and is almost homogeneous in acoustic texture. Further to the north

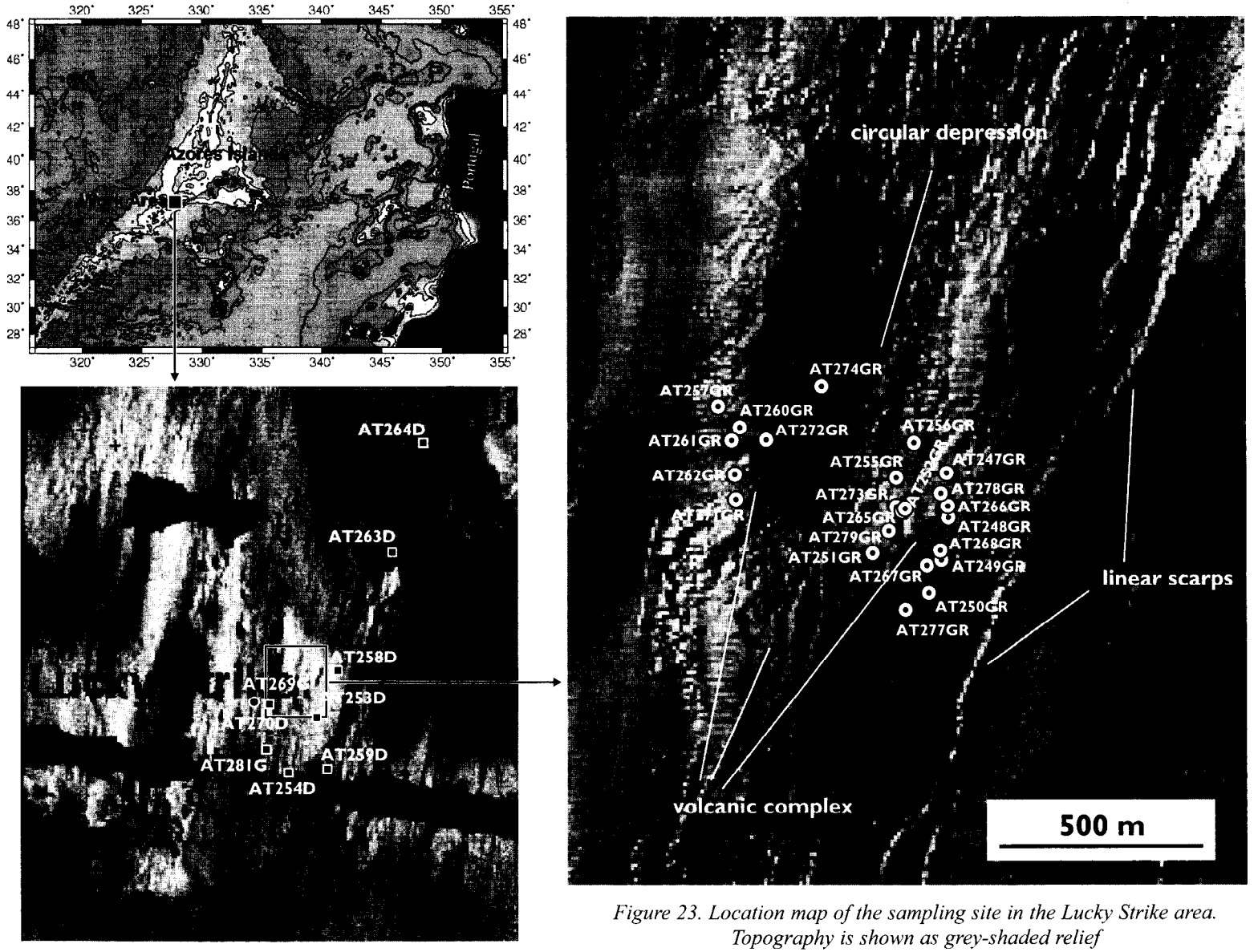

Figure 23. Location map of the sampling site in the Lucky Strike area. Topography is shown as grey-shaded relief

and south, by ~5 km, there are increasingly large areas of highly reflective and acoustically mottled textured terrain. Between 15 and 20 km north and south of the centre of the volcanic complex are low backscatter intensity regions, cut by 015° trending bright linear reflectors. At some 25 km north and south of the centre of the central volcano, lobate-shaped, homogeneous regions of high backscatter occur, 4 km long by 2 km wide.

II.2. AIMS AND OBJECTIVES

To address the question of evolution of the central volcanic complex, a number of TV-controlled grab and dredge stations were sampled. All dredge sites were chosen on the basis of TOBI 30kHz deep-tow sidescan sonar data and multibeam bathymetry data. The extent of sediment cover and an impression of the lava texture (sheet or pillowed) were identified in this way, as well as fracture and fault structures of at least 2 m high. The sample locations for the TV grab sampling were selected using the digital event log produced during the LUSTRE 96 cruise (Fig. 23). The coordinates were taken from the ARGO database. In places the pictures from the ARGO electronic still camera were used to evaluate the nature of the bottom in order to facilitate the TV Grab surveying. Volcanic material was collected from the cones at the centre of the volcanic plateau, from terraces at increasing depth and distance north from the centre, and from two distinctive sheet flows at the far northern end of the segment.

A deep-towed 30 kHz OREtech sidescan sonar survey was run in order to obtain an acoustic image of the central volcanic summit. An attempt was made to core sediment ponds seen on TOBI and OREtech images, subbottom profile records and bathymetry.

II.3. MAIN RESULTS

II.3.1. 30 kHz Sidescan Sonar OREtech Imagery and 7 kHz Sub-bottom Profiling

J. MONTEIRO, B. MURTON, L. PINHEIRO AND P. SHASHKIN

A sidescan sonar line was occupied across the central volcanic complex, crossing the central depression between the three cones, from approximately northeast to southwest (from 37°18.8'N; 32°19.3'W to 37°16.6'N; 32°14.3'W) over a distance of approximately 10 km. The instrument was towed ~100 m above the seafloor at a speed of 0.5 kts.

The sub-bottom profiler revealed sediment ponds to the west of the central volcanic plateau, lying in a small valley at the foot of the western inner rift wall. The profile reveals a large, flat plateau with a central depression and adjacent cone at 32°16'W and steep flanks to the east and west. The plateau is off-set vertically in the west (i.e. the small 015° striking valley) where the seafloor generally slopes eastwards. Several scarps rise to the west of the small valley floor above which the seafloor slopes to the west. The eastern flank is smooth with two small 50 m high hummocky mounds at its base.

The OREtech 30 kHz sidescan sonar image has a range of 1 km each side of the nadir. The area at the foot of the western-most inner valley wall is characterised by bright backscattering lines of hummocky textures indicative of small pillow lava ridges trending 40°. However, the OREtech profile shows these mounds to be less than 10 m high and they are probably partially buried by sediment.

The western flank of the central volcanic plateau is revealed as rough terrain that is traversed by two or three fault scarps 100 m apart. The western lower plateau top has more sediment cover and is also traversed by 10-12 individual parallel faults with a similar 15° strike but each separated by 50 m. Fresh lavas occur at the top of the 15° trending ridge to the west of the small valley, and on the valley floor.

The three central cones are strongly backscattering indicating both rough and sediment-free outcrop. The southern and northeastern cones have radial structures centred on their summits. These

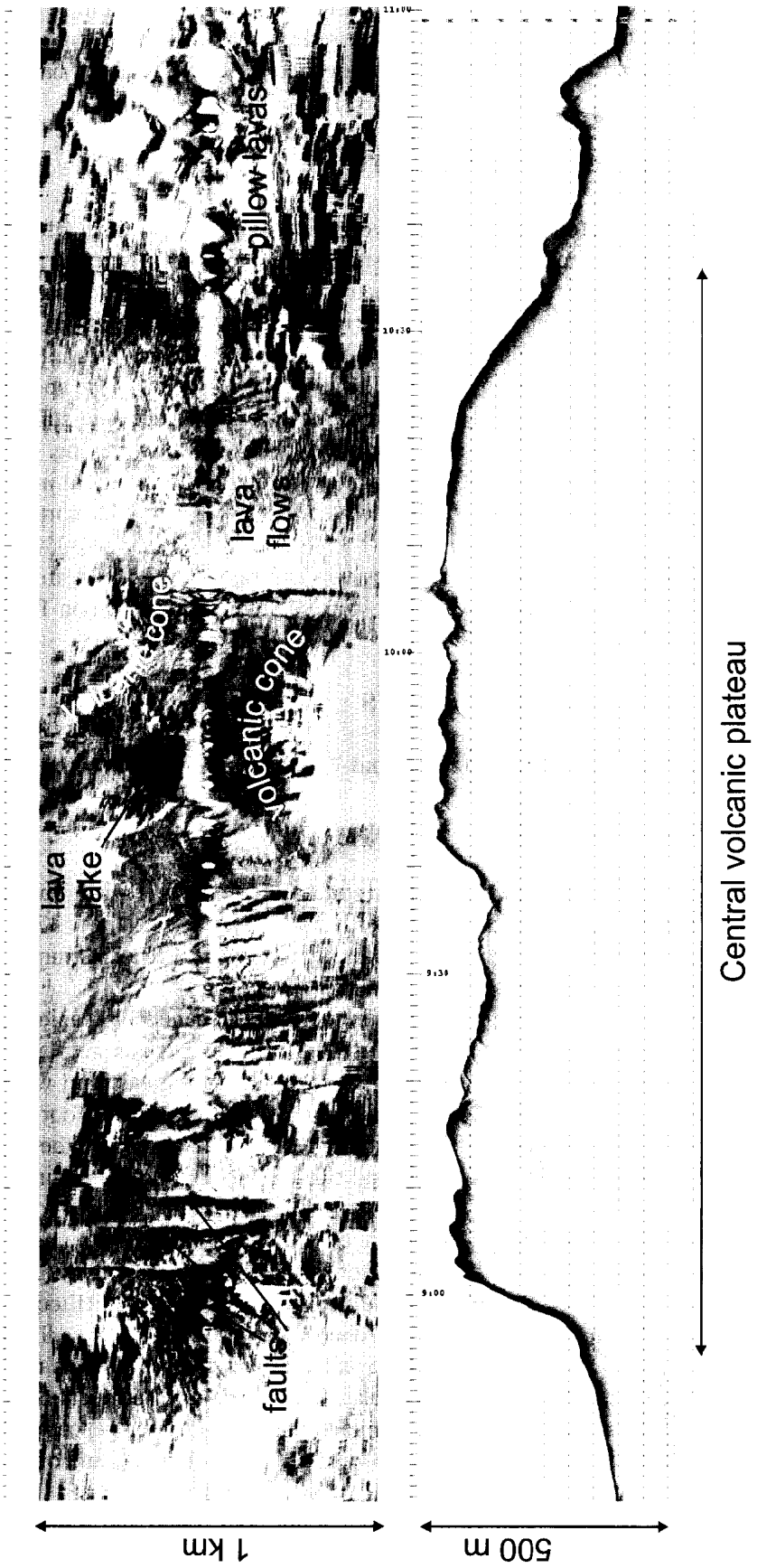

Figure 24. 30 kHz sonograph and bottom profiler record ORAT-38.

are closely spaced (~25 m apart), parallel curved features that throw shadows away from the sidescan sonar's nadir. This indicates a morphology of circular scarps facing inwards towards the centre of the volcanic cones. The lava lake lying between the three cones is visible as a circular depression, surrounded by smooth textured terrain that, from previous work and this cruise, is known to contain the hydrothermal activity as well as the hyaloclastite deposits.

Smooth and strongly backscattering terrain extends east from the three central cones for a further 2 km until terminated by a linear boundary and bright reflector trending 15°. These features coincide with the eastern limit of sheet flows and the location of the eastern-most, major west-facing fault scarp. However, on the OREtech profile, this change in texture is marked only by a 5-10 m high slope. To the east of the limit of sheet flows the seafloor has low backscatter characteristic of sediment cover. The eastern flank of the plateau comprises a mottled backscatter texture indicating pillow type flows. The texture has an east-west fabric, indicating the pillow forms are elongated in a down-slope direction.

The foot of the eastern plateau flank has a hummocky texture indicative of small (20-40 m high) pillow mounds. These features characterise the seafloor for the remaining eastern section of the sidescan sonar image.

II.3.2. Bottom Sampling

B. MURTON, J. BIGGS, P. FERREIRA, M. DA CUNHA, A. HILARIO, I. TEIXEIRA, M. QUARTAU, A. STEPANOV, A. PINTO AND SEDIMENTOGICAL TEAM

24 stations within the hydrothermal field were successfully sampled with TV-guided grab (Figure 23 and Table 4). 2 CTD stations were also done above large vents discovered in 1992 during FAZAR expedition and called Eiffel Tower and Statue of Liberty. The stations were attempting to observe anomalies in a water column related to a hydrothermal activity. 8 dredging station were done outside of the Lucky Strike Field in order to sample the floor and walls of the central graben and slopes of the neo-volcanic rise. One gravity core was collected 4 km away from the field in order to assess the character of pelagic sedimentation and supply of fine, hydrothermally-derived material. The position of the stations and brief description of samples are given in Table 4.

II.4. CONCLUSIONS

J. MONTEIRO, B. MURTON, L. PINHEIRO, A. PINTO AND M. IVANOV

The lava samples confirmed that the three central cones are composed of highly vesicular (<90%), plagioclase phyric (rounded crystals 2-8 mm long and 5-8%) slightly altered basalts. These rocks are mainly pillow types. Included in this volcanic group are bedded hyaloclastite deposits that have lenticular-shaped bedding structures comprising fresh black vesicular glass fragments (1-2 mm in diameter) in a matrix of 2-5 mm thick layers of green-coloured altered angular glass shards. In places hyaloclastite deposits up to 30 cm thick were recovered that have a variety of layers of altered glass, manganese and iron oxide layers (1-2 mm thick) and lenses and layers of fresh black glass fragments. Some of these layers grade upwards towards finer grained material, while others grade upwards towards coarser grained deposits. Some hyaloclastites include interbedded layers of shell debris and 2-3 mm diameter spherulites of either volcanic glass or manganese oxide.

The central northern plateau comprises glassy avesicular sheet flows with infolded and rubble-textured surfaces. These are aphyric and coated with manganese oxide and iron oxide staining. Interiors are vitreous and fresh looking. Some coral was collected from these rocks, and all samples were blackened by manganese oxide and were dead.

The western upper-flank of the central plateau comprises old palagonitic and iron oxide coated pillow lavas. The form of the pillows are elongated and are not flattened, indicating eruption local-

Table 4. Sampling sites in the Lucky Strike area.

Core No	Latitude	Longitude	Depth, m	Sample Description
AT-247GR	37°17.520' N	32°16.512' W	1620	Sample retreived from the chimney area believed to be inactive at the present time. Manganese crust on one side with a diameter of ~ 5 cm. Some layers with coarse pyrite crystals < 1mm in size. Chalcopyrite crystals (? 1 mm) are present. Atacamite?[Cu_2 (Cl, $OH)_3$] found at the bottom of the structure. Abundant chalcopyrite present, especially at the base on the larger diameter/lower end of the rock. Sphalerite? possibly present. Anhydrite present as gang mineral.
AT-248GR	37°17.425' N	32°16.510' W	1665	Sample retreived from the chimney area believed to be inactive at the present time. Sample recovered possibly from the wall of the chimney. Manganese crust on one side of the rock sample. Pyrite crystals < 1mm in size. Anhydrite (possibly) and silica present as gang minerals. Metaliferous sediment. Poorly sorted sand/gravel. Possibly disintegrated sulphide. A few shell fragments. Smells muddy but not pungent. Granules are angular. Massive sulphide present in abundance. Very poorly sorted granules, angular to sub-angular. Dark brown sandy clay with gravel. Abundant rock fragments. Darker than sample AT 247 GR.
AT-249GR	37°17.342' N	32°16.522' W	1685	Numerous boulder-sized fragments of pillow lava represented by porphyry basalt. Pumice like, very vesicular angular fragments. Massive with no internal structure. Plagioclase 0.1 – 1.5 cm crystals ~ 7 %. Hyaloclastic layers; 5 mm thick, sediment intercalated 2 cm thick. Glass shards 0.1 – 3 mm in diameter.
AT-250GR	37°17.275' N	32°16.525' W	1701	10-15 l of a mixture of iron, silica and manganese materials. Orange-brownish colour; very heterogenous give striform layers. It seems to consist of clay minerals between different components. Numerous fragments of altered aphyry basalt and few fragment of porphyry basalt. Shell debris (*Bothimodiolus* spp.).
AT-251GR	37°17.356' N	32°16.657' W	1685	Iron oxide and manganese crust with brown sediments. Black colour. Irregular surface. Ten small samples obtained. Total weight ~ 200 g.
AT-252GR	37°17.442' N	32°16.594' W	1673	Blocks of pillow lava. Large and small pieces of lobate flows – black vesicular glassy matrix with plagioclase phenocrysts, rounded and upto 6 % glassy margins and flow banding of vesicules inside. Oxide and manganese coating. Interior fresh and black coloured. Shell debris (*Bothimodiolus* spp.).
AT-253D	37°17.440' N 37°17.340' N	32°16.521' W 32°16.441' W	1670 1667	Angular fragments of vesicular plagioclase; phyric basalt. Many are tabular or curved i.e. lobate flows. Some may be pillow lavas. Black to dark brown colour, pelagonite alteration of glassy rims. Some scoria also present.
AT-254D	37°16.498' N 37°16.340' N	32°15.790' W 32°15.782' W	1750 1720	Fragments of ropey flows with glassy skin and glassy and crystalline interior. A few large (1 cm in diameter) plagioclase phenocrysts. Some dead corals. Large alive deep-water sponge.
AT-255GR	37°17.503' N	32°16.610' W	1680	Mud formed from completely decomposed by the hydrothermal alteration rock Mud contains well preserved mineralization formed essentially by pyrite and unidentified black mineral. The sample is like sandstone-poorly consolidated. All grains have round shapes. About 25 small samples.

Table 4. Continuation

AT-256GR	37°17.571' N	32°16.576' W	1668	Hydrothermal breccia with fragments of different types of lava – pillow and more massive lavas. It is possible to see silica precipitate layers. Lavas have suffered hydrothermal alteration. Very rich in silica. Grey in colour; many vesicules and phenocrysts (up to 1 cm) of plagioclase. Inside the vesicules there are many microcrystals of pyrite. Middle stage of hydrothermal alterations between the AT 252 GR (Breccia of pillow and massive lavas and hyaloclastites) and the silicified samples of AT 255 GR.
AT-257GR	37°17.640' N	32°16.958' W	1640	Small amount of white to grey sediment and algae. No rocks.
AT-258D	37°19.197' N 37°19.058' N	32°15.595' W 32°15.503' W	1930 1920	Small fragments of folded and tabular sheet flow-vitreous interior, aphiric, low percentage vesicularity. Encrusted with dead manganese coated corals.
AT-259D	37°15.211' N 37°15.482' N	32°15.980' W 32°15.992' W	1969 1883	Very light brown clayey silt and some sand. Well sorted. Yellowish to brown very fine plastic sediment.
AT-260GR	37°17.600' N	32°16.916' W	1690	Sulphide minerals present; mainly pyrite (< 1 mm) and some chalcopyrite? Fine grained. Layered structure. Some holes have plenty of pyrite crystals. Assocaited with the holes are some coloformic pyrite with botryoidal shape. Limonite on one side of the sample < 1 cm.
AT-261GR	37°17.575' N	32°16.932' W	1690	Fragment of a chimney. Sulphide mineralogy: pyrite and chalcopyrite; Gang minerals include barite. Small pieces of massive sulphide showing some external alteration. There are several areas of well formed barite crystals (< 2 mm). Hydrothermal alterations produce some manganese crust. Chalcopyrite seems to be remobilised and reprecipitated.
AT-262GR	37°17.509' N	32°16.925' W	1720	Fragments of large pillows 0.8 – 1 m in diameter, glassy skin, plagioclase phyric up to 15 %, vesicular up to 25 %. Oxidised red/orange with Mn coating and green (atacamite) staining. Mn oxide especially thick (1 mm) underneath pillow.
AT-263D	37°23.425' N 37°23.337' N	32°13.502' W 32°13.075' W	2654 2579	Only a small quantity of mud was recovered. Yellowish to brown sticky mud. Same as AT 259. It has some sand as well. Very silty and well sorted.
AT-264D	37°27.285' N 37°27.303' N	32°11.753' W 32°11.620' W	2920 2910	Pillow lava of megacryst phyric (plagioclase) with some olivine 0.1 % vesicular. Ropy to smooth glassy margin up to 0.8 cm thick. Little pelagic sediment in crevices. No Mn coating. Some pelogonite alteration. Interior unaltered. Megacryst of plagioclase, some zoned, rounded and euhedral, some with melt inclusions.
AT-265GR	37°17.438' N	32°16.599' W	1685	One big sample (45 x 20 x 15 cm) + 5 smaller samples (10 – 15 cm). Hyaloclastite made of different layers with different colours. Cuting the depositional structures a silicified black massive and hard material. In this material there are disseminated small mm grains of pyrite. Each layer has a thickness of 0.2 – 0.5 cm with mm grain size.
AT-266GR	37°17.448' N	32°16.610' W	1692	Silicified breccia. Small pillow fragments very altered. 50 % vesicularity 1 - 2 mm. External manganese layer 1 mm thick. A rectangular clast (3 x 1 cm) with chlorite alteration observed. More vesicules observed. Other zones are massive and seem to be hyaloclastitic fragments. Small cavity with millimetric vitreous lustre minerals (not identified). Some zones are oxidised (orange/brown colour).
AT-267GR	37°17.332' N	32°16.551' W	1710	Fragment of a chimney. Sulphide mineralogy: pyrite, chalcopyrite and sphalerite? Gang minerals: barite 1-3 mm. Millimetric to centimetric chimneys. Mainly pyrite. Chimney walls are formed by pyrite and chalcopyrite. Probably sphalerite filling the chimney channel

Table 4. Continuation

AT-268GR	37°17.361' N	32°16.525' W	1700	Sulphide mud, poorly sorted. Dark brown but some fragments also present. Layer is coarse clasts and plagioclase crystals at bottom. Finer at top. Slump like structures with sediment clasts . Layers of glass and fresh vesicular lava. Base of hyaloclastite is mud. Coarse to fine upward grading volcaniclastic deposit.
AT-269G	37°17.980' N	32°19.303' W	2026	About 17 cm long sequence of silty-clayey sand and foraminiferal ooze.
AT-270D	37°17.896' N 37°17.839' N	32°18.860' W 32°18.633' W	1771 1730	Three small fragments; silica rich with millimetric metallic minerals (pyrite). Very similar to sample AT 255 GR. Without any vesicularity.
AT-271GR	37°17.461' N	32°16.924' W	1712	Active hydrothermal vent. Fragment of chimneys. Sulphide mineralogy: pyrite, chalcopyrite and sphalerite. Gang minerals: anhydrite, barite and silica. Some of the channels are filled by unconsolidated sphalerite (black powder). There is abundant amorphous silica. On one sample it is possible to see the mineralogical zonation typical of the hydrothermal processes: From the centre to the periphery - pyrite; sphalerite; sphalerite + chalcopyrite (+ bornite (??)) - pyrite - anhydrite.
AT-272GR	37°17.588' N	32°16.858' W	1710	Active chimneys. Sulphide mineralogy: pyrite; chalcopyrite and sphalerite. Gang minerals: anhydrite and silica. Copper rich massive ore mainly formed by pyrite and chalcopyrite. Chalcopyrite with strong alteration, showing blue - red tints. Chimneys of massive ore with several sizes. Oxidation on the outside; manganese crusts -hydrothermal oxidation by diffuse discharge.
AT-273GR	37°17.446' N	32°16.611' W	1675	Fragments of chimneys. Sulphide mineralogy: pyrite, chalcopyrite, sphalerite and tetrahedrite-tenantite (?). Gang minerals: anhydrite (?) and silica. Massive copper rich ore. Five samples. Some channels filled by massive chalcopyrite.
AT-274GR	37°17.682' N	32°16.857' W	1660	Reddish brown clayey gravel. poorly sorted probably sulphide mud. Some angular rock fragments in gravel size. Some white fragments. Same as AT 247.
AT-277GR	37°17.270' N	32°16.543' W	1707	Active vent. Several centimetric to decimetric chimneys covered by anhydrite. Sulphide mineralogy: pyrite, chalcopyrite and sphalerite. Gang minerals: anhydrite. Massive sulphide - mainly pyrite. Grain size fine to very fine. Internal texture of the chimneys show rapid grow of the anhydrite through the fluid flow direction. No alteration (inside or outside).
AT-278GR	37°17.472' N	32°16.524' W	1665	Three pieces of massive sulphides. Sulphide mineralogy: pyrite, chalcopyrite and sphalerite. Gang minerals: anhydrite (?). Ore formed mainly by pyrite (> 90%), some sphalerite and rare chalcopyrite. Sphalerite sometimes occurs as layers into a fine-grained pyrite. Intense external alteration. Ore samples associated with red sediments (mud). Some holes in the massive sulphides filled by sub-milimetric chalcopyrite and / or sphalerite crystals. Layers of very fine massive pyrite.
AT-279GR	37°17.400' N	32°16.625' W	1703	Dark/rusty clayey sandy gravel, runny, very poorly sorted material. Hylaoclastite, lower layers (1 cm thick) of green glass shards-middle layer of shell debris (mussels), upper layer 0.5 cm of black glass with beds of glass 1 - 2 mm in diameter.
AT-280GR	37°16.484' N	32°15.799' W	1750	Fragments of basalt. Sheet flow with glossy margin. Avesicular, plagioclase phyric.
AT-281D	37°18.800' N 37°18.795' N	32°15.685' W 32°16.175' W	1880 1750	Fragmented welded pillow type crusty lava. Infolds of glass skin into a glassy interior. Aphyric and avesicular.

ly on steep slopes, confirming the TOBI 30 kHz sidescan sonar imagery and submersible observations of small hummocky mounds in this area. These are aphyric and avesicular (<1%) with vitreous matrix. The glass margins are mostly weathered or absent.

On the eastern central plateau, several tall and steep peaks are observed on the TOBI images. Sampling these recovered two flow types: glassy sheet flows, 5 cm thick with droop and drip structures underneath that are plagioclase phyric (5%) and moderately vesicular (<40%) with Mn coating especially to the under side. A dead and Mn-blackened coral sample was also taken here. The other flow type is pillowed with a few megacrysts of plagioclase (<2 cm long) and less than 1% of olivine crystals, 1-2 mm long. These samples are avesicular, rubble textured with infolds of glass altered to palagonite and iron-oxide stained. The matrix is vitreous.

Samples from mid-way along the northern half of the segment are of pillow and sheet flows. The pillows are rubble textured with infolded glass, avesicular and aphyric with palagonite alteration. The sheet flows include some lobate or pillowed structures, are plagioclase phyric with olivine enclosed in the plagioclase, and have a glassy avesicular matrix. The glass is fresh and virtually unaltered.

The far northern site recovered avesicular pillow lavas with megacrysts of plagioclase (<1.5 cm long) enclosing some olivine (1-2 mm) towards their outer margins. These samples are fresh and have a coating of iron oxide only.

Geological Interpretation of Volcanic Evolution

The central volcanic complex is a composite feature. Interplay between brittle tectonics and volcanic activity is linked to magma evolution and styles of eruption. From the evidence collected by previous studies and the new data collected during this cruise, a model is proposed for the tectono-volcanic evolution of this complex.

A volcanic stratigraphy is identified based on the position, degree of alteration and sediment cover and relative stratigraphic ages of lavas derived from sidescan sonar imagery. The following model is based on mechanisms of magma buoyancy to control the maximum height of the central volcanic complex. The buoyancy mechanism is the result of density differences between the column of magma (from the surface to the depth of magma storage) and the basaltic crust forming the ocean floor. Volcanic eruption is limited and ceases when the height and density of the magma column feeding the top of the volcanic complex is equal to the depth and density of the crust overlying the magma reservoir. Thus the maximum height of the central volcano is achieved when the magma and crust are in isostatic equilibrium.

The oldest lavas form the base of the volcanic plateau and are avesicular, aphyric glassy pillow types. These were erupted relatively slowly forming moderate gradients at their flow fronts that combined to form lobate terraces. These terraces are visible on the bathymetry data especially to the southeast of the central cones and also form the western and eastern flanks of the plateau. At this time, tectonic activity was compensated for by eruption and no major graben system was formed. As the plateau grows in height, reaching some 200 m above its base, pauses in volcanic activity allowed tectonic strain and subsidence to accumulate. This resulted in the eruption of more fractionated lavas that included large megacrysts of plagiocase. Emptying of the magma reservoirs and/or convective overturn caused by replenishment by new batches of melt at this time allowed olivine crystals to be stirred-up from the base of the magma chambers and erupted with the megacrysts of plagioclase. The relatively evolved composition and presence of megacrystals of plagioclase lead to a local increase in viscosity of the lavas allowing steep features to form such as those on the western central plateau.

At the top of the volcanic complex, the three volcanic cones represent the maximum height of the volcano. As they represent isostatic equilibrium between the magma column and crustal depth to the magma chamber, further volcanic eruption either ceases or can only occur if the magma density decreases. In the case of the three cones, magmatic evolution has occurred allowing plagioclase crystals to grow and increasing the volatile content of the magma. Assimilation of altered crust may also

have increased the volatile contents of these magmas during long residence time in a magma chamber beneath the complex. Despite a depth of 1700 m, the volcanic activity at these three cones was pyroclastic, with the formation of hyaloclastite and volcanic breccias. Lenticular structures in the bedded hyaloclastite recovered from the depression between the three cones, and the coarsening-upwards grading of some layers indicate surge deposition during volcanic explosions. Magma vesiculation, of up to 90% in these lavas, assisted explosive eruption and magma fragmentation causing the pyroclastic deposits. Evidence of layers of shell debris and oxidised horizons between hyaloclastic layers indicates that the explosive activity was sporadic. Concentric faulting of the summits of two of the three cones indicates that gaseous eruption and explosive activity led to partial subsidence of the summit. Although explosive, the volcanic activity at this time was of a low volume.

At some time during the pyroclastic activity of the three summit cones, tectonic deformation became dominant over volcanic accretion. The result was graben formation, and subsidence by at least 100 m, of the central volcanic complex. Because the volcano was now no longer in isostatic equilibrium, magma effusion rates rapidly increased resulting in extensive sheet flow formation that partially infilled the newly forming graben. Initially these sheet flows were vesicular and plagioclase phyric, having essentially the same composition as the three pyroclastic cones. However, later sheet flows were aphyric and avesicular, reflecting the degassing of the magma and its replenishment by new magma batches.

The northern-most sheet flows in the segment are aphyric but contain some megacrysts of plagioclase with minor olivine. This reflects rapid effusion but after long magma residence time. The low volatile content may indicate a different mantle composition for these rocks. The presence of both large megacrysts of plagioclase and small olivine crystals may indicate that a new batch of primitive magma entered the magma chamber immediately before the eruption, and perhaps triggered the eruption by magmatic overturn.

Links between volcanic and hydrothermal activity

Hydrothermal activity has affected mainly the pyroclastic deposits. The younger sheet flows and the lava lake in the central depression are not involved in hydrothermal mineralsation. This indicates that the most intense hydrothermal circulation was established during the period of magma accumulation and volcanic stagnation. This was also the time of pyroclastic activity and formation of the summit cones.

The off-axis bathymetry for the Lucky Strike segment shows that the formation of the central volcanic complex has been a long-lived process in this region of the Mid-Atlantic Ridge. If the above model linking volcanic and tectonic cyclicity to hydrothermal activity is correct, than a test for the hypothesis will be the presence of relict pyroclastic deposits and hydrothermal deposits on the summits of the off-axis remains of the central volcanic complex What is unclear at this stage is the timing of the cycles of activity. However, the thickness of the lithosphere in the segment centre, and its ability to accumulate stress before brittle failure during which time volcanic stagnation occurs resulting in sporadic low volume eruption, the formation of a magma chamber, and the establishment of hydrothermal circulation is probably the key to the duration of the volcano-tectonic cycles.

III. NORTH-EAST ATLANTIC EUROPEAN MARGIN (LEG 3)

III.1. PORCUPINE SEABIGHT MOUTH: SHORT STUDY

A. AKHMETZHANOV, N.H. KENYON, B.CRONIN AND M. IVANOV

Continental rises are believed to be depocentres for terrigenous sediment fed from the continental shelf. The floor of the Bay of Biscay has well developed canyon mouth fans that are still active during the Holocene (Zaragosi et al., 2001) but little is known of the neighbouring rise, west of the Porcupine Seabight (Fig. 25). The Porcupine Seabight lies west of the Celtic Sea and of the western Irish shelf. The Gollum Channel, an unusual tributary channel system draining the southern Porcupine Seabight, has been mapped by Kenyon et al. (1978). Initial study of cores, deep towed sidescan sonar and high-resolution seismic profiles during TTR-7 cruise (Kenyon et al., 1998) show that the Gollum

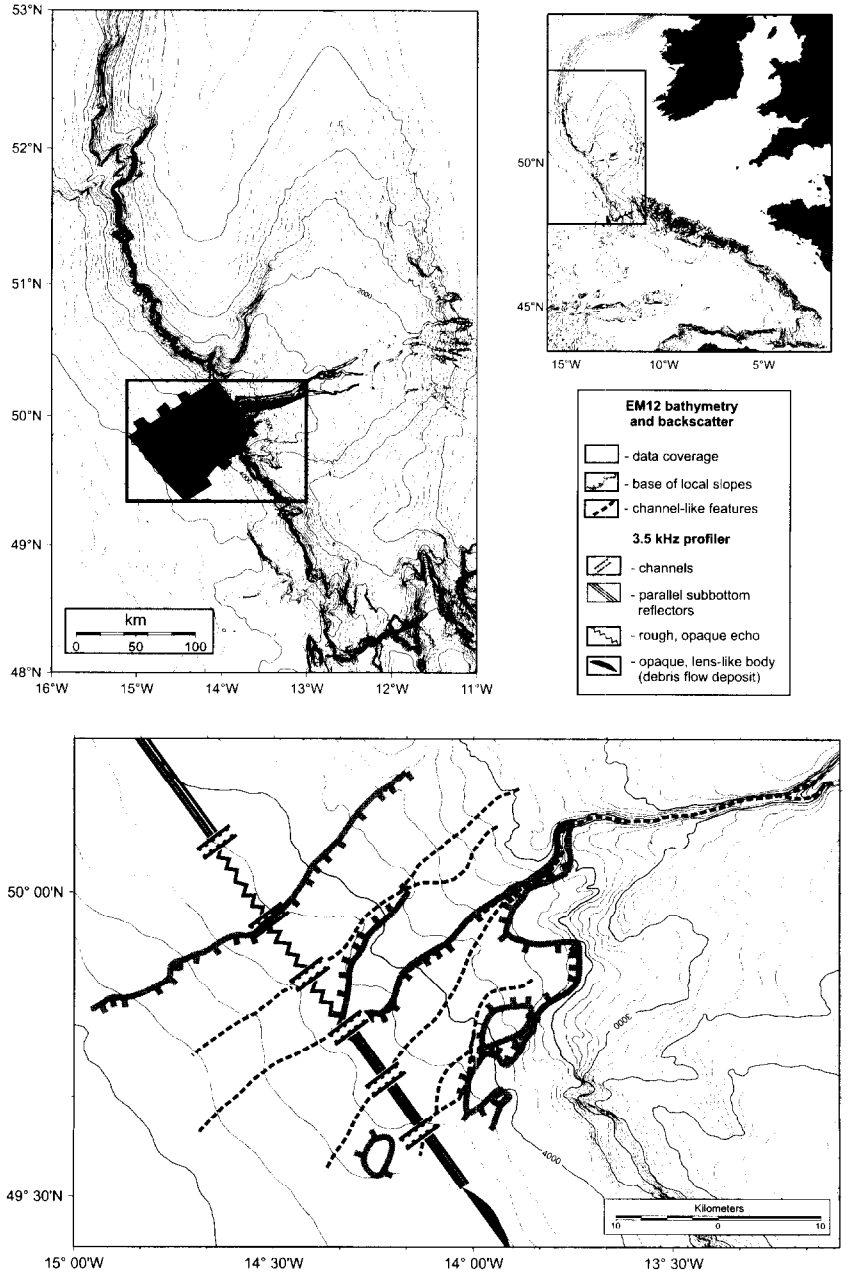

Figure 25. Location map and interpretation of data of the 3.5 kHz survey across Porcupine Seabight mouth.

Channel system is relatively inactive. The rise is mapped here for the first time by an EM12 swath bathymetry system (Charles Darwin Cruise 116) and further investigated by a high resolution seismic profile obtained during the TTR-10 cruise on the transit to the eastern Rockall Trough.

The floor of the Porcupine Seabight is bounded by a relatively steep step down to the continental rise. The Gollum Channel is about 400 m deep where it makes a sharp turn to the south to cut through this step (Fig 25). On the rise a number of shallow channels (20-30 m deep) can be recognised on the bathymetry but only two of them can be seen on the map of backscattering values. Both of the latter seem to emanate from the Gollum system. One is traceable to the edge of the newly mapped area and is slightly sinuous, the other is straight. The single 3.5 kHz profile shows crossings of both of these shallow channels (Fig. 26). More small channels connect with V shaped re-entrants in the foot of the neighbouring slopes. There appears to be a broad deep in front of a prominent valley in the southern end of the Porcupine Bank. This valley is a prominent feature in the digital GEBCO bathymetric map (Fig. 26), originally compiled for this region by Hunter and Kenyon (1984), and seems to start well down the slope. A rough, opaque echo, believed to be characteristic of terrigenous deposition (e.g. Damuth, 1975), is limited to this deep. It is interpreted to be the result of either turbidites and/or a debris flow deposit that has come from the valley in the southern Porcupine Bank. The profile across the channels that extend from the Gollum Channel system has a different character, being smoother and with some subbottom refectors (Fig. 26). This character could represent fine grained overbank turbidites and/or hemipelagic sedimentation.

In conclusion it seems that the Gollum Channel system has been relatively inactive during the Holocene compared to the nearby margin of the Bay of Biscay. Holocene bedload transport paths feed the shelf edge above the active deep sea Celtic Fan with sand (Johnson et al., 1982) whereas bedload transport paths do not reach the shelf edge above the Gollum Channel system.

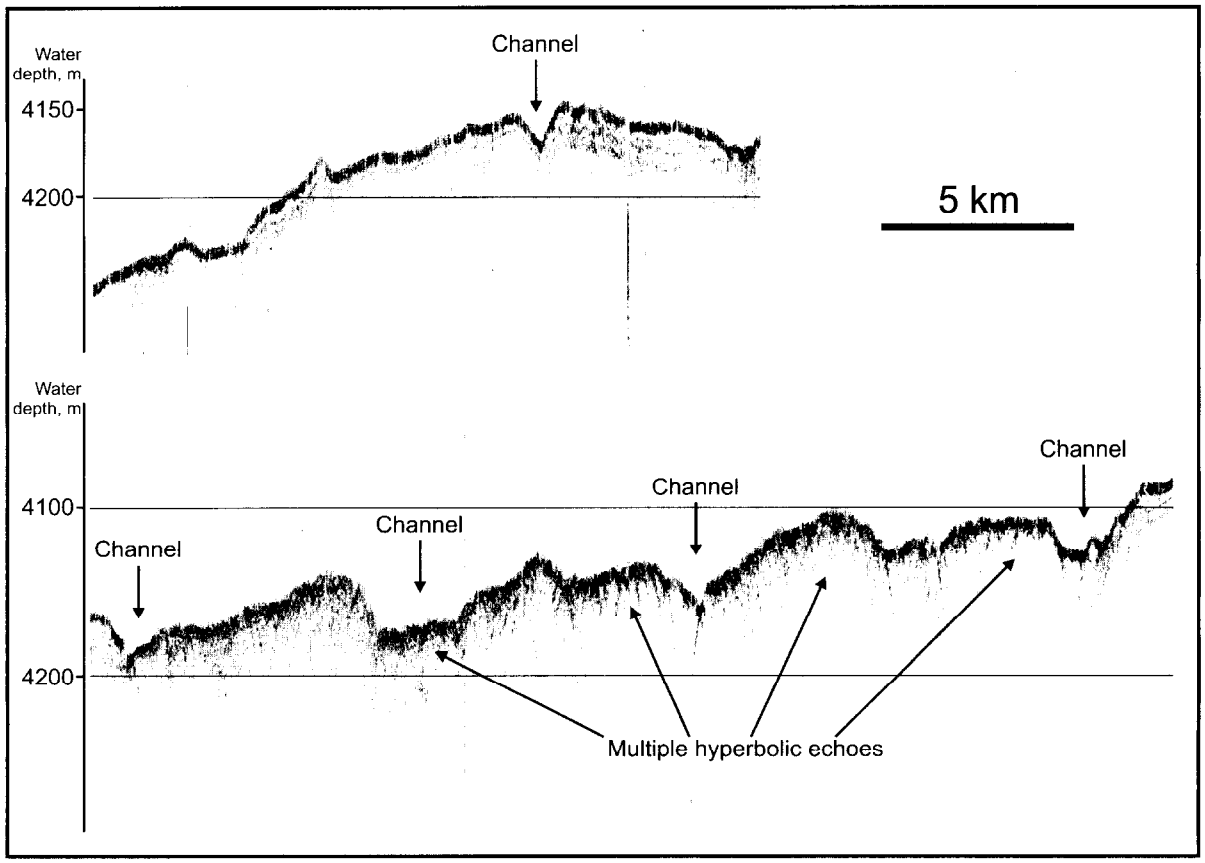

Figure 26. Fragments of 3.5 kHz record showing the character of the seabed in the area beyond Porcupine Seabight Mouth.

III.2. NORTHEASTERN ROCKALL TROUGH MARGIN

III.2.1. Introduction

A. AKHMETZHANOV, B. CRONIN AND M. IVANOV

The increase of oil exploration activities in deep-water parts of the European continental margin have led to a requirement for environmental surveys. These have been undertaken on the Rockall Trough margins in the period of 1996-99. An extensive set of sidescan sonar date has been obtained providing a detailed picture of the modern geological processes taking place on the continental margin. The development of canyon systems and slope instability features are the most important issues in the area.

9.5 kHz GLORIA and 30 kHz TOBI imageries have been obtained over a series of canyons south of the Donegal Fan. The canyons have well seen finger-like heads. Where mapped they have a uniformly low backscattering material within them. It is believed to be sand but its nature is not clear. The possible options are a deposit of a coarse grained contourite or sand spillover from the shelf, as along slope transport of sand is known from the upper slope (Kenyon, 1986). The canyons have a narrow waist and then open into areas on the lower slope where there are fields of small sediment waves. High backscatter on the sidescan sonographs suggest that they may be gravels. There is not much evidence for sand body architecture from the lobes beyond canyons. An investigation of the canyon mouth lobe could resolve several questions such as:

- What type of deposits does one get laterally and distally from the wave fields?
- Are there any debris flow deposits?
- Can one divide the lobe into zones, as on the Bering Sea lobes (Kenyon and Millington, 1995)
- What is the date of the last event?

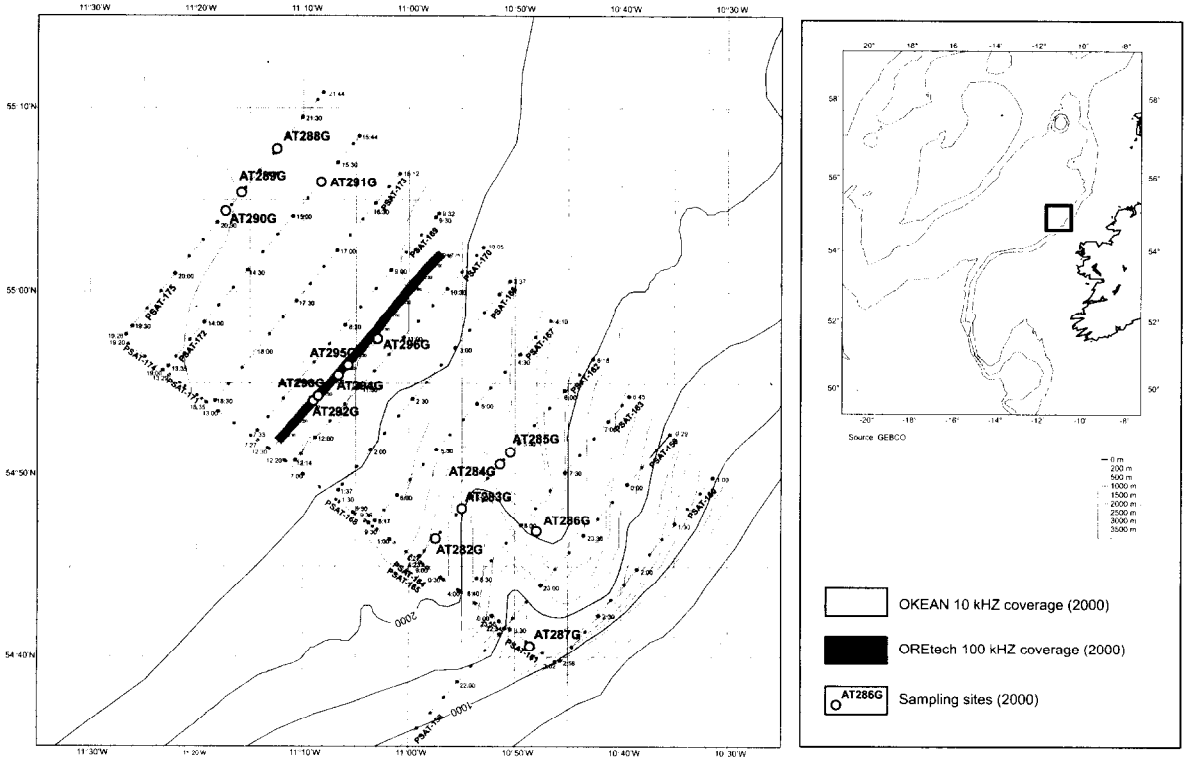

Figure 27. Location map of a canyon study area on the Eastern Rockall Trough margin.

To address these questions the investigation strategy included a preliminary survey with 3.5 kHz hull-mounted bottom profiler, 10 kHz OKEAN sidescan sonar and single channel seismic profiling. On the basis of these data a deep-towed 100 kHz OREtech line was run across the canyon mouth lobe, including crossing the sediment wave fields. Further groundtruthing was aimed at collecting cores from the upper canyon, in the canyon axis and extensively over the lobe (Fig. 27).

TOBI data are confidential and are only occasionally referred to in the text of this report.

III.2.2. Single Channel Seismic Profiling

D.J. MILLER, A. VOLKONSKAYA, I. KUVAEV, I. DENISENKO, K. IVANOVA, S. SHKARINOV, P.-M. BRUDDER, G. DUPONT

A total of 18 profiles were recorded totalling 434 km of seismic data. The survey speed was approximately 6 knots. Profiles PSAT 158, 159, 160, 162, 163, 166, 167, 169, 170, 172, 173 and 175 were acquired in a NE-SW (strike) direction and spaced at about 6 km. Profiles PSAT 161, 164, 165, 168, 171 and 174 were shot in a SE-NW (dip) direction comprising one continuous line in the downslope direction (Fig. 27).

During the interpretation of the acquired seismic lines a total of eight different sequences or seismic units were identified on a basis of seismic character, amplitude and reflector terminations (Fig. 28). In the description below, depth to sea floor is given in metres and thickness of sub-bottom - in ms TWTT.

Line PSAT 158

Line PSAT 158 is the southwestern prolongation of line PSAT 159. It extends 4 km across the middle continental slope in a slightly oblique direction in relation to bathymetric contours. The general sea floor slope direction in the profile is towards the northeast where a canyon can be seen between time marks 21:55 and 22:15. Directly northeast of this feature a large mound is seen which may be interpreted as the levee of the main canyon present in line PSAT 159. From the southwest end of the line to time mark 21:55 the sea floor topography is smooth to undulating. A channel can be observed at time mark 21:18 that appears to be the surface expression of a palaeochannel.

The acoustic basement (sequence 1), the lowermost unit, is overlain by sequence 3 where reflectors are diffuse to partially continuous towards the southwest. This unit is absent in the northeastern margin of the canyon. Acoustically transparent sequence 4 overlies sequences 1 and 3. Sequence 5 fills the paleolows left by the erosional surface which cuts into the upper part of sequence 4 and sequence 6 covers the palaeochannel deposits, between time marks 21:18 and 21:40, with high amplitude continuous reflectors (possible turbidites). Sequence 8, interpreted as a hemipelagic unit, covers most sediments on the profile. The stratigraphic relationship observed between the units on either side of the canyon implies that a fault probably controls the canyon, with the footwall being on the southwestern side and the hanging wall on the northeastern side.

Line PSAT 159

Immediately downslope from line PSAT 160 is line PSAT 159. This profile cuts the continental slope through the proximal part of the studied canyon system. The line has an approximate length of 4.2 km and water depths varying from nearly 1270 metres on highs between canyons to 1850 metres inside the canyon valleys. Sea floor relief is very irregular with one major canyon feature on the profile containing various intracanyon V-shaped channels that should represent tributary systems that feed into the main valley downdip.

As a consequence of an airgun control system failure (irregular release), the central part of this line is of poor quality, between time marks 22:45 and 0:05. However an interpretation was still

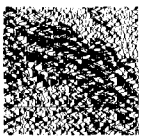

SEQUENCE 1: Acoustic basement. High to low amplitude and low frequency discontinuous reflectors on the deeper portions of the seismic section.

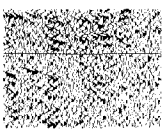

SEQUENCE 2: Partially transparent acoustic sequence with scattered low to middle amplitude chaotic reflectors. Overlies the acoustic basement in the more distal parts of the area.

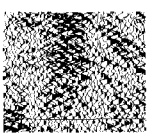

SEQUENCE 3: Low amplitude discontinuous reflectors. Overlies the acoustic basement and underlies sequence 4 in the more proximal profiles.

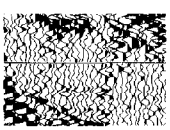

SEQUENCE 4: Acoustically transparent sequence with very scattered low to middle amplitude reflectors. Usually underlies sequence 5 and is present throughout all of the surveyed area.

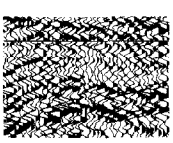

SEQUENCE 5: Discontinuous to locally chaotic middle to high amplitude reflectors. Normally overlying sequence 4 and underlying sequence 6 or slump deposits.

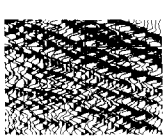

SEQUENCE 6: Continuous parallel high to middle amplitude reflectors generally overlying sequence 5 or slump deposits and underlying sequence 8.

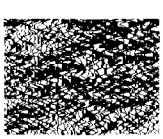

SEQUENCE 7: Continuous parallel high amplitude reflectors generally occurring in a sub-horizontal to horizontal fashion. Associated with channel/canyon fill deposits.

SEQUENCE 8: Continuous transparent sequence present on all of the area directly underlying the sea floor.

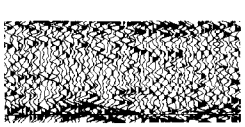

Slump deposits: Sequences with transparent to chaotic seismic character generally related to steep slopes in canyon areas or occurring as sheet deposits in the distal parts of the surveyed area.

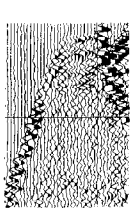

Faulted block deposits: Chaotic seismic character deposits associated to the down-thrown block of gravitational faults along steep slopes in canyon areas.

Figure 28. Brief description of the seismic sequences which were identified on the Eastern Rockall Trough margin.

attempted with the purpose of correlating with adjacent profiles.

The top boundary of the acoustic basement (sequence 1) reaches 2.65 s TWTT in the deepest part of the channel system and 1.88 s TWTT at it's uppermost level. Overlying the basement is sequence 4, an acoustically transparent unit with highly irregular upper and lower surfaces. Apparently this sequence contains most of the erosional remnants in the major palaeocanyon at this level of the system. Overlying sequence 4 is sequence 5 which is restricted to the intercanyon highs. Transparent sequence 8 overlies the higher levels of the observed canyon system sequences on this profile.

Line PSAT 160

Positioned on the southeastern extreme of the survey area, line PSAT 160 transects the canyon head region along the continental slope in a NE-SW alongslope (strike) direction (Fig. 29). Water depths range from approximately 800 m on the intercanyon highs to 1250 m in canyon thalwegs. The sea floor relief along the line is characterised by an irregular topography mainly due to the presence of three canyons occurring from the southwest end to time mark 1:40. These canyons have steep sides and V-shaped profiles, therefore being interpreted as dominantly erosive features. Between time marks 2:20 and 2:30 a subtle channel occurs which appears to be fault controlled. At the northeast extreme of the profile another discrete channel is observed.

The most basal unit appearing on the profile is sequence 1 (acoustic basement) with discontinuous high to low amplitude reflectors and upper contact at 1.45 ms TWTT on the northeast extreme. On the southwestern side of the line, sequence 3 overlies the basement, pinching out towards the northeast. Throughout most of the profile the acoustically transparent sequence 4 appears as somewhat irregular lenticular packages overlying the acoustic basement, on the northeastern and central areas, and sequence 3 on the southwestern area. Sequence 5, a thick (up to nearly 250 ms TWTT) unit with diffuse moderate to low amplitude reflectors, covers sequence 4 throughout most of the profile, except between time marks 1:40 and 2:15 where it either overlies the basement, pinches out, or was eroded away. Underlain by sequence 5 is sequence 6, displaying parallel high amplitude reflectors and an erosive upper boundary covered by probable hemipelagic sediments represented by sequence 8. From

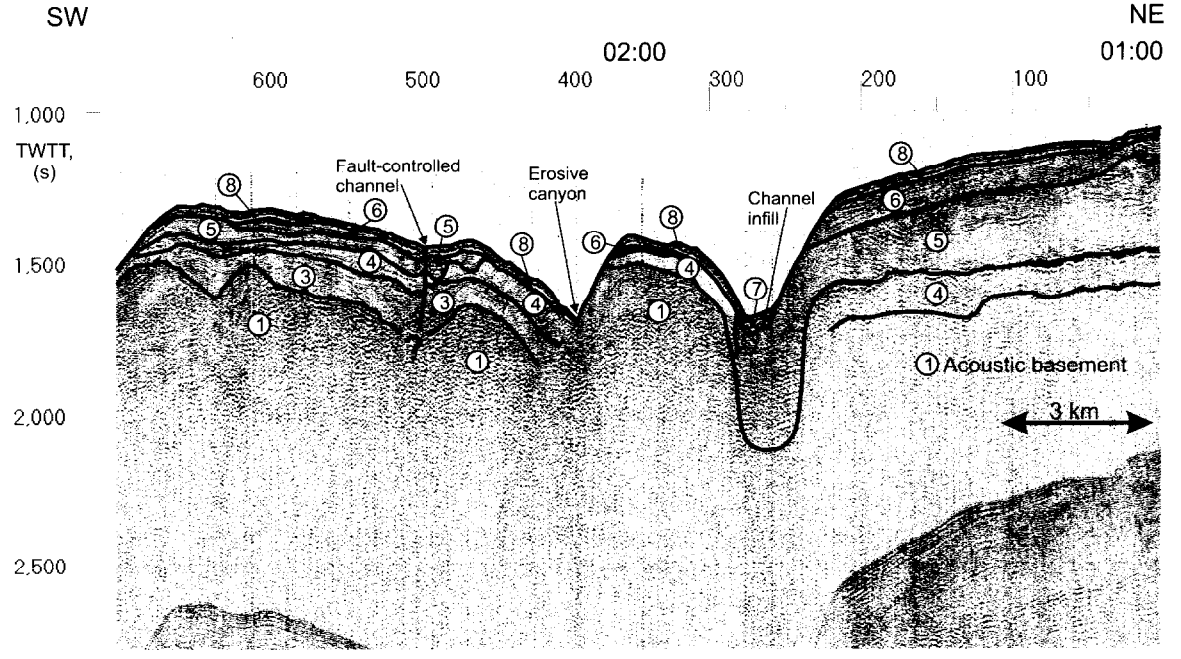

Figure 29. Line PSAT-160 depicting the seismic sequences and features present in the head area of the canyon system.Numbers indicate sequences discussed in the text.

time marks 1:50 to 2:15 sequence 8 overlies sequence 4, possibly due to erosive events in association with tectonic movements. Inside the canyon valley, between time marks 1:44 and 1:48, a parallel high amplitude reflector confined unit named sequence 7 is seen, representing channel infill deposits.

Line PSAT-161

This profile is located along the slope in a SE-NW direction. The water depth varies from1200 to 1950 m. A V-shaped channel is seen on the upper part of the section followed by a smooth slope and a mounded structure towards the north-west.

The acoustic basement with high amplitude and low frequency discontinuous reflectors (sequence 1) can be seen on most of the line. Its depth varies from 3.5 s TWTT below the sea level in the SE part of the line and reaches the sea floor at the 3:30 time mark. The acoustic basement is covered by the transparent facies 4 which underlyes the sequence 3. The thickness of sequence 4 increases downslope, reaching 3.5 s TWTT in the lowest part of the slope (NW). Sequence 5 is represented by two lens-like bodies with irregular shape. They could be either buried slumps or palaeochannels. Sequence 5 is overlain by the transparent sequence 8, which follows the sea floor and has a thickness of about 20 ms TWTT.

Line PSAT 162

Continuing down from line PSAT 163, line PSAT 162 cuts the lower continental slope of the canyon system in a SW-NE strike or alongslope direction in water depths varying from 1900 to 2400 m (Fig. 30). The line crosses a relatively irregular terrain, which is characterised by the presence of a large canyon at the centre of the profile, an apparently younger less mature canyon on the northeastern side and an undulating sea floor on the intercanyon highs. The central canyon has a clear U-shape (flat bottom) indicating that it has a dominantly depositional character. Terraces are quite pronounced on the slopes and levees are evident on the flanks. Palaeochannels are present on the higher terrains.

Sequence 1 (acoustic basement) appears only on the central part of the profile as irregular,

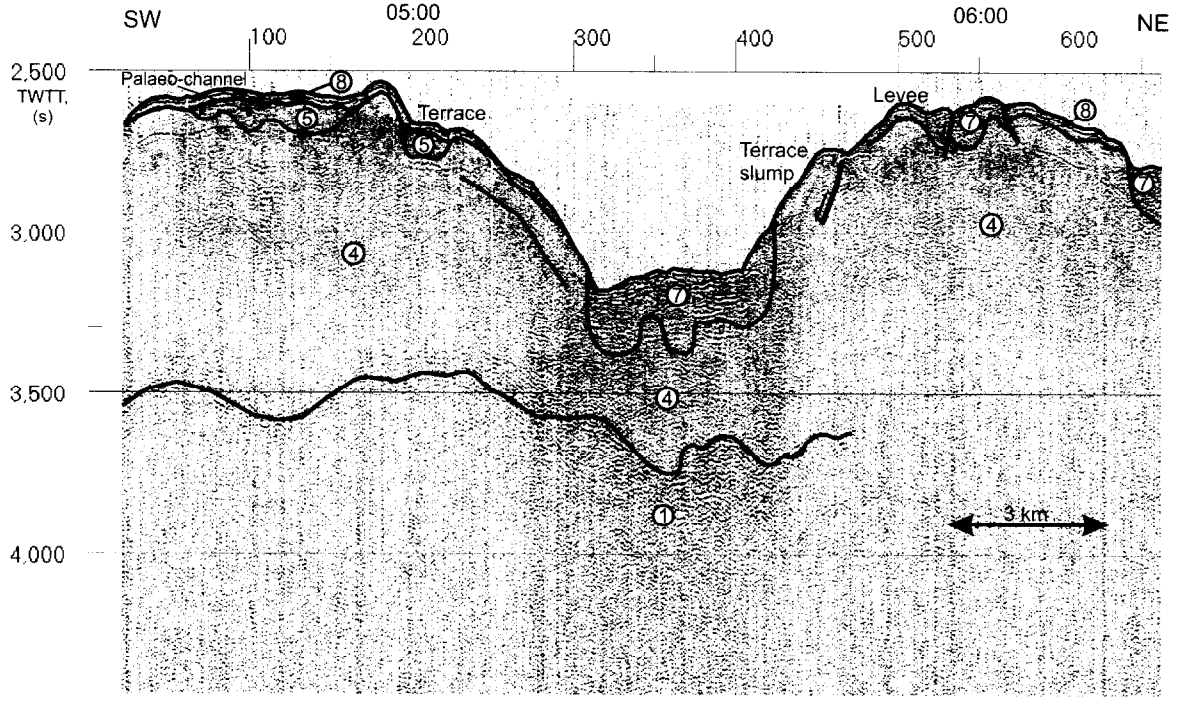

Figure 30. Line PSAT 162 showing the seismic sequences and the most prominent features on the lower slope part of the canyon system.

moderate to low amplitude, locally faulted reflectors. A very thick sequence 4 overlies the basement with a high irregular upper surface. The palaeochannels forming this erosive surface were filled by sequence 5, which is characterised by moderate amplitude diffuse reflectors. The topmost sequence on intercanyon highs is sequence 8, which is not continuous along all the profile. Both canyons seen on the profile are filled by sub-horizontal to horizontal high amplitude reflectors onlapping on either side of the troughs comprising sequence 7. Gravitational faults are identified on the northeastern palaeochannel and on the northeastern flank of the central canyon. Slump deposits associated with the terraces are also observed on the profile.

Line PSAT 163

Running in a NE-SW alongslope (strike) direction, line PSAT 163 is immediately downslope from line PSAT 159. It transects the canyon system along the middle to lower continental slope and has depth ranges from approximately 1650 m at the southwest end to 2230 m inside the deepest canyon. The seabed topography is characterised by two canyons in the central area of the profile. These canyons are U-shaped with relatively confined thalwegs and steep sides. In the southwestern part of the profile, the sea floor relief becomes undulating with two mounds that might represent levees from adjacent channels. The largest of these mounds, between time marks 8:10 and 8:20, is underlain by an acoustic turbid zone that can be interpreted as a fracture zone, a side echo or even a gas pocket, despite the fact that no fluid escape features are known in this area. The central intercanyon high displays a peculiar channel feature at its top with possible infill deposits. The upper outer edge of the southwestern canyon appears to have a fault related slide deposit on the down-thrown block of the fault.

Identified as the most basal unit on this profile is sequence 1, the acoustic basement, which is overlain by a transparent thick (400-800 ms TWTT) sequence 4. Towards the northeastern end of the profile a topographic high displays sequence 5 overlying sequence 4 with very unusual concave up reflectors being covered by the acoustically transparent and convex up sequence 8. In order to explain the origin of this feature a complex combination of geologic processes would be necessary. Perhaps, some type of uncommon seismic artifact may have produced such a feature. If so, seismic modeling would be necessary to prove such a hypothesis. On the opposite side of the line (SW) sequence 6, with continuous high to moderate amplitude reflectors, overlies sequence 4. On the same side sequence 8 truncates sequence 6 and pinches out against the canyon wall. Inside the northeastern canyon, from time marks 7:20 to 7:30, channel fill deposits onlapping on to the canyon walls compose sequence 7. Slump deposits are observed on either side of the central intercanyon high.

Line PSAT164

The survey was interrupted because of the problems with the air gun.

Line PSAT165

This line is located in the SW part of the study area. The water depth is around 1365 m at the beginning of the line (SE) coming down to 2475 m at the 1:20 time mark. It is a high sloping dip line running down the middle to lower continental slope and reaching the continental rise, where it becomes flatter. A mound is observed at time mark 0:30 where a small channel is present on the southeastern side.

Four different acoustic sequences are recognised on this line. The acoustic basement (sequence 1) is marked by low to middle amplitude and low frequency discontinuous reflectors on the deeper part of the seismic section and is covered by sequence 4. The thickness of this sequence is about 200 ms TWTT at the beginning of the profile and reaches almost 400 ms TWTT at the time mark 0:30 after which it remains constant to the end. This acoustically transparent sequence with very scattered low to middle amplitude reflectors is the thickest unit observed on the current seismic data. Transparent

sequence 8 which covers sequence 4 is observed in three places at time marks 0:05, 0:30 and 1:05. It represents deposits located directly under the sea floor and its thickness is about 20-25 ms TWTT. Acoustic sequence 7 which is characterised by continuously parallel reflectors occurring in a horizontal fashion appears on the uppermost and lowermost parts of the slope. It is hard to detect the base of this section since the amplitude fades gradually. The thickness of this unit varies from 100 ms TWTT at the deepest part of the infill and pinches out laterally. There are two slump bodies in the middle of the line, which covers a large part of the slope.

Line PSAT 166

Characterised by the presence of three very well defined canyons, line PSAT 166 is located on the continental rise from a depth of 2325 to 2550 m. Its direction is SW-NE, running parallel and downslope from line PSAT 167. The three canyons display quite evident channel infill deposits and a broad U-shape profile (depositional character).

The basal unit (sequence 1) can be identified at an approximate depth of 2900 m showing faint and discontinuous low to locally high amplitude reflectors. With a thickness from 200 to 700 ms TWTT, sequence 4 overlies the basal unit (acoustic basement) displaying a transparent seismic character and an erosive unconformity as an upper boundary. Between time marks 3:08 and 3:12 and at the northeastern end of the profile, sequence 6 appears as continuous moderate amplitude reflectors overlying sequence 4. Channel infill deposits represented by sequence 7 onlap onto sequence 4 in the three canyons. Although not continuous through the entire profile, transparent sequence 8 covers the upper layers with an average thickness of 35 ms TWTT. Significant slump deposits are present from time mark 2:50 to 3:15, associated with canyon slope instabilities.

Line PSAT 167

Located in the central part of the surveyed area, line PSAT 167 has a NE-SW direction transecting the lower slope portion of the canyon system in a strike or alongslope direction. The sea floor relief is complex with a water depth variation of 2170 to 2520 m. Two canyons, which display the presence of channel fill and slump deposits, are crossed by the line. A third canyon, also showing these types of deposits, can be partially observed at the southwestern end of the profile. The U-shape profile of the canyons implies that, at the present stage, they appear to have a more depositional character rather than an erosional or by-pass nature.

On the deeper levels of the line the acoustic basement (sequence 1) is represented as a unit of low to moderate amplitude reflectors unit between 4.05 and 4.15 seconds TWTT. Overlying it is the acoustically transparent sequence 4, which can reach a thickness of up to 1 second TWTT. Below the central canyon, sequence 4 is overlain by sequence 5 which presents discontinuous low to moderate amplitude reflectors and a thickness of 180 ms TWTT. The contact between these latter units can only be traced between the 5:00 to 5:25 time marks which makes it discontinuous throughout the section. Overlying sequence 4, between time marks 4:40 and 4:45, is sequence 6 displaying continuous high amplitude reflectors. Inside the canyons, continuous high amplitude parallel sub-horizontal to horizontal reflectors are observed corresponding to sequence 7 (channel fill deposits). Covering all units above is sequence 8, an acoustically transparent package directly below the sea floor. Slump deposits appear to be present along the slopes of the central and northeastern canyons.

Line PSAT 168

Line PSAT 168 is located in a SE-NW direction. The water depth varies from 2470 m at the beginning to 2640 m at the end of the line. The bottom topography is almost flat along the line, but between 6:35-6:50 time marks two hill-like structures can be observed. They are separated by a low flat rise.

The acoustic basement is marked by high amplitude and low frequency discontinuous reflectors. Acoustically transparent sequence 4 with very scattered low to middle amplitude reflectors covers the acoustic basement along the whole line. From time mark 7:07 to the end of the line partially transparent acoustic sequence 2 with scattered low to middle amplitude chaotic reflectors can be observed. It is situated in the middle of unit 4 and has a thickness of up to 180 ms TWTT. Between time marks 6:35-6:56 a wide and gentle uplift, where sequence 4 reaches the sea floor, can be observed. Both sides of this uplift are controlled by subvertical normal faults. To the southeast of this uplift the sedimentary succession that covers sequence 4 consists of a lens-like body of canyon fill deposits (sequence 7), which is 150-500 ms TWTT thick. Directly underlying the sea bottom is a continuous transparent sequence 8. Its present thickness is 20-40 ms. To the northwest of the uplift (time mark 7:10) sequence 4 is covered by a thin (max thickness 20 ms TWTT) sequence 5 with discontinuous to locally chaotic middle to high amplitude reflectors. On top of sequence 5 an acoustically transparent buried slump body can be observed. Sequence 6 with continuous parallel high to middle amplitude reflectors overlies this slump. It has a thickness of 100-150 ms TWTT. Right below the sea bottom, sequence 8 overlies sequence 6 downdip from the uplift.

Line PSAT 169

With a SW-NE alongslope (strike) direction, line PSAT 169 crosses the canyon system along the continental rise. It's depth varies from 2600 to 2700 m. The sea floor relief is gentle, showing a slightly higher slope on the northeast side than on the southwest side of the line.

The lowermost unit identified is sequence 1 (from 3.9 to 4.1 seconds TWTT) which represents the acoustic basement. Through the northeastern half of the profile (from time mark 8:30) sequence 2, with low to moderate amplitude intermittent reflectors, overlies the acoustic basement. It's thickness reaches 180 ms TWTT. However, in the southwestern half the acoustic basement is overlain by a thick acoustically transparent sequence 4, which is underlain by sequence 2 in the northeastern half. Directly above sequence 4 occurs sequence 5 with very discontinuous reflectors, a thickness of 20 to 120 ms TWTT and a highly eroded upper surface where four buried slump deposits are clearly observed. Overlying sequence 5 and the slump deposits is sequence 6, a unit with a thickness of 20 to 40 ms TWTT and continuous high to middle amplitude reflectors which may represent turbiditic deposits accumulated on paleolows. Sequence 8 covers all of sequence 6 and a buried slump, portraying a transparent character with a thickness of up to 60 ms TWTT, on the southwestern end of the profile.

Line PSAT 170

As in line PSAT 166, which is immediately upslope, line PSAT 170 also displays three canyons along the profile. However, in this line the canyons show a broader cross-section, lens like convex up infill deposits and lower intercanyon areas, indicating that the profile crosses a highly depositional site. The line has a NE-SW direction crossing the distal part of the system in an alongslope trend across the continental rise. The average water depth along the line is approximately 2520 m. The bottom topography is smooth with the most elevated part on the northeastern side.

Sequence 1 (acoustic basement) is overlain by sequence 2, which is represented by a package of low to middle amplitude reflectors. Above sequence 2 occurs sequence 4, displaying elevated thickness (mainly in the northeastern end), acoustic transparency and an irregular erosional upper contact. Occupying the palaeovalleys is sequence 5, which was deposited over sequence 4 and underlies sequence 7 (a continuous parallel high amplitude reflector unit). This latter sequence is also a channel fill related unit. Long sheet / lens-like slump deposits occur within sequence 7 and over sequence 5 (towards the southwestern end). The most recent sediments (sequence 8) drape the entire profile with an average thickness of 40 ms TWTT. Two faults are interpreted at time marks 10:25 and 11:10, which indicate that the northeastern and central canyons are probably fault controlled.

Line PSAT 171

Trending SE-NW line PSAT 171, is a relatively short profile connecting lines PSAT 170 and PSAT 172. This profile is located across the continental slope and crosses the distal part of a canyon. The relief of the sea floor is regular and water depth is approximately 3345 m. This line is characterised by the following overall subsurface architecture.

The top of the acoustic basement is very visible along the line and represented by low to middle amplitude and middle frequency continuous reflectors. It is covered by transparent acoustic sequence 2 with scattered very low amplitude chaotic reflectors. Sequences 5 and 6 are both moderate to low amplitude packages. They are not very well visible along the line. Between sequence 5 and sequence 6 is an acoustically transparent body, which could be a buried slump. The uppermost sequence in this succession is the continuous transparent sequence 8, present on all the line and directly underlying the sea floor. Its thickness is 30 ms TWTT.

Line PSAT 172

Line PSAT 172 is the next line in the downslope direction of line PSAT 173. It runs SW-NE in water depths of approximately 2650 m along the distal part of the surveyed area on the continental rise. Sea floor relief is very smooth with a slight increase in slope and elevation towards the northeast. All layers within the sedimentary succession appear to be lying horizontally to sub-horizontally.

The oldest sequence on the profile is sequence 1 (acoustic basement). Overlying it is the sequence 2 with a relatively constant thickness (around 360 ms TWTT) and low amplitude discontinuous reflectors on its upper levels. Covering sequence 2 is sequence 4, showing a transparent acoustic character, much like the lower and middle levels of sequence 2. Above sequence 4 a, unit with moderate to high amplitude reflectors and 30 to 100 ms TWTT in thickness was identified as sequence 5. Sheet-like to tabular massive buried slump deposits overlie sequence 5. These deposits show an increase in thickness in the downslope direction. Sequence 6, displaying high amplitude parallel bedding reflectors, overlies the slumps through much of the profile and may represent distal turbiditic deposits. Sequence 8 drapes all the sedimentary succession, displaying an average thickness of 40 ms TWTT. A fault was interpreted at time mark 15:23, which might be responsible for the observed offset of the layers in the northeastern end of the profile.

Line PSAT 173

Line PSAT 173 is a NE-SW trending line that cuts the distal part of the canyon system on the continental rise in an alongslope (strike) direction. Depths range from 2625 to 2760 m. The seabed topography is soft with a slightly higher relief at the northeastern side of the profile (Fig. 31).

The acoustic basement occurs as a series of low amplitude diffuse reflectors on the deeper part of the section. Overlying it is sequence 2, with scattered low amplitude discontinuous reflectors and thickness of approximately 300 to 400 ms TWTT. Directly above it lies sequence 4, with overall low amplitude to transparent seismic character and thickness from 60 to 180 ms TWTT. Underlain by sequence 4 is sequence 5 represented by diffuse to partially continuous reflectors, maximum thickness of 95 ms TWTT and highly eroded upper boundary. A continuous sheet-like sequence of buried slump deposits covers sequence 5 with an irregular to undulating upper contact. The topographic lows left by the irregular slump upper boundaries were filled by sequence 6 that might represent distal turbidite deposits considering the continuous high amplitude nature of its reflectors. Sequence 8 tops the whole stratigraphic sequence with a rather uniformly thick (40 ms TWTT) transparent layer.

Line PSAT 174

Line PSAT 174 has a SE-NW downslope direction. The water depth varies from 2670 m at the

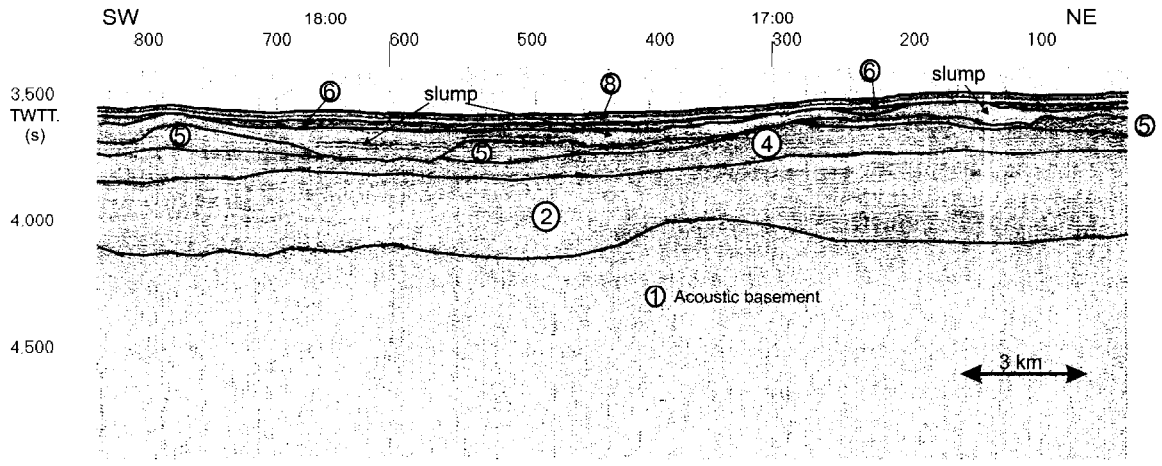

Figure 31. Line PSAT-173 displaying the main seismic sequences present on the distal part of the system.

beginning of the line and slowly increases to 2715 m at the end of the line. The relief of the sea bottom is almost flat.

High amplitude and low frequency discontinuous reflectors mark the acoustic basement on the deepest part of the seismic section. It is covered by a partially transparent acoustic sequence 2 with low to middle amplitude chaotic reflectors. The base of this sequence varies from a depth of 4160 ms TWTT (beginning of line) and slowly increases to 4275 ms TWTT (end of line). Sequence 2 has a thickness of about 340-370 ms TWTT. The top of this sequence is represented by a high frequency, middle amplitude reflector. Acoustically transparent sequence 4, with scattered middle to low amplitude reflectors, overlies sequence 2 and underlies sequence 5 on the rest of the line. The base of sequence 5 is located at a depth of 3680 ms TWTT at the beginning of the line (SE), with an extreme of 3650 ms TWTT at time mark 16:45, slowly decreasing to 3690 ms TWTT from 16:45 to the end of the line (NW). Slump deposits with transparent to chaotic seismic character unconformably overlie sequence 5. The base of the slump deposits varies from a depth of 3660 to 3710 ms TWTT and is quite regular. They are about 50-60 ms TWTT thick and their base is seen by changing amplitudes of the reflectors from high to low. Sequence 5 has a maximum of around 95 m thickness at the beginning of the line (SE). The base of this sequence is characterised by changing amplitudes of reflectors from low to high. Sequence 6 with parallel high amplitude reflectors overlies the slump deposits. The youngest sequence 8 with continuous transparent reflectors occurs in a sub-horizontal fashion. Its thickness varies from 30 to 40 ms TWTT. The base of sequence 8 roughly follows the bottom topography.

Line PSAT 175

Seismic profile PSAT 175 is located on the northwest limit of the survey area, being the furthermost line in the distal downslope direction of the studied area. It runs in a SW-NE alongslope (strike) direction through the continental rise across the dominantly depositional part of the canyon system. Water depth ranges from nearly 2650 to 2730 m. Sea floor topography is very smooth, exhibiting a higher relief towards the northeast.

Low frequency and amplitude reflectors towards the base of the line represent the acoustic basement (sequence 1). Sequence 2 directly overlies the basement with an average thickness of around 380 ms TWTT. Acoustically transparent sequence 4, with an erosional upper boundary, covers sequence 2 while being directly overlain by sequence 5. This latter sequence exhibits a diffuse to locally continuous seismic character with moderate to high amplitude reflectors in a sedimentary package that is clearly thicker on the northeastern half of the profile. Between time mark 20:00 and the southwestern end of the line a buried slump deposit occurs between sequences 4 and 5. A continuous sheet-

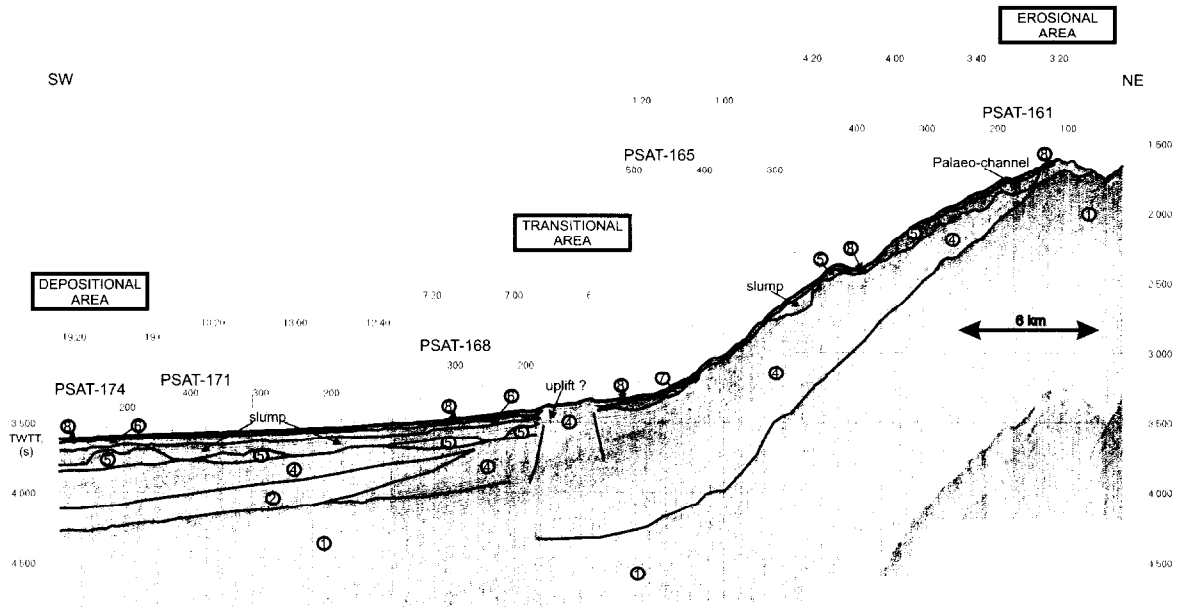

Figure 32. "Long" dip seismic line showing main features and seismic sequences present in the study area.

like to locally lenticular buried slump deposit is also observed, overlying sequence 5 through the entire line. This deposit underlies sequence 8 on the southwestern part of the profile and is overlain by sequence 6 towards the northeast. Sequence 8 covers almost all of sequence 6, except from time marks 20:06 to 20:10 where it pinches out. A northeast dipping fault reaching the sea floor was interpreted on the northeastern part of the line.

"LONG" DIP LINE

The "long" dip line which consisted of lines PSAT-161, PSAT-165, PSAT-168, PSAT-171, and PSAT-174, demonstrates the internal structure of the study area in SE-NW direction (Fig. 32). This line can be divided into two main parts. These parts are characterised by different sedimentary successions. The southeastern part is a slope which characterised by numerous slumps and former channels filled with lens-like bodies of sediments. The northwestern part of the line is characterised by a comparatively flat bottom and represents the depositional basin. Seven different acoustic facies fill this basin. These two parts are separated by an uplift which presumably could be controlled by two bounding faults.

Preliminary interpretation of the seismic sequences

A brief preliminary interpretation of the seismic sequences was attempted in order to understand their origin and the possible relations between them. This interpretation was done on a basis of the individual characteristics of each sequence and their relative position within the depositional, transitional and erosional settings observed.

The acoustic basement remains at a relatively constant depth through the dominantly depositional part of the studied area. It deepens at the base of the slope and outcrops at the upper slope due to the more erosional nature of the proximal area (Fig. 6).

Sequence 2 occurs as tabular layers at the distal part of the area and pinches out against sequence 4 towards the more transitional part of the system. This indicates that sequences 2 and 4 were probably deposited simultaneously in the transitional area. Therefore, sequence 2 may represent distal and transitional slump, debris flows and turbidite deposits accumulating in one or more troughs while sequence 4 could be interpreted as a product of relatively continuous hemipelagic, pelagic and mass wasting deposition. Sequence 4 shows a greater thickness at the base of the slope, decreasing towards the distal areas and being highly eroded on the upper slope.

Restricted to the upper slope is sequence 3 which may be composed of slope hemipelagic sediments that have been partially eroded away. Underlain by sequence 4 through most of the area is sequence 5, present on both the distal and proximal parts of the system. This sequence generally occurs as palaeochannel infill deposits in the proximal parts whereas in the distal regions it may represent fine-grained turbidites and debris flows formed by the erosion of sequence 4 updip.

Also occurring in the distal as well as the upper parts of the system is sequence 6. The distal packages may correspond to fine grained turbidite deposits while the proximal ones could be slope hemipelagic and fine grained sand spillover deposits accumulated on the intraslope lows.

Found as canyon and channel infill deposits is sequence 7, which occurs only on the proximal and transitional parts of the system where U-shaped valleys are present. Covering most of the surveyed area is sequence 8 which corresponds to the most recent hemipelagic and pelagic sediments. Specific canyon infill deposits (sequence 7) are not covered by sequence 8. This could mean that in these canyons recent localized activity might have taken place.

Slump and faulted block individual units are evident throughout most of the stratigraphic succession. The most recent ones are very frequently related to canyon slope instabilities.

In map view, sidescan sonar and bathymetric data show that the canyons do not run parallel, as would be expected if strictly erosional in nature. Therefore, a structural control on the canyons can be inferred which could also be responsible for local possible uplifts observed in the seismic data.

Further studies are necessary to investigate the sequence of events and depositional model for this canyon system. The acquisition and analysis of deep multi-channel seismic, more high resolution sidescan sonar and seabed sampling are suggested for a better understanding of the geologic processes involved in the past and present canyon system.

III.2.3. 3.5 kHz Hull-mounted Sediment Profiler Data

B. Cronin, S. Deleu, V. Galaktionov, A. Mille, S. Shkarinov, A. Stadnitskaya, R. Swift, A. Teles and A. Akhmetzhanov

The 3.5 kHz hull-mounted profiling survey was carried out simultaneously with the seismic and OKEAN data acquisition, at a speed of 6 knots. The data were of superb quality, and were used initially for the siting of gravity core locations (when the airgun needed repair in the middle of line PSAT 164). Subsequently we used the profiles more systematically to describe the shallow subsurface and the sea floor topography. In the sections below we described briefly the broad characteristics of each line. A series of 15 acoustic facies (labeled AF-XX) were observed and a scheme is presented to show these facies and their characteristics (Figure 33). These facies are used to aid description of the different profiles. The profiles are also presented in their raw and interpreted forms as 3-dimensional visualizations, which aid understanding of the down- and along-slope development of the various features studied, whether canyons, transparent lenses or wedges or some other feature. For the purpose of mapping the facies out this scheme can be generalised (Fig. 34).

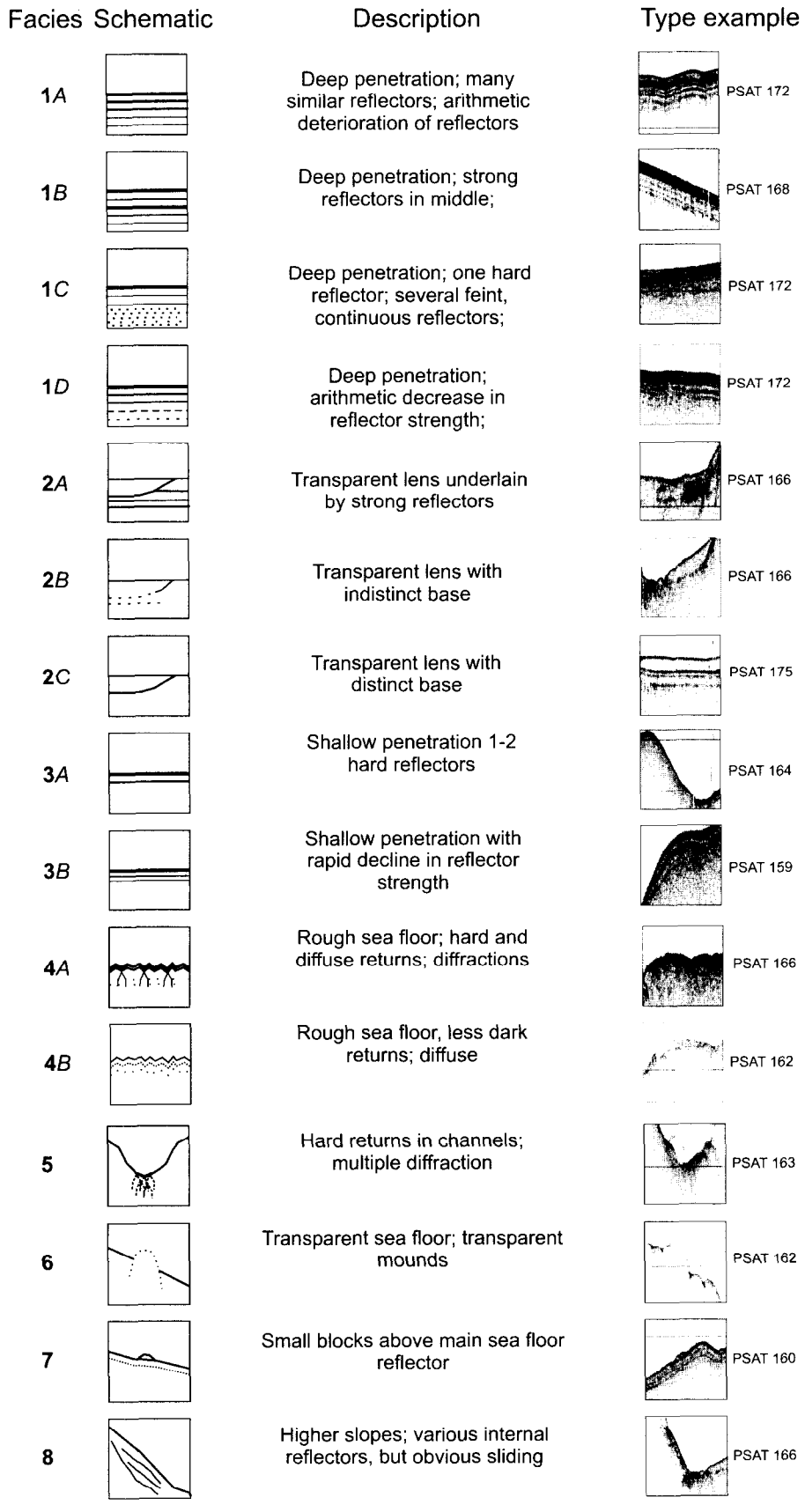

Figure 33. Acoustic facies observed in a canyon study area on the Eastern Rockall Trough margin.

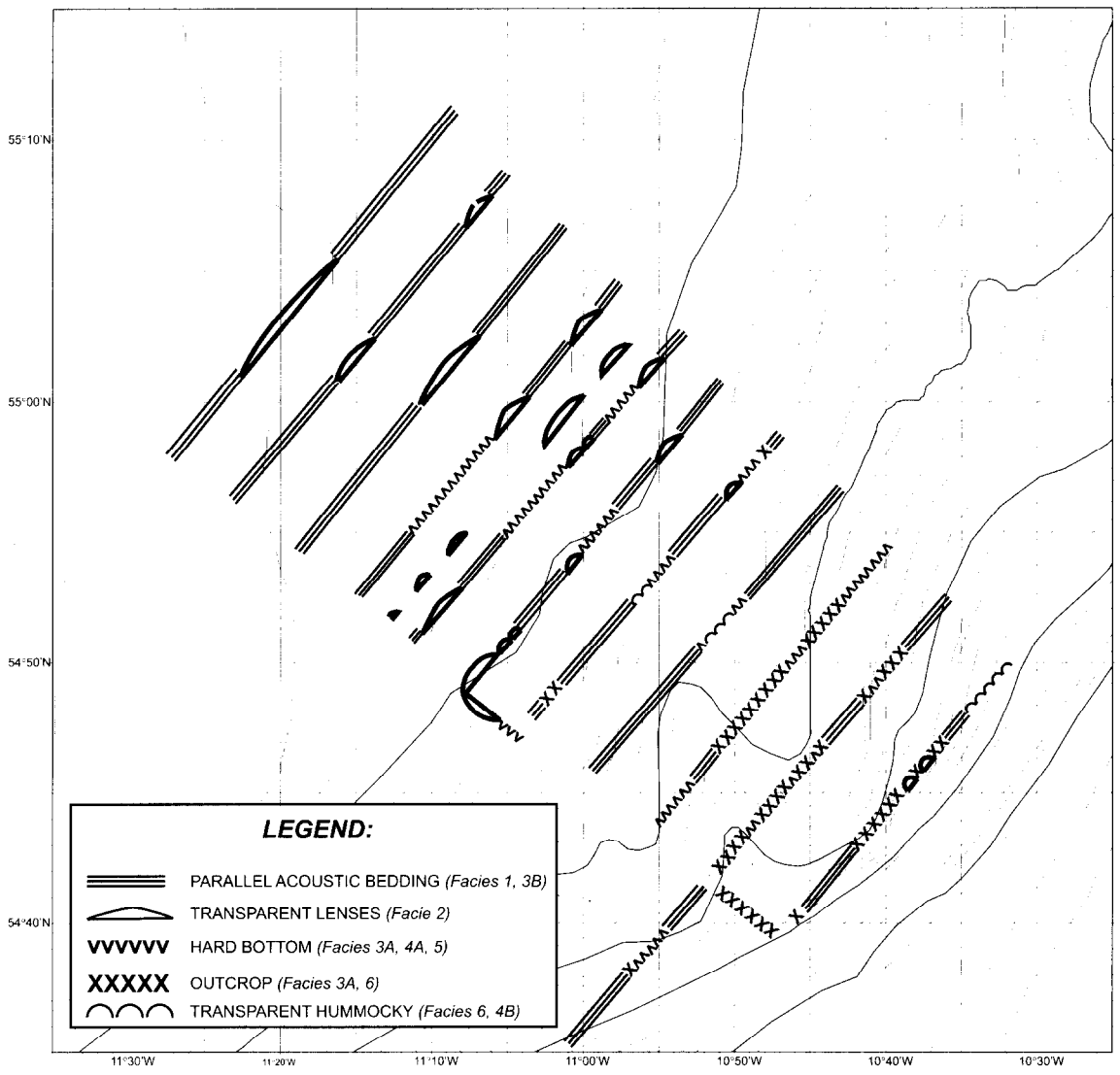

Figure 34. Map showing generalized distribution of 3.5 kHz acoustic facies.

Description of 3.5 kHz records

PSAT 159

Profile 159 is perpendicular to the local slope dip, and the depth ranges from 1270 to 1895 m. The profile crosses a series of steeply incised channels, within a broader canyon (22:43 to 0:03) or large channel. Within the canyon the acoustic response is typically weak, with facies AF-5 occasionally observed at the base of the channels (e.g. 23:33). Slump structures (AF-2B) are observed on some of the channel slopes (23:25 & 23:40). The topographic highs bordering the channel/canyon system show typically strong acoustic response with moderate to deep penetration (AF-1D; e.g. 0:07 to 0:29 and 22:14 to 0:29). Although the system appears more complex in this region of the profile the 'classic' channel profile observed downslope on line 162 is somewhat evident, with terraces and several thalwegs. The line is interpreted to reflect a confluence of several local peripheral channels converging into the main canyon body.

PSAT 160

Line 160 is situated parallel to the slope. Its depth range is from 800 to 1400 m. The section

comprises four main topographical features, represented by ridges separated by V-shaped depressions. From northeast to southwest we observe a slope running from 800 to 1300 m (between 1:00 and 1:50). The slope is characterized by high reflectivity, and the underlying acoustic pattern is highly dispersive. A ridge separating the two main channel depressions is seen at 2:00, separating channels with floors at 1300 m, with acoustic facies AF-1C across that area. Each channel floor has strong diffractions associated with it. A second ridge is found between 2:10 and 3:10, with a depth of 1100 m at 2:50, and a saddle at 2:20 with a small channel incision with diffractions. The ridge has acoustic facies AF-1D. From 3:05 to 3:35 a smaller ridge is seen and the northern side has higher reflectivity. This ridge forms the north wall of a third channel incision. The section is interpreted as another strike section through the main canyon system on the slope, with two well defined channels becoming tributary to one another within a broader deep-water valley. The acoustic character of the walls either side of the valley indicate levee build up and hemipelagic drape, in contrast to the more erosive profiles across the two channel thalwegs.

PSAT 161

This is a downslope profile from 1090 m to 1870 m. On the profile, one large (c.150 m) topographic high and two minor highs (c. 5-10 m) are seen. On the northern slope of the largest high, three mound structures show characteristically poor acoustic response (AF-6, from 03:04 to 03:20). On the southern slope, two structures with disturbed geometry occur (e.g. 03:26, AF-2C), with 5 m thick packages of rotated internal reflectors. Across the profile, penetration is typically poor, the exception being in the lowermost part of the profile where two layers may be distinguished in the mound located there (AF-3B). The mounded structures are interpreted as possible carbonate mounds located on local highs. The disturbed packages are interpreted as slumps.

PSAT 162

This line is sub-parallel to the local slope dip, the depth ranges from c. 1865 m to 2410 m. The profile covers a deep-channel system with several associated structures: levees, overbank area, terraces and channel thalweg. The channel has the typical characteristics of a 'steerhead' channel profile. The topographic high has moderate acoustic response (AF-3B between 04:28 and 04:50) with 1-2 layers observed beneath the sea floor; whilst the eastern high has a rougher surface, with variable penetration, with rare sub-bottom structure (AF-4A). The channel (4:57 - 5:35) is c. 450 m deep with the channel slopes of poor acoustic response. Slump structures (AF-2B) are interpreted on both the eastern and western slopes (e.g. 5:07). Within the channel is a body of sediment with non-parallel internal reflectors (AF-4B). The levee to the west of the channel shows poor acoustic response with no internal structures observed (AF-6, at 04:55). This structure was cored (see sections below).

PSAT 163

This section is parallel to the slope. The highest point is 1720 m and the lowest is 2250 m. There is one large valley with a mounded structure in the centre, dividing the valley into two. On the first slope (7:15) there are some disturbed structures interpreted as slumps. On the valley floor, there is a mounded structure with weak reflectors. Between the two valleys there is a large mound structure with two peaks and poor acoustic response. Another mound of this type is seen in the second valley. At the lower part of the slope (8:45) there are three acoustic reflectors within a topographic 'bump', then a second 'bump' with strong reflectors. At 8:50 we observe another mound with three acoustic reflectors. The profile is interpreted as a cross-section through the channel system, with local slumping and some mounds of unknown origin.

PSAT 164

This profile is downslope, from the highest point at 1690 m to the lowest at 2500 m. A mound with very poor acoustic response is seen at the start of the line. Several other mounds are seen, including one at 8:50 with three internal reflectors. There are several disturbed packages on the slope. The profile is interpreted as a dip section through the slope, with several candidate carbonate mounds and slumps.

PSAT 165

Another downslope section, partly along the same line as line 164, which was stopped due to airgun failure. The profile runs from 1400 m (highest point) to 2570 m (the lowest point). Until time 0:25 only one strong reflector is observed at the sea floor, with no deeper penetration. At this point a mound with three reflectors is seen, and repeated at 0:52 though with only one reflector. After this a disturbed structure interpreted as a slump is observed until 1.15, where the acoustic response is very poor. To the end of the profile we observe two strong reflectors below the sea floor. The latter package of sediment is interpreted as a slump body.

PSAT 166

This line is orientated towards the northeast, passing across the middle of the survey area. The depth ranges between 2350 and 2590 m. The topography is rough with the occurrence of mounded features at various scales (including ridges) and channel-like features. Two of the channels are filled with acoustically transparent deposits (AF-2B; locally AF-2A and AF-2C), and usually have U-shaped (depositional) profiles. Another channel has high reflectivity on its floor, with a rough pattern and high acoustic penetration (AF-1B). Some slumps are also interpreted on the slopes of the intervening ridges (AF-1C). Most of the ridges in this profile are found to be sections of slope separating the individual channels.

PSAT 167

This line is orientated southwestwards, passing across the middle of the surveyed area, with depths ranging from 1670 to 1910 m. The topography is again rough with steep ridges separating channels, slump bodies on their slopes and at the toes of slope. Two main channels are observed of which one is quite a considerably deep canyon feature (~600 m deep). Slumped features are seen on the margins of many of the canyon walls (AF-8). The acoustic facies in general are highly variable across the section, with AF-1B found both at the top of ridges and on the floor of canyons. AF-1C is found on steep slopes and is perhaps a function of poor penetration, and facies AF-6 is also found on some steep slopes between smaller channels. The section is interpreted as an erosion-dominated strike section through a trunk canyon with minor influence of tributary channels, where slumping and mass wasting on a larger scale are common. The canyon has a 'steerhead' geometry in profile.

PSAT 168

This line is oriented northwestwards, profiling downslope on the lower reaches of the area surveyed. Depth ranges from 1800 to 2025 m. The profile is characterized by some disturbed features on the slope, interpreted as slumps. The lower half of the profile comprises AF-1B.

PSAT 169

This profile is oriented northeastwards, crossing the lower reaches of the surveyed area.

Depths range from 2595 to 2665 m, which is a relatively flat area compared with earlier lines. A general strong reflector character with rough topography is observed on this line, similar to the updip line PSAT 166. The highest part of the profile, from 2595 m between 9:35 and 9:10, is characterized by deep penetration AF-1A, which passes downdip towards a prominent topographic high at 9:02 into a transparent lens on the sea floor. This abruptly stops short of the high, forming a prominent step. The high has AF-3A acoustic character, and is overlain downdip by another transparent lens (AF-2A) of limited lateral and dip extent, that is confined to the slope area between 8:50 and 8:35. The flattest and lowest area between 8:05 and 8:34 is characterized by high reflectivity and moderate to poor penetration (AF-3A). This passes abruptly to AF-4A, then AF-1A, 1B and back to AF-1A at the end of the profile, across another minor topographic bump at 7:34. The line is interpreted as a strike section through the lower part of the system, and is dominated by debris flow processes.

PSAT 170

Line 170 is a relatively flat profile, running from 2510 to 2670 m downslope. The topography is irregular, with erosional features (e.g. 11:30), mounds (e.g. 10:43 and 10:21), topographic highs (e.g. 12:13), and transparent lenses (e.g. 10:23-10:32, 10:53-11:02 and 12:04-12:11). Some of these lenses trace laterally, usually updip, onto flatter or steeper areas of slope. Most of the section is characterized by AF-1 facies, with 1A, 1B, 1C and 1D found through the section. Two dislocations, dipping downslope, were observed at 10:21 and 10:49. The profile is interpreted as a dip section going downslope, and dominated by mass-wasting processes. Debris flows and slump bodies, slump scars and syn-sedimentary faults are all recognized.

PSAT 171

This profile is a dip-section (perpendicular to slope) between depths 2630 and 2760 m. The section is smooth with some linear dislocations of reflectors but no disturbed zones or transparent lenses. The highest part of the slope comprises AF-2A, and this passes downslope through AF-1A, AF-1D (where the dislocations are) and back to AF-1A. The profile is interpreted as a slope section with hemipelagic sediments and local synsedimentary, initial slump faults. Mass wasting is not seen and the section thickens downslope.

PSAT 172

This profile is the updip equivalent of lines 173 and 175, which are comparable profiles. The area profiled is a relatively flat strike section between water depths of 2680 and 2740 m. The area described is a low relief valley between 13:32 and 15:22, with the same extremes in water depth as the profile. The centre of the valley is described by a transparent lens (AF-2C) that is <5 m thick and 4 km wide. The eastern margin passes from a thick transparent lens abruptly into thick parallel reflectors (AF-1D) which are overlain by a thin part of the transparent lens to 14:16. The thin lens onlaps the eastern valley margin, and passes to AF-1A for the remainder of that valley margin and wall. The western margin is much more abrupt at 14:38, with a vertical sharp contact between that edge of the lens and the AF-1A deep penetration facies, which continues up to the brow of the western margin of the valley. Outside the valley, from 15:22 to the end of the line, facies AF-1D predominate. A very thin transparent lens appears to onlap the outside channel part of the section at 15:26. The section is interpreted as a combined erosional/depositional area within a confined 'fairway', where a debris flow infills an eroded topography. Possible coarser facies fill the rest of the valley, but otherwise the area is characterized by deep penetration and thus probably hemipelagic, sediments. Undulose patterns in the section on the west margin testify to sedimentary creep towards the axis of the fairway, probably due to the steeper slope on that margin. Outside the valley, sediments onlap the brow, or possible levee, of the fairway.

PSAT 173

This line represents one of the more distal cross-sections of the surveyed area, with depth ranges between 2650 and 2720 m. The section is relatively flat, and is characterized by two transparent lenses (AF-1B), both of which pass laterally into more continuous reflectors (AF-1D and AF-4A) across a sharp, sub-vertical contact (16:14 & 17:24). The thickest lens (<7 m) is partially on a slope to the east where it onlaps (16:52). This lens occupies part of a downslope-oriented, low relief valley. The other half of the valley is occupied by AF-4A, which passes out of the valley and upslope into deeper penetrating AF-1A. The profile is interpreted as a strike section across a channel mouth depositional area occupied by slump or debris flow deposits and candidate coarser material, bordered on the valley slopes either side by hemipelagic material.

PSAT 174

This profile is a dip-section (perpendicular to slope) between depths 2680 and 2720 m. The profile is very similar to PSAT 171, with little acoustic variation, ranging from AF-1A in the upper part to AF-1D in the lower part. The line is interpreted as a slope section with no mass wasting evident.

PSAT 175

This profile is the lowest strike profile on the slope/rise. It is relatively flat, with a deeper centre than at its margins, with depths ranging from 2685 to 2750 m. A broad valley is described between 19:10 and 21:40 (most of the width of the profile) between those depths mentioned above. The axial part of the valley comprises a transparent lens which is almost sheet like, with an abrupt termination against more penetrative reflector facies to the west at 20:02, though a small, upper part of the lens continues to 19:53 where it onlaps topography. The eastern edge of the lens onlaps the valley margin at 20:45, though the thickest part, as with the western edge, terminates against or passes into diffuse and then sharp, deeply penetrative reflectors at ~20.28 ms. There is a possible linear, subvertical, dislocation on the western margin of the valley, at 19:12. The eastern margin does not have an equivalent feature, though reflector packages appear to have a low-relief undulation between 20:06 and 21:16. The profile is interpreted as a strike section across the slope in an area downdip from a channel mouth. There is evidence for erosion here, with a terraced erosive cut that is filled by debris flow material, probably muddy. The western margin of the general valley or fairway is controlled by syn-sedimentary faulting (at least, locally). The eastern margin is characterized by possible sedimentary creep, giving the wavy appearance to the reflectors. Note the potential similarity between these creep features and what might be interpreted as contourites.

3D Visualisation of Irish Margin Slope

A three-dimensional visualization of the Irish Margin has been reconstructed (Fig. 35) using the 3.5 kHz profiles and clearly shows the areas with different slope morphology. The subbotom reflectors indicated that these areas also have different sediment dynamics.

III.2.4. Sidescan Sonographs

A. AKHMETZHANOV, M. IVANOV AND P. SHASHKIN

10 kHz OKEAN imagery

A complete acoustic coverage of the canyon area was obtained. Although the resulting 10 kHz acoustic image lacks significant amount of details seen on the 30 kHz TOBI map, it does show the

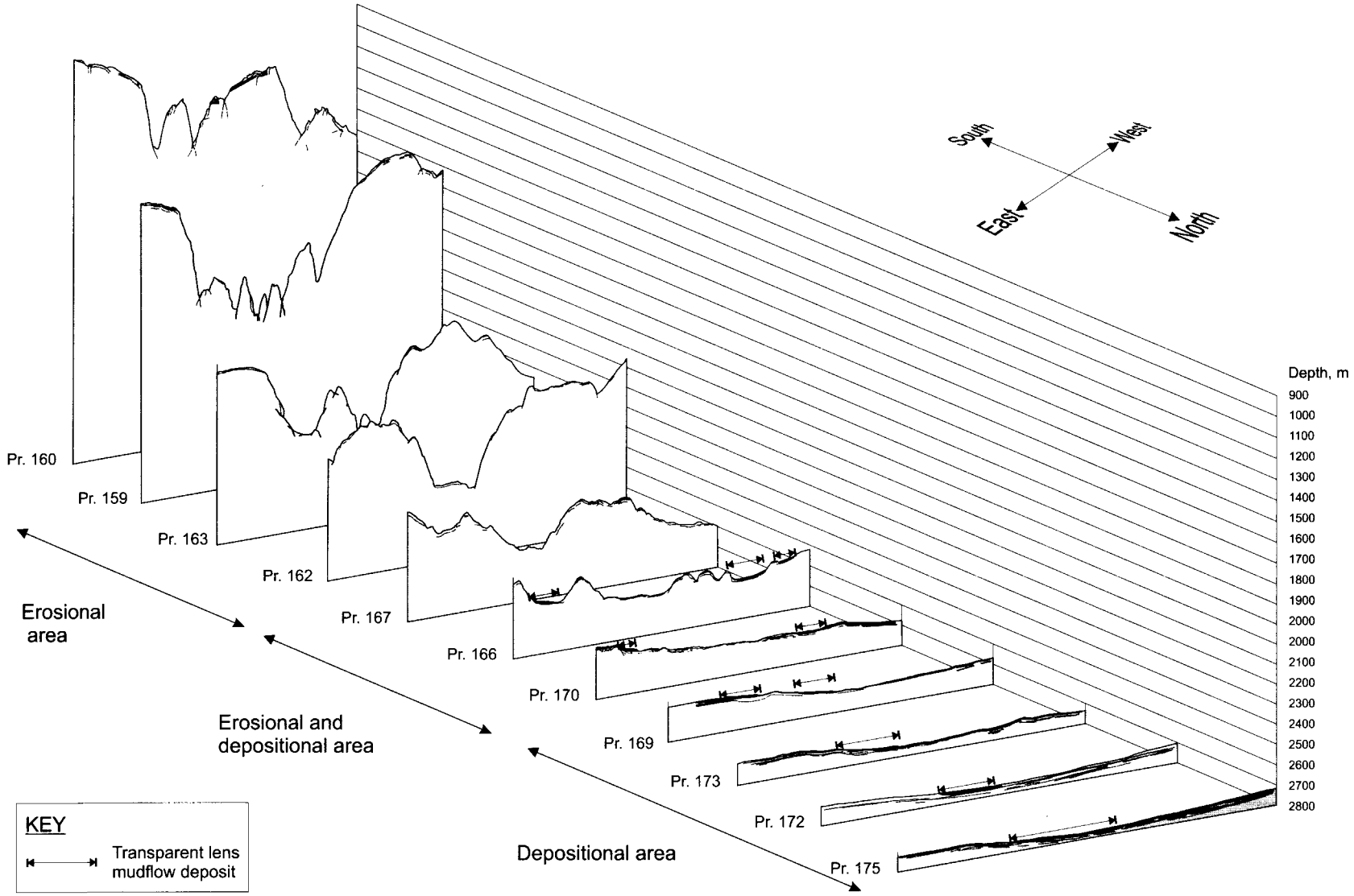

Figure 35. 3-D visualization of the 3.5 kHz profiles showing areas with different slope morphology and with different sediment dynamics.

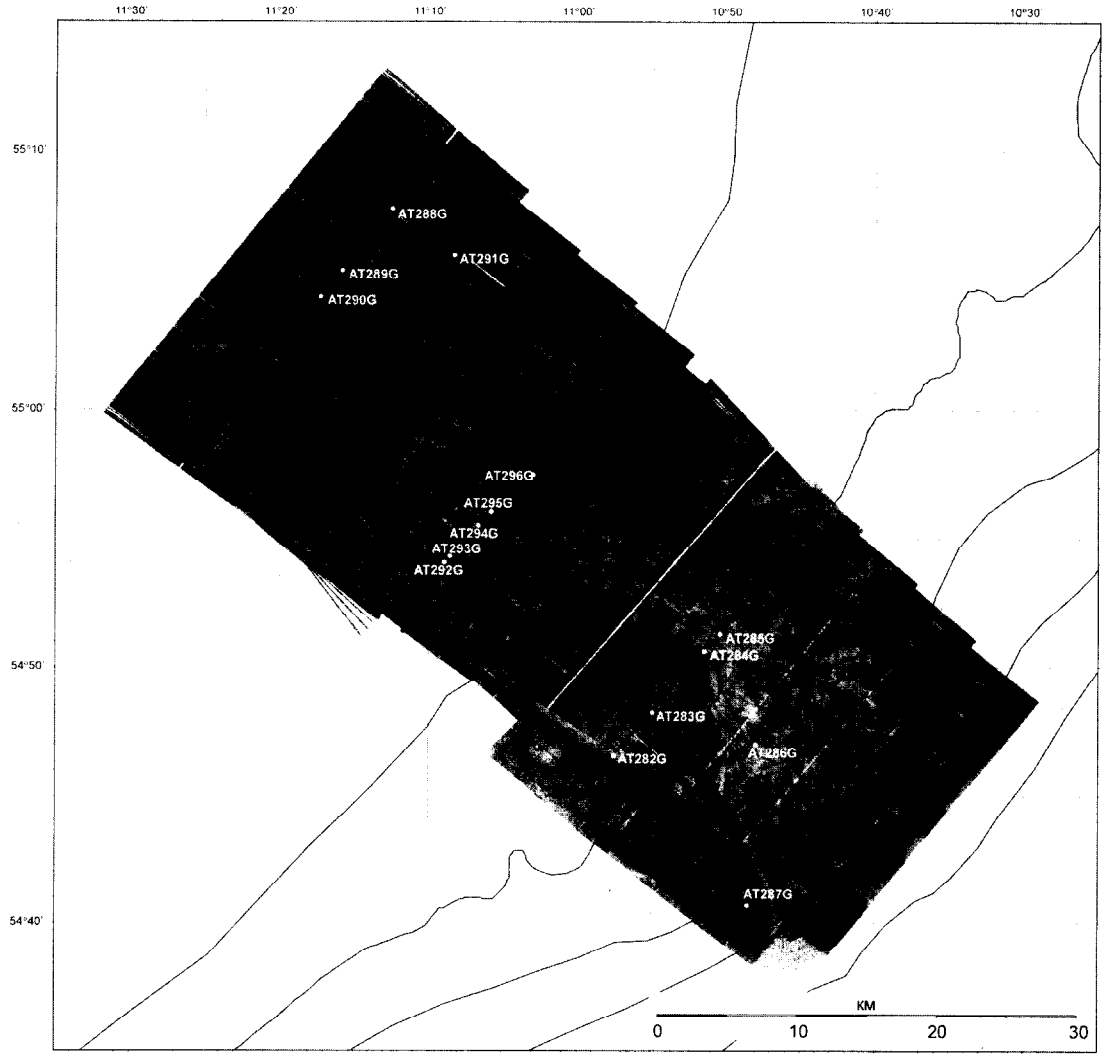

Figure 36. OKEAN mosaic of a canyon area on the Eastern Rockall Trough margin.

major elements of the canyon system. The best expressed feature on the image is a low backscattering canyon head area which has a characteristic "cauliflower" shape. It is found in the depths between 1500 and 1800 m. A few small tributary canyons were noted higher up slope to the southwest. They also have a low backscattering infill. The canyon has a short and narrow waist with high backscattering walls in depths between 1800 and 2000 m. Below 2000 m the slope gradient noticeably decreases and the canyon opens into the basin plain. The OKEAN image shows a patchy pattern with some trends suggesting sediment transport from the canyon further into the basin.

100 kHz OREtech profile

The OREtech deep-towed 100 kHz side scan sonar with 7 kHz sediment profiler provided detailed imaging of the canyon lobe area at a depth of about 2600 m. The line is about 24 km long and located halfway between the 3.5 kHz profiler and OKEAN/seismic lines PSAT 169 and PSAT 170. On the profiler record a broad depression corresponding to the canyon axis is seen. The lowermost part of the depression is found at the depth of 2680 m and represents a 2.5 km wide valley with a flat floor. Two gullies about 60-120 m wide are found within the valley, one of which has a V-shaped profile and is almost 30 m deep. To either side of the valley the depth gradually decreases up to 2580 m on the northeastern flank.

The sonograph has a very variable contrasting backscatter pattern and 5 major acoustic facies are distinguished: 1) Lower backscatter, uniform monotonous; 2) Lower backscatter, patchy; 3) Contrasting backscatter, lineation; 4) High backscatter, wavy; 5) High backscatter, patchy. Interpretation of the facies is significantly facilitated by the subbottom profiler record which shows a generally stratified sequence with a number of clearly identified acoustically transparent lenses and places where the seabed has evidence of erosion. The lenses are up to 20 m thick and have lateral extension up to 4 km. Similar lenses have been found in many different places on the continental margins, particularly on the glaciated ones, and recognised as muddy debris flows. These lenses correspond to facies 2, 5 and sometimes to 1. The patchy character of the facies is due to the rough upper surface of debris flows (Fig. 37). Variations of backscatter can be explained by the different thickness

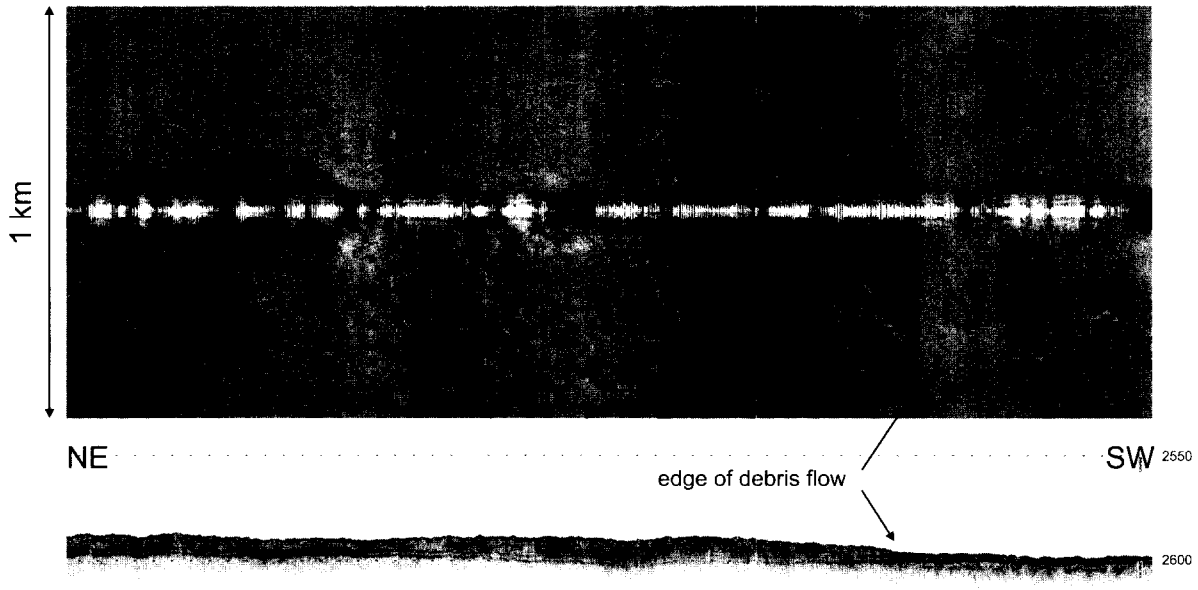

Figure 37. Fragment of ORAT-39 100 kHz sonograph and subbottom profiler record showing debris flow.

of hemipelagic draping. The lower backscatter corresponds to the thicker draping. Most of the debris flows are found on the flanks of the depression. Often the sonograph shows sharp boundaries between high and low backscattering areas which are correlated with the edges of the debris flows. In the central part of the depression the seafloor is dominated by facies 3, 4 or 1. Seabed lineation (facies 3) is more common and is particularly well expressed within the valley (Fig. 38). Subbottom profiler record shows evidence of seabed erosion such as truncated reflectors or well-marked gullies. Facies 4 forms elongate fields of relatively limited width (up to 1 km) and on the subbottom profiler records in most cases it corresponded to eroded portions of the seafloor, such as the gullies. However the largest field crossed by the sidescan line does not show evidence for erosion on the profiler record (Fig. 39). This possibly means that the high backscatter is caused by a thin, below profiler resolution, layer of coarse material. Several cores taken from this facies recovered a thin (up to 3 cm) layer of washed out gravel and pebbles which is a good candidate for the cause of the high backscatter.

III.2.5. Ground-truthing of 3.5 kHz Profiler, OKEAN and OREtech Sidescan Sonographs

G. Akhmanov, A. Mazzini, A. Akhmetzhanov, B. Cronin, A, Stadnitskaya and Sedimentological Team

Seventeen gravity cores (Table 5) were collected on the basis of backscatter acoustic facies

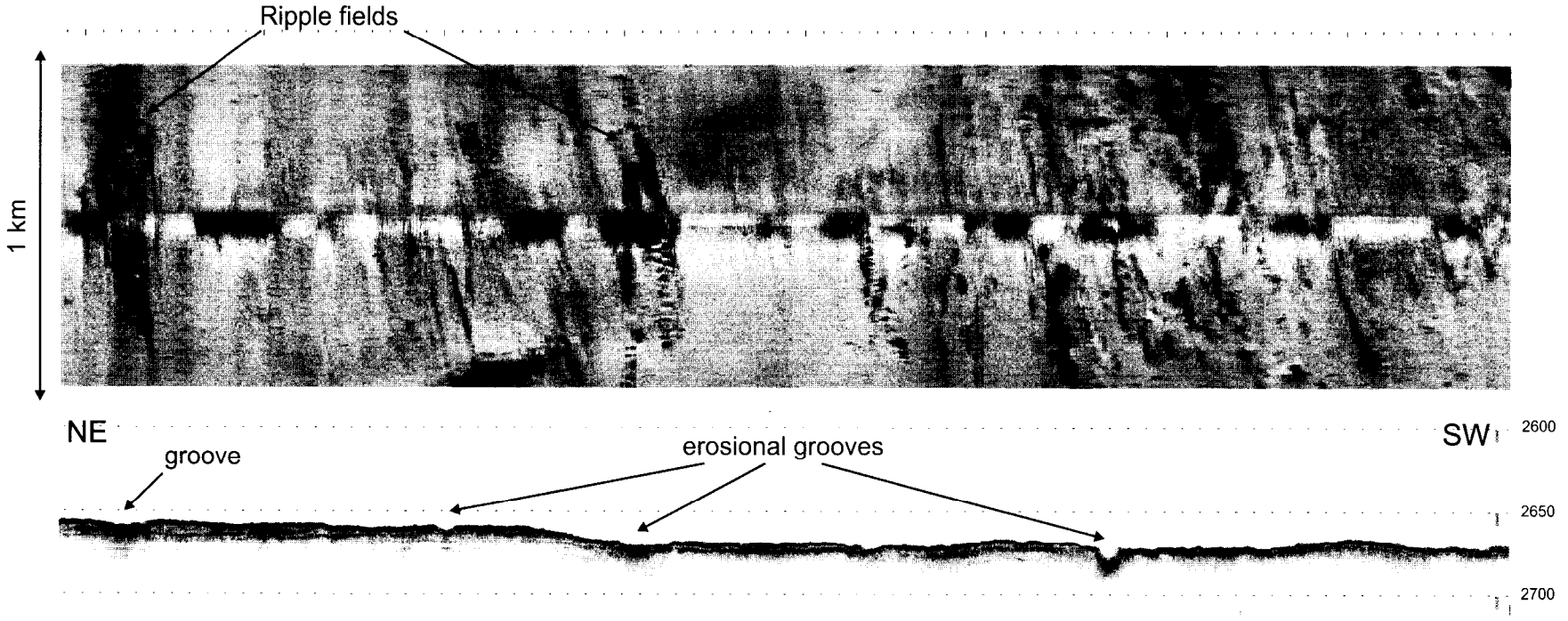

Figure 38. Fragment of ORAT-39 100 kHz sonograph and subbottom profiler record showing evidence of erosion in the axial part of the canyon.

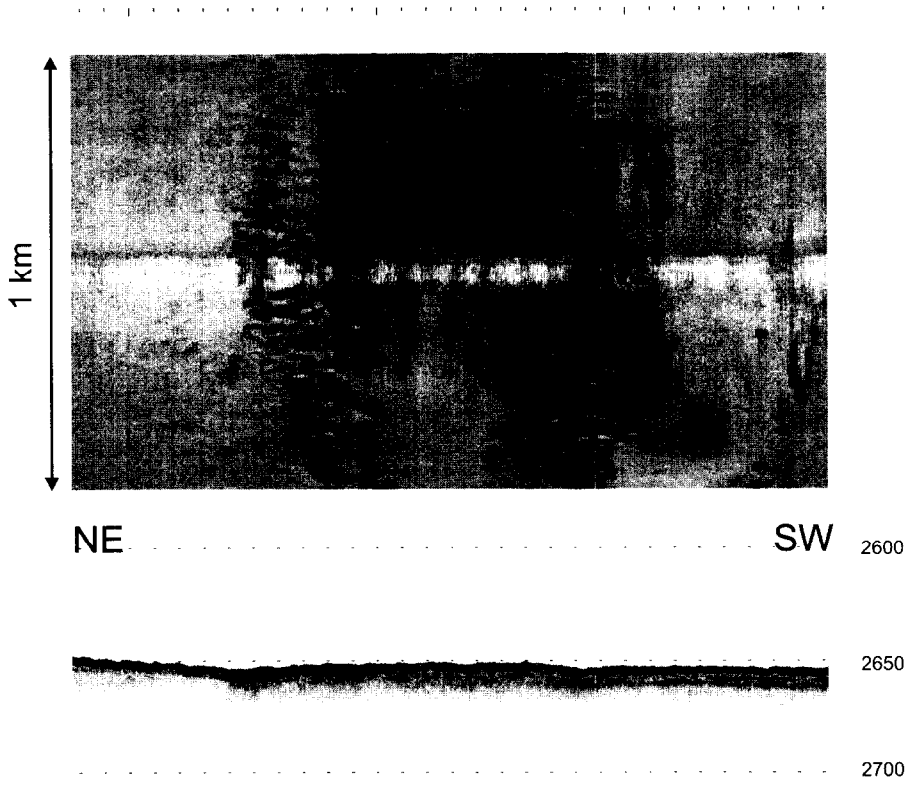

Figure 39. Fragment of ORAT-39 100 kHz sonograph and subbottom profiler record across a strongly backscattering ripple field.

from the OREtech profile ORAT 39 and its 7.5 kHz profiler and the 3.5 kHz profiler sections. In this section we discuss the gravity cores from three different geological/physiographic parts of the Eastern Rockall Trough deep-water slope, and see how the sedimentary layering may explain the backscattering on the OKEAN and OREtech sonographs. These three areas are: (i) Canyon Head region; (ii) Lower Slope region and (iii) Upper Rise region. In all regions, a pattern-coding of the core numbers at their locations (as shown on the sonograph details) is used. A stippled pattern is used for those cores where sand (of both turbidity current and bottom-reworking/contour current origin) was recovered, a grey pattern for reworked mud (both muddy debris flow and slump origin), a pebble pattern for prominent layers of clast supported gravel of enigmatic or compound origin, and a white pattern for hemipelagic sediment. The same patterns are used in the core logs (see Annexe I).

Canyon Head Region

Six gravity cores were taken in the Canyon Head region: four in a transect across the upper reaches of the main deep-water canyon (AT-282G to AT-285G), one from the floor of the same canyon approximately 8 km nearer the shelfbreak up the canyon axis (AT-286G) and one core was taken from a mound off the canyon flank in the extreme SW of the surveyed area, approximately 17 km updip from the canyon transect.

Canyon Transect

The canyon transect from 3.5 kHz profiler data is shown in Figure 40, which is a strike section, or along-slope section, through the canyon. This figure also shows the OKEAN (line PSAT-162) image from the area in the immediate vicinity of the transect.

Table 5. General information on the cores sampled on the Eastern Rockall Trough margin.

Core No	Date	Time, GMT	Latitude	Longitude	Cable length, m	Depth, m	Recovery, cm
AT-282G	14.08.00	11:56	54°46.552' N	10° 57.532' W	1940	1940	351
AT-283G	14.08.00	14:04	54°48.226' N	10° 54.938' W	1940	1940	88
AT-284G	14.08.00	16:10	54°50.604' N	10° 51.459' W	2405	2410	60
AT-285G	14.08.00	17:49	54°51.276' N	10° 50.410' W	2358	2366	367
AT-286G	14.08.00	20:10	54°46.989' N	10° 47.997' W	2033	2020	282
AT-287G	14.08.00	22:45	54°40.677' N	10° 48.565' W	1240	1240	15 cm^3
AT-288G	15.08.00	23:54	55°07.784' N	11° 12.479' W	2705	2705	211
AT-289G	16.08.00	02:00	55°05.405' N	11° 15.830' W	2730	2730	380
AT-290G	16.08.00	04:03	55°04.381' N	11° 17.279' W	2742	2740	434
AT-291G	16.08.00	06:35	55°06.001' N	11° 08.319' W	2687	2691	419
AT-292G	17.08.00	00:32	54°54.061' N	11° 08.941' W	2665	2667	428
AT-293G	17.08.00	02:10	54°54.307' N	11° 08.550' W	2662	2662	186
AT-294G	17.08.00	04:02	54°55.507' N	11° 06.660' W	2670	2670	55
AT-295G	17.08.00	05:47	54°56.044' N	11° 05.799' W	2670	2670	309
AT-296G	17.08.00	08:04	54°57.499' N	11° 02.984' W	2650	2650	341
AT-297G	17.08.00	16:10	55°30.035' N	09° 52.480' W	965	980	22
AT-298G	17.08.00	17:23	55°31.499' N	09° 50.001' W	826	834	399

Core AT-282G was targeted in an area of multiple layering on the 3.5 kHz profiler data, which was known to be outside the canyon and was thought to be the overbank area to the main canyon. The backscattering on the OKEAN is medium to low. A linear feature at the core location running NW-SE and then dog-legging towards the canyon is seen, and is probably a buried channel or canyon. The core is not thought to penetrate this feature. The core recovered bedded hemipelagic sediment and three sand layers, between 2.4 and 3.5 m, that contained siliciclastic material with foraminifera and local dropstones.

Core AT-283G was targeted on a topographic high between the overbank and canyon axis

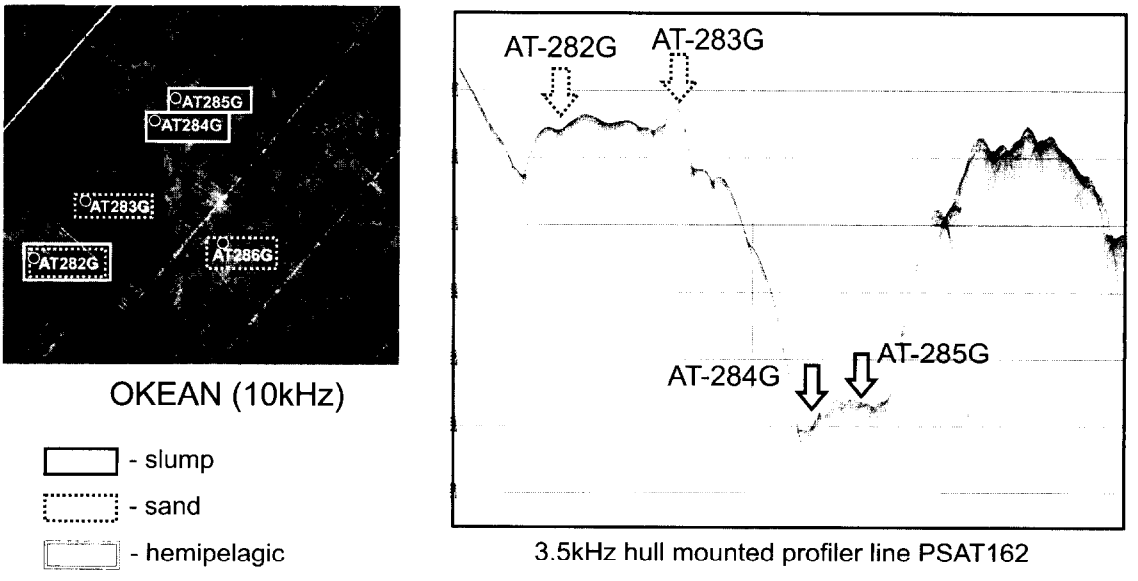

Figure 40. Cores from the canyon head region

areas, and was thought to be the highest part of the canyon levee, with a transparent mound structure clearly visible on the 3.5 kHz data. The OKEAN sonograph shows medium-high backscatter (though this is somewhat obscured by the ship's track and by a nearby acquisition anomaly on the sonograph). The core location is off the inferred buried channel from the last core station. The station is on the same general area of inferred slump as the last station. The core recovered bedded sands and foraminiferal ooze, though it is dominated throughout by sand. Penetration was poor (0.8 m), and this was thought to be due to the core hitting deeper, impenetrable sand below this level.

Core AT-284G was targeted on the deepest part of the canyon, or the inferred canyon thalweg, where the 3.5 kHz profiler showed a hard, shallow penetration acoustic response with some diffractions. On the OKEAN, the backscatter is medium and the sedimentary body is clearly part of the cauliflower area of the canyon head region and is interpreted as slump structures from the canyon wall. This slump feature separates areas of low backscatter in the cauliflower area from higher backscatter down canyon on the OKEAN image. This slump may have been responsible for ponding of sandy sediment in the head region. The core recovered hemipelagic sediment and hit the top of a possible muddy slump interval, though core penetration was poor (0.6 m).

Core AT-285G was targeted on a mounded feature on the canyon floor, with highly irregular sea floor topography, hard return and diffractions on the 3.5 kHz profiler, which was thought to be a slump mass on the canyon floor. On the OKEAN the backscattering is medium, a little higher than at the last station, but clearly in the axis of the main canyon at the downdip end of the cauliflower structure. The core recovered a hemipelagic sequence with intercalations of slumped material. The slumped intervals were dewatered and extremely sticky in texture, and it took the sampling team and a number of onhand strongmen from the crew almost 30 minutes to extract the sediment from the core-liner.

Core AT-286G: Canyon Head core

Core AT-286G was taken approximately 7 km up-canyon towards the headwall of the cauliflower pattern imaged on the OKEAN mosaic (Fig. 36). The core station was not targeted on the profiler, with which it does not coincide, but rather with the sonographs. On the OKEAN, the location is one of low backscatter within the central part of the cauliflower structure. A deep canyon with high backscatter margins is seen clearly within the cauliflower. The core was targeted at the most axial, or central part of the canyon floor, where it was expected that we might recover sand. The exercise, based entirely on sonograph images, was successful. The core recovered intercalated thick sandy layers (the thickest recovered on the margin) and hemipelagic sediments.

Core AT-287G: Marginal mound feature

Core AT-287G was targeted using the 3.5 kHz profiler on a mounded structure on the flank of the main canyon even further up the canyon reaches. The structure, despite the unusual depth, was targeted as a possible mound or at least as some sort of enigmatic feature. The structure was one of several such features of the same size seen between 3.10 and 3.20 on PSAT-161, at water depths between 1240 and 1280 m. On OKEAN, the core station is in a localised area of high backscatter, situated on the flank or just outside a major SSW-NNE trending canyon which feeds into the SW part of the cauliflower structure. There was no recovery in the gravity corer, but there was sand and clasts (dropstones) in the core catcher, suggesting that the features were unlikely to be carbonate mounds.

General comments about the Canyon Head region

The cauliflower-shaped head area is seen particularly well on the OKEAN. On OKEAN, stacked linear canyon and channel features and tributaries with low backscatter are interpreted as a major phase of erosion and sand deposition in the head area that does not persist today. On 3.5 kHz the dominant sedimentary bodies overprinting this older phase are slumped bodies and mudflows. Most of

the smaller-scale mudflows and slumps are directed towards the canyon and channel axes, in other words from the sides of the canyons. This indicates that the system is largely now not a sand-transporting one. One such slump body, cored twice, is thought to have blocked the main canyon axis, and subsequent sand transportation may have been ponded behind it. In targeting sand with the gravity corer, it was found that coring the topographic highs near canyons, coring on areas of low backscatter very near the head of the system, or getting a sample from the deepest part of a V-shaped thalweg, was the most reliable way. Other areas of potential sand were too deep below the sea floor (seen on OKEAN) to be sampled by the 6 m gravity corer, largely due to the thickness of the slumped masses. The overbank area in particular (e.g. AT-282G) showed that relatively recent large sandy turbidity currents were moving through the canyon, and overbanking into this region. This is particularly impressive when one considers the width (17 km) and depth (~800 m) of the canyon. The timing of these flows is thought to be during the end of the last glacial period, confirmed by biostratigraphy and their association with dropstones.

Lower Slope Region

Five cores were collected in the mixed erosional-depositional, lower slope area of the Irish Margin (Fig. 41). Cores AT-292G to AT-295G were all selected on the basis of their backscatter characteristics on OREtech, in combination with information about seafloor topography and acoustic response from the 7.5 kHz profiler. The cores were taken in another strike (along-slope) transect across the slope. Cores AT-292G and AT-293G were targeted on depositional features on the profiler, and cores AT-294G and AT-295G were targeted on erosional features on the profiler. Core AT-296G was targeted on a very high backscattering area with characteristic ripple-like pattern seen on the TOBI image, where the seafloor topography was unknown.

Core AT-292G was taken on an area of medium backscatter on OKEAN, and low backscatter on OREtech (Fig. 41). On the profiler the sub-bottom is characterized by deep penetration and multiple layering. A transparent layer was observed on the profiler, and this can be traced laterally under station 293. The core recovered a thick mudflow capped by Holocene marl.

Core AT-293G was taken on an area of medium-high backscatter on OKEAN and medium to high backscatter on OREtech. On the profiler the seafloor reflects strongly but otherwise is the same as the previous station. These two cores were taken to test the reason for the difference in backscatter on OKEAN and OREtech. The core recovered a mudflow capped by a marl, but separated by a 0.05 m thick clast-supported gravel layer.

Core AT-294G was taken on an area of medium-high backscatter on OKEAN and a low backscatter on the OREtech. On the profiler this area is in a shallow, V-U shaped channel with a thin layer of transparent acoustic response underlain by stronger returns and poor penetration. The core had poor recovery, with a Holocene marl capping sand. The marl is interpreted to correspond to the transparent acoustic facies on the 7.5 kHz, and the sand to be the top of the higher amplitude acoustic facies below the channel base. The depth of the sand (0.38 m) explains the relative lack of penetration of the OREtech, which does not show this layer.

Core AT-295G was taken on an area of medium backscatter on OKEAN and low backscatter on OREtech. On the profiler the core is from the middle of a zone of strong reflectivity within a flat-bottomed, shallow depression. The core recovered a thick hemipelagic sequence with no sand, draped by Holocene marl. The feature is interpreted as an inactive, draped channel feature.

Core AT-296G was taken from an area of medium backscatter on OKEAN. The core recovered a thick hemipelagic interval capped by a Holocene marl, and separated by a thin clast-supported gravel (reworked dropstone) layer, identical to that seen in AT-293G.

General comments on the Lower Slope area

The two sidescan sonar systems, also compared with confidential TOBI data, allow 3D analy-

sis of the upper sedimentary layers in what is a unique ground-truthing exercise for the TTR programme, in combination with 3.5 kHz, 7.5 kHz and seismic profiling across the same transect. The high backscattering gravel layer seen on TOBI is less evident on OKEAN because it is not thick enough, and not as evident on OREtech because it is partially buried. The same can be said for sand-filled features such as the narrow linear channel seen on TOBI, which is not seen on OKEAN but is

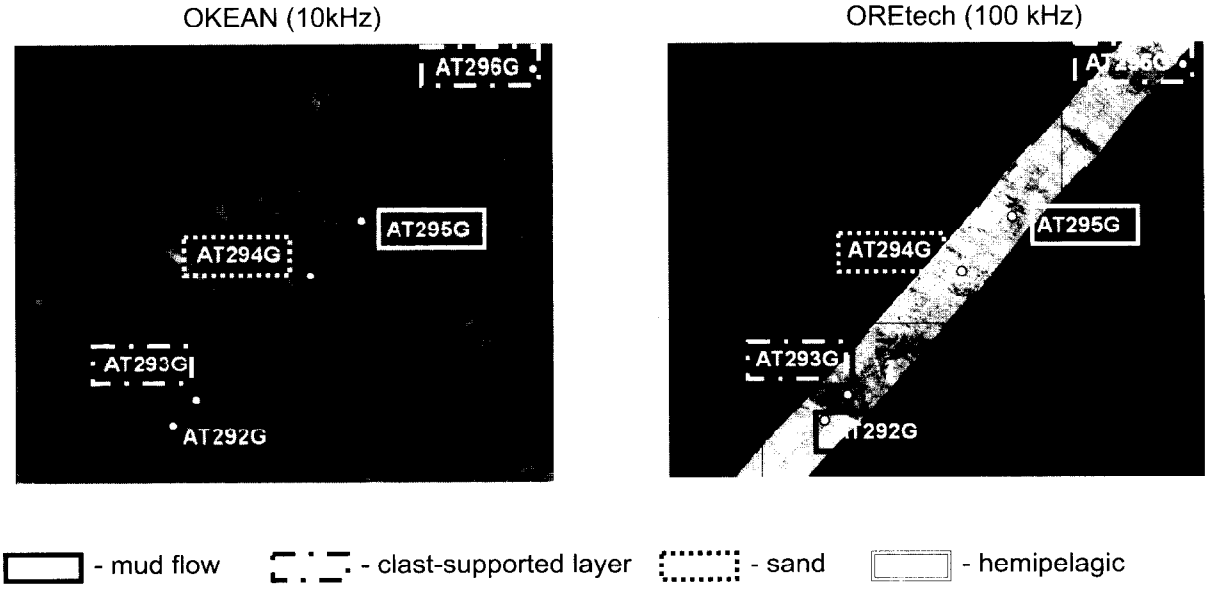

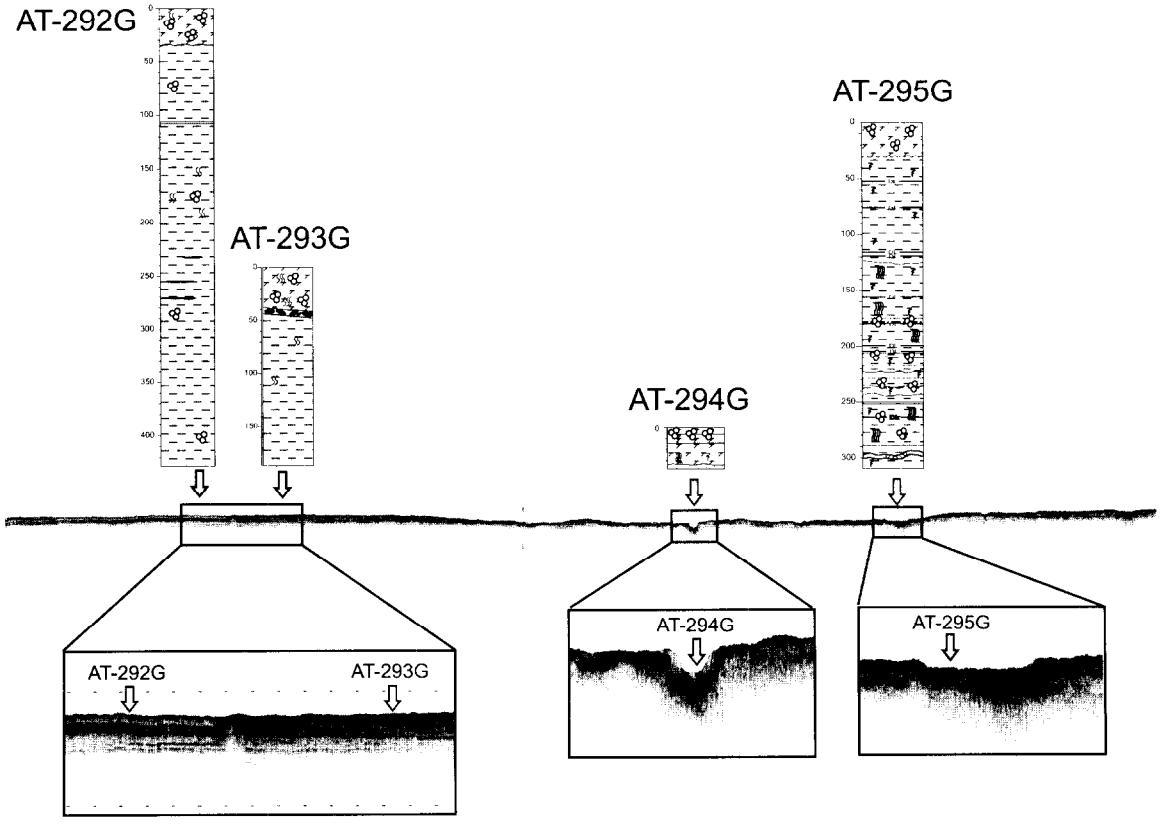

Figure 41. Cores from the lower slope portion of the canyon.

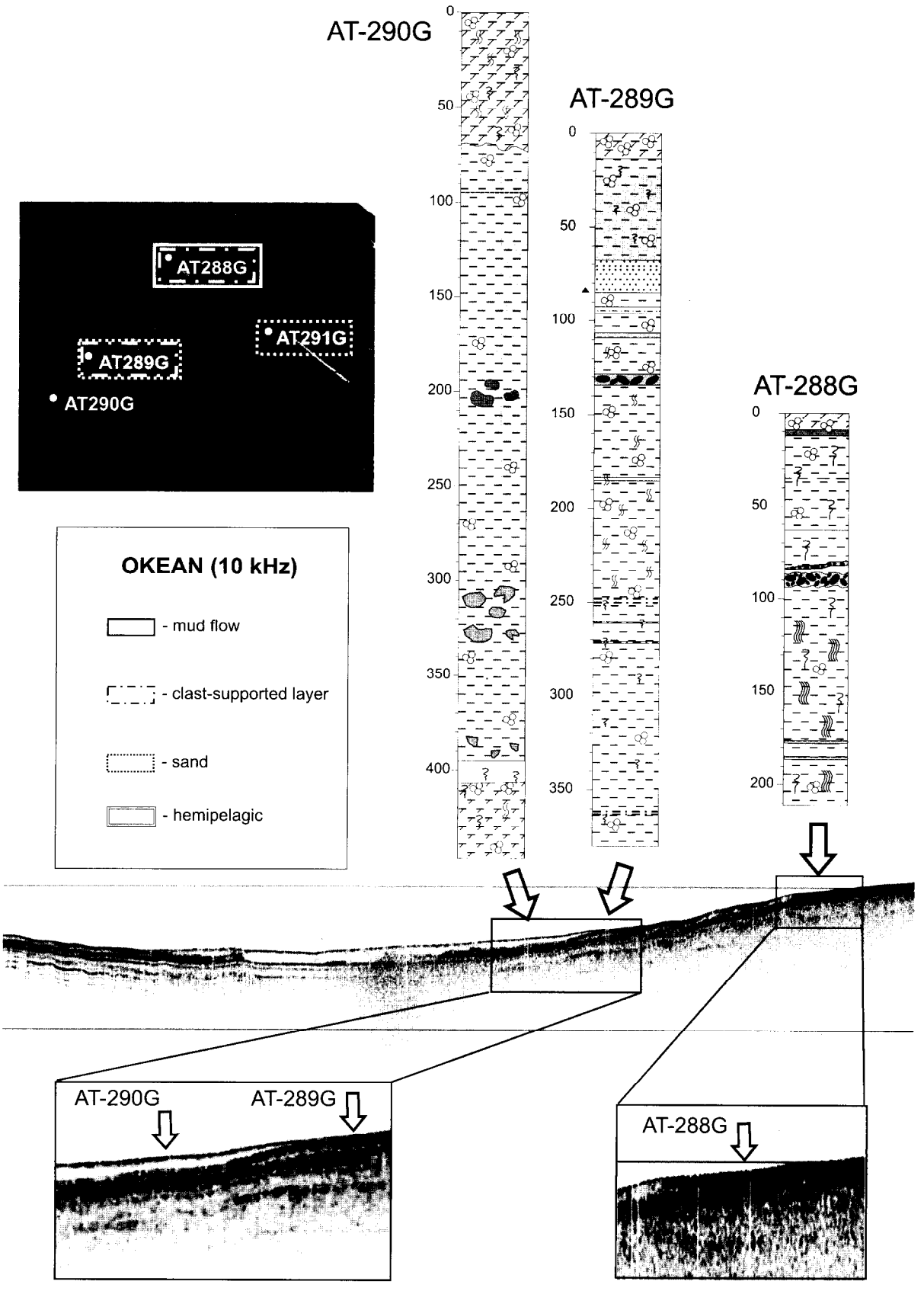

Figure 42. Cores from a portion of the canyon within the upper rise.

perhaps seen in a field of linear features (acoustic facies 10 on OREtech). The transparent lens seen on the profile to the SW is attributed to the (cored) mudflow which is buried by the gravel layer in the centre of the profile. It is a sheet-like lens extending across half of the profile, and is thought to terminate at this locality rather than be eroded out. The mudflow complexity inferred from the profiler and cores is not as straight-forward to interpret from any of the sonographs, but it is interpreted here that there are many, interfingering mud flows possibly coming from different local directions. This is in agreement with conclusions from the Canyon Head region, that the system is now dominated by reworking of intraslope mud. The gravel layers sampled at 293 and 296 are thought to be one and the same. Therefore we could infer that the central part of the profile was an erosive fairway (low relief area of erosion) which truncated the gravel, and possibly the transparent lens underneath. We conclude that there was therefore major erosion in the Lower Slope area as late as the immediate pre-Holocene.

Upper Rise Region

Four cores were taken in the Upper Rise area. Cores AT-288G to AT-290G were targeted on different acoustic facies on the 3.5 kHz profile line PSAT-175. This section is a slope-parallel, strike transect in the depositional area of the Irish Margin (Fig. 42).

Core AT-291G was targeted on an area of medium backscatter on OKEAN line 172.

Core AT-288G was targeted on the edge of a very thin transparent lens, on a topographic high otherwise characterized by medium penetration, multiple layering (which deteriorates rapidly) in the sub-bottom. The area is outside the wide, shallow valley that corresponds to the area downdip of the main canyon mouth. The core recovered a hemipelagic sequence with two clast-supported layers at 0.85 and 0.9 m. These are overlain by silty hemipelagic sediments, which may correlate with the sands in AT-289G, and it is capped by Holocene marl. The gravel layers are of different thickness. Two thin, silty-sandy layers were recovered towards the bottom of the core.

Core AT-289G was targeted on the edge of the shallow valley, on an undulose low-angle slope. The 3.5 kHz profile shows the feather edge of a thin transparent lens underlain by a strong reflector and some deeper strong reflectors. The core recovered a thick sequence, with the Holocene marl underlain by a thin mudflow, underlain by several graded silty-sandy layers (max. thickness 0.2 m) interbedded with hemipelagic sediments, a thin, clast-supported gravel at 1.3 m, and a thick package of hemipelagics without dropstones. Several thin silty layers are seen between 2.5 and 2.7 m.

Core AT-290G was targeted on an area of slightly higher backscatter on the OKEAN, where the transparent lens on the 3.5 kHz is thicker, and nearer the deepest part of the shallow valley. The core recovered a thick sequence, with the Holocene marl underlain by a 3.7 m thick mudflow with various layers of dropstones, some clast-supported, at its lower parts. The mudflow is underlain by *in situ* Holocene sediments.

Core AT-291G was targeted on an OKEAN area of slightly lower backscatter. Most of the sequence is represented by bioturbated grey clay sometimes with parallel bedding. A few thin fine sand turbidites were observed.

Canyon heads further north

Two cores were collected from another canyon head located further to the northeast. TOBI imagery shows that the canyon head also has a cauliflower shape and is characterised by a very weak backscatter, while the surrounding seafloor is of strong backscatter.

Core AT-297 was take from the area of weak backscatter and recovered about 20 cm of fine-grained medium-sorted polimictic sand without visible structure. This confirmed our original suggestion on the cause of the low backscatter. Core AT-298 recovered an almost 4 m long sequence of homogeneous dark grey clay with some silty admixture.

III.2.6. Main Conclusions

A. AKHMETZHANOV AND M. IVANOV

The study of a canyon on the northeastern Rockall Trough margin showed that the system is inactive at the present time as most of the cores were capped by the Holocene draping. It was suggested that the last pulse of active downslope sediment transport took place in immediate pre-Holocene time. Debris flows were found mostly on the flanks of the canyon while the axial zone showed numerous evidence of erosion. Sand was not particularly common in the studied area. It can be suggested that significant amounts of sand are trapped in the canyon head area possibly due to slumps blocking the narrower waist area. Abundant traces of seabed erosion found immediately beyond the canyon mouth indicate that this area is a bypass zone and sand deposition can also occur further into the basin plain. Thin layers of gravel are possibly a result of deposits from a grain flow. The presence of such deposits together with the rippled pattern on the sidescan sonar sonographs indicate that in this part of the slope gravity flows still had significant energy.

Comparison with the Umnak turbidite system (the Bering Sea) shows the analogy of the bypass zone with the zone of longitudinal bedforms in the channel-mouth (Kenyon and Millington, 1995), which also suggests that sand deposition can be expected further into the basin.

III.3. NORTHERN ROCKALL TROUGH AND SOUTHERN FAEROE CONTINENTAL MARGIN

P. BARNETT AND TTR-10 SHIPBOARD SCIENTIFIC PARTY

III.3.1. Objectives

With the available ship-time, it was intended to make a number of deployments of the TV-guided grab system. The majority of the deployments were targeted on areas of the "White Zone" that have proved to be (or are likely to be) impossible to sample using conventional core and grab samplers. The areas were located on the Wyville-Thomson Ridge and southern Faeroe Plateau. Some additional work was also proposed in the Darwin Mounds area to enable sampling of coral growths in a precise and minimally destructive manner (i.e. in contrast with trawling or dredging techniques).

III.3.2. Methodology

Site selection

The site selection was carried out prior to the TTR cruise, primarily using data from previous surveys of the Faeroes Plateau, in particular the TOBI imagery obtained by SOC during RV *Darwin* cruises in 1996 and 1998 (Masson et al., 1997; Bett and Masson, 1998).

Once at the location the precise site selection was carried out using the visual display of the seafloor from the TV grab to select a site of interest at each locality. Typically only 1 grab was taken at each locality, with the exception of AT-312GR/AT313 where 2 samples were made due to the failure of the initial grab to bring up any sediment or biomass.

Deployment and grab operation

The TV grab was operated in conjunction with the RV *Professor Logachev*'s 3.5kHz sub-bottom profiler. This enabled the approximate location of the grab to the seafloor to be determined, by comparison of the profiler information and the amount of cable deployed for the grab. There is a degree of error induced by deviation from the vertical during the descent of the grab towards the seafloor, as a result of the surface movement of the RV *Professor Logachev* and subsurface currents.

There are three main areas from which the TV grab is operated: (1) the control booth, (2) the navigation unit on the Bridge and (3) the Deep Water Exploration Laboratory (DWEL). The control booth is positioned next to the crane mechanism which lowers/raises the grab mechanism, and has a single TV screen to view the relayed visual information from the grab. The DWEL has three TV screens - 1 colour, 2 black and white - which show the relayed information. The chief scientist in charge of the shift on duty watches the screens during the period the seafloor is visible - looking for suitable sample sites, and gives the command when to lower the grab to collect a sample through a direct communications link with both the control booth and the Bridge. During observation the movement of the ship is controlled from the bridge using a Dynamic Positioning System, this is achieved through the constant exchange of instructions from the DWEL, regarding heading and distance, to the Bridge. Of the screens in the DWEL one displays the TV images and two display the video footage - from separate cameras onboard the grab. Visual records of the TV grab images are recorded directly onto VHS video in the DWEL. The lighting onboard the TV grab is operated by a DWEL technician, through a control box that is linked directly to the grab.

Sampling of material

Once a grab sample is onboard the sampling team systematically sample the material. For the

purposes of the data acquisition the sample team focuses on biological specimens. Initially photography of the surface sediments is carried out, with no flora/fauna removed. Once this is complete the biological specimens are removed and placed in 5-litre buckets, they are then transported to the main deck where they are laid out. The grab is then opened and the material deposited on the deck, with another photograph taken. 10 litres of the sediment is then sieved for further biological specimen retrieval, any material of interest retrieved is presented alongside the biological specimens obtained from the surface. The specimens are then photographed with a corresponding station number, and recorded on 'biological survey' forms. Records are also made of the nature of the surface sediments using 'lithological description' forms. Two samples of sediment are also taken - 1 from both the upper- and sub-surfaces (c. 300 g each) - along with extraction of any clasts of interest. Once photographed and recorded the biological specimens are preserved. Some of the more dominant species which are surplus to requirements are placed in a 'touch tank' so that those aboard can see some living examples of the flora and fauna being examined.

Preservation methods

The majority of specimens recovered are preserved. There are 3 methods of preservation being used in this survey: formaldehyde, BSB and freezing.

The majority of specimens are preserved using formaldehyde, this enables subsequent analysis of nutritional information. The formaldehyde (40% concentration) is mixed with tap water to a ratio of 1:9, which produces a formalin solution of 4% concentration. Samples to be preserved are placed in another 5-litre bucket, which is filled to a height 4 cm clear of the samples with the formalin solution, the bucket is then sealed and labeled.

Polyps of living coral obtained are broken from the main body of the coral and preserved in 30ml vials containing BSB, this enables genetic analysis at a later date by the Natural History Museum in London.

Freezing at -12°C is used for the preservation of coral for genetic material for DNA analysis of mother:daughter relationships. However, it must be noted that there were limited amounts of coral and this was the least preferred method of preservation.

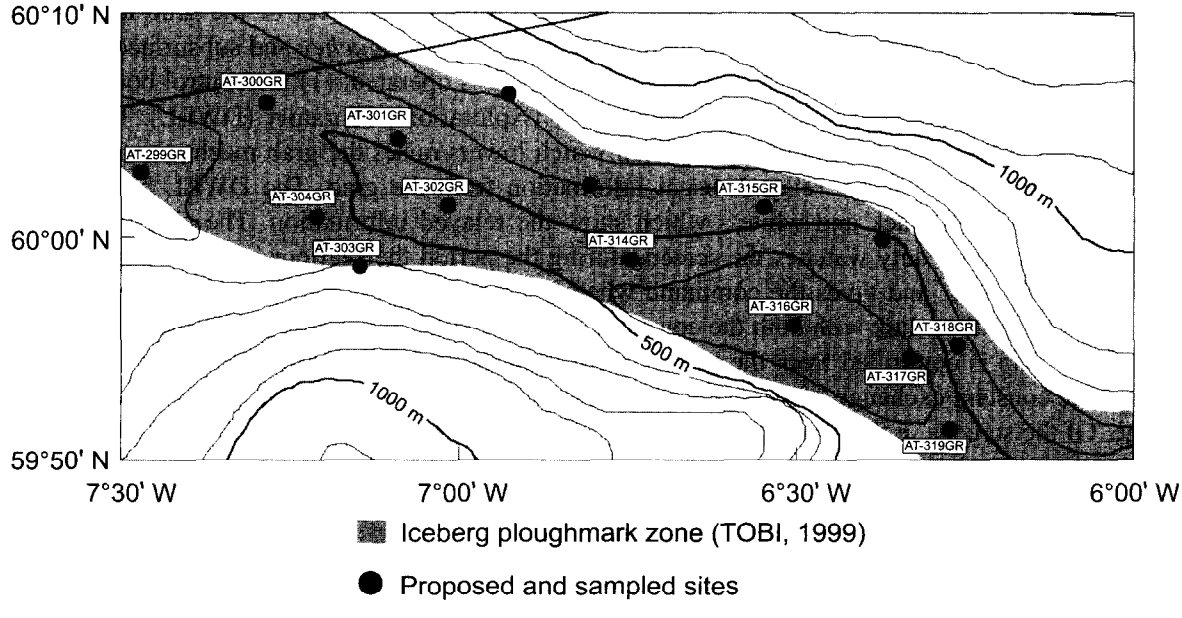

Figure 43. Location map of the environmental survey on the Wyville-Thomson Ridge.

III.3.3. Summary of Work

Wyville-Thomson Ridge (Fig. 43)

The upper reaches of the Wyville-Thomson Ridge pose a challenge to conventional sampling, having extensive areas of dense cobble / boulder cover (the iceberg plough mark area of the DTI 1999 TOBI survey). Video-controlled giant grab sampling was therefore proposed for all those sites already assessed by WASP during the DTI 1999 survey and the additional WASP sites proposed for RRS Charles Darwin cruise 123 (a total of 16 sites). Sampling of the recovered material will primarily aim to provide a qualitative assessment of the composition of the large macrobenthos / megabenthos present. This information will be used to support the quantitative data derived from the corresponding WASP deployments. Given the nature of the seabed and the quality of the grab samples, the recovered sedimentary material is unlikely to be of any value to chemical analyses (e.g. hydrocarbon determinations). However, it is conceivable that potential hydrocarbon contamination could be determined by the analysis of tissue samples from the recovered biological

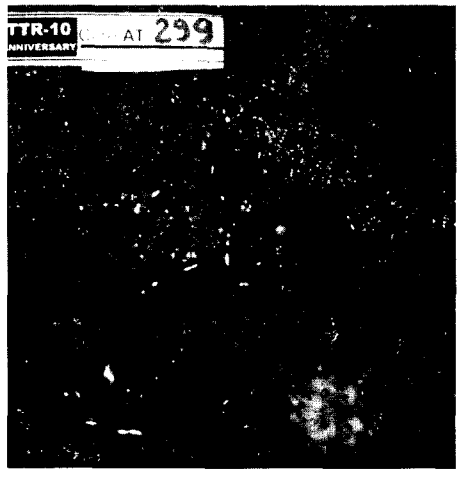

Figure 44. Surface sediment sampled from the Wyville-Thomson Ridge.

Table 6. General information on the samples collected during environmental surveys in the northern Rockall Trough, Wyville-Thomson Ridge and southern Faeroe Plateau area.

Site	*Station #*	*Latitude*	*Longitude*	*Cable length, m*	*Profiler depth, m*
WTR	AT-299	60° 03.006' N	07° 27.964' W	535	520
WTR	AT-300	60° 05.992' N	07° 17.035' W	526	500
WTR	AT-301	60° 04.303' N	07° 05.522' W	535	535
WTR	AT-301	60° 04.302' N	07° 05.519' W	540	535
WTR	AT-302	60° 01.556' N	07° 01.180' W	455	452
WTR	AT-303	59° 58.494' N	07° 08.996' W	640	641
WTR	AT-304	60° 00.995' N	07° 12.785' W	488	484
DM	AT-305	59° 47.898' N	07° 23.396' W	952	952
DM	AT-306	59° 48.105' N	07° 23.543' W	950	949
DM	AT-307	59° 49.445' N	07° 21.884' W	949	950
DM	AT-308	59° 48.662' N	07° 22.989' W	945	946
DM	AT-311	59° 49.057' N	07° 22.199' W	955	955
DM	AT-312	59° 49.646' N	07° 21.653' W	948	946
DM	AT-313	59° 49.510' N	07° 22.021' W	947	945
WTR	AT-314	59° 58.795' N	06° 45.002' W	392	392
WTR	AT-315	60° 01.495' N	06° 32.991' W	473	470
WTR	AT-316	59° 56.000' N	06° 30.007' W	360	361
WTR	AT-317	59° 54.502' N	06° 20.002' W	490	491
WTR	AT-318	59° 55.002' N	06° 15.994' W	577	581
WTR	AT-319	59° 51.512' N	06° 16.495' W	426	427
FP	AT-320	60° 13.407' N	06° 09.998' W	1171	1165
FP	AT-321	60° 12.014' N	06° 04.993' W	1210	1224
FP	AT-322	60° 12.998' N	05° 50.004' W	1112	1110

WTR - Wyville-Thomson Ridge
DM -Darwin Mounds (Northern Rockall Trough)
FP - Southern Faeroe Plateau

material. Geological assessment and analysis of recovered rock samples may also be of value. Some observations made from WASP deployments during the DTI 1999 survey suggest the possibility of mineral coatings (e.g. manganese) on some rocks in the area.

A total of 12 stations were sampled in the area with the TV-guided grab (AT-299GR - AT-303GR and AT-314GR - AT-319GR) (Table 6). Most of the samples were represented by a succession of fine to coarse sand, rich in forams and lithoclastic grains. The sediment was fining downward with increasing clay content. The surface is scattered with dropstones of different lithology, varying in size from 0.5 cm to 15 cm and with a uniform roundness (Fig. 44). Often ripples were observed. Biomass samples taken included shrimps, shells, sponges, polyps, echinodermata, seastars (ophiura) and bryozoa.

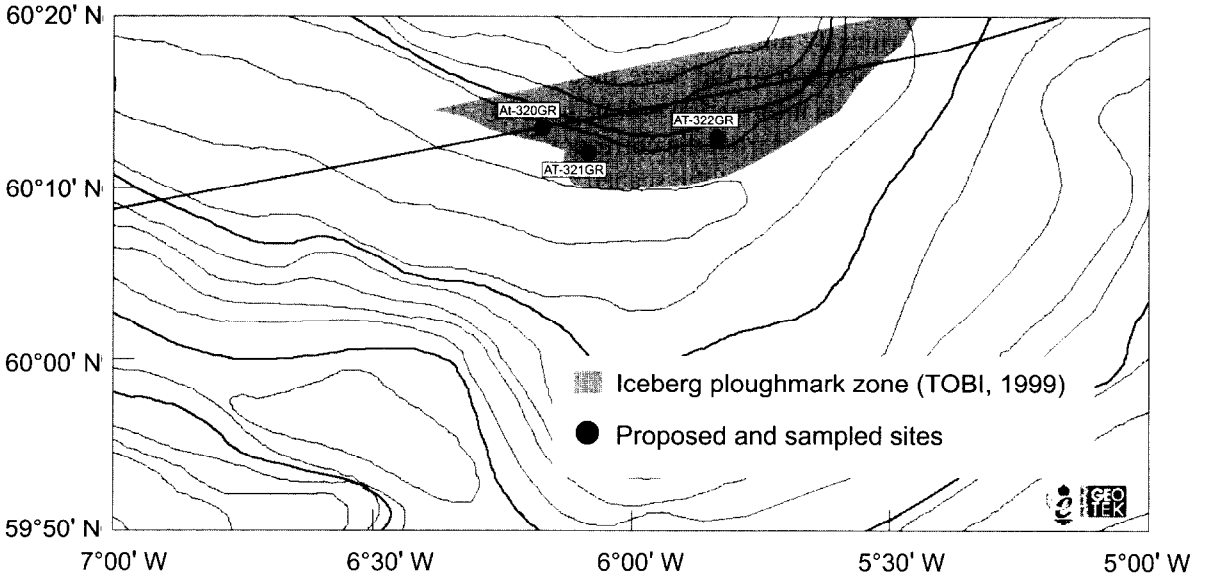

Figure 45. Location map of the environmental survey on the southern Faeroe Plateau.

Faeroe Plateau (Fig. 45)

A second area that has proved problematic to conventional sampling is the area of dense gravel cover on the lower slope of the Faeroe Plateau, where it meets the floor of the Faeroe Bank Channel. Three video-controlled giant grab sampling sites were proposed and sampled (AT-320GR - AT-322GR) in an area that has already been assessed from a SOC deep-towed video survey in 1999. The aims of this sampling was the same as with the Wyville-Thomson Ridge area.

Samples were represented by brownish polymictic medium - coarse sand, medium sorted, with shell fragments and numerous dropstones of different sizes (1-300 mm diameter), roundness and lithology (sandstone, mudstone, quartzite, basalt and others) (Fig. 46).

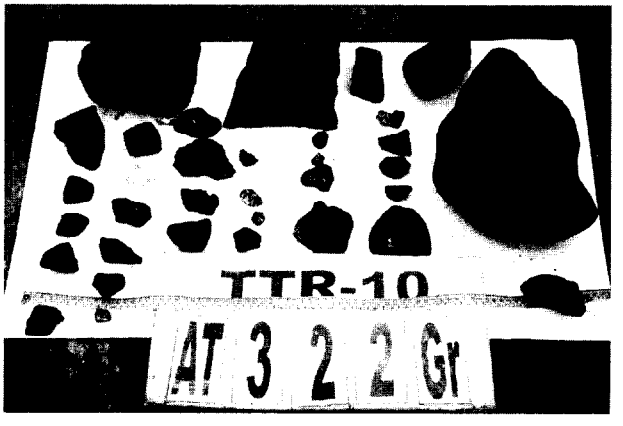

Figure 46. Large glaciagenic debris sampled in the southern Faeroe Plateau area.

Darwin Mounds (Northern Rockall Trough)(Fig. 47)

The Darwin Mounds are named after the SOC research vessel that discovered them. Mounds of this type had never before been observed until they were discovered during a TOBI sidescan sonar survey. The mounds on TOBI sidescan image appear as subcircular targets, typically 50-100 m across. Extending to the southwest of many of the mounds are tails with downcurrent preferred orientation. Later the site was revisited with the WASP (Wide Angle Survey Photography) camera and flash system and coring was done. Colonies of deep-water corals were recovered from the mounds and changes in the biological communities in the tail areas were noticed (Bett and Masson, 1999).

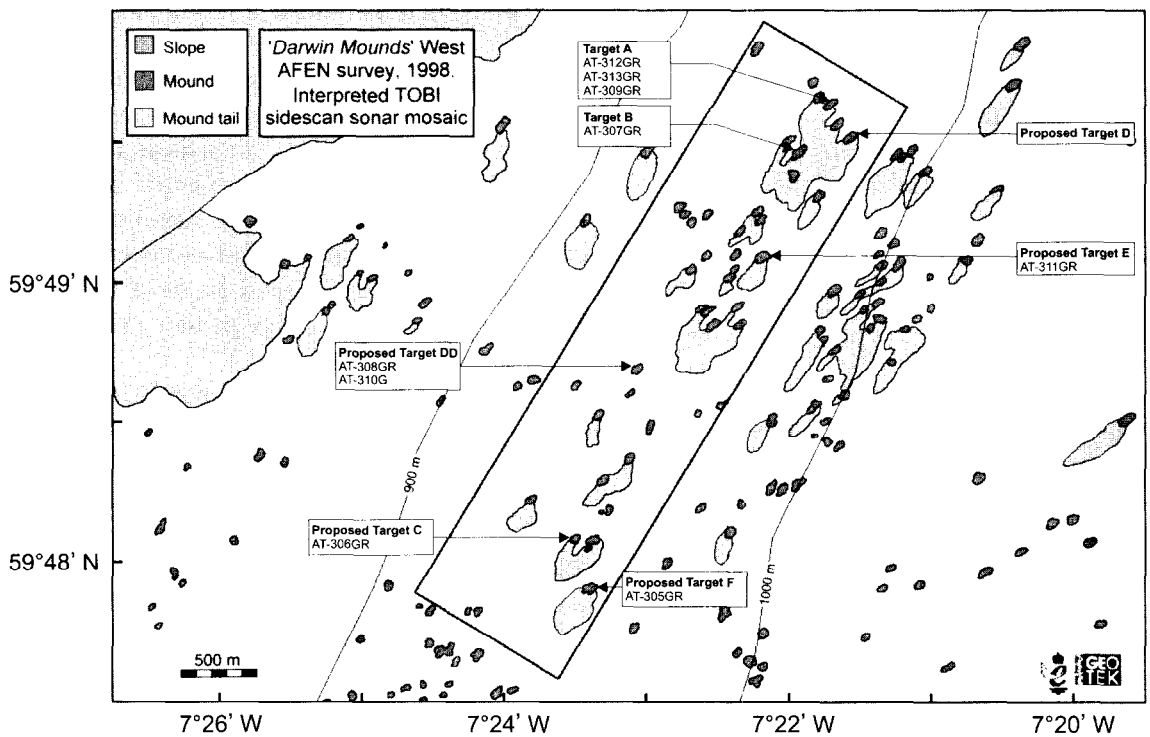

Figure 47. Location map of the environmental survey in the Darwin Mounds area (Northern Rockall Trough).

Three mound sites (A, B and C) were planned to be sampled to make an assessment of intra- and inter-mound variability at different horizontal ranges across the Darwin Mounds west field. The nominal sites selected give approximately order of magnitude variation in horizontal range (A-B 380 m; A-C 3345 m). The resultant samples were intended to serve several purposes:

· Confirmation of the coral species as *Lophelia pertusa*
· Identification of any other coral present (e.g. *Madrepora oculata*)
· Identification of associated species of large macrobenthos and megabenthos
· Research genetic status of *Lophelia* locally and regionally
· Research nutritional status of *Lophelia*
· Supply live material for additional laboratory based research

7 stations were sampled with the TV-guided grab (AT-305GR - AT-308GR, AT-311GR - AT313GR) and 2 stations with the gravity corer (AT-309G and AT310G). The small size of the mounds limited the success rate and abundant samples of coral branches and associated bottom fauna were collected only from 3 stations AT-307GR, AT-308GR and AT312GR. Samples from other stations mainly contained polymictic medium to fine, well sorted sand, often with a rippled surface and very little bioturbation. Gravity cores contained a small amount of fine-grained, well-sorted sand.

III.4. SOUTHERN VØRING PLATEAU

III.4.1. Introduction

S. BOURIAK, A. VOLKONSKAYA

Geological settings

The Norwegian-Greenland Sea is a relatively young oceanic basin, formed by seafloor spreading during the last 56 Ma. It is surrounded by passive continental margins and represents the northernmost extension of the Atlantic Ocean.

Based on bathymetry, morphology and structural elements, the Norwegian continental margin is subdivided into three main units: the More, Vøring and Lofoten-Vesteralen margin provinces. The Vøring Plateau, with an area of approximately 35000 km^2, is flanked by the Lofoten basin in the north and the Norway basin in the southwest (Eldholm et al., 1987). It is a marginal structural high buried beneath a relatively thin veneer of Cenozoic sediments and bounded on its landward side by the Vøring Plateau Escarpment (Rabinowitz et al., 1992). Thick Cenozoic sediment accumulations characterise the area and part of the depocentre coincides with the Storegga Slide, located south of the Vøring Plateau (Jansen et al., 1987). On the marginal Vøring Plateau, diapir fields are present (Hjelstuen et al., 1997).

The potential for sediment deposition in the Norwegian-Greenland Sea responded strongly to the glacial-interglacial paleoclimatic fluctuations in the Quaternary. The regional pattern of sediment flux to the deep seafloor changed considerably (Eldholm et al., 1987). The mainly glacial Quaternary deposits near the shelf edge in the Storegga Slide area vary between 100 and over 300 m in thickness (Bugge et al., 1988).

The Storegga Slide, situated on the passive Norwegian margin south of the Vøring Plateau, is known as one of the world's biggest underwater slides. The headwall, the steepest part of the slide, is 290 km long and has an average slope gradient of 10-20°. The slide deposits are up to 450 m thick, the total run-out distance is approximately 800 km and the total displaced volume of sediments is estimated to be in the order of 5500 km^3. The slide scar area, including distal deposits, is approximately 34000 km^2 (Bugge et al., 1987).

The occurrence of gas hydrates on the Vøring Plateau (seismic observation of bottom simulating reflector - BSR) and their possible relationship with the initiation of the Storegga Slide on the Norwegian shelf edge have been discussed previously (e.g. Bugge et al., 1987; Bugge et al., 1988; Mienert et al., 1998; Bouriak et al., 2000). Bugge et al. (1987) hypothesised that the main triggering mechanism for the slides was likely to have been earthquake loading with a possible contribution of ice loading for the first slide event. From the observation that inferred gas hydrates are located at the same depth as part of the gliding plane, decomposition of hydrates may have contributed to the triggering of the slides, after an earthquake suddenly reshaped the pore pressure distribution in the sedimentary column, leading to liquefaction and weakened sediments (Bugge et al., 1987).

Recently some arguments contradicting this hypothesis have been adduced. It has been shown, that sliding did not necessarily lead to decomposition of hydrates in the area and, even if it had, it could have caused only a negligible increase in pore pressure of the sediments (Bouriak et al., 2000). Moreover, during the TTR-8 Cruise of RV *Professor Logachev* in 1988, the BSR was observed not only below the undisturbed sediments of the Vøring Plateau, but also below the slide deposits (Bouriak et al., 1998, Bouriak et al., 2000). The independence of the BSR from whether there was sliding above it or not, was considered as an indirect evidence of the minor relevance of the sliding to hydrate dissociation and vice versa (Bouriak et al., 2000). Indeed, the question of the interrelation between sliding and gas hydrate decomposition in the area remains discussible and further research is required.

Gas hydrate occurrence is also suggested by fluid escape features on the sea floor surface. Small pockmarks and dome-like elevations were reported 15-20 km to the north of the north head-wall of the slide, having been imaged by various sidescan sonars (Vogt et al., 1999; Bouriak et al., 2000).

Objectives

TTR-10 studies in the area, located at the northern edge of the Storegga Slide and extending to the south-western edge of the Vøring Plateau, were aimed at continuing the survey conducted there during the TTR-8 expedition in 1998. There were 3 main objectives: (1) to continue seismic mapping of the BSR, both below the slide on the SE and at the plateau on the NW, trying to better understand the distribution and spatial extent of inferred gas hydrates, (2) to continue sidescan sonar imaging of fluid escape features of the sea-floor surface of the plateau, and (3) to carry out additional bottom sampling with TV-controlled grab and gravity corer from these features. All this was aimed at achieving a better understanding of the formation and dynamics of gas hydrates and, generally, of the fluid regime in the area, as well as at finding more evidence for or against the hypothesis that the decomposition of gas hydrates could have contributed to slope failures.

III.4.2. Seismic and OKEAN Profiling

A. VOLKONSKAYA, S. BOURIAK, D. MILLER

Introduction

A total of 25 profiles were recorded totalling 755.5 km of seismic data (Fig. 48). The survey speed was approximately 6 knots. The lines were run in a SW-NE direction, along the continental slope (PSAT 178, 179, 180, 181, 182, 183, 184, 187, 189, 190, 192, 193, 195, 196, 198) and are connected by seven short lines (PSAT 186, 191, 194, 197, 200, 201, 202) and two long lines (PSAT 185 and 199) crossing the continental slope in a NW-SE direction. Another line (PSAT 186) was run in S-N direction. The water depth in the study area varies between 600 and 1450 metres. The acoustic penetration achieved was down to 1300 ms TWTT.

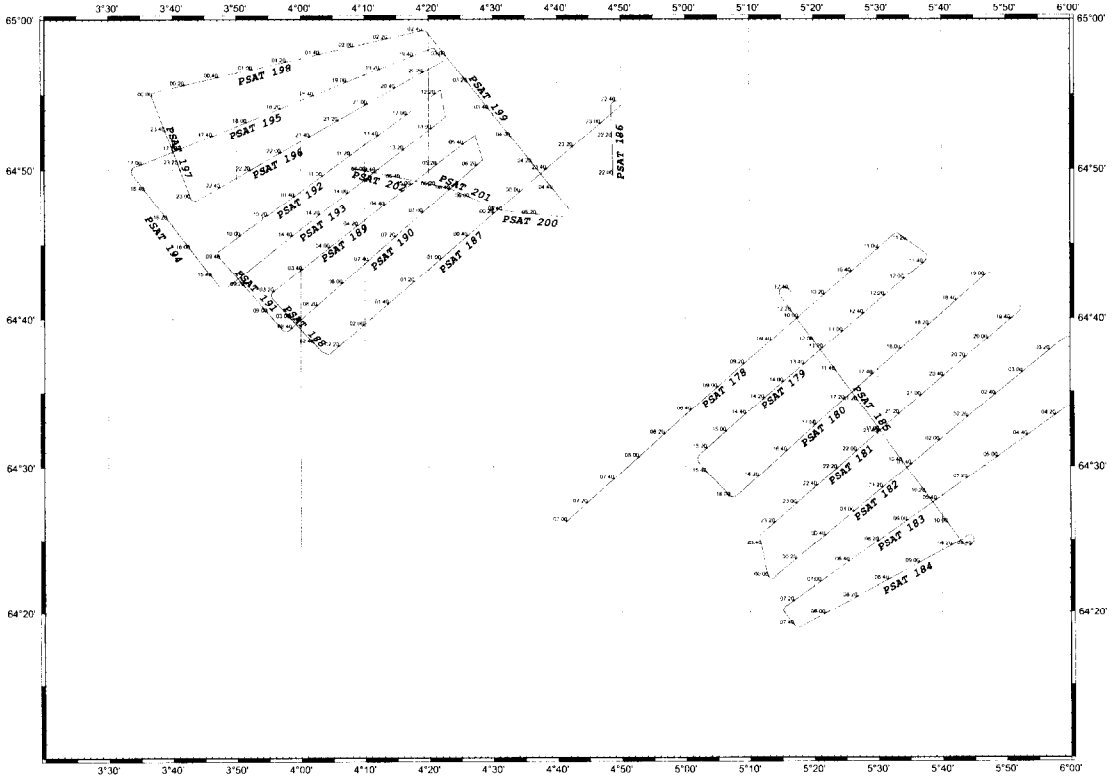

Figure 48. Vøring Plateau study area location map. PSAT - seismic and OKEAN lines

Seismic data interpretation

During the interpretation of the acquired seismic lines, a total of seven different sequences or seismic units were identified on the basis of seismic character, amplitude and reflector terminations (Fig. 49.). All sequences are dipping to the SSE, generally parallel with the surface slope.

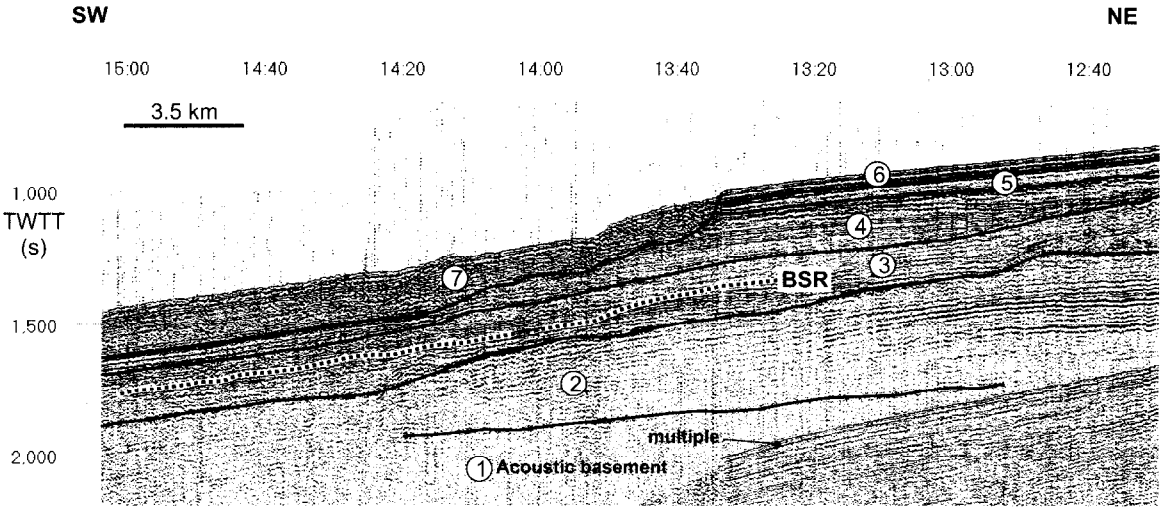

Figure 49. Fragment of seismic line PSAT 179 with the main seismic sequences indicated.

Sequence 1 forms the acoustic basement with a chaotic internal structure. The top of this sequence is a smooth reflector with medium amplitude, which is found all over the study area whenever it lies within the penetration depth. The depth of the reflector is 600-1150 ms (TWTT) deep.

Sequence 2 also has a broad distribution and is composed of a set of discontinuous reflectors with low amplitude. The upper part of this sequence shows a few reflectors, more continuous with higher amplitude. The top of this sequence is at a depth of 1000 ms (TWTT) in the SW part of the area and 600 ms (TWTT) in the NE part. The thickness of sequence 2 is 200-400 ms (TWTT).

Sequence 3 shows very diffuse, low amplitude, discontinuous reflectors. Its thickness varies from 250 to 150 ms (TWTT) because of low amplitude undulations in relief of the top and bottom of

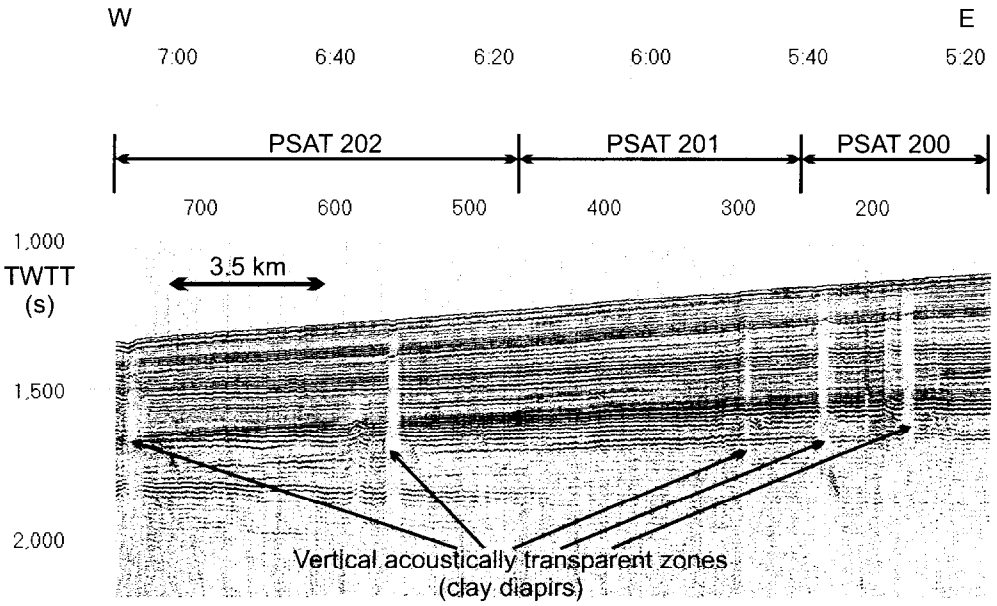

Figure 50. Seismic lines PSAT 200-202 showing a group of possible clay diapirs.

the sequence. In some places a significantly increased amplitude of the signal is observed, forming "bright spot" acoustic anomalies. Within this unit the BSR (bottom simulating reflector) was distinguished. It is a continuous high amplitude reflector with reversed polarity, roughly following the sea bottom topography at about 300 ms (TWTT) below the sea bottom and cross-cutting the internal reflectors of the unit. In the northern part of the studied area the sequence is disturbed by the presence of acoustically transparent narrow vertical zones crossing the whole sedimentary succession and interpreted as clay diapirs (Fig. 50). These transparent zones can still be traced within sequence 2. The top of sequence 3 is eroded in the SW part of the area and contains lens-like bodies of buried slump deposits with very diffuse, low amplitude, discontinuous reflectors. Their thickness is about 100-150 ms (TWTT).

Sequence 4 displays continuous moderate to high amplitude reflectors with minor internal discontinuities. The top of the sequence is represented by a prominent high-amplitude reflector. In the northern part of the area the sequence contains "bright spot" acoustic anomalies probably related to the presence of free gas (Fig. 51).

Sequence 5 displays a well-layered pattern of numerous parallel reflectors of moderate to high amplitude. The top of the sequence is a strong reflector traced over the whole study area.

Sequence 6 only appears in the north-eastern part of the area. Two sub-sequences can be distinguished within the sequence. They are represented by alternate bands of high to very high continuous reflectors.

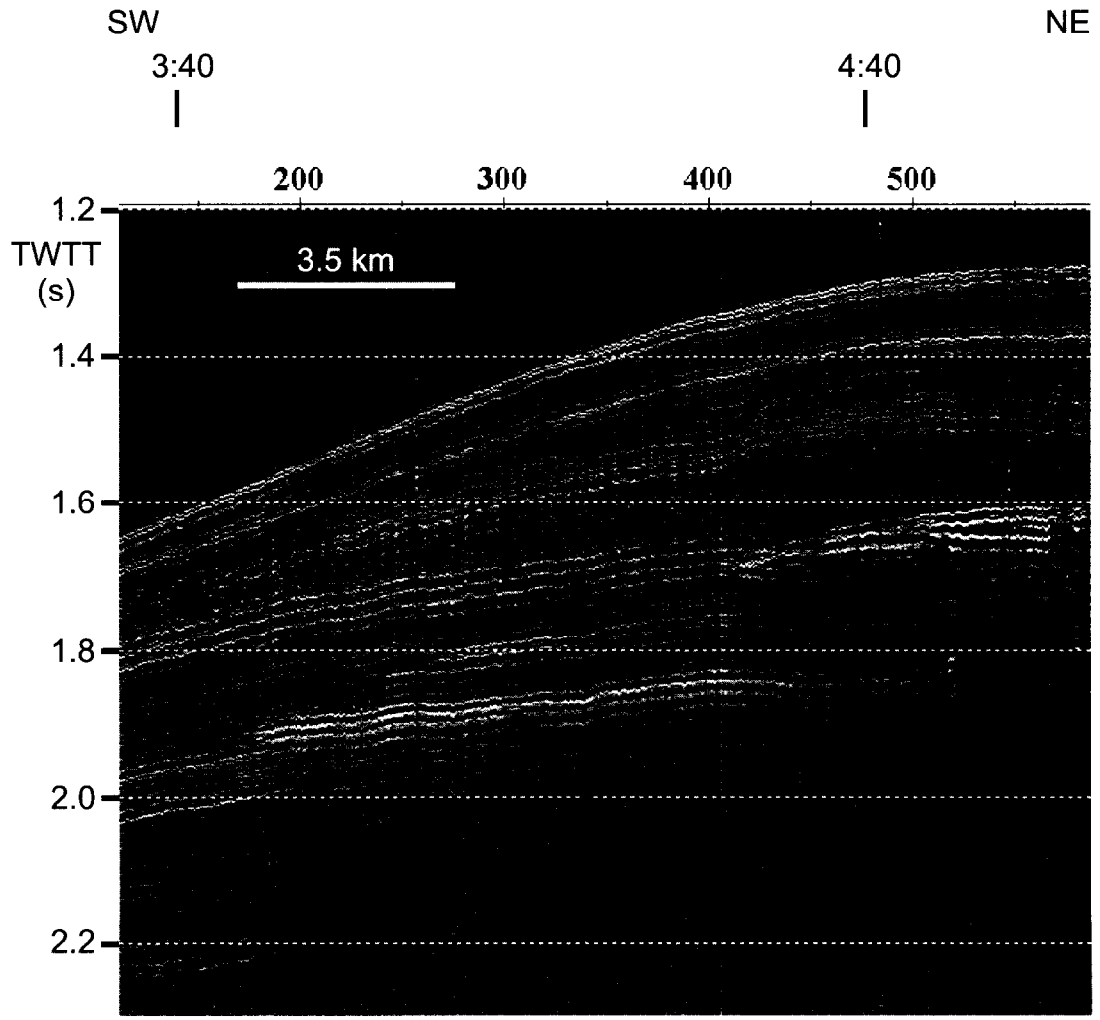

Figure 51. Fragment of seismic line PSAT 189 showing "bright spot" acoustic anomaly within the sequence 3.

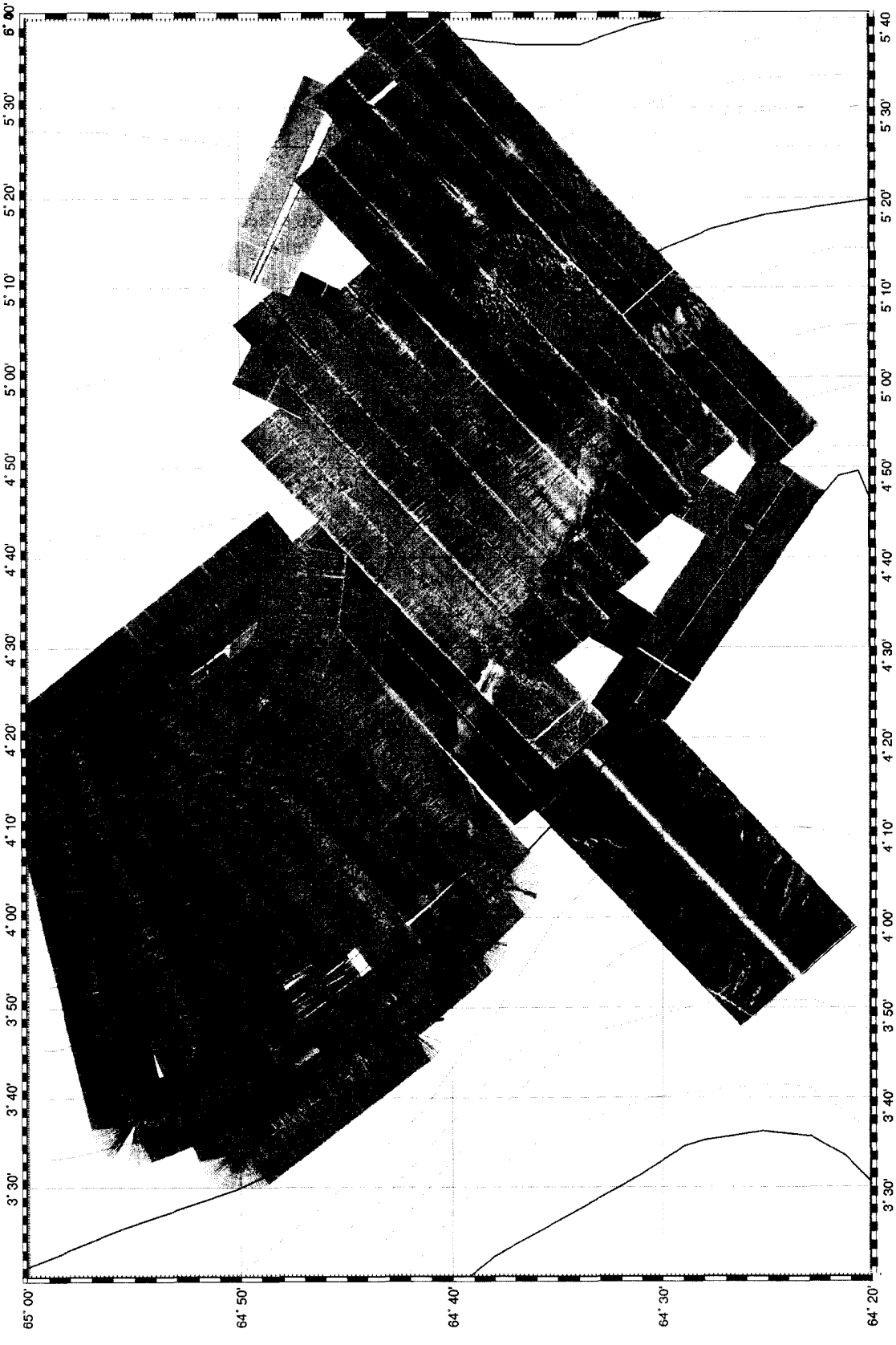

Figure 52. OKEAN image of the study area on the Vøring Plateau. Coverage obtained during TTR-8 cruise is also shown.

Sequence 7 is found only within the Storrega Slide and seems to be sediments removed from sequence 6. It is a very heterogeneous sequence, which displays transparent acoustic facies and very high amplitude reflectors which are continuous as well as chaotic. This sequence could represent the most recent slide deposits.

OKEAN survey

Due to weather conditions the OKEAN survey had to be skipped for lines PSAT-178 - PSAT-185 and was carried out only along lines PSAT-186 - PSAT-202. The new OKEAN data extended to the northwest the OKEAN coverage obtained in this area in 1998 during TTR-8 cruise (Kenyon et al., 1999). The new image (Fig. 52) showed mainly a weakly backscattering seafloor with numerous isometric spots of high backscatter up to 200 m in diameter. Detailed survey of these structures in 1998 showed that in most instances they represent large pockmarks and sometimes outcropping tops of mud diapirs.

III.4.3. Bottom Sampling

G. AKHMANOV, A. MAZZINI, A. STADNITSKAYA, M. IVANOV, E. KOZLOVA, D. OVSYANNIKOV, A. STEPANOV, A. SAUTKIN, I. PASECHNIK, I. BELENKAYA, V. BLINOVA, L. MAZURENKO, AND N. GALIN

The main goal of the sampling programme on the Vøring Plateau was to sample fluid escape structures on the seafloor and also to check out several possible mud diapirs. 8 sites were sampled. 4 with TV-guided grab and 4 with a gravity corer (Table 7, Annexe I).

Core AT-323GR

The core was collected from the the inferred mud volcanic structure called "Tobic". The sample consisted of large carbonate crusts with shell and coral debris within a carbonate matrix. In the lower part of the sample there were layers of fine clayey sand and silty clay. The sample had a strong smell of H_2S.

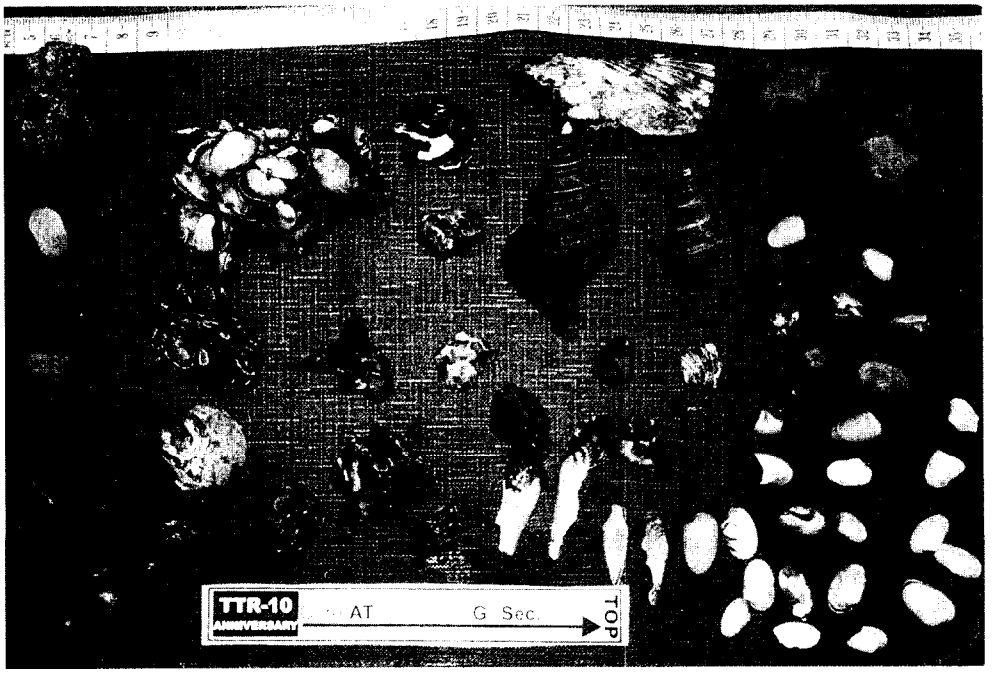

Figure 53. Fragments of rocks, bivalve and gastropod shells from the site AT-323GR.

Table 7. General information on the cores sampled on the Vøring Plateau.

Core No	Date	Time, GMT	Latitude	Longitude	Cable length, m	Depth, m	Recovery, cm
TTR-10-AT-323GR	24.08.00	13:47 14:08	64°40.876' N 64°40.907' N	05°15.814' E 05°15.749' E	717 719	723	
TTR-10-AT-324G	24.08.00	15:04	64°40.901' N	05° 15.741' E	723	724	490
TTR-10-AT-325GR	24.08.00	18:46 19:35	64°46.113' N 64°46.141' N	04°48.709' E 04°48.661' E	789 795	794	
TTR-10-AT-326G	24.08.00	20:28	64°46.104' N	04° 48.713' E	794	794	526
TTR-10-AT-327G	26.08.00	08:54	64°49.989' N	04° 09.286' E	1008	1008	573
TTR-10-AT-328G	26.08.00	10:57	64°49.170' N	04° 18.586' E	950	964	573
TTR-10-AT-329GR	26.08.00	13:20 13:44	64°47.548' N 64°47.479' N	04°30.391' E 04°30.454' E	872 875	890	
TTR-10-AT-330GR	26.08.00	16:54 17:40	64°47.118' N 64°47.079' N	04°48.403' E 04°48.381' E	785 792	801	

Core AT-324G

The sample was collected in the vicinity of the previous station. The core recovered a sequence of silty clay with some rock clasts which were up to 1 cm in diameter in the middle part of the core.

Core AT-325GR

The grab was taken from a depression seen on the 3.5 kHz profiler record and interpreted as a possible pockmark. The sample was represented by a homogeneous grey clay with *Pogonophora* in the upper part.

Core AT-326G

Another attempt to groundtruth an inferred pockmark. The core recovered an intensively bioturbated section of uniform silty clay.

Core AT-327G

The station was planned on the basis of the OKEAN image and meant to groundtruth a small isometric patch of high backscatter interpreted as a possible pockmark. The recovered section was represented by bioturbated grey clay with some hydrotroilite.

Core AT-328G

The core was taken from a pockmark well seen on a seismic line. A sequence of homogeneous grey silty clay with some hydrotroilite was recovered

Core AT-329GR

Another sample from a pockmark seen on a seimic line. The grab sample was represented by homogeneous grey silty clay with some hydrotroilite. Some *Pogonophora* were found in the upper part of the sample. Faint smell of H_2S was detected.

Core AT-330GR

Another sample from a pockmark. Grey homogeneous clay with significant silty admixture.

III.4.4. Main Results

S. BOURIAK AND M. IVANOV

The investigations enabled mapping of distribution of BSR zone in the southeastern part of the area. The boundary of the zone can be traced 15 km to southeast, where it disappears. This may indicate that the formation of the Storegga Slide was not directly related to the dissolution of gas hydrates. In the northwest of the study area the boundary is found within the undisturbed sedimentary section of the Vøring Plateau up to 64°30'N and possibly continues further north but lack of time prevented mapping of the continuation of the zone.

The investigation also provided a new insight into the problem of gas hydrates formation in the area. The previous model (Bouriak et al., 2000), postulating the presence of two independent zones with a BSR, turned out to be very simplified. The new data revealed that there are at least four separate zones where a BSR is found and they extend approximately parallel to the contours. These zones are possibly related with certain stratigraphic intervals where lithological conditions are favourable for gas hydrate formation. The BSR is found in places where these intervals cross the hydrate stability field which follows the present seafloor relief.

The sidescan sonar survey extended and outlined the area of fluid escape structures on the Vøring Plateau studied by TTR in 1998 (Kenyon et al., 1999). The sampling confirmed the interpretation of the acoustic data.

REFERENCES

Baptista, M.A., Miranda, P. M. A. and Mendes Victor, L. (1998). Constraints on the source of the 1755 Lisbon tsunami inferred from numerical modelling of historical data. *Journal of Geodynamics*, 25 (2), 159-174.

Bett, B., and Masson, D., 1998. Atlantic Margin environmental surveys. In Depth, Southampton Oceanography Centre, 3, 4-5.

Bett, B.J., and Masson, D., 1999. Biological zonation of bathyal carbonate mounds formed under a prevailing bottom current. North-East Atlantic Slope Processes: Multi- Disciplinary Approaches, 24-27 January 1999, SOC, UK. Incorporating: TTR-8 Post Cruise Conference; 4th ENAM II Workshop; IGCP Workshop 432 - Contourites and Bottom Currents. Southampton Oceanography Centre, 19.

Bolli, H.M., Saunders, J.B. and Perch-Nielson, K. 1985. Plankton Stratigraphy. Cambridge University Press. 1032 pp.

Bolshakov, A.M., and Yegorov, A.G., 1987. Use of phase-equilibrium degassing in gas investigations. *Oceanology*, 27(5), 652-653.

Bouriak, S., De Mol, B., Baturin, M., Yakovlev, E., 1999. Southern Vøring Plateau: Seismic profiling data. In Kenyon, N., Ivanov, M. & Akhmetzhanov, A. (eds.), Geological Processes on the Northeast Atlantic Margin: preliminary results of geological and geophysical investigations during the TTR-8 cruise of RV *Professor Logachev*, 1998, 81-83.

Bouriak, S., Vanneste, M, and Saoutkine, A., 2000. Inferred gas hydrates and clay diapirs near the Storegga Slide on the southern edge of the Vøring Plateau, offshore Norway. *Marine Geology*, 163, 125-148.

Bugge, T., Befring, S. Belderson, R.H., Eidvin, T., Jansen, E., Kenyon, N.H., Holtedahl, H., Sejrup, H.P. 1987. A giant three-stage submarine slide off Norway. *Geo-Marine Letters*, 7, 191-198.

Bugge, T., Belserson, R.H., Kenyon, N.H., 1988. The Storegga Slide. *Philosophical Transactions of the Royal Society of London*, 325, 357-388.

Damuth, J. E., 1975. Echo character of the western equatorial Atlantic floor and its relationship to the dispersal and distribution of terrigeneous sediments. *Marine Geology*, 18, 17-45.

Eldholm, O., Thiede, J. & Taylor, E., 1987. Evolution of the Norwegian Continental Margin: background and objectives. in Eldholm, O., Thiede, J. & Taylor, E., Proceedings of the Ocean Drilling Program, initial reports, Leg 104, 5-25.

Fouquet, Y., 1999. Where are the large hydrothermal sulphide deposits in the oceans? In Cann, J.R., Elderfield, H. & Laughton, A. (Editors), Mid-Ocean Ridges. Cambridge University Press , 211-224.

Fouquet, Y., Knott, R., Cambon, P., Fallick, A., Rickard, D., and Desbruyeres, D., 1996. Formation of large sulfide mineral deposits along fast spreading ridges. Example from off-axial deposits at 12.43N on the East Pacific Rise. *Earth and Planetary Science Letters*, 144(1/2), 147-162.

Grimison, N.L., Chen, W-P., 1988. Source mechanisms of four recent earthquakes along the Azores-Gibraltar plate boundary. *Geophysical Journal*, 92(3), 391-401.

Hindson, R.A., Andrade, C., 1999. Sedimentation and hydrodynamic processes associated with the tsunami generated by the 1755 Lisbon earthquake. *Quaternary International*, 56, 27-38.

Hjelstuen, B.O., Eldholm, O., and Skogseid, J., 1997. Vøring Plateau diapir fields and their structural and depositional settings. *Marine Geology*, 144, 33-57.

Hunter, P. and Kenyon, N.H., 1984. Bathymetry of Porcupine Seabight and Porcupine Bank. 3 charts at 1:274,000. Unpublished Report of Institute of Oceanographic Sciences, UK.

Jansen, E., Befring, S., Bugge, T., Eidvin, T., Holtedahl, H. & Sejrup, H.P., 1987. Large submarine

slides on the Norwegian continental margin: sediments, transport and timing. *Marine Geology*, 78, 77-107.

Johnson, M.A., Kenyon, N.H., Belderson, R.H. and Stride, A.H., 1982. Sand transport. In: Stride, A.H. (ed), *Offshore tidal sands*. London, Chapman & Hall, 58-94.

Kenyon N.H., Ivanov M.K., and Akhmetzhanov A.M. (eds), 1998. Cold water carbonate mounds and sediment transport on the Northeast Atlantic margin. Preliminary results of geological and geophysical investigations during the TTR-7 cruise of RV *Professor Logachev* in co-operation with the CORSAIRES and ENAM 2 programmes. *IOC Technical Series*, 52, 178 pp.

Kenyon, N.H., Belderson, R.H. and Stride, A.H., 1978. Channels, canyons and slump folds on the continental slope between south-west Ireland and Spain. *Oceanologica Acta*, 1: 369-380.

Kenyon, N.H., Belderson, R.H., 1973. Bedforms of the Mediterranean undercurrent observed with sidescan sonar. *Sedimentary Geology*, 9, 77-99.

Kenyon, N.H., Ivanov, M.K. and Akhmetzhanov, A.M. (eds.), 1999. Geological Processes on the Northeast Atlantic Margin. *IOC Technical Series*, 54, UNESCO, 141 pp.

Kenyon, N.H., Ivanov, M.K., Akhmetzhanov, A.M. and Akhmanov, G.G., (eds), 2000, Multidisciplinary study of geological processes on the Northeast Atlantic and Western Mediterranean margins. *IOC Technical Series* 56, UNESCO, Paris, 119 pp.

Kenyon, N.H., Millington, J., 1995. Contrasting deep-sea depositional systems in the Bering Sea. In: Pickering, K.T., Hiscott, R.N., Kenyon, N.H., Ricci Lucchi, F., Smith, R.D.A. (eds). *Atlas of deep water environments: architectural style in turbidite systems*. London, Chapman & Hall, 196-202.

Langmuir, C., Humphris, S., Fornari, D., Van Dover, C., Von Damm, K., Tivey, M.K., Colodner, D., J.-L. Charlou, Desonie, D., Wilson, C., Fouquet Y., Klinkhammer, G. & Bougault, H., 1997. Hydrothermal vents near a mantle hot spot: the Lucky Strike vent field at 37°N on the Mid-Atlantic Ridge. *Earth and Planetary Science Letters*, 148, 69-91.

Masson, D.G., Bett, B.J., and Birch, K.G., 1997. Atlantic margin environmental survey. *Sea Technology*, 38(10), 52-59.

Mienert, J., Posewang, J., Baumann, M., 1998. Gas hydrates along the northeastern Atlantic margin: possible hydrate-bound margin instabilities and possible release of methane. In: Henriet, J.-P., and Mienert, J. (eds) *Gas Hydrates: Relevance to World Margin Stability and Climate* Change. Geological Society, London, Special Publications, 137, 275-291.

Nelson, C.H.. Baraza, J., and Maldonado, A. 1993. Mediterranean undercurrent sandy contourites, Gulf of Cadiz, Spain. *Sedimentary Geology*, 82, 103-131.

Parson, L., Gracia, E., Coller, D., German, C., and Needham, D., 2000. Second-order segmentation; the relationship between volcanism and tectonism at the MAR, 38N-35 40N. *Earth and Planetary Science Letters*, 178(3/4), 231-251.

Rabinowitz, P.D., Baldauf, J.G., Garrison, L.E. & Meyer, A.W., 1992. Ocean drilling on passive continental margins. in Watkins, J.S., Zhiqiang, F. & McMillen, K.J. (eds.); *Geology and Geophysics of Continental Margins*, American Association of Petroleum Geologists, 399-414.

Rice, D. D and Claypool, G. E., 1981. Generation, accumulation, and resource potential of biogenic gas. *AAPG Bulletin*, 65, 5-25.

Sartori, R., Torelli, L., Zitellini, N., Peis, D., and Lodolo, E., 1994. Eastern segment of the Azores-Gibraltar line (central-eastern Atlantic): an oceanic plate boundary with diffuse compressional deformation. *Geology*, 22(6), 555-558.

Torelli, L. E. A., 1997. The giant chaotic body in the Atlantic Ocean off Gibraltar: new results from a deep seismic reflection survey. *Marine and Petroleum Geology*, 14(2): 125-138.

Tyson, R.V., 1995. Sedimentary organic matter: organic facies and palynofacies. London, Chapman & Hall. 615 pp.

Vogt, P., Gardner, J., Crane, K., Sundvor, E., Bowels, F., and Cherkashev, G. 1999. Ground-truthing 11- to 12-kHz sidescan sonar imagery in the Norwegian-Greenland Sea: Part I: Pockmarks on the Ventnesa Ridge and Storegga slide margin. *Geo-Marine Letters*, 19, 97-110.

Zaragosi, S., Le Suave, R., Bourillet, J.-F., Auffret, G.A., Faugeres, J.-C., Pujol, C., and Garlan, T., 2001. The deep-sea Armorican depositional system (Bay of Biscay), a multiple source, ramp model. *Geo-Marine Letters*, 20(4), 219-232.

Zitellini, N., Chierici, F., Sartori, R. and Torelli, L. (1999). The tectonic source of the 1755 Lisbon earthquake and tsunami. *Annali di Geofisica*, V. 42, 49-55.

ANNEX I. CORE LOGS

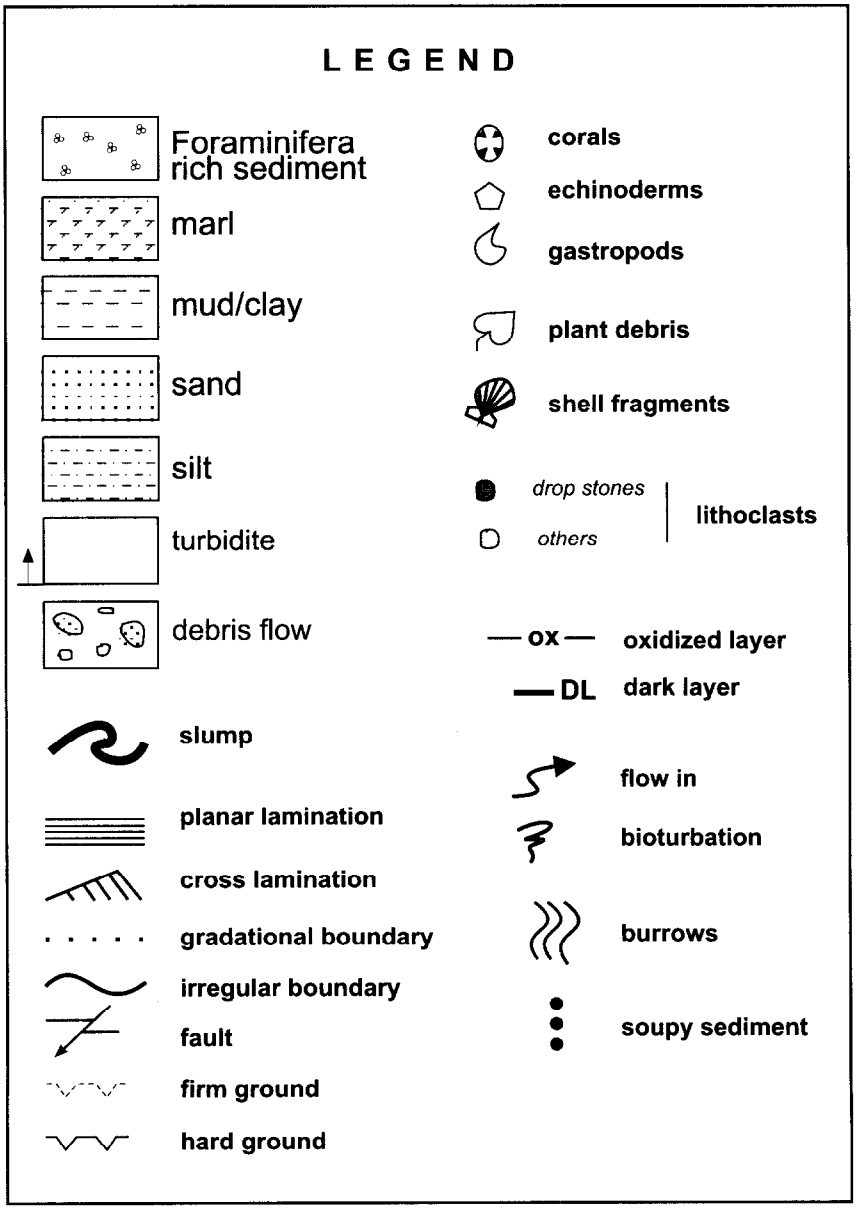

ANNEXE I. CORE LOGS (LEG 1, The Marques de Pombal structure)

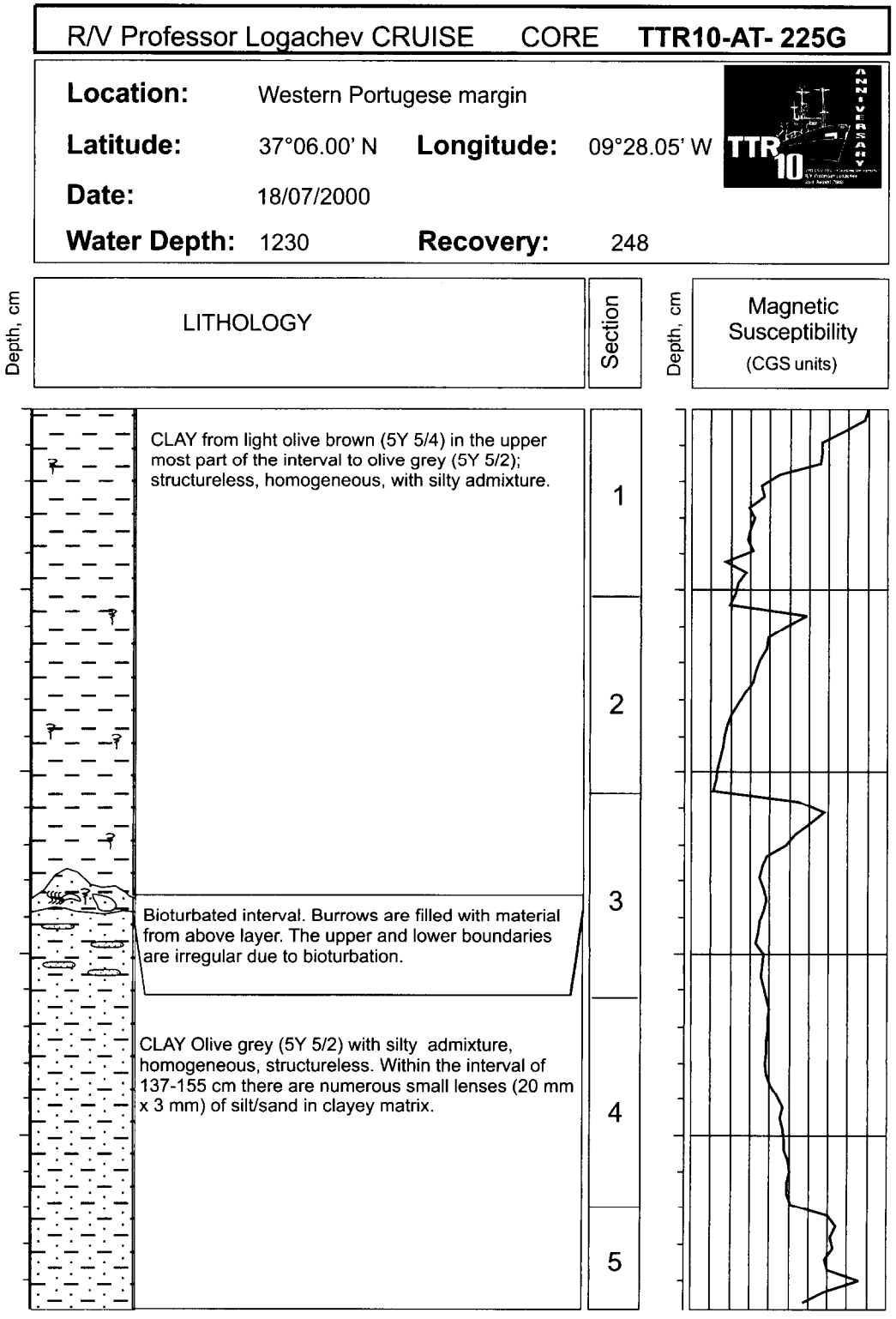

Core log TTR-10-AT-225G

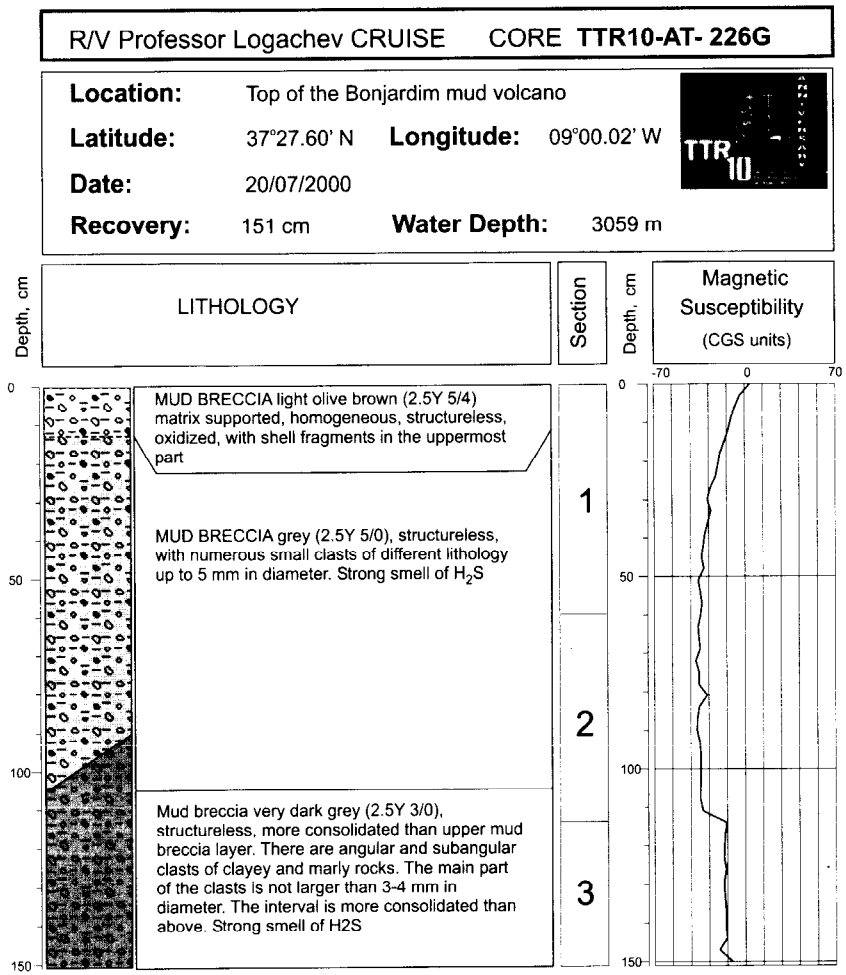

Core log TTR-10-AT-226G

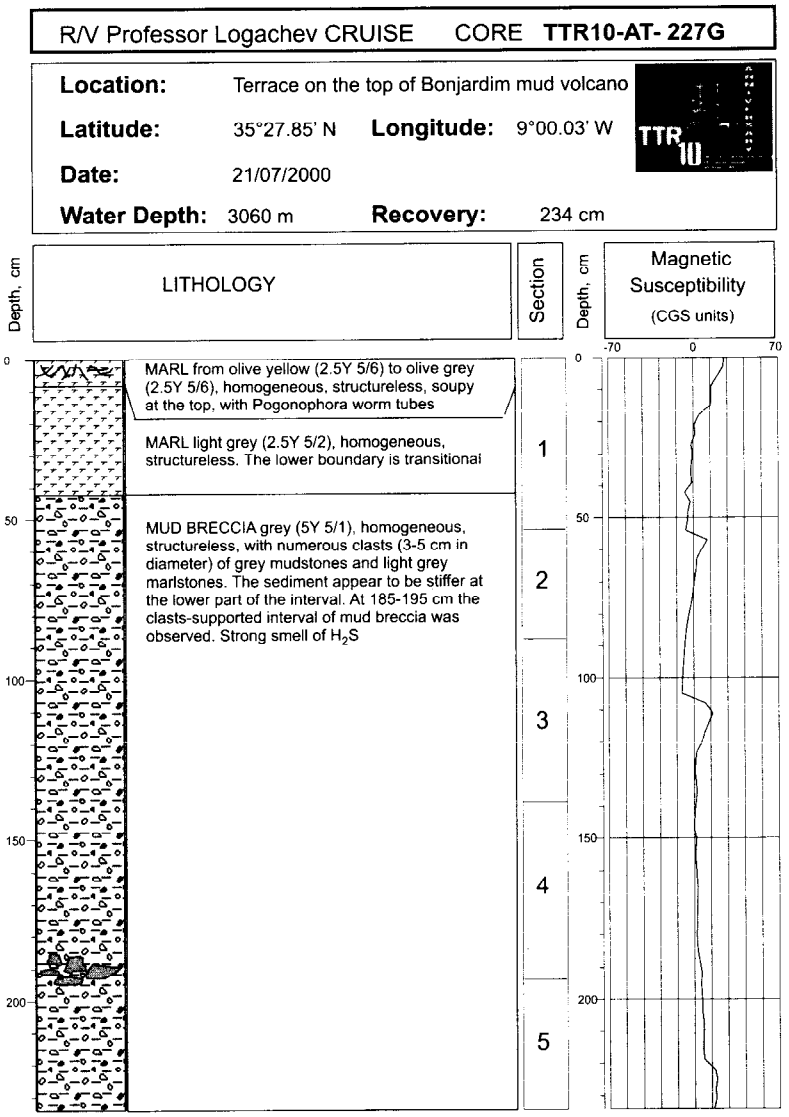

Core log TTR-10-AT-227G

ANNEX I. CORE LOGS (LEG 1, Algarve margin and Gulf of Cadiz)

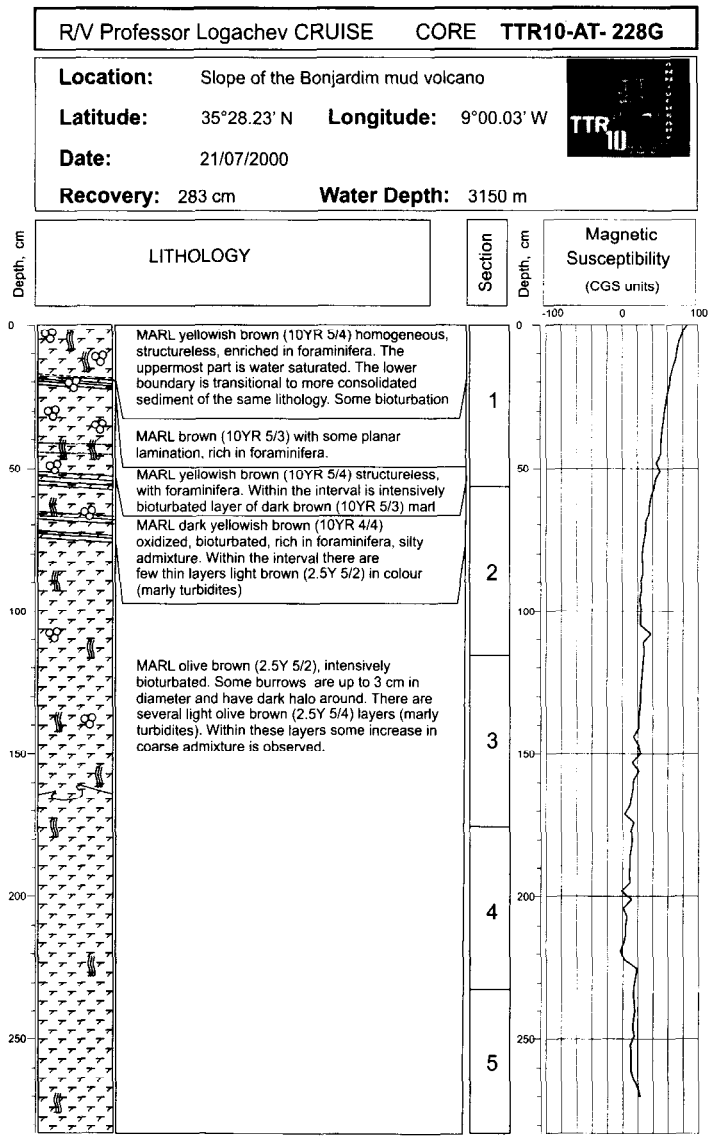

Core log TTR-10-AT-226G

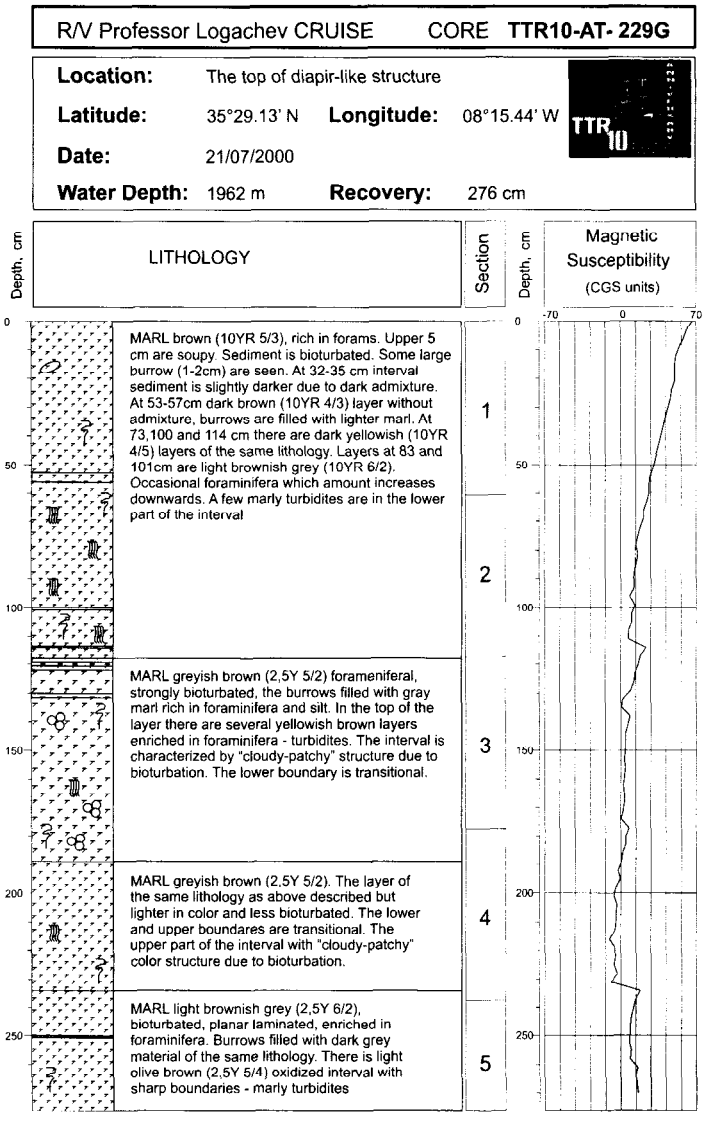

Core log TTR-10-AT-227G

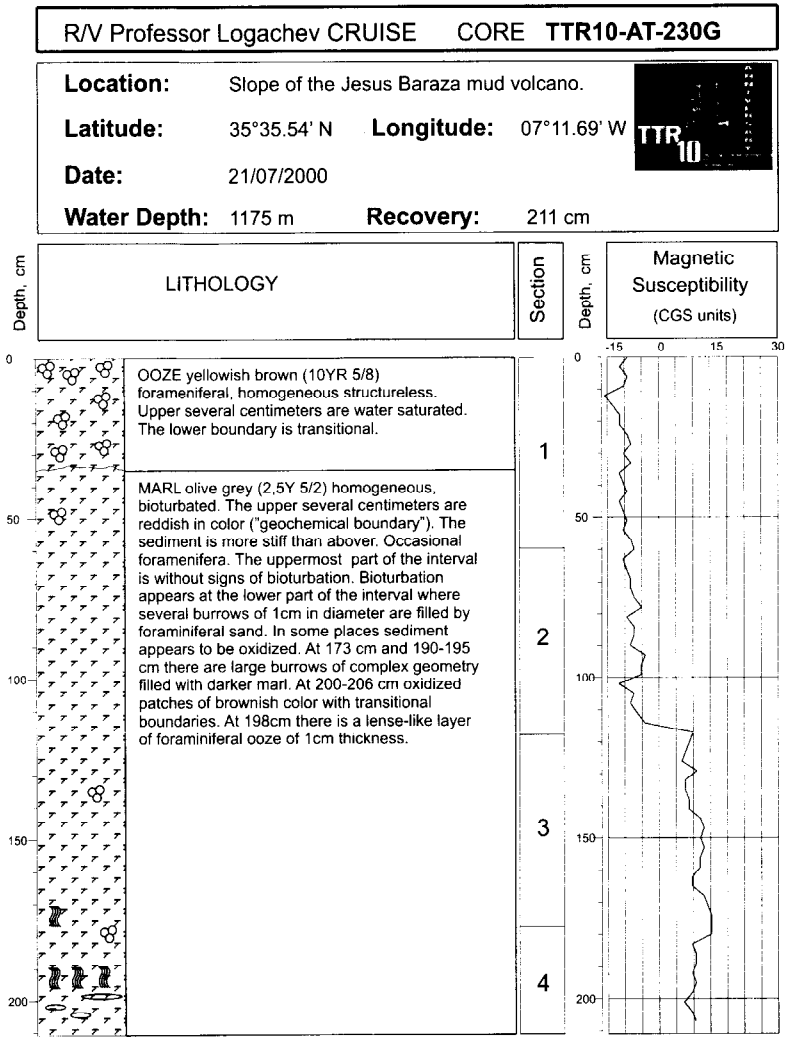

Core log TTR-10-AT-230G

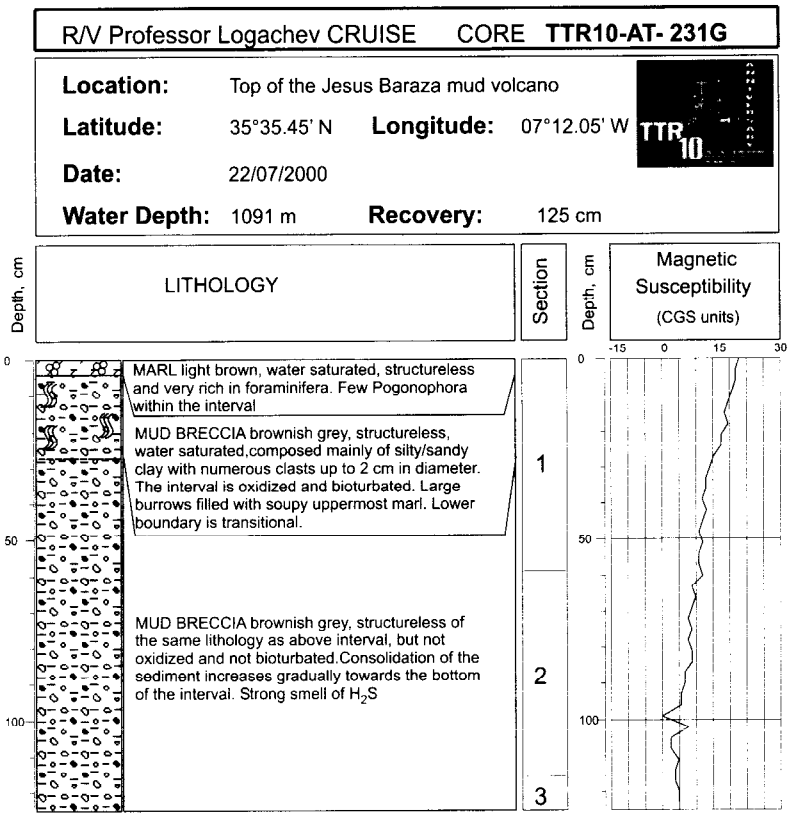

Core log TTR-10-AT-231G

ANNEX I. CORE LOGS (LEG 1, Algarve margin and Gulf of Cadiz)

R/V Professor Logachev CRUISE CORE **TTR10-AT- 233G**

Location: Top of the carbonate mound on the Moroccan margin

Latitude: 35°31.06' N **Longitude:** 07°08.96' W

Date: 22/07/2000

Water Depth: 955 m **Recovery:** 36 cm

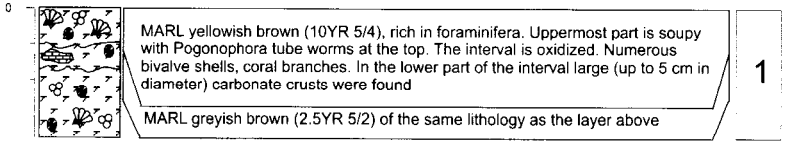

Core log TTR-10-AT-233G

R/V Professor Logachev CRUISE CORE **TTR10-AT- 234G**

Location: Top of the diapir structures

Latitude: 35°25.72' N **Longitude:** 7°10.56' W

Date: 22/07/2000

Water Depth: 1140 m **Recovery:** 241 cm

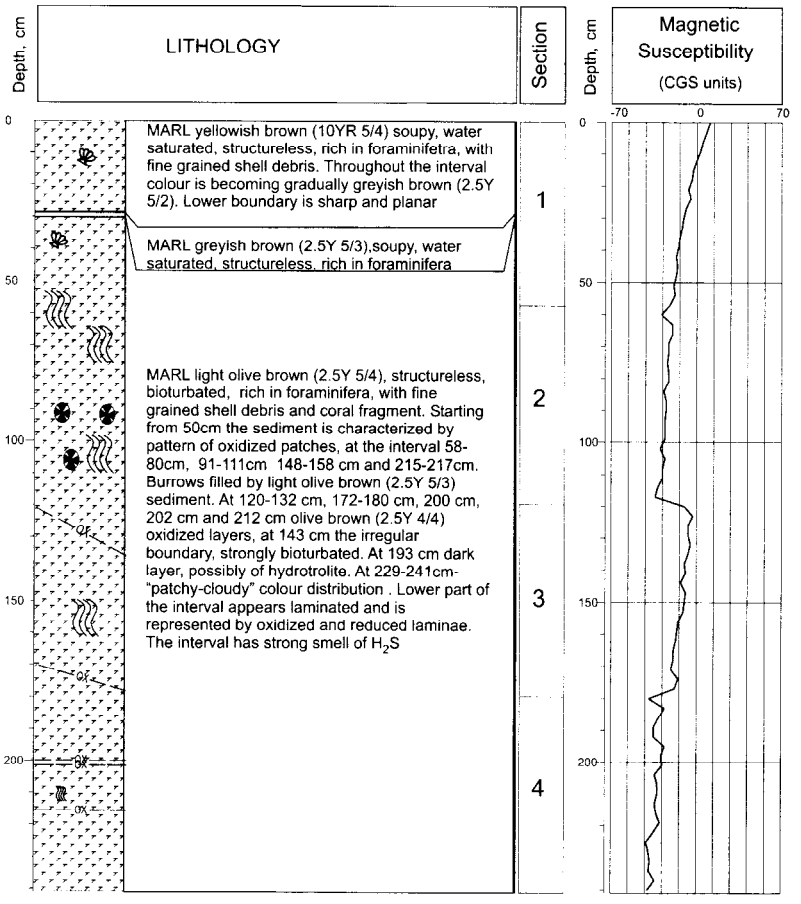

Core log TTR-10-AT-234G

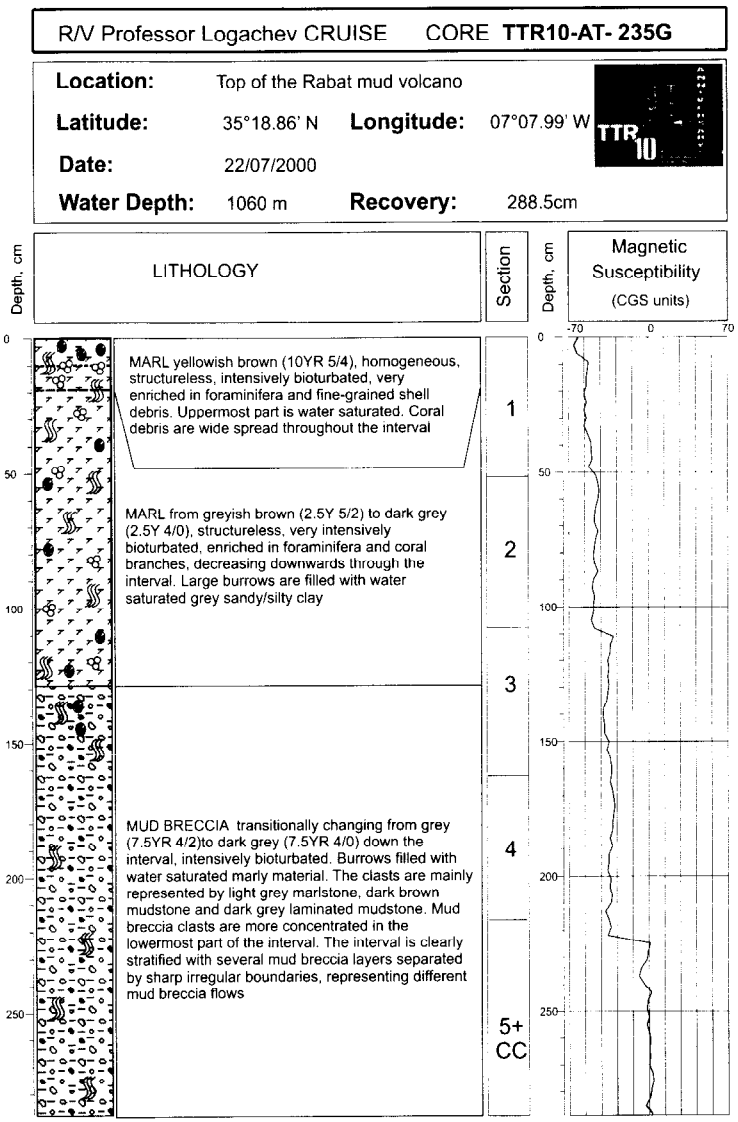

Core log TTR-10-AT-235G

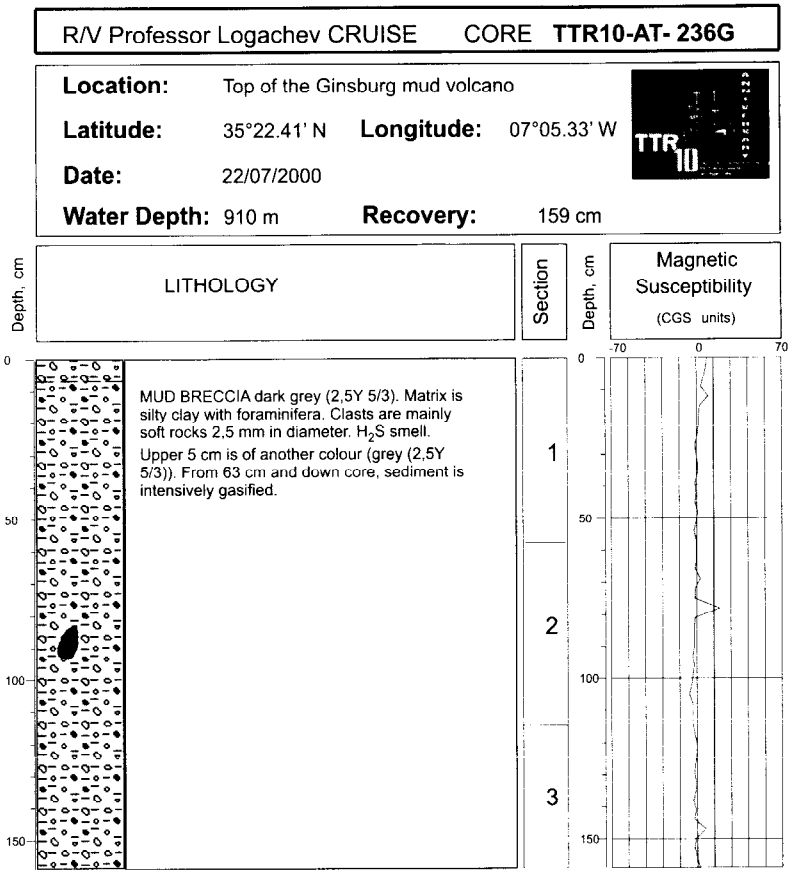

Core log TTR-10-AT-236G

ANNEX I. CORE LOGS (LEG 1, Algarve margin and Gulf of Cadiz)

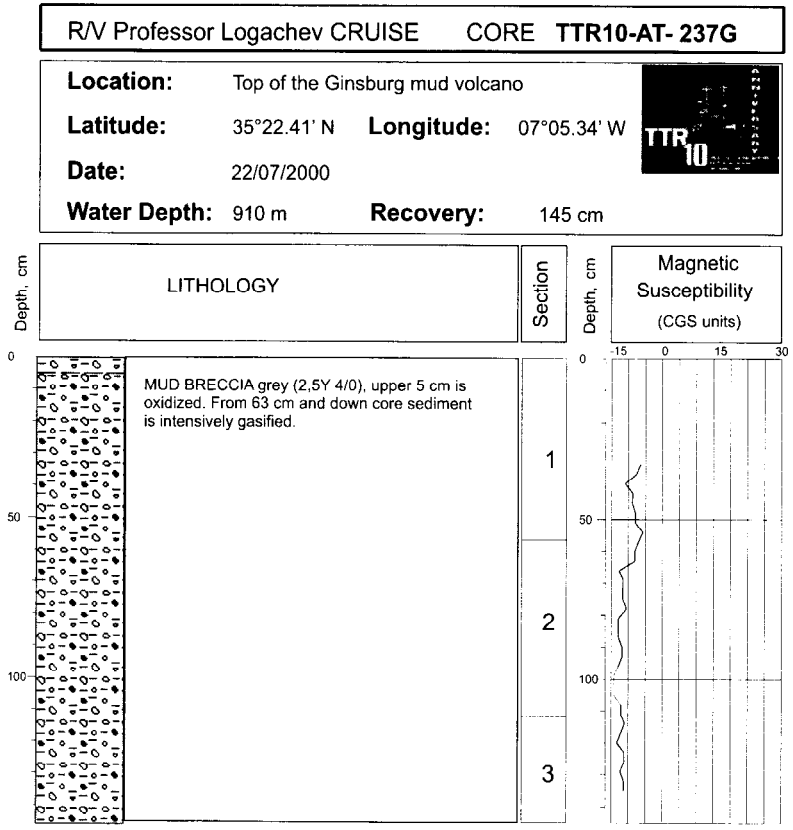

Core log TTR-10-AT-237G

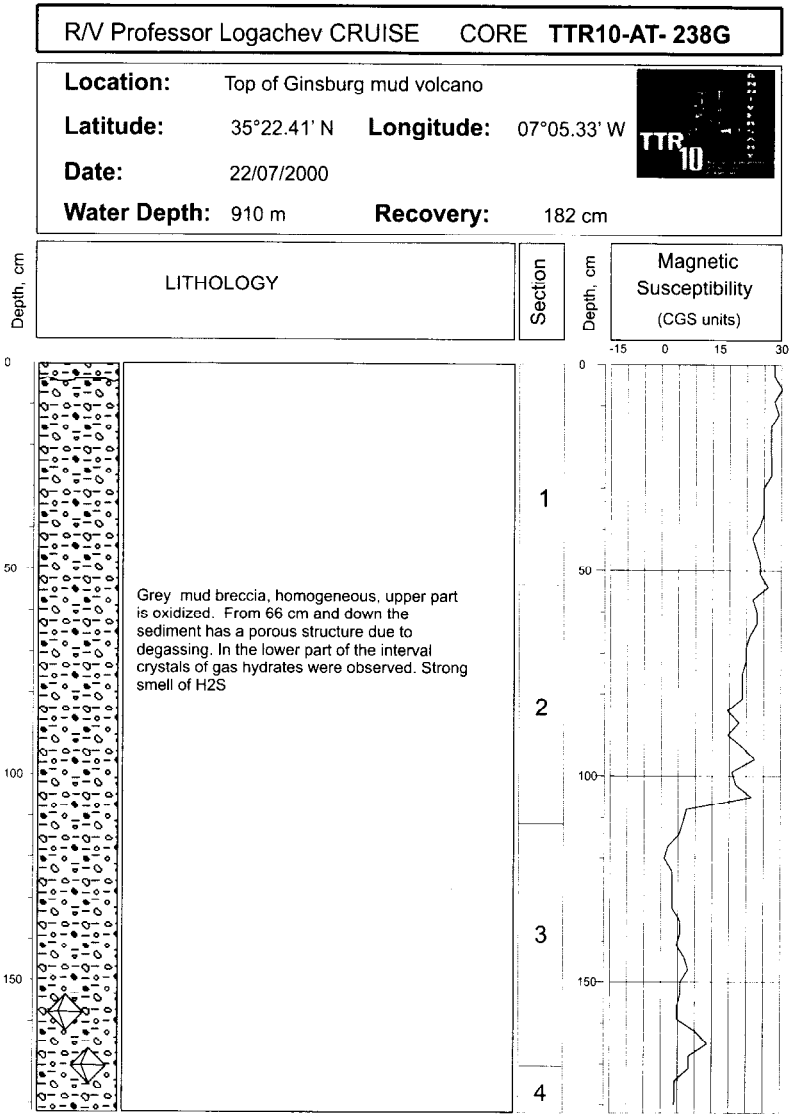

Core log TTR-10-AT-238G

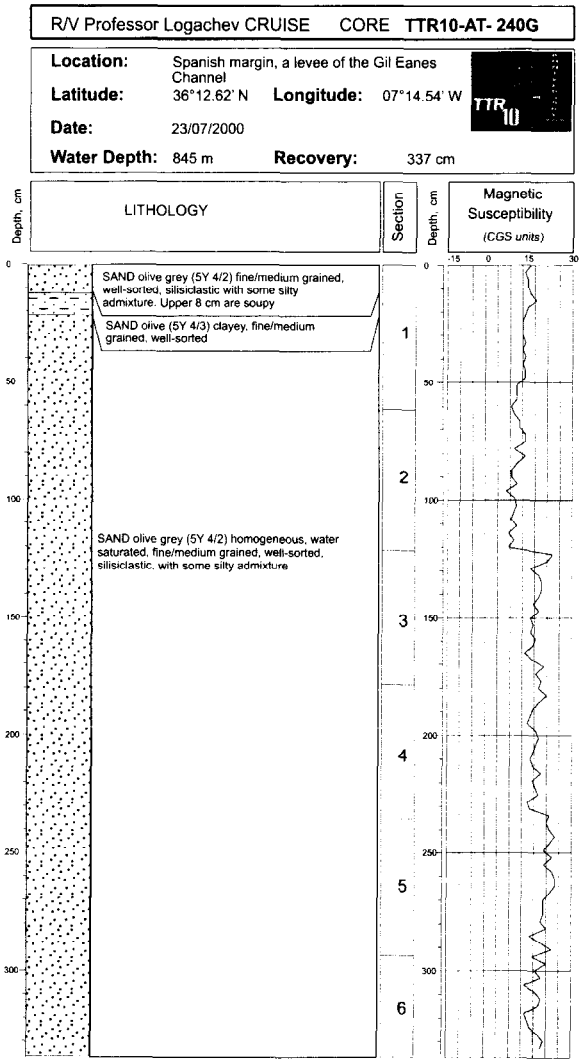

Core log TTR-10-AT-240G

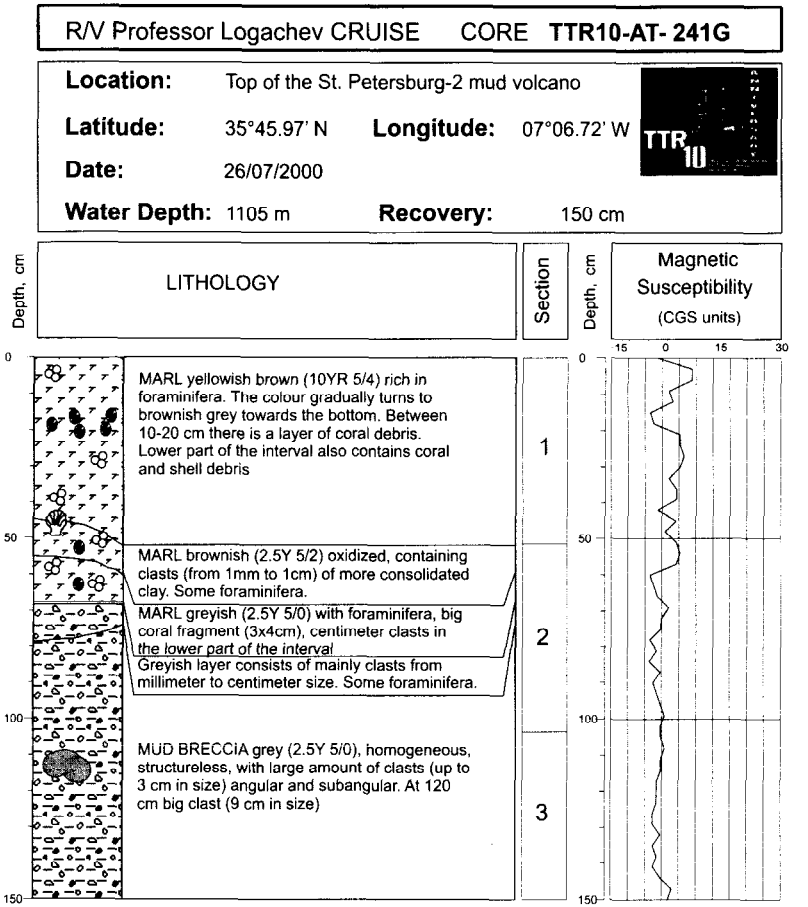

Core log TTR-10-AT-241G

ANNEX I. CORE LOGS (LEG 1, Algarve margin and Gulf of Cadiz)

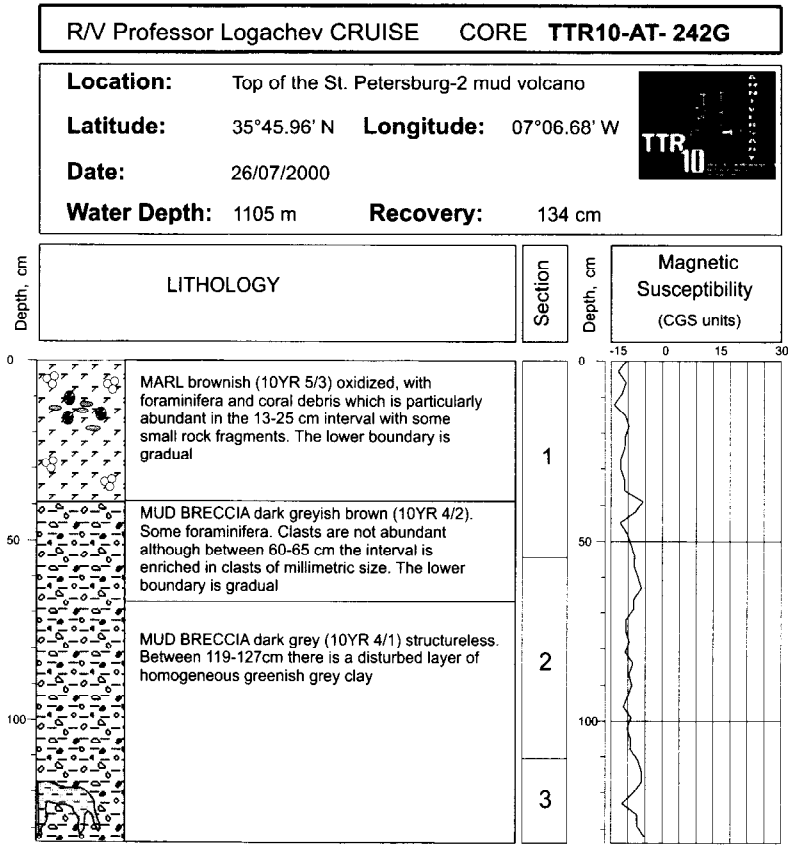

Core log TTR-10-AT-242G

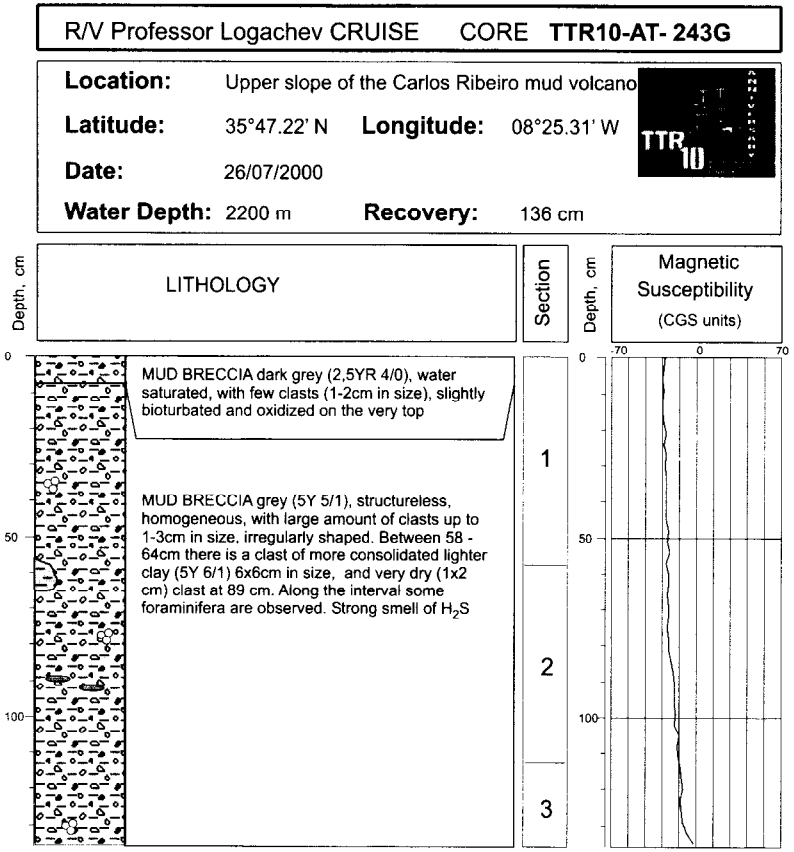

Core log TTR-10-AT-243G

ANNEX I. CORE LOGS (LEG 1, Algarve margin and Gulf of Cadiz)

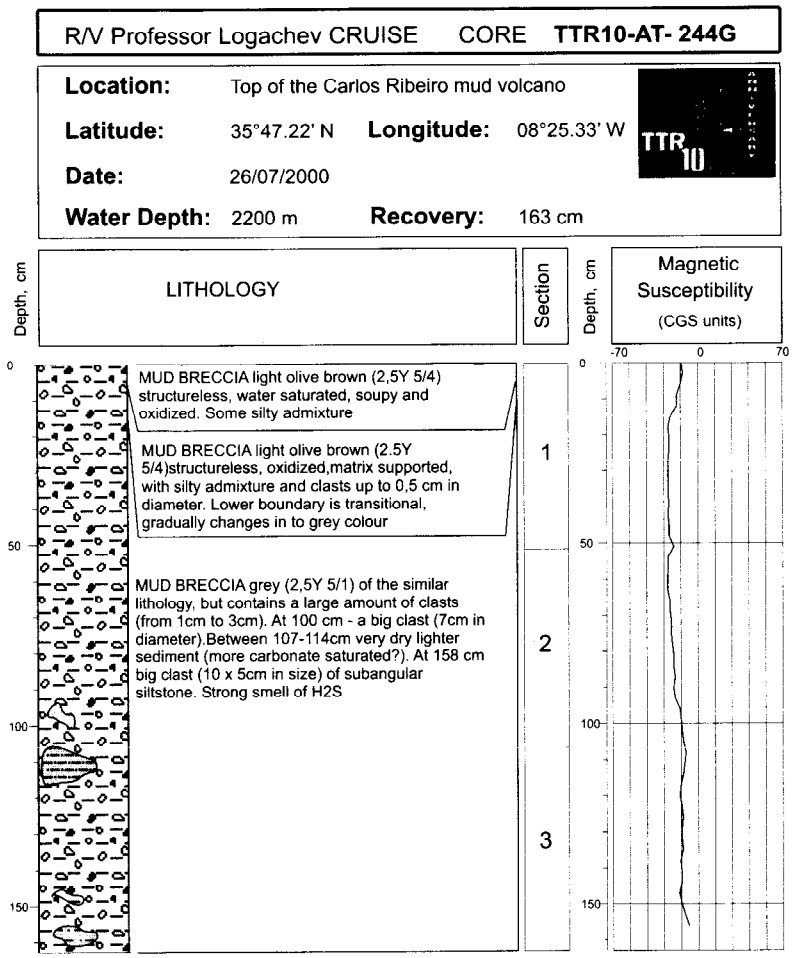

Core log TTR-10-AT-244G

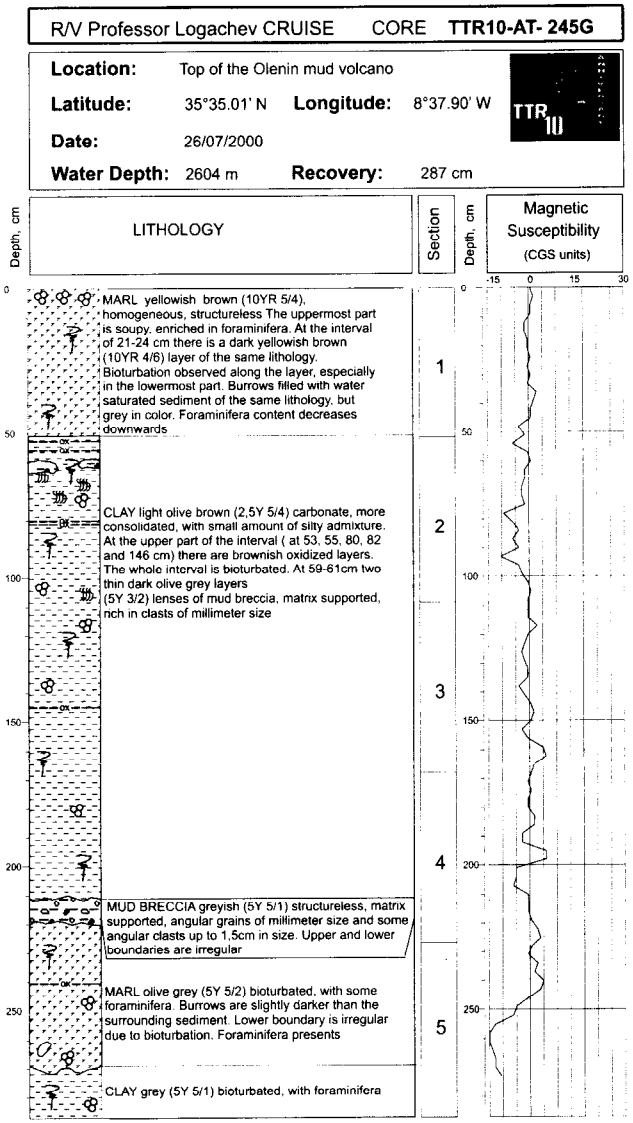

Core log TTR-10-AT-245G

ANNEX I. CORE LOGS (LEG 1, Algarve margin and Gulf of Cadiz)

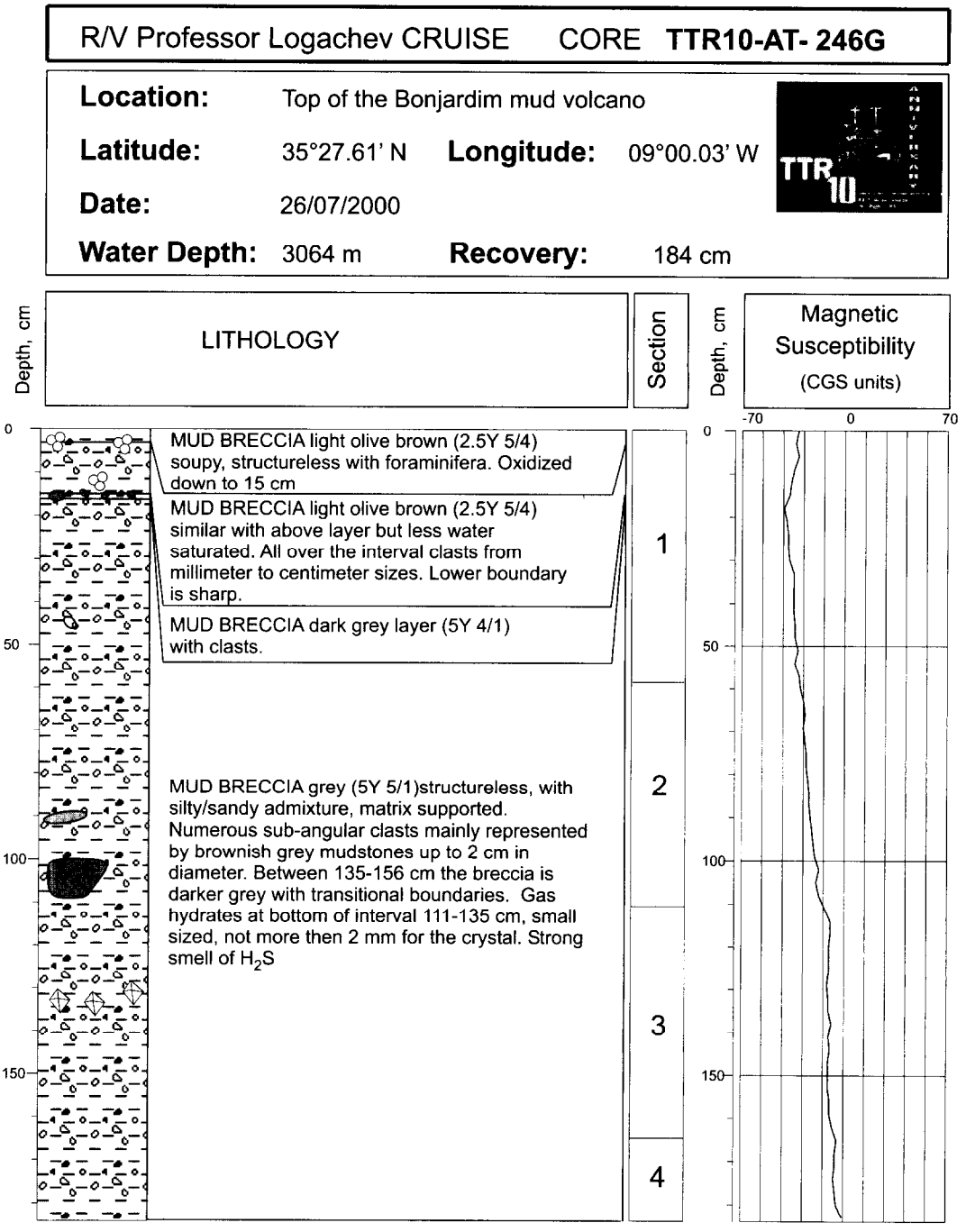

Core log TTR-10-AT-246G

ANNEX I. CORE LOGS (LEG 3, Northeastern Rockall Trough Margin)

R/V Professor Logachev CRUISE TTR-10 CORE TTR10-AT- 282G

Location: Irish margin, channel overbank.

Latitude: 54°46,552' N Longitude: 10°57,532' W

Date: 14/08/2000

Water Depth: 1940 m

Recovery: 351 cm

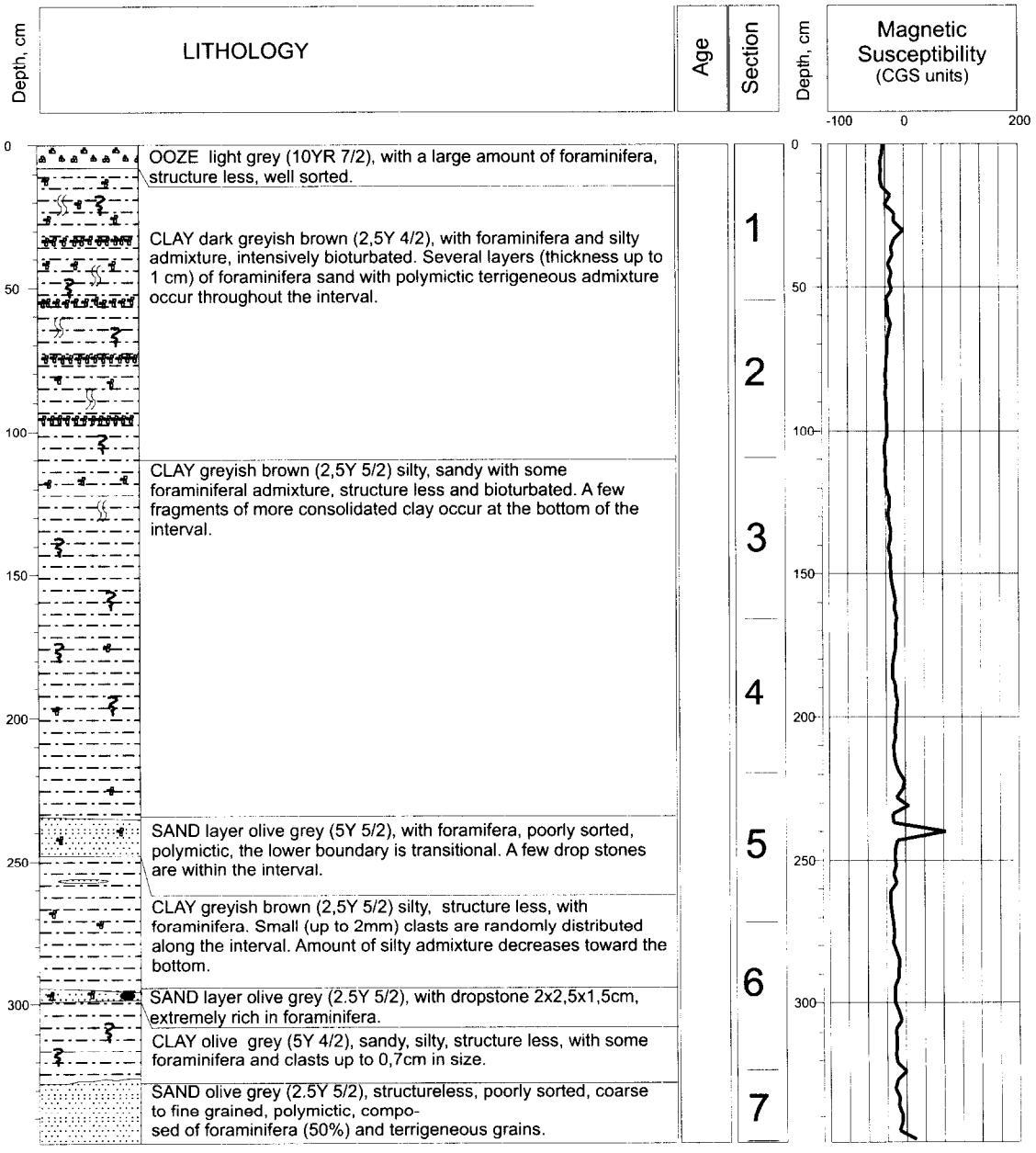

Core log TTR-10-AT-282G

ANNEX I. CORE LOGS (LEG 3, Northeastern Rockall Trough Margin)

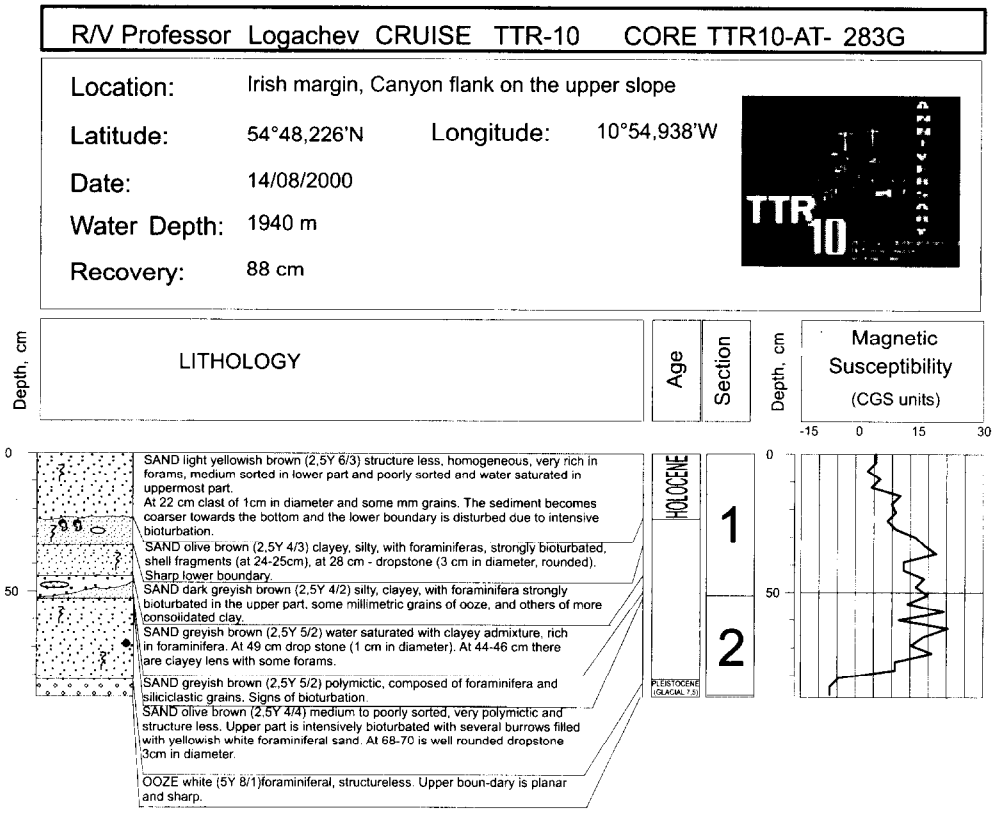

Core log TTR-10-283G

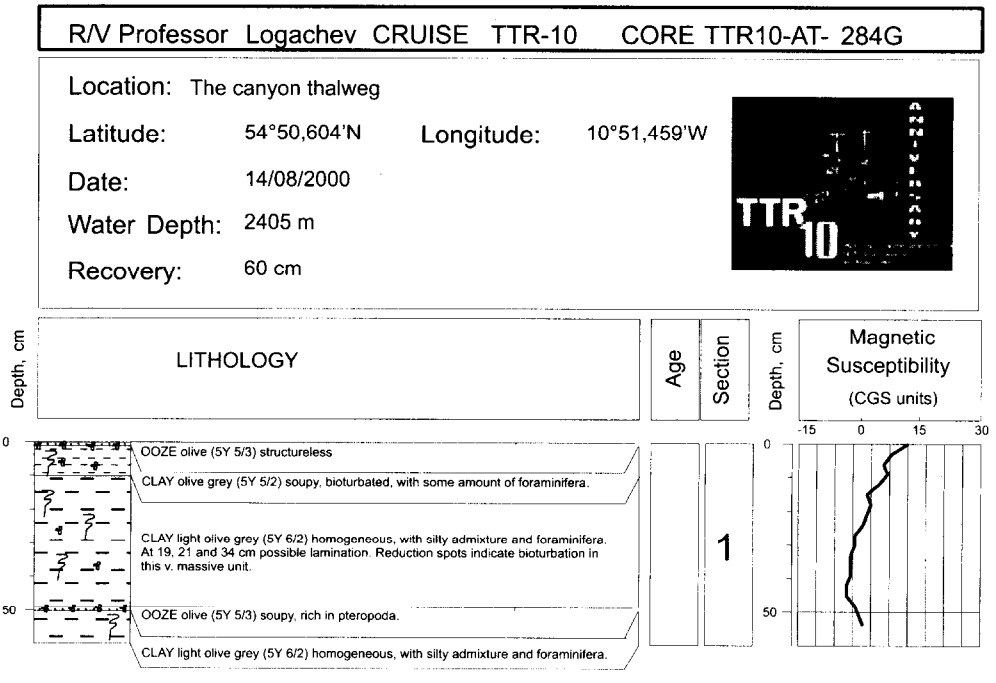

Core log TTR-10-AT-284G

ANNEX I. CORE LOGS (LEG 3, Northeastern Rockall Trough Margin)

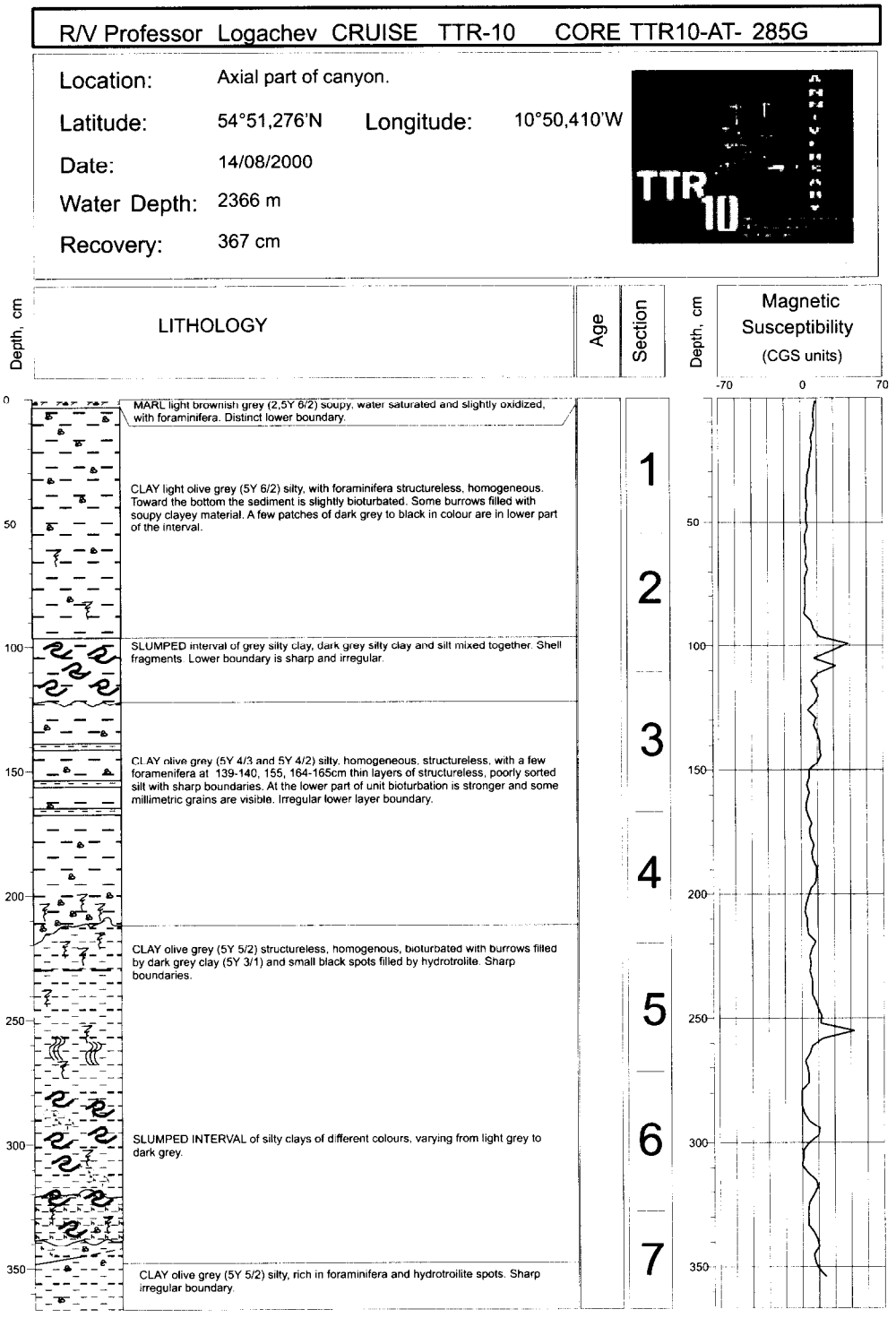

Core log TTR-10-AT-285G

ANNEX I. CORE LOGS (LEG 3, Northeastern Rockall Trough Margin)

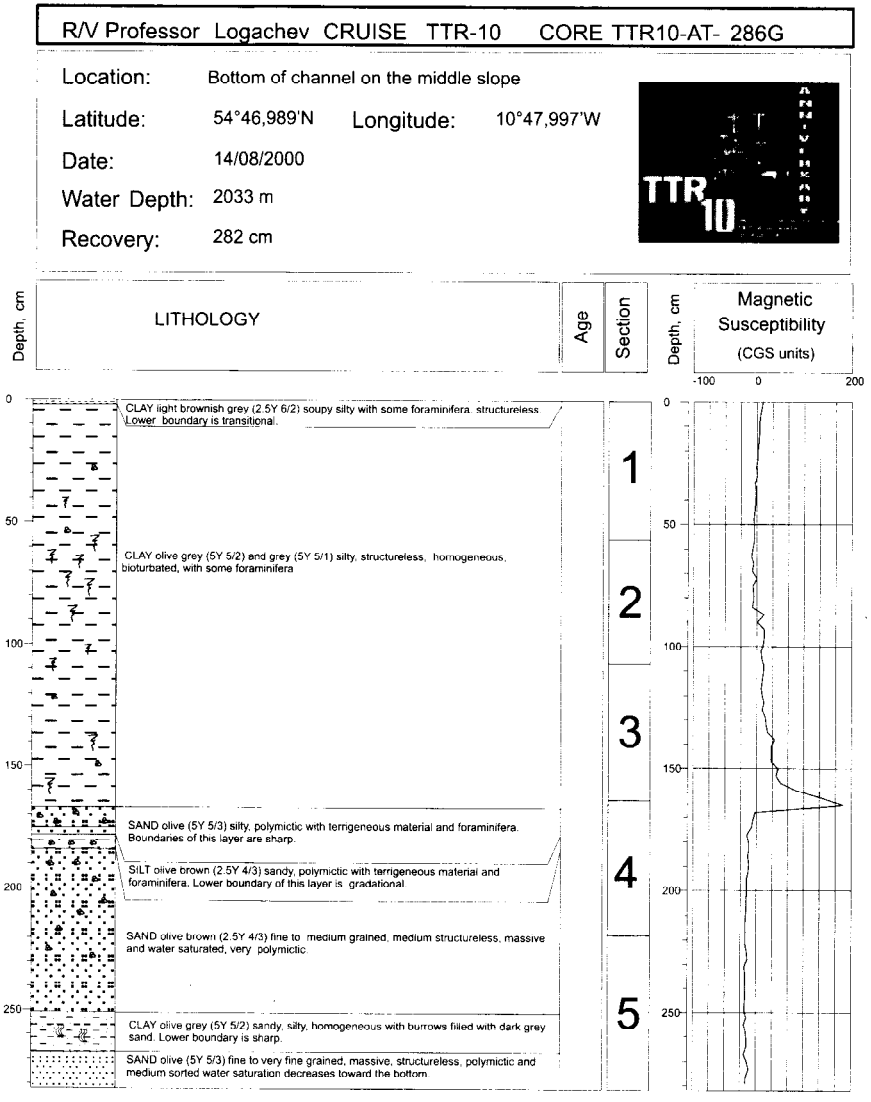

Core log TTR-10-AT-286G

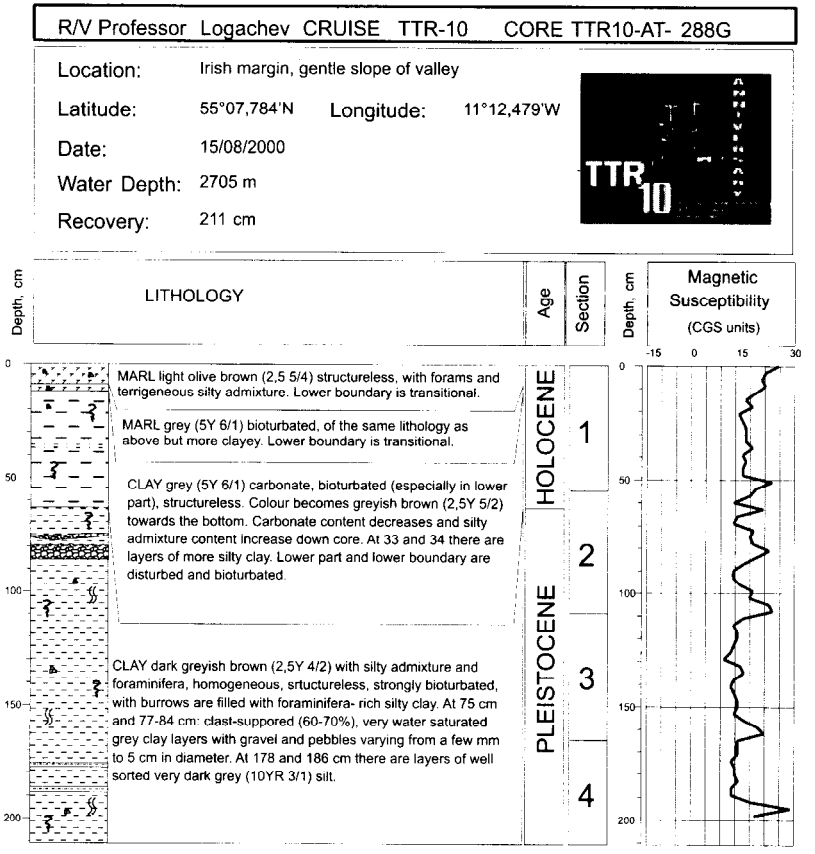

Core log TTR-10-AT-288G

ANNEX I. CORE LOGS (LEG 3, Northeastern Rockall Trough Margin)

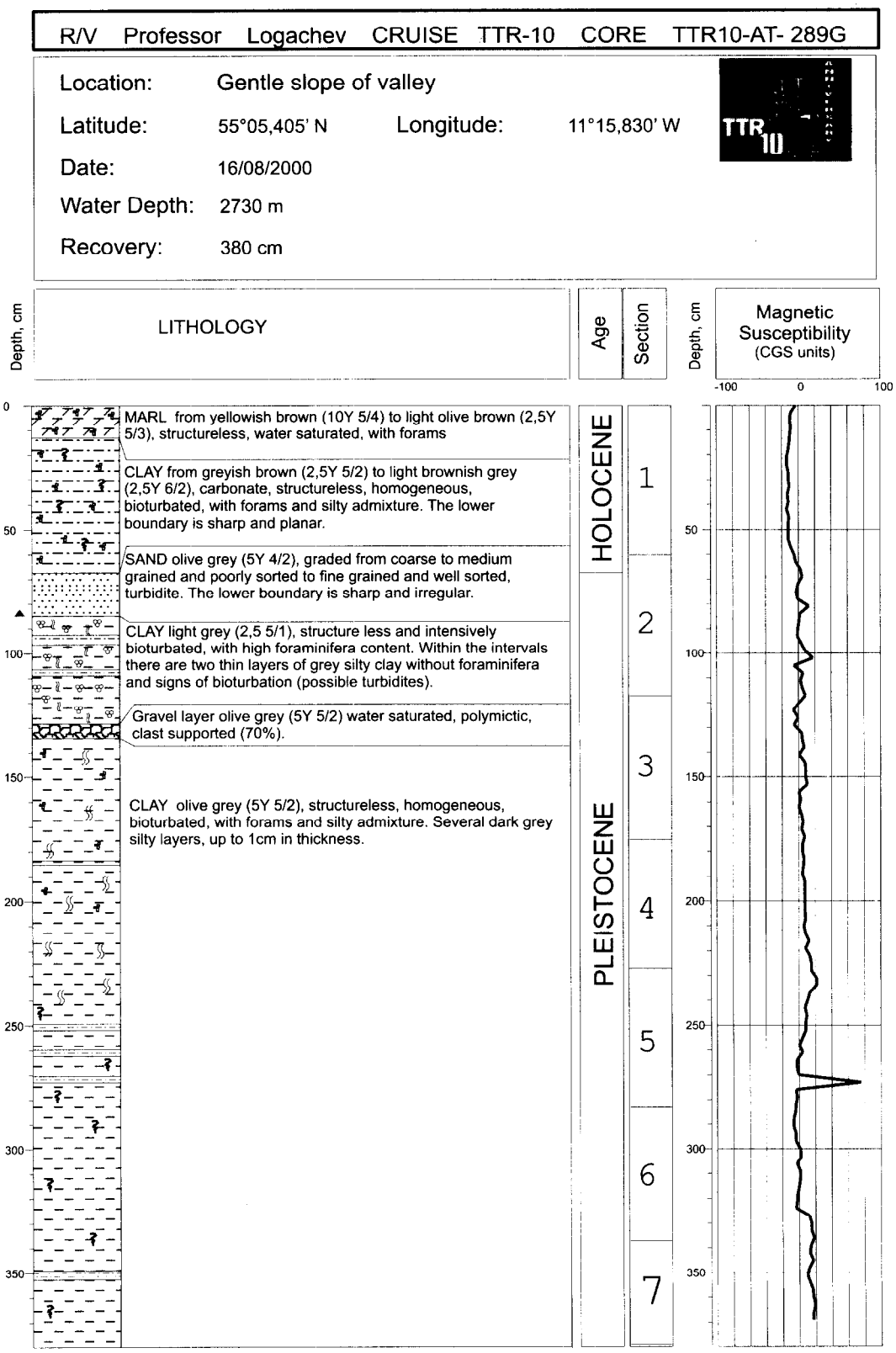

Core log TTR-10-AT-289G

ANNEX I. CORE LOGS (LEG 3, Northeastern Rockall Trough Margin)

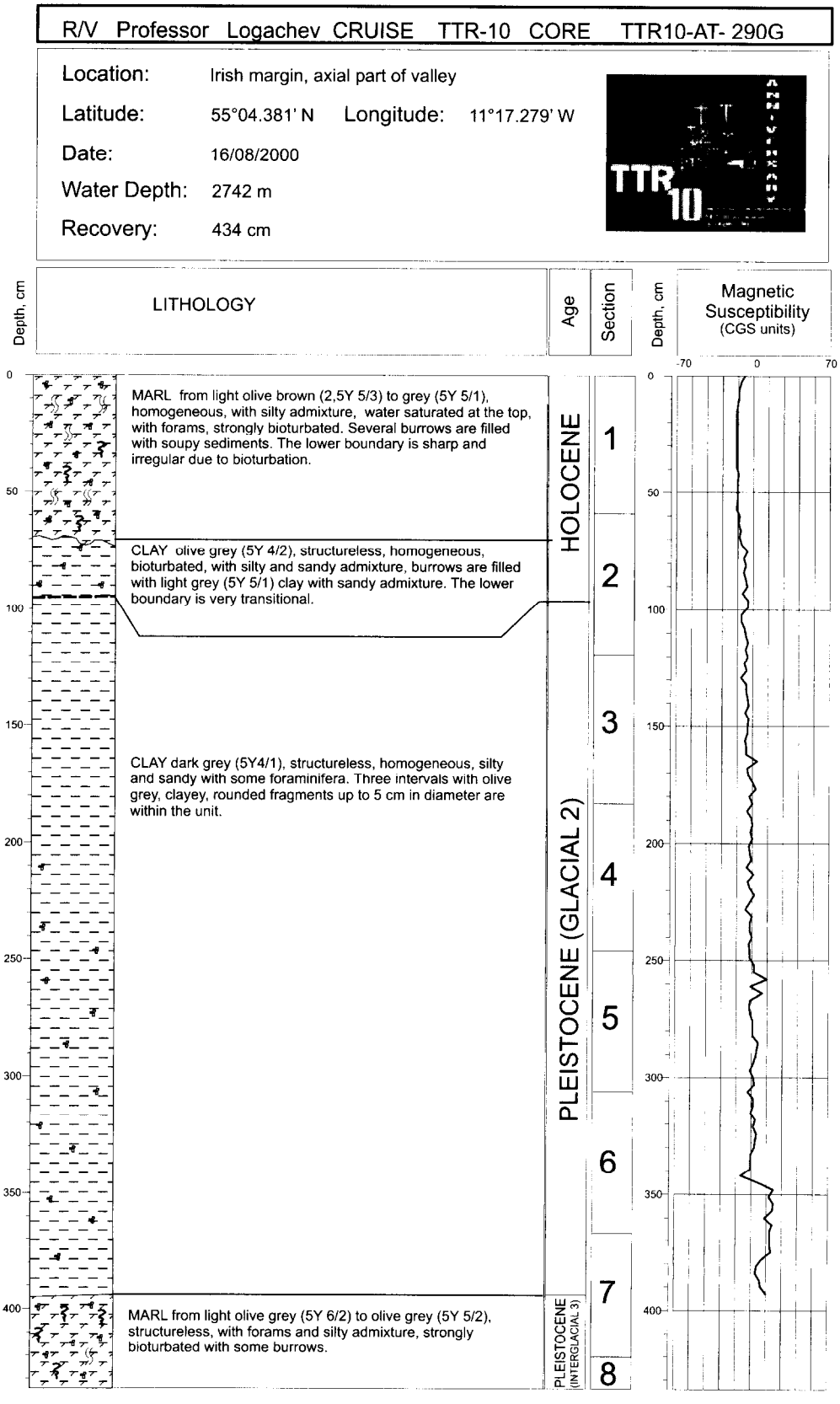

Core log TTR-10-AT-290G

ANNEX I. CORE LOGS (LEG 3, Northeastern Rockall Trough Margin)

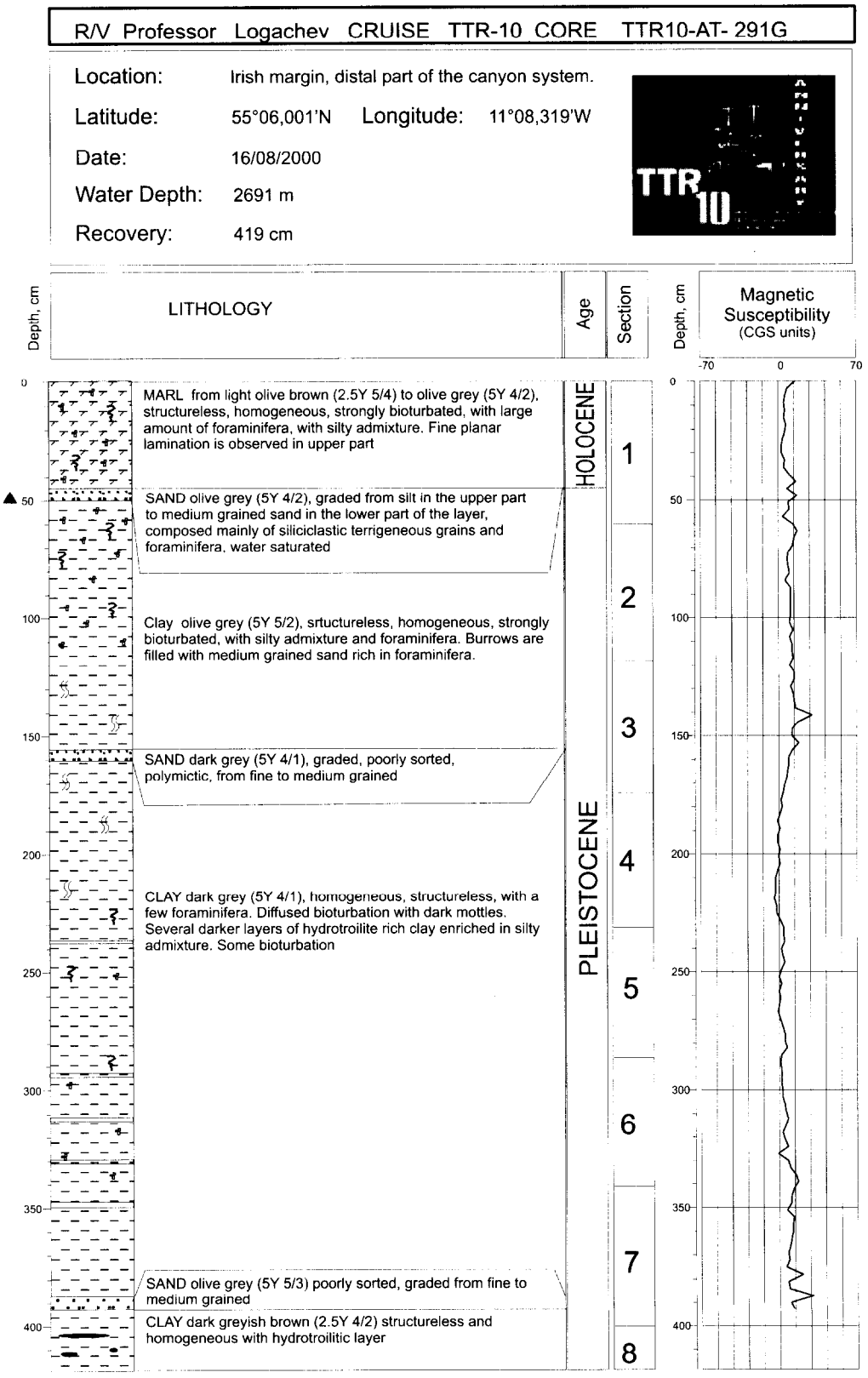

Core log TTR-10-AT-291G

ANNEX I. CORE LOGS (LEG 3, Northeastern Rockall Trough Margin)

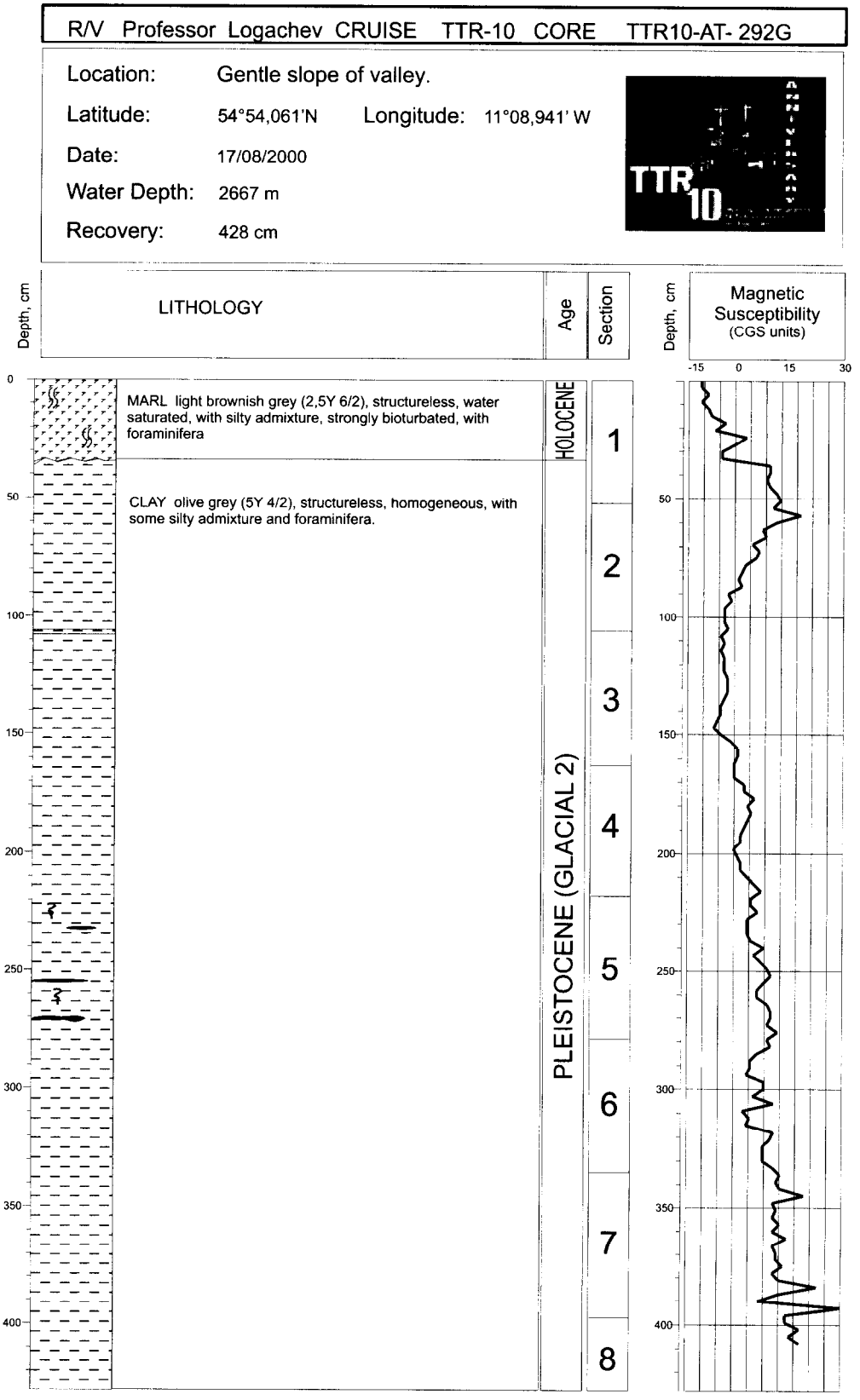

Core log TTR-10-AT-292G

ANNEX I. CORE LOGS (LEG 3, Northeastern Rockall Trough Margin)

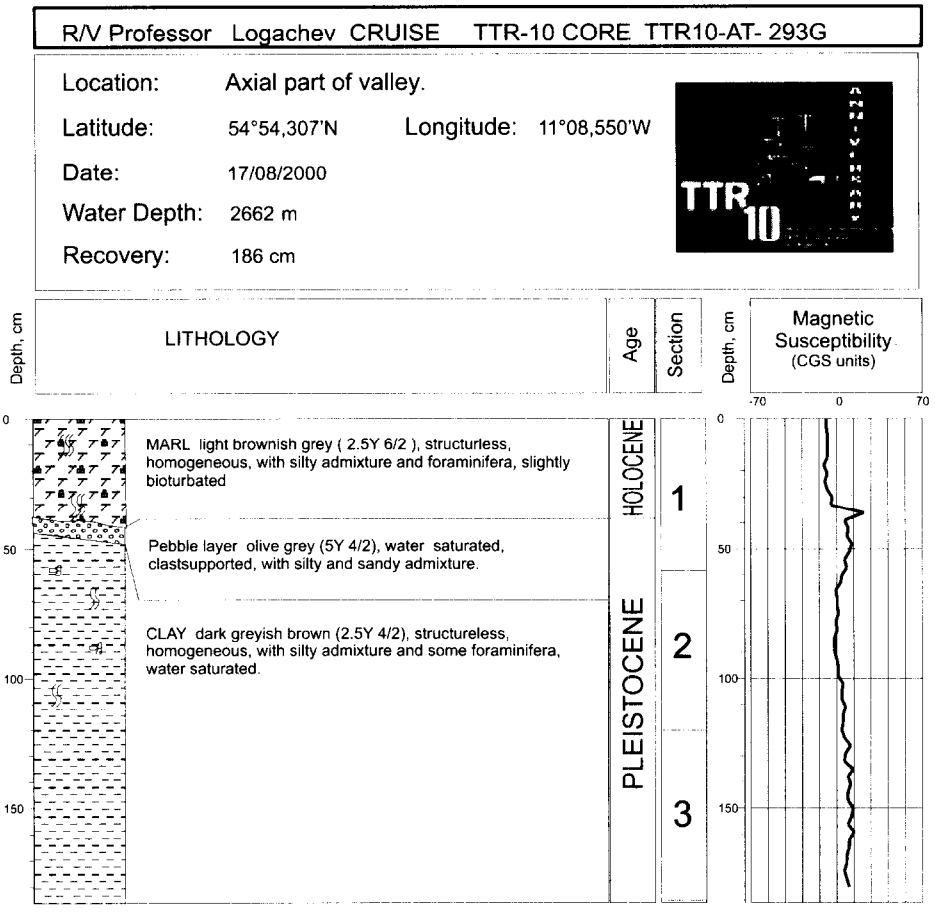

Core log TTR-10-AT-293G

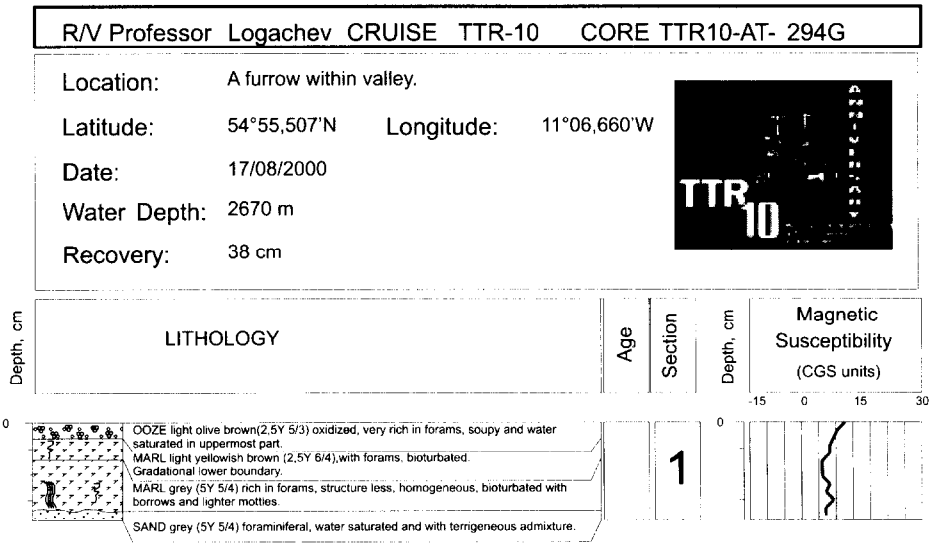

Core log TTR-10-AT-294G

ANNEX I. CORE LOGS (LEG 3, Northeastern Rockall Trough Margin)

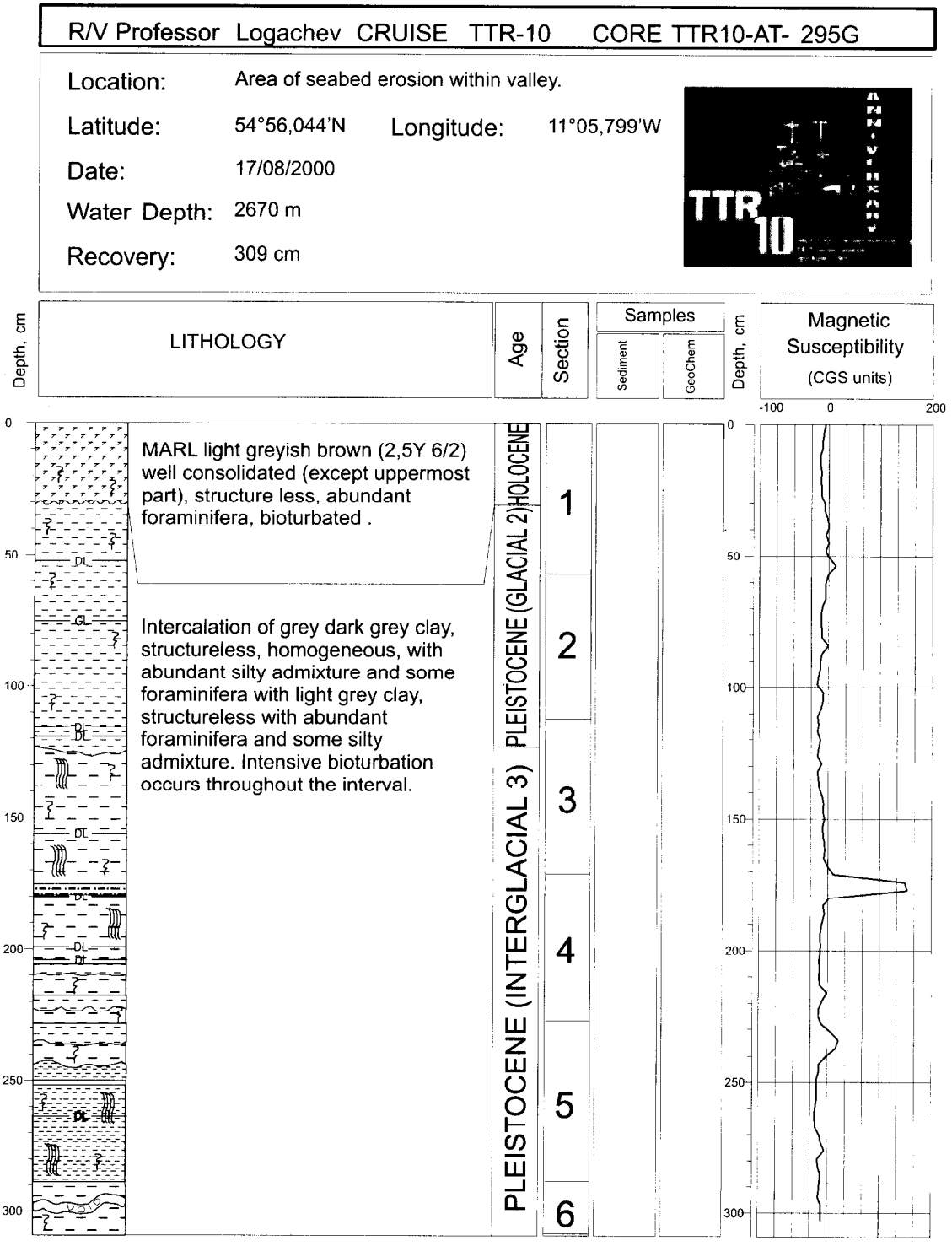

Core log TTR-10-AT-295G

ANNEX I. CORE LOGS (LEG 3, Northeastern Rockall Trough Margin)

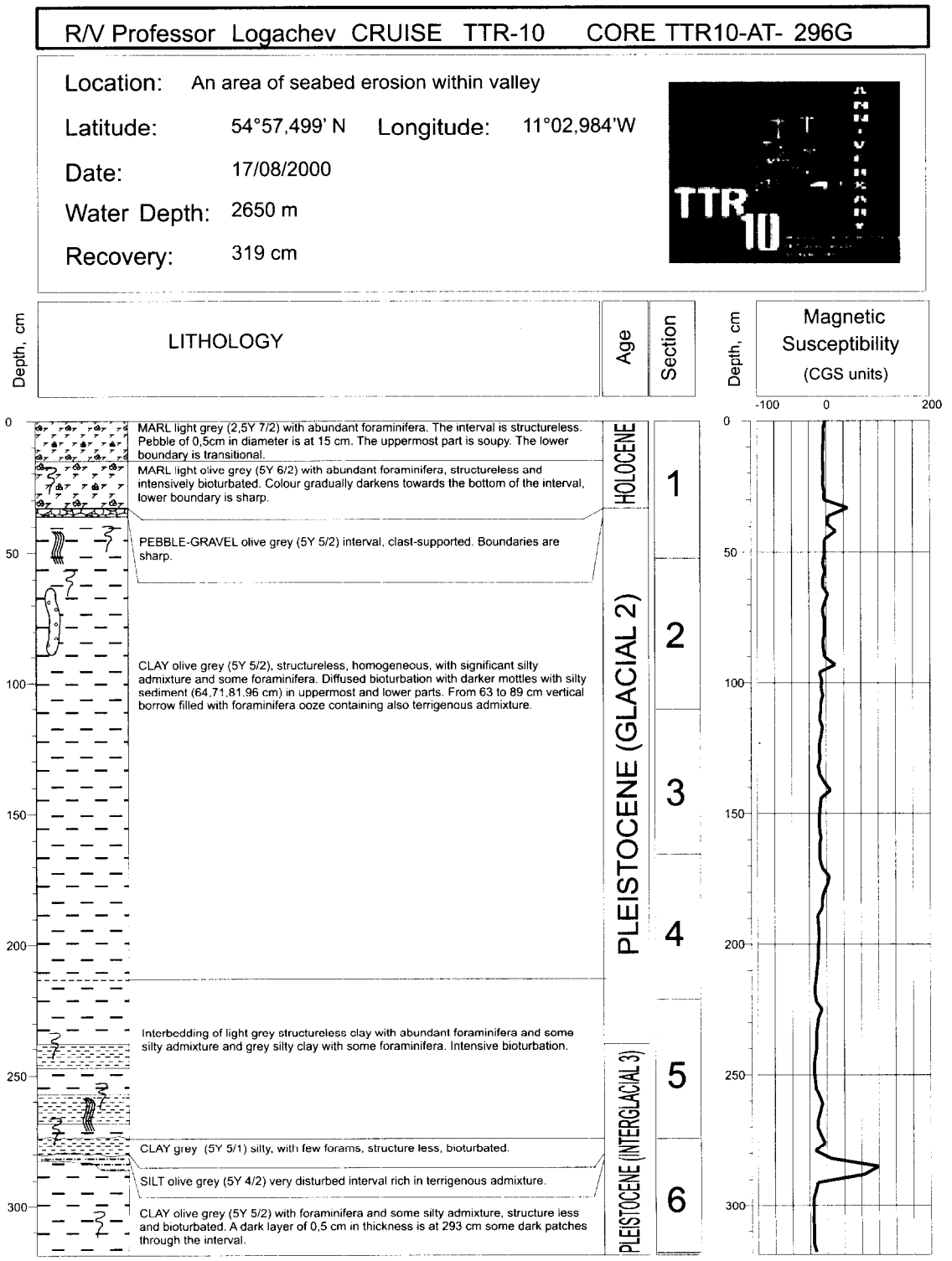

Core log TTR-10-AT-296G

ANNEX I. CORE LOGS (LEG 3, Northeastern Rockall Trough Margin)

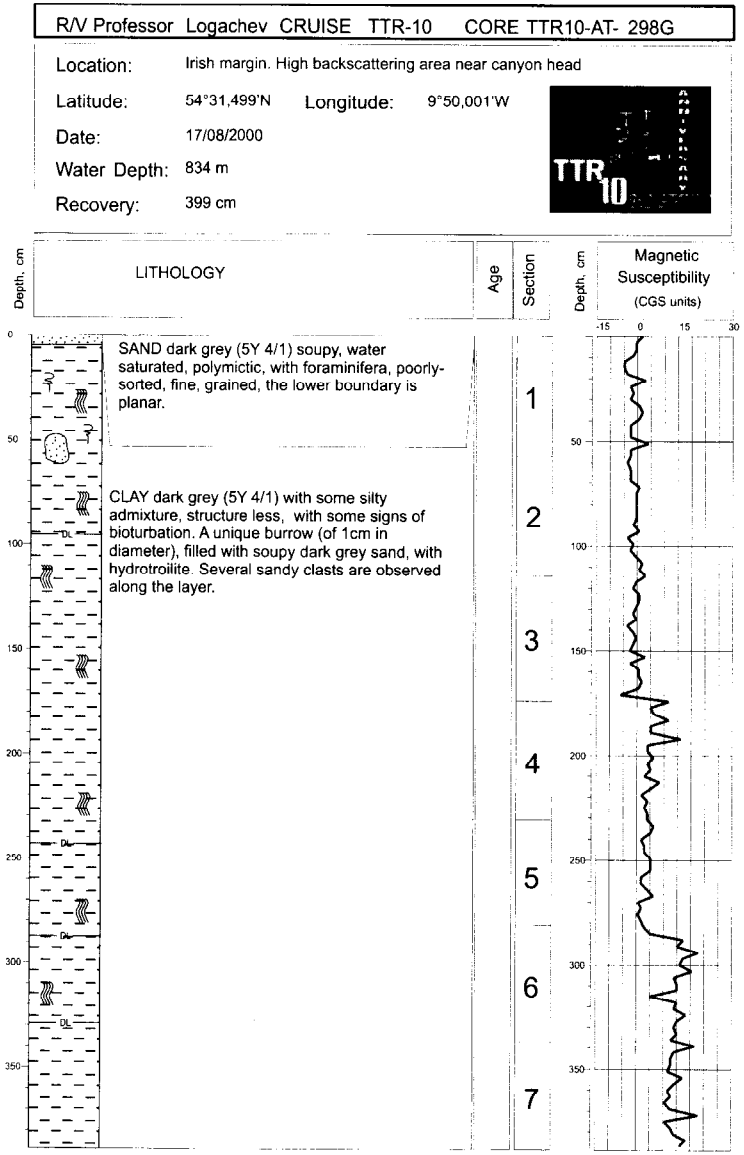

Core log TTR-10-AT-298G

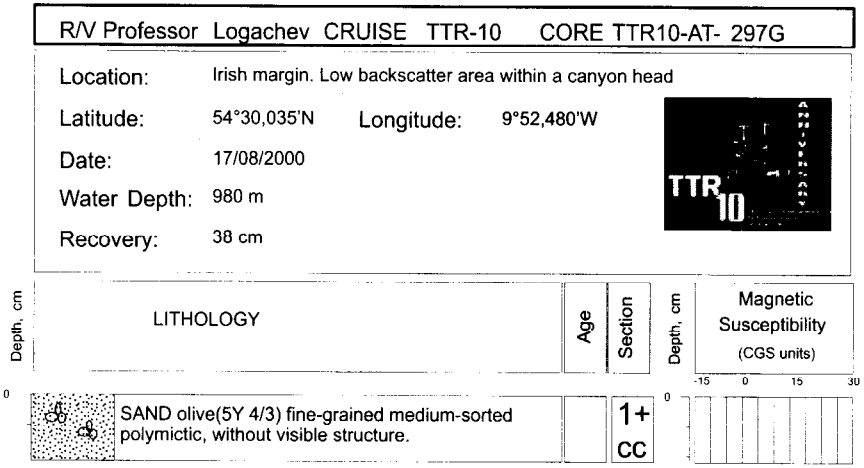

Core log TTR-10-AT-297G

ANNEX I. CORE LOGS (LEG 3, Vøring Plateau)

R/V Professor Logachev CRUISE TTR-10 CORE TTR10-AT- 324G

Location: Voring Plateau. In the vicinity of an inferred mud volcano

Latitude: 64°40,901'N Longitude: 5°15.741'E

Date: 24/08/2000

Water Depth: 724 m

Recovery: 490 cm

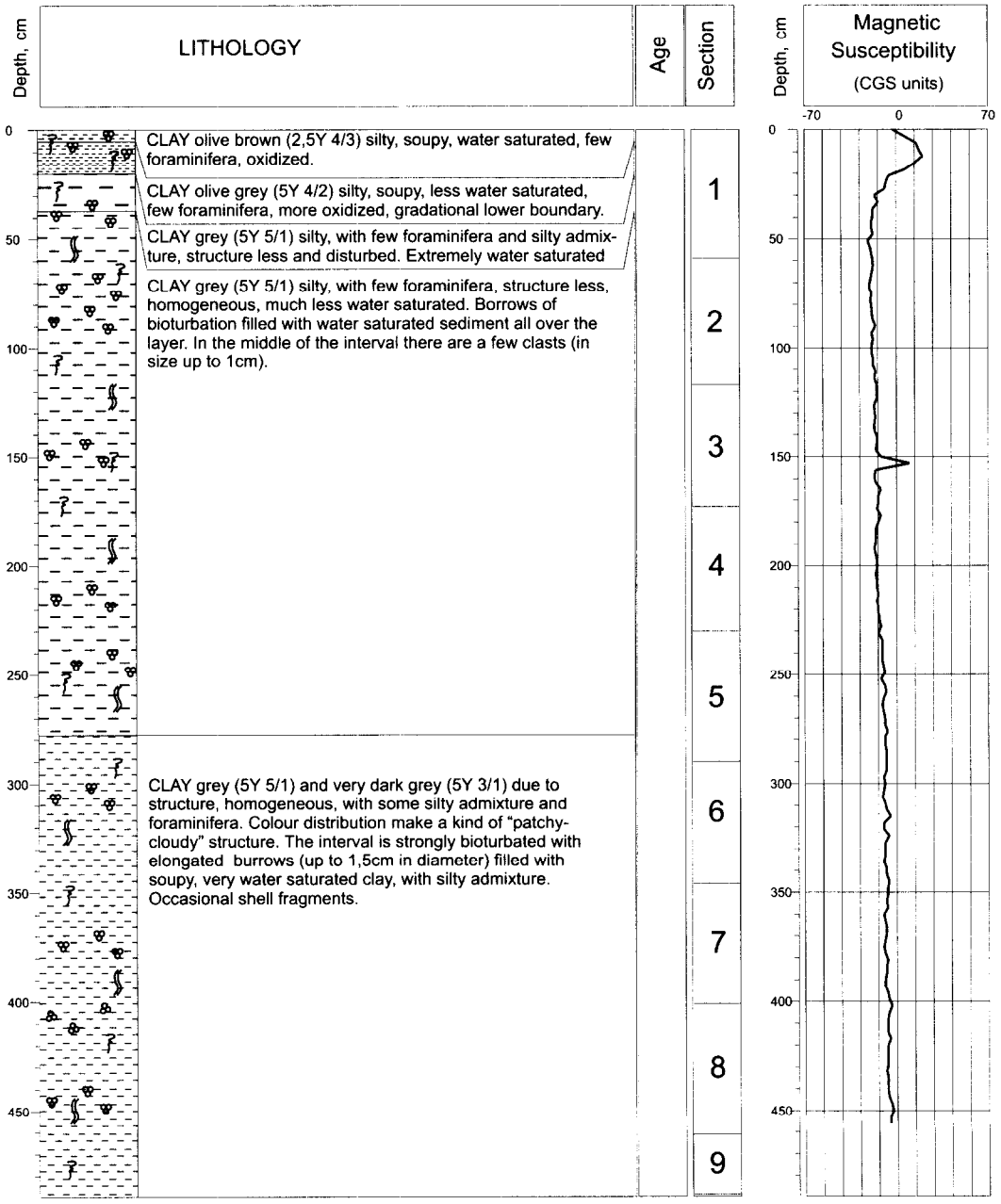

Core log TTR-10-AT-324G

ANNEX I. CORE LOGS (LEG 3, Vøring Plateau)

R/V Professor Logachev CRUISE TTR-10 CORE TTR10-AT- 326G

Location: Voring Plateau. Possible pockmark

Latitude: 64°46,104'N Longitude: 4°48,413'E

Date: 24/08/2000

Water Depth: 794 m

Recovery: 557 cm

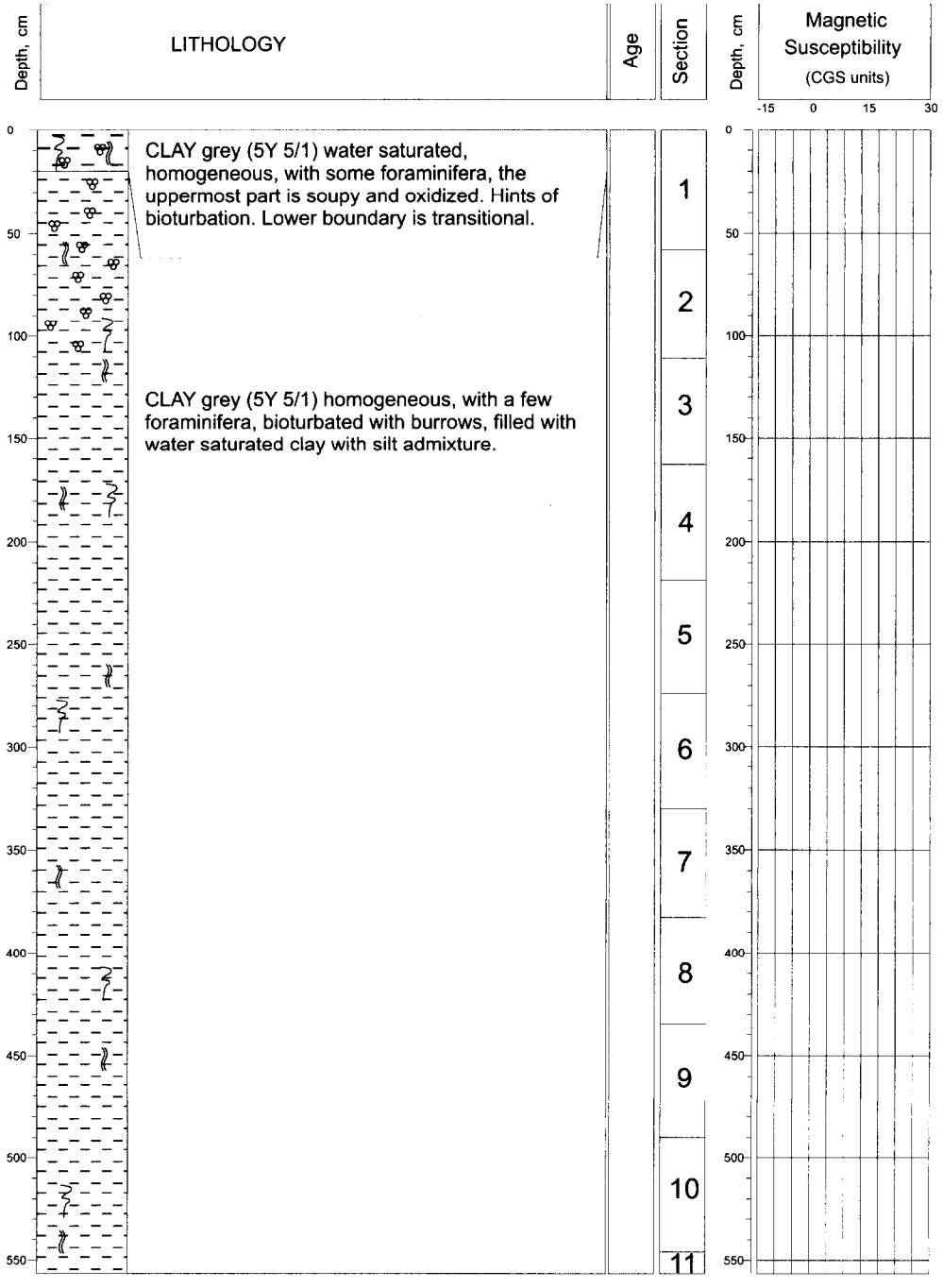

Core log TTR-10-AT-326G

ANNEX I. CORE LOGS (LEG 3, Vøring Plateau)

R/V Professor Logachev CRUISE TTR-10 CORE TTR10-AT- 327G

Location: Voring Plateau. Possible pockmark

Latitude: 64°49.989'N Longitude: 4°09.286'E

Date: 26/08/2000

Water Depth: 1008 m

Recovery: 573 cm

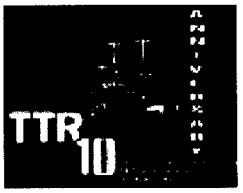

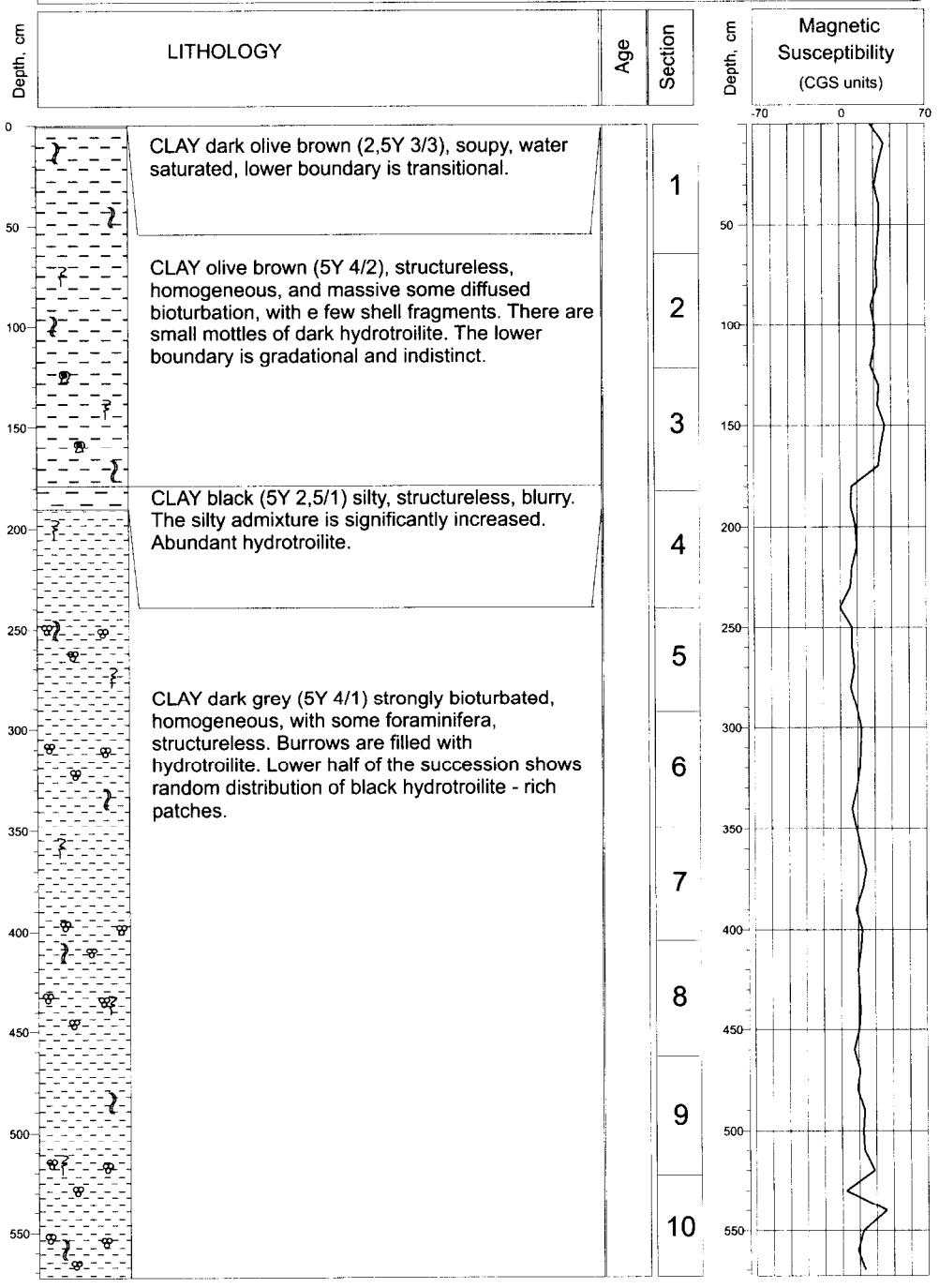

Core log TTR-10-AT-327G

ANNEX I. CORE LOGS (LEG 3, Vøring Plateau)

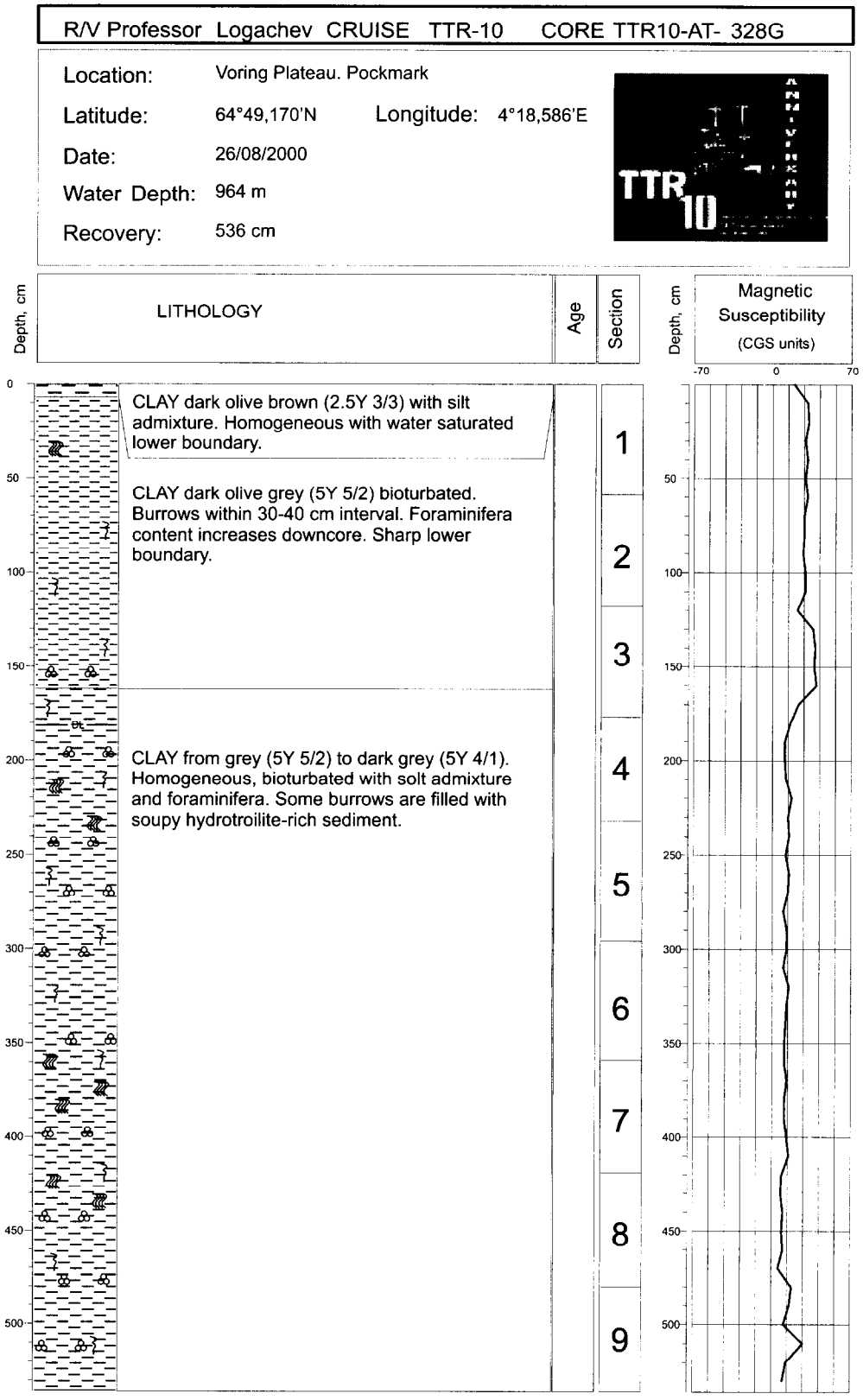

Core log TTR-10-AT-328G

ANNEX II. LIST OF TTR-RELATED REPORTS

Limonov, A.F., Woodside, J.M. and Ivanov, M.K. (eds.)., 1992. Geological and geophysical investigations in the Mediterranean and Black Seas. Initial results of the "Training through Research" Cruise of RV *Gelendzhik* in the Eastern Mediterranean and the Black Sea (June-July 1991). *UNESCO Reports in Marine Science*, 56, 208 pp.

Limonov, A.F., Woodside, J.M. and Ivanov, M.K. (eds.), 1993. Geological and geophysical investigations of the deep-sea fans of the Western Mediterranean Sea. Preliminary report of the 2nd cruise of the RV *Gelendzhik* in the Western Mediterranean Sea, June-July, 1992. *UNESCO Reports in Marine Science*, 62. 148 pp.

"Training-Through-Research" Opportunities Through the UNESCO/TREDMAR Programme. Report of the first post-cruise meeting of TREDMAR students. Moscow State University, 22-30 January, 1993. *MARINF*, 91, UNESCO, 1993.

Limonov, A.F., Woodside, J.M. and Ivanov, M.K. (eds.), 1994. Mud volcanism in the Mediterranean and Black Seas and Shallow Structure of the Eratosthenes Seamount. Initial results of the geological and geophysical investigations during the Third UNESCO-ESF "Training-through-Research" Cruise of RV *Gelendzhik* (June-July 1993). *UNESCO Reports in Marine Science*, 64, 173 pp.

Recent Marine Geological Research in the Mediterranean and Black Seas through the UNESCO/TREDMAR programme and its "Floating University" project, Free University, Amsterdam, 31 January-4 February 1994. Abstracts. *MARINF*, 94,UNESCO, 1994.

Limonov, A.F., Kenyon, N.H., Ivanov, M.K. and Woodside J.M. (eds.), 1995. Deep sea depositional systems of the Western Mediterranean and mud volcanism on the Mediterranean Ridge. Initial results of geological and geophysical investigations during the Fourth UNESCO-ESF 'Training through Research" Cruise of RV *Gelendzhik* (June-July 1994). *UNESCO Reports in Marine Science*, 67, 171 pp.

Deep-sea depositional systems and mud volcanism in the Mediterranean and Black Seas. 3rd post-cruise meeting, Cardiff, 30 January - 3 February 1995. Abstracts. *MARINF*, 99, UNESCO, 1995.

Ivanov, M.K., Limonov, A.F. and Cronin, B.T. (eds.), 1996. Mud volcanism and fluid venting in the eastern part of the Mediterranean Ridge. Initial results of geological, geophysical and geochemical investigations during the 5th Training-through-Research Cruise of RV *Professor Logachev* (July-September 1995). *UNESCO Reports in Marine Science*, 68, 127pp.

Sedimentary basins of the Mediterranean and Black Seas. 4th Post-Cruise Meeting, Training-through-research Programme. Moscow and Zvenigorod, Russia, 29 January-3 February. Abstracts. *MARINF*,100, UNESCO, 1996.

Woodside, J.M., Ivanov, M.K. and Limonov, A.F. (eds.), 1997. Neotectonics and Fluid Flow through Seafloor Sediments in the Eastern Mediterranean and Black Seas. Preliminary results of geological and geophysical investigations during the ANAXIPROBE/TTR-6 cruise of RV *Gelendzhik*, July-August 1996. Vols. 1, 2. *IOC Technical Series*, 48, UNESCO, 226 pp.

Gas and Fluids in Marine Sediments: Gas Hydrates, Mud Volcanoes, Tectonics, Sedimentology and Geochemistry in Mediterranean and Black Seas. Fifth Post-cruise Meeting of the Training-through-

research Programme and International Congress, Amsterdam, The Netherlands, 27-29 January 1997. *IOC Workshop Reports*,129, UNESCO, 1997.

Geosphere-biosphere coupling: Carbonate Mud Mounds and Cold Water Reefs. International Conference and Sixth Post-Cruise Meeting of the Training-through-Research Programme, Gent, Belgium, 7-11 February 1998. *IOC Workshop Reports*, 143, UNESCO, 1998.

Kenyon, N.H., Ivanov, M.K. and Akhmetzhanov, A.M. (eds.), 1998. Cold water carbonate mounds and sediment transport on the Northeast Atlantic Margin. *IOC Technical Series*, 52, UNESCO, 178 pp.

Kenyon, N.H., Ivanov, M.K. and Akhmetzhanov, A.M. (eds.), 1999. Geological Processes on the Northeast Atlantic Margin. *IOC Technical Series*, 54, UNESCO, 141 pp.

Geological Processes on European Continental Margins. International Conference and Eighth Post-cruise Meeting of the Training-Through-Research Programme, University of Granada, Spain, 31 January - 3 February 2000. *IOC Workshop Reports*, 168, UNESCO, 2000.

Kenyon, N.H., Ivanov, M.K., Akhmetzhanov, A.M. and Akhmanov, G.G., (eds), 2000, Multidisciplinary study of geological processes on the Northeast Atlantic and Western Mediterranean margins. *IOC Technical Series,* 56, UNESCO, Paris, 119 pp.

Geological processes on deep-sea European margins. International Conference and Ninth Post-Cruise Meeting of the Training-through-research Programme. Moscow/Mozhenka, Russia, 28 January - 3 February 2001. *IOC Workshop Reports,* 175. UNESCO, 2001, 76 pp.

IOC Technical Series

No.	Title	Languages
1	Manual on International Oceanographic Data Exchange. 1965	(out of stock)
2	Intergovernmental Oceanographic Commission (Five years of work). 1966	(out of stock)
3	Radio Communication Requirements of Oceanography. 1967	(out of stock)
4	Manual on International Oceanographic Data Exchange – Second revised edition. 1967	(out of stock)
5	Legal Problems Associated with Ocean Data Acquisition Systems (ODAS). 1969	(out of stock)
6	Perspectives in Oceanography. 1968	(out of stock)
7	Comprehensive Outline of the Scope of the Long-term and Expanded Programme of Oceanic Exploration and Research. 1970	(out of stock)
8	IGOSS (Integrated Global Ocean Station System) – General Plan Implementation Programme for Phase 1. 1971	(out of stock)
9	Manual on International Oceanographic Data Exchange – Third Revised Edition. 1973	(out of stock)
10	Bruun Memorial Lectures. 1971	E, F, S, R
11	Bruun Memorial Lectures. 1973	(out of stock)
12	Oceanographic Products and Methods of Analysis and Prediction. 1977	E only
13	International Decade of Ocean Exploration (IDOE), 1971-1980. 1974	(out of stock)
14	A Comprehensive Plan for the Global Investigation of Pollution in the Marine Environment and Baseline Study Guidelines. 1976	E, F, S, R
15	Bruun Memorial Lectures, 1975 – Co-operative Study of the Kuroshio and Adjacent Regions. 1976	(out of stock)
16	Integrated Ocean Global Station System (IGOSS) General Plan and Implementation Programme 1977-1982. 1977	E, F, S, R
17	Oceanographic Components of the Global Atmospheric Research Programme (GARP). 1977	(out of stock)
18	Global Ocean Pollution: An Overview. 1977	(out of stock)
19	Bruun Memorial Lectures – The Importance and Application of Satellite and Remotely Sensed Data to Oceanography. 1977	(out of stock)
20	A Focus for Ocean Research: The Intergovernmental Oceanographic Commission – History, Functions, Achievements. 1979	(out of stock)
21	Bruun Memorial Lectures, 1979: Marine Environment and Ocean Resources. 1986	E, F, S, R
22	Scientific Report of the Intercalibration Exercise of the IOC-WMO-UNEP Pilot Project on Monitoring Background Levels of Selected Pollutants in Open Ocean Waters. 1982	(out of stock)
23	Operational Sea-Level Stations. 1983	E, F, S, R
24	Time-Series of Ocean Measurements. Vol. 1. 1983	E, F, S, R
25	A Framework for the Implementation of the Comprehensive Plan for the Global Investigation of Pollution in the Marine Environment. 1984	(out of stock)
26	The Determination of Polychlorinated Biphenyls in Open-ocean Waters. 1984	E only
27	Ocean Observing System Development Programme. 1984	E, F, S, R
28	Bruun Memorial Lectures, 1982: Ocean Science for the Year 2000. 1984	E, F, S, R
29	Catalogue of Tide Gauges in the Pacific. 1985	E only
30	Time-Series of Ocean Measurements. Vol. 2. 1984	E only

(continued on inside back cover)

No.	Title	Languages
31	Time-Series of Ocean Measurements. Vol. 3. 1986	E only
32	Summary of Radiometric Ages from the Pacific. 1987	E only
33	Time-Series of Ocean Measurements. Vol. 4. 1988	E only
34	Bruun Memorial Lectures, 1987: Recent Advances in Selected Areas of Ocean Sciences in the Regions of the Caribbean, Indian Ocean and the Western Pacific. 1988	Composite E, F, S
35	Global Sea-Level Observing System (GLOSS) Implementation Plan. 1990	E only
36	Bruun Memorial Lectures, 1989: Impact of New Technology on Marine Scientific Research. 1991	Composite E, F, S
37	Tsunami Glossary – A Glossary of Terms and Acronyms Used in the Tsunami Literature. 1991	E only
38	The Oceans and Climate: A Guide to Present Needs. 1991	E only
39	Bruun Memorial Lectures, 1991: Modelling and Prediction in Marine Science. 1992	E only
40	Oceanic Interdecadal Climate Variability. 1992	E only
41	Marine Debris: Solid Waste Management Action for the Wider Caribbean. 1994	E only
42	Calculation of New Depth Equations for Expendable Bathymerographs Using a Temperature-Error-Free Method (Application to Sippican/TSK T-7, T-6 and T-4 XBTs). 1994	E only
43	IGOSS Plan and Implementation Programme 1996-2003. 1996	E, F, S, R
44	Design and Implementation of some Harmful Algal Monitoring Systems. 1996	E only
45	Use of Standards and Reference Materials in the Measurement of Chlorinated Hydrocarbon Residues. 1996	E only
46	Equatorial Segment of the Mid-Atlantic Ridge. 1996	E only
47	Peace in the Oceans: Ocean Governance and the Agenda for Peace; the Proceedings of *Pacem in Maribus* XXIII, Costa Rica, 1995. 1997	E only
48	Neotectonics and fluid flow through seafloor sediments in the Eastern Mediterranean and Black Seas – Parts I and II. 1997	E only
49	Global Temperature Salinity Profile Programme: Overview and Future. 1998	E only
50	Global Sea-Level Observing System (GLOSS) Implementation Plan – 1997. 1997	E only
51	L'état actuel de l'exploitation des pêcheries maritimes au Cameroun et leur gestion intégrée dans la sous-région du Golfe de Guinée *(under preparation)*	F only
52	Cold water carbonate mounds and sediment transport on the North East Atlantic Margin. 1998	E only
53	The Baltic Floating University: Training Through Research in the Baltic, Barents and White Seas – 1997. 1998	E only
54	Geological Processes on the North East Atlantic Margin (8th training-through-research cruise, June-August 1998. 1999	E only
55	Bruun Memorial Lectures, 1999: Ocean Predictability. 2000	E only
56	Multidisciplinary Study of Geological Processes on the North East Alantic and Western Mediterranean Margins (9th training-through-research cruise, June-July 1999). 2000	E only
57	*Ad Hoc* Benthic Indicator Group - Results of Initial Planning Meeting, Paris, France, 6-9 December 1999. 2000	E only
58	Bruun Memorial Lectures, 2001: Operational Oceanography - a perspective from the private sector. 2001	E only
59	*In preparation*	
60	Interdisciplinary Approaches to Geoscience on the North East Atlantic Margin and Mid-Atlantic Ridge (10th training-through-research cruise, July-August 2000). 2001	E only